5-18-2016 12:00 AM

Role of Fatty Acid omega-Hydroxylase 1 and Abscisic Acid in Potato Tuber Suberin Formation

Meg Haggitt
The University of Western Ontario

Supervisor
Dr. Mark Bernards
The University of Western Ontario

Graduate Program in Biology
A thesis submitted in partial fulfillment of the requirements for the degree in Doctor of Philosophy

Role of *Fatty Acid omega-Hydroxylase 1* (*FAωH1*) and Abscisic Acid in Potato Tuber Suberin Formation

Thesis format: Integrated-Article

By

Meghan L. Haggitt

Department of Biology, Faculty of Science

A thesis submitted in partial fulfillment
of the requirements for the degree of
Doctor of Philosophy

SCHOOL OF GRADUATE AND POSTDOCTORAL STUDIES
THE UNIVERSITY OF WESTERN ONTARIO
LONDON, ONTARIO, CANADA

Abstract

Suberin is a complex biopolymer composed of two distinct but covalently-linked domains. The first domain is composed of polymerized phenolic monomers, whereas the second domain is predominately fatty acid derivatives esterified with glycerol. Deposited in specialized cells during development or in response to abiotic stress, suberin functions as a barrier against water loss and pathogen attack. In potato, more than 65% of suberin monomers undergo ω-hydroxylation, representing a major class of fatty acids in the final biopolymer. The ω-hydroxylation reaction is catalyzed by Cytochrome P450 (CYP) proteins, of which few have been characterized to date. In 2009, *CYP86A33* from potato was identified and implicated as the main suberin-associated ω-hydroxylase by another research group through RNA*i* gene silencing; although functional characterization of *in vitro* protein was unsuccessful. Simultaneously, I identified and characterized gene expression patterns for three *CYP86A* and *CYP94A* ω-hydroxylase genes in potato. From this expression analysis, I identified *CYP86A33* as the primary candidate for a suberin-associated ω-hydroxylase, from which ω-hydroxylase activity was confirmed through an *in vitro* enzyme assay with recombinant protein. Following an *in silico* analysis of the *CYP86A33* promoter region, which identified many ABA-responsive promoter elements, an extensive analysis of the effects of ABA on gene expression and suberin biosynthetic regulation was conducted. Using a biosynthetic inhibitor of ABA production, fluridone, I investigated the effects of ABA on suberin regulation by inhibiting ABA *de novo* biosynthesis with or without the addition of exogenous ABA. Using wounded potato tubers, three parallel timecourse experiments were conducted with different treatments to quantify the ABA concentration, suberin-associated gene expression, and soluble and

insoluble aliphatic monomer deposition into the suberin biopolymer. Expression of suberin-associated genes, including *CYP86A33*, was reduced post-wounding with fluridone treatment. Similarly, insoluble aliphatic monomer accumulation was nearly eliminated from suberin in fluridone-treated tissues, exhibiting both chain length and monomer class specific effects. These fluridone effects on gene expression and suberin deposition were rescued through the addition of exogenous ABA. Overall, ABA was shown to have a regulatory post-wounding effect on the gene expression of key suberin-associated genes, with concomitant downstream impact on aliphatic suberin deposition.

Key words: *Solanum tuberosum*, potato, suberin, CYP86A33, FAωH1, ω-hydroxylation, abscisic acid, fluridone, wounding

Statement of Co-Authorship

The following people contributed to the publication of the work undertaken as part of this thesis:

University of Western Ontario, London, Canada: Meghan L. Haggitt

University of Western Ontario, London, Canada: Anica Bjelica

Author details and their roles:

Bjelica A, Haggitt ML, Woolfson KN, Lee DNP, Makhzoum AB, Bernards MA. 2016. Fatty Acid ω-Hydroxylases from *Solanum tuberosum*.

Accepted pending revisions to Plant Cell Reports

Located in Chapter 2, discussed in Chapter 4

Candidate was the secondary author, who identified *CYP86A33*, cloned *CYP86A33* and its promoter, created promoter deletion construct library (12 constructs), and conducted semi-quantitative RT-PCR tissue-specific expression analysis. AB completed all complementation assays, including aliphatic suberin analysis, and promoter analyses. KNW conducted qPCR to repeat tissue-specific expression for publication. DNPL created the *CYP86A33* minimal promoter construct for the P2 allele. ABM established hairy root cultures in the lab group. MAB supervised the lab work and wrote the manuscript.

Haggitt ML, Woolfson KN, Zhang Y, Kachura A, Bjelica A, Bernards MA. Differential Regulation of Polar and Non-Polar Metabolism During Wound-Induced Suberization in Potato (*Solanum tuberosum*) tubers.

In preparation for submission to The Plant Cell

Located in Chapter 3, discussed in Chapter 4

Candidate was the first author, who co-designed and conducted ABA and FD treatments on wound-healing potato tissue, isolated the wounded tissue, conducted semi-quantitative RT-PCR and non-polar metabolite analysis. KNW conducted qPCR to repeat tissue-specific expression for publication. YZ conducted the parallel ABA quantification in treated potato tissued. AK repeated the ABA and FD experiment and prepared the polar metabolites for analysis. AB conducted the polar metabolite analysis. MAB evaluated the polar metabolites, supervised the lab work and wrote the manuscript.

Acknowledgements

Firstly, I extend my sincere and utmost gratitude to my supervisor, Dr. Mark Bernards. Your guidance and leadership throughout my Ph.D study created a truly enjoyable environment to work in, and I learned a great deal that far exceeded my field of study.

In addition, I thank my advisory committee, Dr. Denis Maxwell and Dr. Chris Guglielmo. You have both impacted my development as a researcher and provided guidance throughout my degree, for which I am truly grateful. Special thanks to Dr. Maxwell for acting as a reader for my thesis, your thoughtful insights were appreciated. Besides my formal advisors, there were so many other professors who provided guidance throughout my time at Western, including but not limited to Dr. Kathleen Hill, Dr. Susanne Kolhami, Dr. Norm Huner, Dr. Yolanda Morbey, Dr. Sheila Macfie and Dr. Charlie Trick. Thank you for your generosity with your time, it will be remembered.

I also thank my fellow lab mates over the years whom I have had the pleasure of working with, in particular Andrea Neculai, Dr. Dimitre Ivanov, Anica Bjelica, Dr. Yanni Zhang, Dr. Leon Kurepin and Trish Tully. Many hours we spent pondering the world while we worked at our lab benches, and I truly enjoyed the lively and diverse discussions. Also, thank you to all the past and present fellow graduate students on 4th floor NCB and beyond. Thank you for the stimulating and often unpredictable discussions. I will remember the many grad club lunches and laughs we had over the years.

I am very grateful to my parents, Lois and Glenn Hayter, for their incredible support and guidance. As I have grown up I have realized the incredible gifts you gave me, including the solid belief I could achieve whatever I put my mind to and the knowledge that you will always be there to encourage and support me every step of the way. I have not always chosen the conventional path, but you never doubted that I would get there in my own time. I love you both and I am grateful to have you in my life.

Words cannot express the extraordinary gratitude I have for my incredible partner in life, Dave Haggitt. So often I am asked how I balance it all in my life, and the answer is being partnered with you. I have never met another person who approaches the world with such a kindness, generosity and true appreciation for how to fully support others in their goals. Saying that I am lucky to have chosen you as my partner in life is an understatement and, with having spent more than half our lives together already, I can't imagine it any other way. As you have been right alongside me through my entire education, I feel this achievement belongs in part to you. You handled the many, many nights of solo childcare with amazing grace, and I am so thankful for your love and leadership in our family.

Last but definitely not least, my two beautiful little ladies, Taya and Lexi. As you grow up I know you too will have the chance to build a life you love to live, find incredible people to surround yourself from which to learn, and choose follow your passions. I hope I can infuse in you a love of learning as great as mine, so that you may find your own amazing opportunities to explore the world.

Table of Contents

List of Figures

List of Tables

List of Appendices

List of Abbreviations

α	Alpha (first carbon that attaches to a functional group (e.g., carbonyl))
α,ω-dioic acid	Carboxyl groups occupy both the α and ω carbons of the carbon chain
ABA	Abscisic acid
ABA/FD	Abscisic acid and Fluridone treatment simultaneously
ABC	ATP-Binding Cassette transporters
ABCG	ATP-Binding Cassette transporters (subfamily G)
ABRE	ABA-Responsive Element
ACP	Acyl Carrier Protein
ALA	5-Aminolevulinic Acid
ANOVA	Analysis of Variance
*ara*BAD	Arabinose promoter
ASFT	*Arabidopsis* Suberin Feruloyl-CoA Transferase
*At*CYP#A#	*Arabidopsis thaliana* Cytochrome P450 protein belonging to # subfamily (for other genus/species the first two initials will change)
*At*MYB41	*Arabidopsis thaliana* myeloblastosis (MYB) transcription factor 41
*Bam*HI	*Bacillus amyloliquefaciens* type II restriction endonuclease
BLASTn	Basic Local Alignment Search Tool for nucleotides
BLASTp	Basic Local Alignment Search Tool for amino acids (proteins)
BSA	Bovine Serum Albumin
BSTFA	Bis(trimethylsilyl)trifluoroacetamide
bZIP	Basic-domain leucine zipper-type transcription factors
C#	Carbon chain with the number of carbon atoms (e.g., C16 is 16)
cDNA	Complementary DNA
CoA	Coenzyme A
cv	Cultivar of potato
CW	Cell wall
CYP	Cytochrome P450 superfamily of proteins
CYP#A	Cytochrome P450 subfamily nomenclature (e.g., CYP86A)
DDM	n-dodecyl β-D-maltoside
DFCI	Dana-Farber Cancer Institute
dH_2O	Distilled water
DMSO	Dimethyl Sulfoxide
DNA	Deoxyribonucleic acid
dNTPS	Deoxyribonucleic triphosphates
DRE/CRT	Dehydration-Responsive Element/C-Repeat
DTT	Dithiothreitol
ECL	Enhanced Chemiluminescence
EDTA	Ethylenediaminetetraacetic acid
ef1- α	*Elongation Factor 1-alpha* gene
ER	Endoplasmic Reticulum
ESI-TOF-MS	Electrospray Ionization Time-of-Flight Mass Spectrometry
EST	Expressed Sequence Tag

FAωH	Fatty Acid ω-Hydroxylase
FAωH1::TAG	FAωH1 protein with 6X HIS tag
FAωO	Fatty Acid ω-Oxidase
FAE	Fatty Acid Elongase complex
FAMES	Fatty acid methyl esters
FAR	Fatty Acyl-CoA Reductase
FAS	Fatty Acid Synthase
FD	Fluridone
FHT	Feruloyl-CoA Transferase
FID	Flame Ionization Detection
FW	Fresh Weight
GC-FID	Gas Chromatography- Flame Ionization Detection
GC-MS	Gas Chromatography-Mass Spectroscopy
GPAT	Glycerol-3-Phosphate Acyl-CoA Transferase
GUS	B-glucuronidase Reporter gene
horst	Hydroxylase of Root Suberized Tissue
IPTG	Isopropyl β-D-1-thiogalactopyranoside
KAS	Keto-acyl Synthases
KCS	3-Ketoacyl CoA Synthase
LC-MS	Liquid Chromatography Mass Spectroscopy
LCR	LACERATA (CYP86A8)
MEGA	Molecular Evolutionary Genetics Analysis software
MeOH/HCl	Methanolic Hydrochloric acid
MQH_20	Milli-Q Ultrapure Water
MS	Mass Spectrometry
MSMO	Murashige and Skoog basal salts with Minimal Organics
4-MUG	4-methylumbelliferyl-β-D-glucuronide
MYB	Myeloblastosis family of transcription factors
MYC	Mycorhizza binding sites
N_2	Nitrogen
NaCl	Sodium Chloride
NADP	Nicotinamide Adenine Dinucleotide Phosphate (oxidized)
NADPH	Nicotinamide Adenine Dinucleotide Phosphate (reduced)
*Nco*I	*Nocardia corallina* type I restriction endonuclease
ω	Omega (terminal carbon farthest from the functional group)
ω-hydroxy ω-OH	Hydroxylated terminal carbon of the fatty acid chain
P1 or P2	FAωH1 Promoter Allele 1 or FAωH1 Promoter Allele 2
P450	Cytochrome P450 superfamily of proteins
PAL	Phenylalanine Ammonia Lyase
PCA	Principle Component Analysis
PCR	Polymerase Chain Reaction
PGSC	Potato Genome Sequencing Consortium
PLACE	Plant Cis-Acting DNA Elements database
PlantCARE	Plant Cis-Acting Regulatory Elements database

PM	Plasma membrane
qPCR	Quantitative Polymerase Chain Reaction
RACE	Rapid Amplification of cDNA Ends
RCN1	*Reduced Culm Number 1*
RNA	Ribonucleic Acid
RNAi	RNA-interference mediated silencing
RNAseq	RNA Sequencing Data from Potato Genome Sequencing Consortium
RT-PCR	Reverse Transcriptase Polymerase Chain Reaction
*Sal*I	*Streptomyces albus* type I restriction endonuclease
SDS	Sodium Dodecyl Sulfate
SDS-PAGE	Sodium Dodecyl Sulfate Polyacrylamide Gel Electrophoresis
Semi-QT PCR	Semi-Quantitative Reverse Transcriptase Polymerase Chain Reaction
SIF	Suberin-Inducing Factor
St	*Solanum tuberosum*
Taq	*Thermus aquaticus*
TAE	Tris-Acetate-EDTA buffer
TBS	TRIS-Buffered Saline
TC	Tentative Contig
T-DNA	Transfer DNA from tumour-inducing (Ti) plasmid in *Agrobacterium*
TEM	Transmission Electron Microscopy
THT	Tyramine Hydroxycinnamoyl Transferase
Tm	Melting Temperature
TMS	Trimethylsilyl
TRIS	Tris(hydroxymethyl)aminomethane
UDP	Uridylyl
UTR	Untranslated Region
VLCFA	Very long chain fatty acids
WAT11	Yeast strain containing *ATR1* NADPH-cytochrome P450 Reductase from *Arabidopsis thaliana*
WRKY	WRKY family of transcription factors
*Xba*I	*Xanthomonas baldrii* type I restriction endonuclease
3D	Three-dimensional
4-MU	4-methylumbelliferone
4-MUG	4-methylumbelliferyl-β-D-glucuronide

Chapter 1

Suberin Biosynthesis and Regulation in Plants

1.1 Introduction

The sessile nature of plants requires the development of unique strategies to deal with stress. To survive pathogen attack and abiotic stress without the ability to physically remove themselves from these conditions, plants expanded their secondary metabolism to produce unique chemicals to combat these challenges. Suberin biosynthesis is one example of complex plant secondary metabolism used as both a pre-formed defense and induced stress response. By integrating products from two major primary metabolic pathways, phenylpropanoid biosynthesis and fatty acid biosynthesis, plants have developed a complex biopolymer that forms a barrier between their dermal cells and the environment. As the production of suberin utilizes primary metabolism through redirecting the plants' metabolites to form the biopolymer, studying the induction of suberin biosynthesis is challengingas the metabolic pathways involved are intricately linked to common metabolic pathways. To begin to explore the regulation of suberin biosynthesis, the starting point was to identify and characterize a biochemical step unique to suberization. In turn, this knowledge may be used as a stepping-stone to develop an understanding of the complex regulation governing the use of these two major metabolic

pathways, which results in the perfectly timed incorporation of many different metabolites into the suberin biopolymer.

The characterization of suberin biochemistry flourished 35 years ago by using chemical degradation of monomer linkages to determine the chemical composition (Riley and Kolattukudy, 1975; Holloway, 1983). However, research on suberin biosynthesis stalled due to lack of tools available to dissect and understand the biochemical regulation, as most suberin-associated reactions were also involved in other plant processes. With the development of molecular tools over the past 20 years, and the expansion to utilizing previous non-model systems in research, researchers now have the ability to investigate previously unanswerable questions. To begin to understand micro-level regulation of suberin-associated genes, which could provide evidence of macro-level biosynthetic regulation, identifying a unique proxy of suberin biosynthesis was a logical place to start. Focusing on aliphatic metabolism, fatty acids exported from the plastid undergo one of two developmental fates: ω-hydroxylation or elongation followed by further reduction or oxidation (Yang and Bernards, 2006). In potato suberin, ~55% of aliphatic monomers have been reported to undergo ω-hydroxylation, a rare biochemical step involved in the production of only two other spatially separate plant biopolymers: cutin and sporopollenin (Holloway 1983, Yang and Bernards, 2006). Thus, the identification and characterization of a suberin-associated ω-hydroxylase in the potato model system was the starting point to begin to explore both micro- and macro-regulation of suberization.

Plant cells require a cell wall exterior to their plasma membrane for structural integrity and to control plant morphology (Cosgrove, 2005). The primary cell wall is

composed of three main polysaccharides: cellulose, hemicellulose and pectin, as well as a lesser amount of protein (Cosgrove and Jarvis, 2012). Cellulose fibrils provide mechanical strength and are embedded in the matrix created from hemicellulose (Keegstra, 2010) and pectins (Harholt et al., 2010). The structurally sound nature of the primary cell wall is complemented by its porosity for water and ion passage, allowing both uptake and passage to adjoining plant cells (Brett and Waldron, 1996). Due to its proximity to the external environment, the primary cell wall has also become a site of many interior and exterior modifications by secondary metabolites in response to abiotic and biotic stresses. Synthesis and deposition of unique plant biopolymers internally or externally of the cell wall allows further protection against pathogens, dehydration and other environmental factors (Ranathunge et al., 2011).

1.2 Plant Environment Interfaces

The outermost physical boundary that separates a plant from its surroundings is predominately composed of lipids. In the green aerial parts of the plant, cutin and cuticular waxes are laid down exterior to the epidermal cell wall (Schreiber, 2010); in the flower anthers, sporopollenin and waxes are deposited on the outer pollen exine wall (Ariizumi and Toriyama, 2011); and in the periderm and underground organs, suberin and suberin-associated waxes are formed interior to the cell wall (Schreiber, 2010; Li-Beisson, 2011). Due to their hydrophobic nature, these three biopolymers function to protect the plant from water loss and pathogen attack (Kolattukudy et al., 1976; Bernards 2002). Two main criteria differentiate cutin, sporopollenin and suberin: 1) sites of

deposition, and 2) presence of poly-phenolic domain associated with the primary cell wall (Bernards, 2002; Heredia, 2003; Schreiber, 2010).

Cutin is a biopolymer that forms a continuous layer over the epidermal cells in aerial plant organs including stems, fruits and leaves. The main function of cutin is to prevent dehydration (Samuels et al., 2008), and it is generally composed of shorter chain ω-hydroxy and mid-chain epoxy fatty acids as well as glycerol (Baker and Holloway, 1970; Walton, 1990; Pollard et al., 2008). Cutin is integrated into the exterior portion of the cell wall creating a polymerized macromolecule impregnated with soluble waxes that are resistant to degradation. Differential deposition and composition of epicuticular wax components as a film or crystals may create a topographical barrier to insects by creating ridges or furrows on the plant surface (Baker, 1982; Eigenbrode and Jetter, 2002).

Sporopollenin forms the tough outer walls of pollen, called the exine, and prevents dehydration of the spore and protection from environmental stress (Kim and Douglas, 2013). Composed of modified aliphatic and phenolic components, including long-chain (>C18) fatty acids as well as phenylpropanoids, sporopollenin is structurally similar to suberin (Wilmesmeier and Wiermann, 1995). Sporopollenin differs from suberin as it is deposited externally to the cellulose/pectin intine wall whereas suberin is deposited interior to the cell wall (Bohne et al., 2003).

Suberin is a complex plant biopolymer deposited between the cell wall and plasma membrane in response to developmental or environmental signals (e.g., dehydration, wounding). Functioning to prevent water loss and pathogen attack (Kolattukudy, 2001), suberin is deposited to varying degrees based on the environmental stimuli perceived by

the plant (Pozuelo et al., 1984; Franke and Schreiber, 2007). Suberin is deposited in a developmentally-regulated manner in only a few cell types or locations, including endodermal and hypodermal cells of the roots (Bonnet, 1968; Peterson et al., 1982), bundle sheath cells of the mesophyll (O'Brien and Kuo, 1975), chalazal region of the seed coat (Franke et al., 2009), floral abscission zones (van Doorn and Stead, 1997), dermal cells of the underground tissues (Espelie et al., 1980), and cork cells of the periderm tissue (Holloway, 1983). Depending on the cell type and location, suberin can be deposited in one of three distinctive manners: as nonlamellar or diffuse suberin, as a Casparian band, or as lamellar suberin. First, nonlamellar or diffuse suberin is deposited in epidermal cells and is characterized by faint bands throughout the cell walls (Peterson et al., 1978). Second, the Casparian band is a developmental deposition in the radial and tangential cell walls of hypodermal and endodermal root cells (Peterson et al., 1978), and functions to create an apoplastic barrier to ion and water flow (Schreiber et al., 1999). Finally, a continuous lamellae layer interior to the primary cell wall, known as suberin lamellae, can be formed in maturing cells in a variety of tissues throughout the plant. Suberin lamellae are characterized by the appearance in transmission electron microscope (TEM) sections of alternating light and dark bands exterior to the plasma membrane (Sitte, 1962). Suberin lamellae surround the entire cell to create an effective diffusion barrier to water and ion passage (Schreiber et al., 2005). Although developmentally specific to a few cell types in the plant, any cell type in response to wounding is capable of producing suberin lamellae in the cells adjacent to a wound site (Kolattukudy, 2001).

The macromolecule of suberin is composed of two domains, a poly-phenolic and a poly-aliphatic, deposited in a specific temporal and spatial pattern (reviewed in Bernards, 2002). First, the poly-phenolic domain is synthesized through up-regulation of phenylpropanoid metabolism (Bernards et al., 1995), and is primarily composed of oxidatively cross-linked hydroxycinnamic acids and their derivatives (including amides and hydroxycinnamoyl alcohols) (Arrieta-Baez and Stark, 2006). As phenolic compounds have anti-microbial properties, it is speculated that these play a role in pathogen resistance (Lulai and Corsini, 1998; Wang et al., 2011). Although the mechanism of transport for these phenolic monomers to the primary cell wall remains unknown, they are subsequently covalently linked to the polysaccharides of the primary cell wall, effectively anchoring the biopolymer interior to the cell wall (Yan and Stark, 2000, Mattenin et al., 2009).

Subsequent to incorporation of the phenolic domain, the synthesis of the poly-aliphatic domain occurs through up-regulation of fatty acid biosynthesis in the plastid. The C16 and C18 fatty acids produced in the plastid (mainly C18) have one of two developmental fates. Yang and Bernards (2006) used carbon flux analysis to show that over 50% of C18 fatty acids are desaturated prior to leaving the plastid and are subsequently oxidized to ω-hydroxylated and α,ω dioic fatty acids. Those fatty acids that were exported from the plastid without desaturation were further elongated to very long chain fatty acids (VLCFA), and either accumulated as free acids, were reduced to primary alcohols or oxidized to n-alkanes (Yang and Bernards, 2006). Subsequently these fatty acids and modified fatty acids are transported to the primary cell wall, where the

phenolics have already been incorporated, and are attached to the phenolic domain (Graça and Santos, 2007). Predominately composed of ω-hydroxy fatty acids and α, ω-dioic acids, the aliphatic domain is a complex matrix bridged by functional groups with ester linkages to glycerol (Moire et al., 1999; Graça and Pereira, 2000; Graça, 2015). In addition to the cross-linked biopolymer, suberin-associated waxes impregnate the aliphatic domain, and consist of long-chain alkanes, alcohols, acids and alkyl ferulates (Kolattukudy et al., 1976; Yang and Bernards, 2006; Schreiber, 2010). These waxes are present in all suberized cells at the plant-environment interface and provide an important barrier to water diffusion (Soliday et al., 1979; Vogt et al., 1983; Schreiber et al., 2005). In combination, the two domains of suberin build a barrier both impermeable to water and resistant to pathogen attack.

Observation of suberin lamellae under TEM creates a striking pattern of alternating light and dark bands (e.g., Serra et al., 2010). Soliday et al. (1979) showed that the inhibition of wax biosynthesis by a fatty acid chain elongation inhibitor resulted in loss of the light band formation. This result indicated that the light bands are most likely composed of suberin-associated waxes, but no direct evidence has been uncovered to support this. Bernards (2002) presented a hypothetical model for the 3D structure of suberin, which suggested that the characteristic TEM alternating light and dark banding pattern of suberin lamellae may be due to the alternating deposition of aliphatic monomers joined by ferulate esters. In loss of function *cyp86a1* (the *Arabidopsis* suberin-associated fatty acid ω-hydroxylase) mutants, the characteristic TEM banding pattern is disrupted (Molina et al., 2009; Serra et al., 2009a). However, both Molina et al. (2009)

and Serra et al. (2010) showed the classic lamellar structure of suberin remained intact with a feruloyl transferase knockdown in *Arabidopsis*, which resulted in a dramatic decrease in ferulate and thus an inability to form the ferulate esters to crosslink the two domains as was hypothesized by Bernards (2002). Recently, Graça et al. (2015) performed a partial depolymerization of the suberin biopolymer identifying two key linkages: a glycerol-α,ω dioic acid-glycerol as the core of the polymer, and a glycerol-ω-hydroxy fatty acid-ferulic acid anchoring the edge of the poly-aliphatics to the poly-phenolics. Further evidence that the glycerol-α,ω dioic acid-glycerol linkage is critical for the lamellar structure was apparent in *cyp86a33* knockdowns as they had significantly impaired monomer production and acylglycerol structure formation (Graça et al., 2015). Graça et al. (2015) now hypothesize that the glycerol- α,ω dioic acid-glycerol linkage may be responsible for the alternating light and dark bands in TEM images, which does not take into account the original wax observations by Soliday et al. (1979). Therefore, due to technical challenges of isolating intact suberin lamellae, the current understanding of suberin ultrastructure remains under debate and is constantly evolving, as new evidence continues to advance our understanding of this complex biopolymer.

1.3 Model Systems for Studying Suberin Biosynthesis

During the past 40 years, three plant systems have been explored to further our understanding of suberin formation. The first species, *Quercus suber* (cork oak), was utilized as it contains a large amount of the suberin biopolymer in cork cells, which form the outer tree bark. However, the long generation time and difficulty administering radiolabeled isotopes for studying suberin biochemistry make this species unattractive as

a model organism. The second species, *Solanum tuberosum*, emerged as an excellent model system, as potato tubers form large quantities of suberized tissue in response to wounding, creating an inducible system for the study of suberin (Kolattukudy, 1984). However, lack of genetic tools available for this species as well as a lengthy time period required for plant regeneration following *Agrobacterium tumefaciens* transformation led researchers to look for a more suitable genetic model system. This led to the examination of a third species, *Arabidopsis thaliana*, which has ample genetic resources and techniques to accelerate the study of cutin and suberin regulation (Ranathunge et al., 2011). Understanding of the genetic regulation of these biopolymers has been accelerated using reverse genetics to identify mutant phenotypes (e.g., Wellesen et al., 2001; Bonaventure et al., 2004; Xiao et al., 2004; Beisson et al., 2007; Lee et al., 2009). The characterization of cutin- and suberin-associated genes has advanced quickly in the past few years with the plethora of molecular tools available in *Arabidopsis*, such as microarrays and large-scale T-DNA insertion lines, as well as the ease to which plant transformation can occur to produce RNAi knockdowns (RNA-interference mediated silencing) (e.g., Hofer et al., 2008; Molina et al., 2009; Serra et al., 2009a, 2009b, 2010; Domergue et al., 2010). However, the small plant size of *Arabidopsis* limits the production of suberin, as it restricts both the surface area available for wounding and quantity of developmental deposition. Thus, due to the limitations with using *Arabidopsis* as the suberin model system, the research focus has shifted back to potato, especially with the release of the diploid *Solanum tuberosum* group Phureja genomic sequence (http://www.potatogenome.net/; known in this thesis as Phureja genome). This has created a unique opportunity to utilize newly developed genetic tools with proven

biochemical methods to advance the study of suberin formation, regulation and deposition.

1.4 Biosynthesis of Suberin Aliphatic Monomers

Determining the composition of the polyaliphatics using solvent extraction and depolymerization techniques has led to the development of a logical biochemical sequence required to produce these monomers (Figure 1.1), which has been used to identify key research targets.

1.4.1 *Fatty Acid Biosynthesis and Desaturation*

Fatty acid biosynthesis occurs in the plastid using a multi-subunit enzyme complex called Fatty Acid Synthase (FAS). For suberin biosynthesis, pyruvate maintains a transient pool of plastidial acetyl-Coenzyme A (CoA) that is utilized to drive fatty acid biosynthesis by: 1) conversion to malonyl-CoA, and 2) formation of bicarbonate by acetyl-CoA carboxylase (Rawsthorne, 2002). Subsequently, the malonyl group of malonyl-CoA is transferred to Acyl Carrier Protein (ACP), which provides the two-carbon unit at each step of elongation through the FAS cycle. Keto-acyl synthases (KAS) catalyze the condensation reactions of malonyl-ACP to the acetyl-CoA backbone, producing C16 or C18 fatty acids (Ohlrogge and Jaworski, 1997). While C16:0-ACP is immediately released from the FAS complex, a large portion of C18:0-ACP is desaturated to C18:1-ACP at position 9 prior to release (Ohlrogge and Jaworski, 1997). ACP is cleaved from the fatty acids by a plastid-localized thioesterase resulting in free fatty acids

for transport. Subsequently, both C16:0 and C18:1 are exported to the cytoplasm where they are activated to CoA esters and have one of two developmental fates, participating in oxidation or elongation reactions (Yang and Bernards, 2006; Li-Beisson et al., 2013).

1.4.2 *ω-Hydroxylation and Subsequent Oxidation*

C16 and C18:1 fatty acid-CoA esters in the cytoplasm are transported to the endoplasmic reticulum (ER) membrane to be ω-hydroxylated. In potato, ω-hydroxylation is a critical reaction as the majority of aliphatic monomers are oxidized to produce ω-hydroxy acids or α, ω-dioic acids (Holloway, 1983; Yang and Bernards, 2006). Five plant

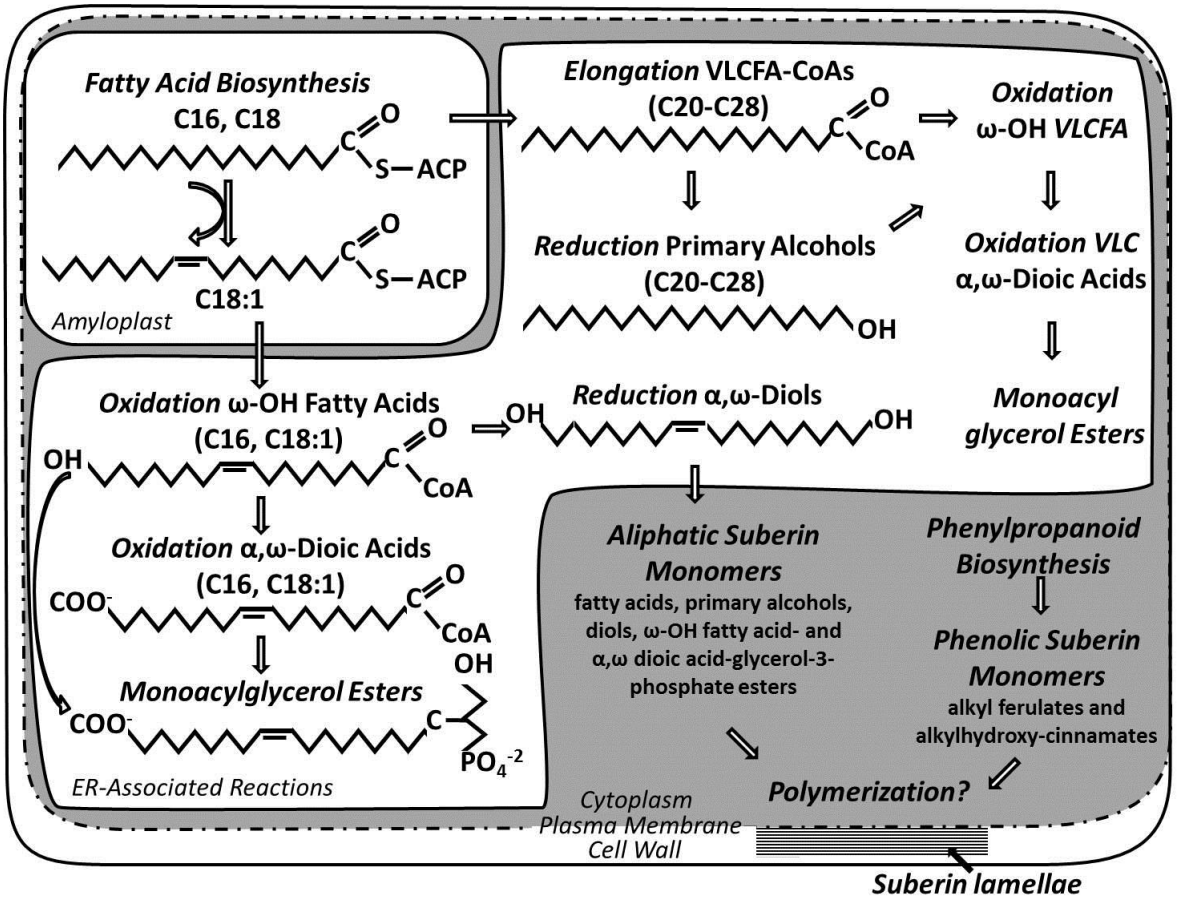

Figure 1.1: Wound-Induced Suberin Biosynthesis in Potato Tubers
Overview of the fatty acid and phenylpropanoid metabolism resulting in suberin monomer production for polymerization into the suberin lamellae. In the plastid (amyloplast), C16 and C18 fatty acids are produced through fatty acid biosynthesis. These fatty acids have two possible developmental fates. First, C16 and C18 fatty acids may be exported to the endoplasmic reticulum (ER) for elongation into VLCFAs, which may be further oxidized or reduced (see top right of figure). In potato, the majority of VLCFAs are C22-C28, with low levels of C16-C20 present in suberin. Second, C18 fatty acids are desaturated to C18:1 in the plastid, which are then exported to the ER where they are oxidized to produce ω-OH fatty acids or α,ω-dioic acids (see bottom left of figure). All modified fatty acids are subsequently exported from the ER to the cytoplasm, where they are incorporated into suberin lamellae with glycerol and the alkyl ferulates and alkyl hydroxycinnamates produced through phenylpropanoid biosynthesis. Suberin lamellae are deposited at the plasma membrane, internal to the primary cell wall. This figure is based on data from Yang and Bernards (2006) and Vishwanath et al., 2015.

Cytochrome P450 monooxygenase subfamilies have been identified to catalyze fatty acid ω-hydroxylation: *CYP86A*, *CYP86B*, *CYP94A* and *CYP77A* and *CYP704B*. CYP monooxygenases of these subfamilies are able to activate molecular O_2 (Werck-Reichhart et al., 2002) and insert one of its O atoms onto the terminal carbon of a fatty acid to produce an alcohol group, which can be further oxidized to a carboxylic acid (Figure 1.2). The second O atom is reduced to water by a CYP450 NADPH reductase, which avoids peroxide production.

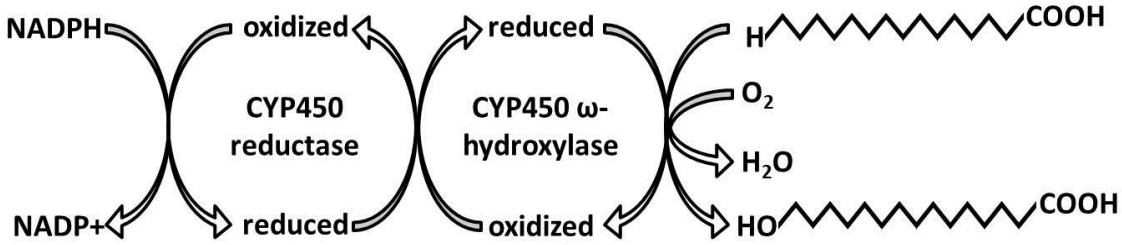

Figure 1.2: CYP450 ω-Hydroxylation of C16 Palmitate.
Simplified view of fatty acid ω-hydroxylation with CYP450 proteins. The incorporation of oxygen (O) into the terminal carbon of the fatty acid requires a CYP450 ω-hydroxylase and a CYP450 NADPH reductase to provide the necessary proton (H^+) and electrons for the generation of water (H_2O).

1.4.3 *Elongation and Further Modification*

Elongation of the C16:0 or C18:1 fatty acyl-CoAs occurs by the addition of two-carbon units by the Fatty Acid Elongase complex (FAE) on the ER (Lee et al., 2009). Similar to fatty acid synthesis, fatty acid elongation occurs through a series of four reactions: condensation, reduction, dehydration and reduction. The condensation reaction is catalyzed by a 3-ketoacyl CoA synthase (KCS), which attach two carbon moieties from malonyl-CoA to the fatty acid-CoA. As suberin and cutin waxes may range from C20-

C32, multiple rounds of fatty acid elongation are required on the same substrate (Kunst and Samuels, 2003). KCS mutants from both *Arabidopsis* (*KCS2*/*DAISY* (Franke et al., 2009; Lee et al., 2009); *KCS9* (Kim et al., 2013) and *KCS20* (Lee et al., 2009) and potato (*KCS6,* Serra et al., 2009b) have reduced accumulation of VLCFAs and their derivatives during cutin and suberin deposition. Once elongated to the desired chain length, VLCFA may enter an acyl reduction pathway to produce primary alcohols (fatty acyl-CoA reductases; *At*FAR1, 4, and 5; Domergue et al., 2010, Vishwanath et al., 2013) and wax esters; or a decarbonylation pathway to form aldehydes, alkanes, secondary alcohols, and/or ketones (Kunst and Samuels, 2003).

1.4.4 *Other Suberin Biosynthetic Reactions*

Glycerol's role in linking acyl monomers together to produce a 3D cross-linked biopolymer was recently verified through partial suberin aliphatic depolymerization, which showed that 90% of all esterified monomers were acylglycerols in wild type potatoes (Graça et al., 2015) (Figure 1.3). However, the role of glycerol in crosslinking monomers was first conceived from potato periderm studies 15 years earlier. Moire et al. (1999) first documented a positive correlation between esterified glycerol monomers and suberin-associated α, ω dioic acids, followed by Graça and Pereira (2000a) characterizing monoacylglycerol esters of ω-hydroxy, α,ω dioic acids as well as alkanoic acids. Together with the evidence for acyl-CoA incorporation into *Vicia faba* cutin (Croteau and Kolattukudy, 1974), these studies suggested a role for glycerol-3-phosphate acyl-CoA transferases (GPATs) in producing the building blocks for suberin. GPAT5 was identified

in *Arabidopsis* as a suberin-associated glycerol-3-phosphate acyltransferase, conjugating glycerol-3-phosphate at the *sn*-2 position with acyl-CoAs or acyl-ACPs (Beisson et al.,

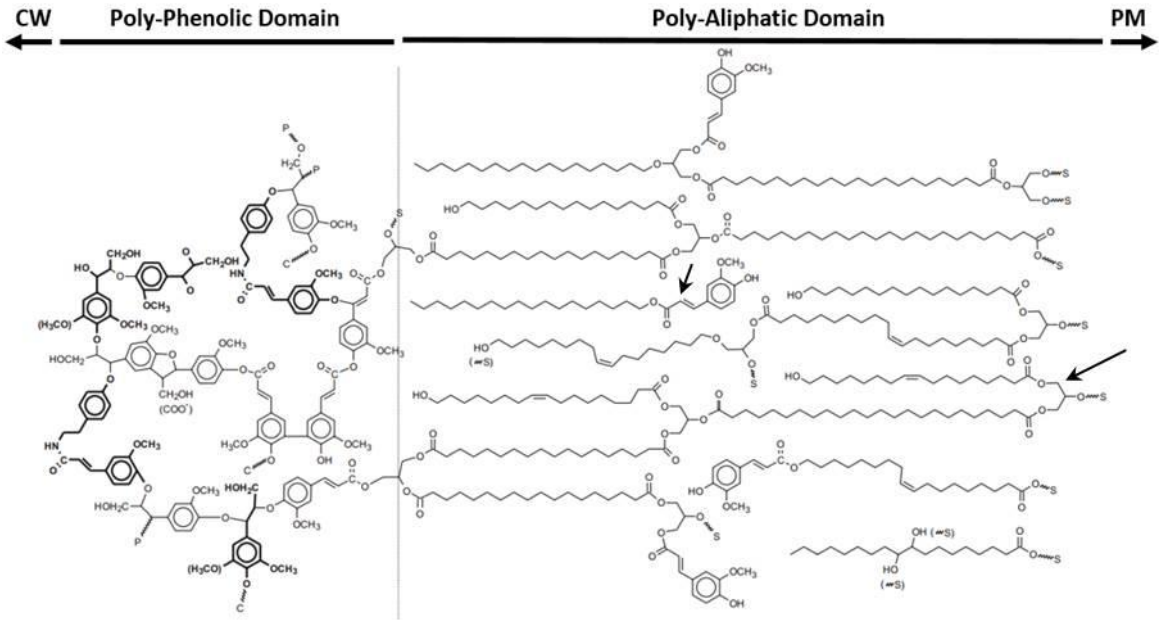

Figure 1.3: Hypothetical Model of Suberin Macromolecular Structure.
Suberin lamellae are deposited exterior to the plasma membrane but interior to the primary cell wall. Covalently-linked to the interior of primary cell wall is a poly-phenolic domain, composed of hydroxycinnamic acids and derivatives (left domain shown above), which is linked to a poly-aliphatic domain (right domain shown above). The poly-aliphatic domain is predominately fatty acids, alkanes, alcohols and ω-hydroxylated fatty acids esterified through functional groups to glycerol (long black arrow) and ferulic acid (ferulate esters, short black arrow), forming a cross-linked matrix. CW, cell wall; PM, plasma membrane. Modified figure from Bernards, 2002.

2007; Li et al., 2007a, b; Yang et al., 2010; 2012). *gpat5* mutants had a 50% reduction in aliphatic suberin and were shown to act synergistically with fatty acid ω-hydroxylases, providing the acyl-glycerol building blocks for suberin biosynthesis (Beisson et al., 2007; Li et al., 2007b).

In addition to production of acylglycerols for incorporation, ω-hydroxyfatty acids and alcohols are esterified to ferulic acid to produce ferulate esters (Figure 1.3), a reaction

catalyzed by feruloyl-CoA transferases (AFST (Kosma et al., 2012 or FHT (Molina et al., 2009; Serra et al., 2010). The potato *fht* mutant greatly reduced alkyl ferulates as well as ω-hydroxylated fatty acids and primary alcohols incorporated into the periderm (Serra et al., 2010).

1.4.5 *Suberin Monomer Transport and Incorporation*

Suberin production is tightly regulated in both a spatial and temporal manner, with wounding initiating a global reorganization of metabolism (Yang and Bernards, 2007). Using Principle Component Analysis (PCA), which is a statistical procedure to create two-dimensions to delineate changes in the metabolome, Yang and Bernards (2007) distinguished shifts in polar and non-polar metabolism throughout the closing layer formation post-wounding. Throughout the first two days post-wounding, the pool of polar metabolites shifts from the predominately sugars, amino acids and organic acids to include suberin-associated phenolics such as ferulic acid. The suberin-associated phenolic monomers produced are anchored to carbohydrates within the cell wall (Mattenin et al., 2009) through ether and carbon-carbon linkages (Yan and Stark, 2000). Once the phenolic domain is attached to the cell wall, it continues to develop towards the plasma membrane through ether bonds between functional groups of the phenolic monomers. After the third day post-wounding, polar metabolism stabilized and remained fairly uniform throughout the remaining closing layer formation. At the same time as polar metabolism stabilizes, the non-polar metabolism begins to change. During days 3 and 4 post-wounding suberin-associated short-chain aliphatics such as C16:0 and C18:1

monomers began to accumulate, which is caused by a shift in non-polar metabolite biosynthesis. A second shift occurs in the later stages of closing layer formation over the wound site, from days 5 to 7 post-wounding, as longer chain aliphatics are being produced for deposition into the suberin macromolecule. Integration of the aliphatic monomers progresses towards the plasma membrane, building a complex matrix of monomers esterified together using glycerol as a bridge (Graça and Pereira, 2000; Graça et al., 2015). In addition, deposited throughout both domains of the suberin biopolymer are the unlinked fatty acids, fatty alcohols and feruloyls that form the soluble waxes.

Metabolic profiling of potato suberin has shown no accumulation in the soluble pool of ω-hydroxy fatty acids and α,ω-dioic acids from days 3 to 7 post-wounding, indicating these monomers are either incorporated in the macromolecule at the rate of production or are shuttled from the site of production to incorporation in a modified form (Yang and Bernards, 2006). Evidence for the process of secreting and assembling precursors has come from two different types of mutants: glycosyltransferase and ATP-binding cassette (ABC) transporters.

In the *ugt80B1* mutant, a UDP-glucose:sterol glycosyltransferase, there is a strong reduction in seed polyester monomers including fatty acids, ω-hydroxylated fatty acids, α,ω-dioic acids and ferulate (DeBolt et al., 2009). Interestingly, TEM showed a lack of suberin lamellae but an accumulation of electron-dense bodies in the cytoplasm, which may be representing the aliphatic precursors (DeBolt et al., 2009). Thus, lipid polyester precursor export or trafficking to the apoplast may involve steroyl glycosides in plant

seeds, which may also be true for other sites of suberin deposition (Ranathunge et al., 2011).

With respect to the role of plasma membrane-associated ABCG transporters, three recent studies have confirmed a strong role in suberin monomer transport for assembly of the macromolecule. *RCN1*, an ABCG transporter, is normally expressed in *Oryza sativa* (rice) root cells that undergo developmental suberin deposition. In the *rcn1* mutant, C28 and C30 aliphatic monomers were greatly reduced resulting in an impaired apoplastic barrier formation during suberization (Shiono et al., 2014). *ABCG1* from potato is normally expressed in roots and tuber periderm, while the RNA*i*-silenced *abcg1* mutant produced morphologically disorganized cell layers with the accumulation of suberin precursors in the periderm (Landgraf et al., 2014). Characterization of a small clade of three *Arabidopsis abcg* mutants revealed that they lacked proper suberin formation in the roots and seed coats resulting in increased permeability and altered suberin lamellae structure (Yadav et al., 2014). Therefore, *ABCG* transporters are required to export suberin components across the plasma membrane for proper assembly of the suberin macromolecule.

1.5 Cytochrome P450 Monooxygenases

The cytochrome P450 superfamily of proteins, knowns as CYPs, consists of functionally conserved proteins that have as little as 20% sequence identity. Found in all organisms, the P450 reaction relies on the activation of molecular oxygen with insertion of one atom of oxygen into the substrate while reducing the other to form water (Figure

1.2; Mansuy, 1998). As one of the largest protein families in plants, CYPs can catalyze a wide variety of reactions having either broad and narrow substrate specificities, and are thought to have expanded through gene duplication for adaption to harsh environments or protection from pests and pathogens (Werck-Reichhart et al., 2002).

In the late 1970's, Kolattukudy's group characterized the ω-hydroxylation reactions of suberin and cutin formation using *Vicia faba* ER-microsomal protein preparations (Soliday and Kolattukudy, 1977) and suberizing potato tuber tissue (Agrawal and Kolattukudy, 1977, 1978; Soliday and Kolattukudy, 1978). Since this research, five plant CYP subfamilies have been identified to catalyze the ω-hydroxylation of fatty acids: *CYP86A*, *CYP86B*, *CYP94A*, *CYP77A* and *CYP704B*. These five subfamilies are capable of fatty acid ω-hydroxylation with different chain length specificity, while CYP94As can also catalyze subsequent oxidation steps leading to a terminal carboxyl group (Le Bouquin et al., 2001). During the past 15 years, suberin- or cutin-associated ω-hydroxylases have been characterized in three of the four subfamilies, providing ideal targets for further study of biosynthetic regulation.

Forty years ago, Kolattukudy's research group elucidated the biochemical steps required to produce ω-hydroxylated fatty acids or α, ω-dioic acids for suberin (Agrawal and Kolattukudy 1977, 1978a, 1978b; Soliday and Kolattukudy, 1977). However, due to the difficult nature of extracting and characterizing membrane proteins, it took the development of molecular tools before suberin-associated ω-hydroxylases received further study. With the use of genomics tools in the past 20 years, ω-hydroxylases have been identified and functionally characterized in *Arabidopsis* (Tijet et al., 1998; Hofer et

al., 2008; Compagnon et al., 2009; Dobritsa et al., 2009), *Nicotiana tabacum* (Le Bouquin et al., 2001), *Vicia sativa* (Pinot et al., 1998, 1999, 2000; Le Bouquin et al., 1999; Kahn et al., 2001; Benveniste et al., 2005), *Petunia hybrid* (Han et al., 2010) and *Solanum tuberosum* (Serra et al., 2009a; Grausem et al., 2014). In addition, larger scale studies have begun to elucidate the breadth of mechanisms involved in suberin biosynthesis including a microarray study for cork oak (Soler et al., 2007), expression studies using RNAi knockdowns and metabolite analysis (Compagnon et al., 2009; Molina et al., 2009; Serra et al., 2009a), a carbon flux analysis of suberin-associated aliphatic metabolism (Yang and Bernards, 2006), and a metabolomics investigation of phenolic and aliphatic metabolism (Yang and Bernards, 2007). However, limited *in vitro* functional characterization of many suberin-associated ω-hydroxylases as well as a general lack of investigation into their regulation has been completed to date.

1.5.1 *CYP86A ω-Hydroxylases*

CYP86A fatty acid ω-hydroxylases were initially characterized in *Arabidopsis* while investigating their role in cutin biosynthesis (Benveniste et al., 1998; Wellesen et al., 2001). Five *CYP86A* ω-hydroxylases were identified in the *Arabidopsis* genome, with *AtCYP86A1* expressed in the roots and the remaining four (*CYP86A2*, *CYP86A4*, *CYP86A7* and *CYP86A8*) expressed in green tissues where the cuticle is present (Duan and Schuler, 2005). Functional characterization of these CYP86As showed conversion of saturated C12 to C16 and unsaturated C18 fatty acids into ω-hydroxy fatty acids using an *in vitro* radioactivity assay, with palmitate (C16) being the preferred substrate

(Benveniste et al., 1998; Wellesen et al., 2001). To date, a range of other *CYP86A* subfamilies members have been characterized through T-DNA knockdowns and RNAi mutants, but no further work has been done to explore the substrate range or specificity of these proteins due to the problematic nature of CYP *in vitro* protein expression.

In 2007, the first indication that *CYP86A1* was involved in suberin biosynthesis came from a transcriptome analysis of cork oak that identified a *CYP86A1*-homolog to be associated with suberin deposition (Soler et al., 2007). Subsequently, *CYP86A1* T-DNA insertion mutants in *Arabidopsis* explored the *in vivo* role of this ω-hydroxylase. The *CYP86A1* knockdown mutants had decreased deposition of total aliphatic suberin, specifically fewer C16 and C18 ω-hydroxy and α,ω-dioic acids (Hofer et al., 2008). In addition, ectopic co-expression of *CYP86A1* and *GPAT5* resulted in an 80% increase in total aliphatics, as well as the novel appearance of suberin-associated C20 and C22 ω-hydroxy and α,ω-dioic acids in *Arabidopsis* leaves and stems (Li et al., 2007). Finally, a potato homolog *CYP86A33* was identified and characterized using RNAi; it had a 60% decrease in aliphatic suberin primarily resulting from reduction in C18:1 ω-hydroxy and α,ω-dioic acids (Serra et al., 2009a). *CYP86A33* down-regulation also significantly increased periderm water permeability and changed the characteristic suberin lamellae organization, resulting in a lack of alternating light and dark bands (Serra et al., 2009a).

1.5.2 *CYP86B ω-Hydroxylases*

The *CYP86B* subfamily shares 45% identity with the *CYP86A* subfamily, with two *Arabidopsis* members *CYP86B1* and *CYP86B2* identified through *in silico* data mining.

Evidence of *CYP86B1* being co-expressed with suberin biosynthetic genes led to the characterization of *cyp86b1* T-DNA insertion and RNAi knockdown mutants (Compagnon et al., 2009). Although total aliphatics remained approximately equal between the wild-type and mutant lines, a strong reduction in C22 and C24 ω-hydroxy and α,ω-dioic acids as well as a corresponding increase in saturated C22 and C24 fatty acids occurred (Compagnon et al., 2009). Interestingly, there was no effect on C16 or C18:1 ω-hydroxylation, indicating chain-length substrate specificity between the CYP86A1 and CYP86B1. In contrast to *cyp86a1*, there were no detectable morphological changes or physiological phenotype with regards to ion content or salt permeability associated with *cyp86b1* (Compagnon et al., 2009).

1.5.3 *CYP94A ω-Hydroxylases and ω-Oxidases*

The CYP94A subfamily is a diverse, it is not only capable of ω-hydroxylation, as is the case for CYP86A and CYP86B, but can also catalyze subsequent oxidation steps leading to α,ω-dioic acids by producing a terminal carboxyl group. The first characterized protein was CYP94A1 from *Vicia sativa*, which showed *in vitro* ω-hydroxylation of saturated C10 to C16 and unsaturated C18 fatty acids (Tijet et al., 1998). In the context of cutin and suberin biosynthesis, it is important to note that CYP94A1 had a low K_m value for palmitate, which is a major cutin and suberin monomer precursor (Tijet et al., 1998). Further investigations into CYP94A1 substrate range showed it could also ω-hydroxylate epoxy- and midchain-hydroxy fatty acids (Pinot et al., 1999), which although absent in potato suberin are formed in many species including cork oak suberin (Holloway, 1983).

A second ω-hydroxylase from *Vicia sativa*, CYP94A2, was also characterized *in vitro*, it had showed shorter chain length specificity from saturated C12 to C16 where C14 (myristate) was the preferred substrate (Le Bouquin et al., 1999).

Evidence of ω-oxidase activity came from characterization of CYP94A5 from tobacco, which was able to ω-hydroxylate C12 to C18 saturated and unsaturated fatty acids as well as C18 mid-chain epoxy fatty acids (Le Bouquin et al., 2001). Furthermore, increasing the incubation time for 9,10-epoxystearic acid led to the formation of 9,10-epoxy-α,ω-octadecanoic acid, which was the first *in vitro* demonstration of a plant enzyme catalyzing the complete oxidation of a fatty acid (Le Bouquin et al., 2001). However, not all plant species that generate α,ω-dioic acids contain *CYP94A* subfamily members (including *Arabidopsis*), indicating it cannot be the sole plant ω-oxidase subfamily.

1.5.4 *CYP77A ω-Hydroxylases*

CYP77A is the most recently identified subfamily of ω-hydroxylases, which have been shown *in vitro* to ω-hydroxylate fatty acids ranging from C12 to C18 in potato (Grausem et al., 2014). Two potato homologs, CYP77A19 and CYP77A20 were expressed in both cutinizing and suberizing tissue, including apical buds, young leaves, stolons, wounded tubers and developing microtubers (Grausem et al., 2014). In addition, CYP77A19 was induced 1 hour post-treatment with jasmonic acid, indicating it may be a part of biotic stress response as well. Previously characterized members of the CYP77A subfamily from *Arabidopsis*, CYP77A4 (Sauveplane et al., 2009) and CYP77A6 (Li-

Beisson et al., 2009), both catalyzed in-chain fatty acid hydroxylation with CYP77A4 also catalyzing epoxidation. While CYP77A6 has been shown to play a role in cutin synthesis, the physiological role of CYP77A4 is unknown. However, it is worth noting that suberized potato tissue does not contain epoxides, and these fatty acid modifications are unique to cutinized tissues.

1.5.5 *CYP704B ω-Hydroxylases*

CYP704B is a relatively newly characterized ω-hydroxylase subfamily, with gene expression restricted to anthers. CYP704B1 (*Arabidopsis*; Dobritsa et al., 2009) and CYP704B2 (*Oryza sativa*; Li et al., 2010) can ω-hydroxylate C16 and C18 fatty acids *in vitro*). Due to the floral expression pattern, *CYP704B* subfamily is likely active primarily in sporopollenin biosynthesis (Wiermann et al., 2005, Dobritsa et al., 2009). As this is a small gene family with only one member in the *Arabidopsis* and *Oryza sativa* genomes, it is likely that its role in the potato plant is restricted to production of the pollen exine biopolymer.

1.6 Regulation and Biosynthesis of Suberin

Due to the sessile nature of plants, they have evolved dynamic responses to injury using secondary metabolites to seal and protect their tissues from invading organisms. In dicot plants, the development of suberin in the existing cells at a wound site is closely followed by the formation of a new phellogen (cork cambium), which initiates cell division and development of the wound periderm (Neubauer et al., 2012). Once the

phellogen is formed, it proceeds to divide outwardly to produce rectangular files of suberizing phellem (cork cells) and inwardly to produce phelloderm. Once adequate numbers of cells have been produced, the phellogen becomes non-meristematic and wound periderm formation is complete (Lulai and Freeman, 2001).

The complex regulation of wound-induced suberin deposition is difficult to determine due to the vast array of biological processes activated by wounding. The first *Arabidopsis* cutin-associated transcription factor, AtMYB41, was identified through ectopic expression that resulted in a malformed cuticle (Cominelli et al., 2008). Upon further evaluation using TEM, Kosma et al. (2014) identified lamellae formation in aerial epidermal walls strongly resembling typical suberin lamellae. Biochemical analysis identified both cutin and suberin-associated monomers, with more than 4.5 times the suberin monomers relative to cutin. Due to the complexity of coordinating gene expression, transport and polymerization to form lamellae, AtMYB41 is likely part of the regulatory network that controls suberin formation under stress conditions (Kosma et al., 2014). Recently, a second wound-responsive transcription factor belonging to the WRKY protein family was characterized in potato, with ectopic expression increasing deposition of hydroxycinnamic acid amides associated with the suberin phenolic domain (Yogendra et al., 2015). Direct binding of *St*WRKY1 to promoters was demonstrated with 4-coumarate:CoA ligase and Tyramine Hydroxycinnamoyl Transferase (THT), two phenolic biosynthetic genes. Silencing of *Stwrky1* expression conferred greater pathogen susceptibility to *Phytophthora infestans* due to decreased secondary cell wall strengthening (Yogendra et al., 2015).

Plant hormones play an integral role in the response to wounding, as their release and *de novo* synthesis alters gene expression and regulates biosynthetic pathways (Lulai et al., 2007a, 2007b, 2008). Four hormones play a role the plant's response to wounding: salicylic acid, jasmonates, ethylene, and abscisic acid (ABA). For the purposes of this thesis, only the role of ABA will be investigated in wound-response and suberin formation. ABA is a terpenoid-derived hormone involved in multiple plant processes including seed dormancy (Koornneef et al., 2002) and the regulation of stress responses to drought (Zhang et al., 2006; Efetova et al., 2007), salt (Zhang et al., 2006) and wounding (Leon et al., 2001). ABA biosynthesis has been extensively studied using mutants from a variety of plant species, which is derived from carotenoid biosynthesis. While the role of ABA in potato tuber dormancy has been explored, the sites of ABA synthesis and catabolism in the tuber are unknown (Destefano-Beltran et al., 2006). During dormancy, levels of endogenous ABA decrease with increased age of the tuber (Kumar et al., 2010), and further evidence suggests that ABA synthesis and catabolism occurs throughout tuber dormancy (Destefano-Beltran et al., 2006).

Thirty-eight years ago, Soliday et al. (1978) began an investigation into the effect of different hormones on suberin deposition in wounded tubers resulting in two important insights. First, there was a significant delay in suberization in the water-washed control tissue, indicating there must be a water-soluble factor involved in the initiation of suberin deposition that was removed with washing (termed Suberization-Inducing Factor (SIF)). Second, ABA treatment significantly enhanced the speed of suberization, but did not alter the maximal amount of suberin deposited. A follow-up study with potato callus cultures

showed ABA-treated tissue began to accumulate suberin-associated aliphatics after an initial 2-day lag, while the control cultures exhibited a 4-day lag before accumulation (Cottle and Kolattukudy, 1982). With regards to phenolic deposition, phenylalanine ammonia-lyase (PAL) activity increased quickly with ABA treatment relative to control cultures, and total phenolic deposition was 3- to 4-fold greater in ABA-treated cultures after eight days (Cottle and Kolattukudy, 1982). However, no further exploration of ABA's regulatory role in wound-induced suberin deposition was completed for the next 25 years.

In 2008, Lulai et al. re-visited the role of ABA in wound-induced suberization and dehydration using fluridone (FD), a phytoene desaturase inhibitor that restricts *de novo* ABA biosynthesis by cutting off the supply of metabolic precursor. Water-treated tuber disks initially showed a sharp decrease in ABA content, followed by an increase in ABA content on day three post-wounding, presumably due to *de novo* biosynthesis, which remained high until day seven. FD-treated tuber disks showed the same initial sharp decrease in ABA concentration, but due to inhibition of *de novo* ABA biosynthesis, the ABA levels failed to increase throughout the remainder of the timecourse (Lulai et al., 2008). To estimate the amount of suberin deposition that accompanied these treatments, fluorescence microscopy was used to estimate the accumulation of phenolic or aliphatic suberin monomers (using autofluorescence or histochemical staining by toluidine blue O and neutral red, respectively). Using this qualitative microscopy rating system, exogenous ABA was shown to increase both phenolic and aliphatic deposition initially, without altering the total suberin deposition. Sharply contrasting the ABA treatment, FD

suppressed accumulation of both phenolic and aliphatic monomer deposition resulting in increased water permeability throughout the 7 day timecourse. FD treatment decreased the activity of PAL by 30%, which in combination with reduced autofluorescence indicated a reduced accumulation of phenolics (Lulai et al., 2008). Joint exogenous ABA and FD reverted the phenolic autofluorescence back to control levels throughout the timecourse. Interestingly, either treatment involving the exogenous ABA substantially increased aliphatic deposition initiation on day 3 post-wounding. However, this effect was short-term as by day 7 there was no difference in accumulation between the control and ABA treatments (Lulai et al., 2008). Thus, the restoration of deposition in both phenolic and aliphatic suberin deposition after exogenous ABA application identified a role for ABA in regulating wound-induced suberin deposition.

In 2010, a follow-up study determined that tuber age significantly impacted ABA content and wound-induced suberin biosynthesis potential, as older tubers had 86% less ABA and reduced PAL transcription which correlated with delayed suberization post-wounding by 5 days versus younger tubers (Kumar et al., 2010). Wound-induced suberin deposition was also slowed relative to younger tubers. Exogenous ABA treatment increased PAL expression in tubers of both ages and restored transcriptional initiation of *PAL* 24 hours post-wounding in the older tubers (Kumar et al., 2010).

1.7 Thesis Rationale and Objectives

To understand the complex regulation of suberin biosynthesis, one must first identify and characterize a unique biosynthetic step of the process. Regarding aliphatic

suberin deposition, the ω-hydroxylation of modified fatty acids presents an ideal step as it is unique to polyester biosynthesis and the majority of potato suberin monomers undergo this modification (Holloway, 1983; Bernards, 2002).

At the beginning of this research project, the potato genome had not been sequenced and suberin-associated ω-hydroxylases had not been identified or characterized in any plant species. Thus, the first step was to use cutin-associated *CYP86As* and *CYP94As* to screen the DFCI Potato Gene Index database, with the goal to identify putative ω-hydroxylases and proceed with *in vitro* protein expression, functional characterization and gene silencing. However, within the timeframe of my project *CYP86A1* was characterized as a suberin-associated ω-hydroxylase in *Arabidopsis* (Li et al., 2007; Hofer et al., 2008), followed by the potato homolog *CYP86A33* using RNA*i* mediated-silencing (Serra et al., 2009a). Since I had also simultaneously cloned *CYP86A33* (referred to herein as *Fatty Acid ω-Hydroxylase 1* (*FAωH1*)) prior to the publication by Serra et al. (2009a) and was in the process of recombinant FAωH1 protein expression for functional characterization, the initial objectives of my project pertaining to *FAωH1* characterization were completed. However, the rest of my objectives were revised from pursuing *FAωH1* gene silencing to exploring *FAωH1* regulation and global regulation of aliphatic metabolism. To investigate the regulation of *FAωH1* expression, with the recent publication of the potato Phureja genome, I completed an *in silico* analysis of the *FAωH1* promoter as well as the Phureja genome to identify additional *CYP86A* and *CYP94A* potato *FAωH*s. From these *in silico* analyses, my project expanded to investigate the effect of ABA in regulating suberin-associated gene expression as well as *CYP86A*

and *CYP94A* potato *FAωH* gene families. In addition to genetic regulation, my objectives focused on the downstream effects from altered transcription of suberin-associated genes, including the role of ABA in aliphatic suberin monomer production, deposition and incorporation during potato tuber wound healing.

References

Agrawal VP, Kolattukudy PE. 1977. Biochemistry of Suberization: ω-Hydroxyacid Oxidation in Enzyme Preparations from Suberizing Potato Tuber Disks. Plant Physiology 59: 667-672

Agrawal VP, Kolattukudy PE. 1978a. Purification and Characterization of a Wound-Induced ω-Hydroxyfatty Acid: NADP Oxidoreductase from Potato Tuber Disks. Archives of Biochemistry and Biophysics 191: 452-465

Agrawal VP, Kolattukudy PE. 1978b. Mechanism of Action of a Wound-Induced ω-Hydroxyfatty Acid: NADP Oxidoreductase Isolated from Potato Tubers (*Solanum tuberosum* L.). Archives of Biochemistry and Biophysics 191: 466-478

Ariizumi T, Toriyama K. 2011. Genetic Regulation of Sporopollenin Synthesis and Pollen Exine Development. Annual Review of Plant Biology 62: 437-460

Arrieta-Baez D, Stark RE. 2006. Modeling Suberization with Peroxidase-Catalyzed Polymerization of Hydroxycinnamic Acids: Cross-coupling and Dimerization Reactions. Phytochemistry 67: 743-753

Baker EA. 1982. Chemistry and Morphology of Plant Epicuticular Waxes. *In* The Plant Cuticle, Linnean Society Symposium Series. Cutler, Alvin and Price (eds), Academic Press, London. Volume 10, pp 139-165

Baker EA, Holloway PJ. 1970. The Constituent Acids of Angiosperm Cutins. Phytochemistry 9: 1557-1562

Beisson F, Li Y, Bonaventure G, Pollard M, Ohlrogge JB. 2007. The Acyltransferase *GPAT5* Is Required for the Synthesis of Suberin in Seed Coat and Root of *Arabidopsis*. The Plant Cell 19: 351-368

Benveniste I, Tijet N, Adas F, Philipps G, Salaün JP, Durst F. 1998. *CYP86A1* from *Arabidopsis thaliana* Encodes a Cytochrome P450-dependent Fatty Acid omega-Hydroxylase. Biochemical and Biophysical Research Communications 243: 688-693

Benveniste I, Bronner R, Wang Y, Compagnon V, Michler P, Schreiber L, Salaün JP, Durst F, Pinot F. 2005. *CYP94A1*, a Plant Cytochrome P450-catalyzing Fatty Acid omega-Hydroxylase, is Selectively Induced by Chemical Stress in *Vicia sativa* Seedlings. Planta 221: 881-890

Bernards, MA. 2002. Demystifying Suberin. Canadian Journal of Botany 80: 227-240

Bernards MA, Lopez ML, Zajicek J, Lewis NG. 1995. Hydroxycinnamic Acid-Derived Polymers Constitute the Polyaromatic Domain of Suberin. Journal of Biological Chemistry 270: 7382-7386

Bird D, Beisson F, Brigham A, Shin J, Greer S, Jetter R, Kunst L, Wu X, Yephremov A, Samuels L. 2007. Characterization of *Arabidopsis* ABCG11/WBC11, an ATP Binding Cassette (ABC) Transporter that is Required for Cuticular Lipid Secretion. The Plant Journal 52: 485-498

Brett CT, Waldron KW. 1996. Physiology and Biochemistry of Plant Cell Walls, Second Edition. Chapman and Hall, London. pp 62-64

Boher P, Serra O, Soler M, Molinas M, Figueras M. 2013. The Potato Suberin Feruloyl Transferase *FHT* which Accumulates in the Phellogen is Induced by Wounding and Regulated by Abscisic and Salicylic Acids. Journal of Experimental Botany 64: 3225-3236

Bohne G, Richter E, Woehlecke H, Ehwald R. 2003. Diffusion Barriers of Tripartite Sporopollenin Microcapsules Prepared from Pine Pollen. Annals of Botany 92: 289-297

Bonaventure G, Beisson F, Ohlrogge J, Pollard M. 2004. Analysis of the Aliphatic Monomer Composition of Polyesters Associated with *Arabidopsis* Epidermis: Occurrence of octadeca-cis-6, cis-9-diene-1,18-dioate as the Major Component. The Plant Journal 40: 920-930

Bonnet HTJ. 1968. The Root Endodermis: Fine Structure and Function. Journal of Cell Biology 37: 199-205

Cominelli E, Sala T, Calvi D, Gusmaroli G, Tonelli C. 2008. Over-expression of the *Arabidopsis AtMYB41* Gene Alters Cell Expansion and Leaf Surface Permeability. The Plant Journal 53: 53-64

Compagnon V, Diehl P, Benveniste I, Meyer D, Schaller H, Schreiber L, Franke R, Pinot F. 2009. CYP86B1 is Required for Very Long Chain omega-Hydroxyacid and alpha, omega-Dicarboxylic Acid Synthesis in Root and Seed Suberin Polyester. Plant Physiology 150: 1831-1843

Cosgrove DJ. 2005. Growth of the Plant Cell Wall. Nature Reviews Molecular Cell Biology 6: 850-861

Cosgrove DJ, Jarvis MC. 2012. Comparative Structure and Biomechanics of Plant Primary and Secondary Cell Walls. Frontiers in Plant Science 3: 204

Cottle W, Kolattukudy PE. 1982. Abscisic Acid Simulation of Suberization. Plant Physiology 70: 775-780

Croteau R, Kolattukudy PE. 1974. Biosynthesis of Hydroxy Fatty Acid Polymers. Enzymatic Synthesis of Cutin from Monomer Acids by Cell-free Preparations from the Epidermis of *Vicia faba* Leaves. Biochemistry 13: 3193-3202

DeBolt S, Scheible WR, Schrick K, Auer M, Beisson F, Bischoff V, Bouvier-Navé P, Carroll A, Hematy K, Li Y, Milne J, Nair M, Schaller H, Zemla M, Somerville C. 2009. Mutations in UDP-Glucose:Sterol Glucosyltransferase in *Arabidopsis* cause *transparent testa* Phenotype and Suberization Defect in Seeds. Plant Physiology 151: 78-87

Destefano-Beltrán L, Knauber D, Huckle L, Suttle JC. 2006. Effects of Postharvest Storage and Dormancy Status on ABA Content, Metabolism, and Expression of Genes involved in ABA Biosynthesis and Metabolism in Potato Tuber Tissues. Plant Molecular Biology 61: 687-697

Dobritsa AA, Shrestha J, Morant M, Pinot F, Matsuno M, Swanson R, Møller BL, Preuss D. 2009. CYP704B1 is a Long-chain Fatty Acid omega-Hydroxylase Essential for Sporopollenin Synthesis in Pollen of *Arabidopsis*. Plant Physiology 151: 574-589

Domergue F, Vishwanath SJ, Joubes J, Ono J, Lee JA, Bourdon M, Alhattab R, Lowe C, Pascal S, Lessire R, Rowland O. 2010. Three *Arabidopsis* Fatty Acyl-Coenzyme A Reductases, FAR1, FAR4, and FAR5, Generate Primary Fatty Alcohols Associated with Suberin Deposition. Plant Physiology 153: 1539-1554

Duan H, Schuler MA. 2005. Differential Expression and Evolution of the *Arabidopsis CYP86A* Subfamily. Plant Physiology 137: 1067-1081

Efetova M, Zeier J, Riederer M, Lee CW, Stingl N, Mueller M, Hartung W, Hedrich R, Deeken R. 2007. A Central Role of Abscisic Acid in Drought Stress Protection of *Agrobacterium*-induced Tumors on *Arabidopsis*. Plant Physiology 145: 853-862

Eigenbrode SD, Jetter R. 2002. Attachment to Plant Surface Waxes by an Insect Predator. Integrative and Comparative Biology 42: 1091-1099

Espelie KE, Sadek NZ, Kolattukudy PE. 1980. Composition of Suberin-associated Waxes from Subterranean Storage Organs of Seven Plants, Parnip, Carrot, Rutabaga, Turnip, Red Beet, Sweet Potato, and Potato. Planta 148: 468-476

Franke R, Höfer R, Briesen I, Emsermann M, Efremova N, Yephremov A, Schreiber L. 2009. The *DAISY* Gene from *Arabidopsis* Encodes a Fatty Acid Elongase Condensing Enzyme involved in the Biosynthesis of Aliphatic Suberin in Roots and the Chalaza-Micropyle Region of Seeds. The Plant Journal 57: 80-95

Franke R, Schreiber L. 2007. Suberin--a Biopolyester Forming Apoplastic Plant Interfaces. Current Opinion in Plant Biology 10: 252-259

Graça J. 2015. Suberin: the Biopolyester at the Frontier of Plants. Frontiers in Chemistry 3: 62

Graça J, Cabral V, Santos S, Lamosa P, Serra O, Molinas M, Schreiber L, Kauder F, Franke R. 2015. Partial Depolymerization of Genetically Modified Potato Tuber Periderm Reveals Intermolecular Linkages in Suberin Polyester. Phytochemistry 117: 209-219

Graça J, Pereira H. 2000. Methanolysis of Bark suberins: Analysis of Glycerol and Acid Monomers. Phytochemical Analysis 11: 45-51

Graça J, Santos S. 2007. Suberin: A Biopolyester of Plants' Skin. Macromolecular Bioscience 7: 128-135

Grausem B, Widemann E, Verdier G, Nosbusch D, Aubert Y, Beisson L, Schreiber L, Franke R, Pinot F. 2014. CYP77A19 and CYP77A20 Characterized from *Solanum tuberosum* Oxidize Fatty Acids *in vitro* and Partially Restore the Wild Phenotype in an *Arabidopsis thaliana* Cutin Mutant. Plant, Cell and Environment 37: 2102-2115

Holloway PJ. 1983. Some Variations in the Composition of Suberin from the Cork Layers of Higher-Plants. Phytochemistry 22: 495-502

Han J, Clement JM, Li J, King A, Ng S, Jaworski JG. 2010. The Cytochrome P450 CYP86A22 is a Fatty Acyl-CoA omega-Hydroxylase Essential for Estolide Synthesis in the Stigma of *Petunia hybrida*. Journal of Biological Chemistry 285: 3986-3996

Harholt J, Suttangkakul A, Scheller H. 2010. Biosynthesis of Pectin. Plant Physiology 153: 384-395

Heredia A. 2003. Biophysical and Biochemical Characteristics of Cutin, a Plant Barrier Biopolymer. Biochimica et Biophysica Acta 1620: 1-7

Höfer R, Briesen I, Beck M, Pinot F, Schreiber L, Franke R. 2008. The *Arabidopsis* Cytochrome P450 *CYP86A1* encodes a Fatty Acid omega-Hydroxylase Involved in Suberin Monomer Biosynthesis. Journal of Experimental Botany 59: 2347-2360

Kahn RA, Le Bouquin R, Pinot F, Benveniste I, Durst F. 2001. A Conservative Amino Acid Substitution Alters the Regiospecificity of CYP94A2, a Fatty Acid Hydroxylase from the Plant *Vicia sativa*. Archives of Biochemistry and Biophysics 391: 180-187

Keegstra K. 2010. Plant Cell Walls. Plant Physiology 154: 483-486

Kim SS, Douglas CJ. 2013. Sporopollenin Monomer Biosynthesis in *Arabidopsis*. Journal of Plant Biology 56: 1-6

Kim J, Jung JH, Lee SB, Go YS, Kim HJ, Cahoon R, Markham JE, Cahoon EB, Suh MC. 2013. *Arabidopsis* 3-Ketoacyl-Coenzyme A Synthase9 Is Involved in the Synthesis of Tetracosanoic Acids as Precursors of Cuticular Waxes, Suberins, Sphingolipids, and Phospholipids. Plant Physiology 162: 567-580

Kim SS, Grienenberger E, Lallemand B, Colpitts CC, Kim SY, de Azevedo Souza C, Geoffroy P, Heintz D, Krahn D, Kaiser M, Kombrink E, Heitz T, Suh DY, Legrand M, Douglas CJ. 2010. LAP6/POLYKETIDE SYNTHASE A and LAP5/POLYKETIDE SYNTHASE B Encode Hydroxyalkyl α-Pyrone Synthases Required for Pollen Development and Sporopollenin Biosynthesis in *Arabidopsis thaliana*. The Plant Cell 22: 4045-4066

Kolattukudy PE. 2001. Polyesters in Higher Plants. Advances in Biochemical Engineering/Biotechnology 71: 1-49

Kolattukudy PE. 1978. Chemistry and Biochemistry of the Aliphatic Components of Suberin. *In* Biochemistry of Wounded Plant Tissues. Kahl (ed), de Gruyter Press, Berlin. pp 43-84

Kolattukudy PE, Dean BB. 1974. Structure, Gas Chromatographic Measurement, and Function of Suberin Synthesized by Potato Tuber Tissue Slices. Plant Physiology 54: 116-121

Kolattukudy PE, Croteau R, Buckner JS. 1976. The Biochemistry of Plant Waxes. *In* Chemistry and Biochemistry of Natural Waxes. Kolattukudy (ed), American Elsevier, New York. pp 289-347

Koornneef M, Bentsink L, Hilhorst H. 2002. Seed Dormany and Germination. Current Opinion in Plant Biology 5: 33-36

Kosma DK, Molina I, Ohlrogge JB, Pollard M. 2012. Identification of an *Arabidopsis* Fatty Alcohol:Caffeoyl-Coenzyme A Acyltransferase Required for the Synthesis of Alkyl Hydroxycinnamates in Root Waxes. Plant Physiology 160: 237-248

Kosma DK, Murmu J, Razeq FM, Santos P, Bourgault R, Molina I, Rowland O. 2014. *AtMYB41* activates ectopic suberin synthesis and assembly in multiple plant species and cell types. The Plant Journal 80: 216-229

Kumar GN, Lulai EC, Suttle JC, Knowles NR. 2010. Age-induced Loss of Wound-Healing Ability in Potato Tubers is Partly Regulated by ABA. Planta 232: 1433-1445

Kunst L, Samuels AL. 2003. Biosynthesis and Secretion of Plant Cuticular Wax. Progress in Lipid Research 42: 51-80

Landgraf R, Smolka U, Altmann S, Eschen-Lippold L, Senning M, Sonnewald S, Weigel B, Frolova N, Strehmel N, Hause G, Scheel D, Böttcher C, Rosahl S. 2014. The ABC Transporter *ABCG1* is Required for Suberin Formation in Potato Tuber Periderm. The Plant Cell 26: 3403-3415

Le Bouquin R, Pinot F, Benveniste I, Salaün JP, Durst F. 1999. Cloning and Functional Characterization of CYP94A2, a Medium Chain Fatty Acid Hydroxylase from *Vicia sativa*. Biochemical and Biophysical Research Communications 261: 156-162

Le Bouquin R, Skrabs M, Kahn R, Benveniste I, Salaün JP, Schreiber L, Durst F, Pinot F. 2001. CYP94A5, a New Cytochrome P450 from *Nicotiana tabacum* is able to Catalyze the Oxidation of Fatty Acids to the omega-Alcohol and to the Corresponding Diacid. European Journal of Biochemistry 268: 3083-3090

Lee SB, Jung SJ, Go YS, Kim HU, Kim JK, Cho HJ, Park OK, Suh MC. 2009. Two *Arabidopsis* 3-ketoacyl CoA synthase genes, *KCS20* and *KCS2*/*DAISY*, are Functionally Redundant in Cuticular Wax and Root Suberin Biosynthesis, but Differentially Controlled by Osmotic Stress. The Plant Journal 60: 462-475

Leon J, Rojo E, Sanchez-Serrano JJ. 2001. Wound Signalling in Plants. Journal of Experimental Botany 52: 1-9

Li H, Pinot F, Sauveplane V, Werck-Reichhart D, Diehl P, Schreiber L, Franke R, Zhang P, Chen L, Gao Y, Liang W, Zhang D. 2010. Cytochrome P450 Family Member *CYP704B2* Catalyzes the {omega}-Hydroxylation of Fatty Acids and is Required for Anther Cutin Biosynthesis and Pollen Exine Formation in Rice. The Plant Cell 22: 173-190

Li Y, Beisson F, Koo AJ, Molina I, Pollard M, Ohlrogge J. 2007a. Identification of Acyltransferases Required for Cutin Biosynthesis and Production of Cutin with Suberin-like Monomers. Proceedings of the National Academy of Sciences of the United States of America 104: 18339-18344

Li Y, Beisson F, Ohlrogge J, Pollard M. 2007b. Monoacylglycerols are Components of Root Waxes and can be Produced in the Aerial Cuticle by Ectopic Expression of a Suberin-associated Acyltransferase. Plant Physiology 144: 1267-1277

Li-Beisson Y. 2011. Cutin and Suberin. *In* Encyclopedia of Life Sciences (ELS). John Wiley and Sons, Ltd. Chichester. pp 1-9

Li-Beisson Y, Pollard M, Sauveplane V, Pinot F, Ohlrogge J, Beisson F. 2009. Nanoridges that Characterize the Surface Morphology of Flowers Require the Synthesis of Cutin Polyester. Proceedings of the National Acacdemy of Sciences of the United States of America 106: 22008-22013

Li-Beisson Y, Shorrosh B, Beisson F, Andersson MX, Arondel V, Bates PD, Baud S, Bird D, Debono A, Durrett TP, Franke RB, Graham IA, Katayama K, Kelly AA, Larson T, Markham JE, Miquel M, Molina I, Nishida I, Rowland O, Samuels L, Schmid KM, Wada H, Welti R, Xu C, Zallot R, Ohlrogge J. 2013. Acyl-lipid Metabolism. The *Arabidopsis* Book 8: e0133. pp 24

Lulai EC, Corsini DL. 1998. Differential Deposition of Suberin Phenolic and Aliphatic Domains and their Roles in Resistance to Infection During Potato Tuber (*Solanum tuberosum* L.) Wound-Healing. Physiological and Molecular Plant Pathology 53: 209-222

Lulai EC, Freeman TP. 2001. The Importance of Phellogen Cells and their Structural Characteristics in Susceptibility and Resistance to Excoriation in Immature and Mature Potato Tuber (*Solanum tuberosum* L.) Periderm. Annals of Botany 88: 555-561

Lulai, EC. 2007. The Canon of Potato Science: Skin-Set and Wound-Healing Suberization. Potato Research 50: 387-390

Lulai EC, Suttle JC, Pederson SM. 2008. Regulatory Involvement of Abscisic Acid in Potato Tuber Wound-Healing. Journal of Experimental Botany 59: 1175-1186

Mansuy D. 1998. The Great Diversity of Reactions Catalyzed by Cytochromes P450. Comparative Biochemistry and Physiology Part C, Pharmacology, Toxicology and Endocrinology 121: 5-14

Mattinen ML, Filpponen I, Järvinen R, Li B, Kallio H, Lehtinen P, Argyropoulos D. 2009. Structure of the Polyphenolic Component of Suberin Isolated from Potato (*Solanum tuberosum* var. Nikola). Journal of Agricultural and Food Biochemistry 57: 9747-9753

Molina I, Li-Beisson Y, Beisson F, Ohlrogge JB, Pollard M. 2009. Identification of an *Arabidopsis* Feruloyl-Coenzyme A Transferase Required for Suberin Synthesis. Plant Physiology 151: 1317-1328

Moire L, Schmutz A, Buchala A, Yan B, Stark RE, Ryser U. 1999. Glycerol is a Suberin Monomer. New Experimental Evidence for an Old Hypothesis. Plant Physiology 119: 1137-1146

Neubauer JD, Lulai EC, Thompson AL, Suttle JC, Bolton MD. 2012. Wounding Coordinately Induces Cell Wall Protein, Cell Cycle and Pectin Methyl Esterase Genes Involved in Tuber Closing Layer and Wound Periderm Development. Journal of Plant Physiology 169: 586-595

Ohlrogge JB, Jaworski JG. 1997. Regulation of Fatty Acid Synthesis. Annual Review of Plant Physiology and Plant Molecular Biology 48: 109-136

O'Brien TP, Kuo J. 1975. Development of the Suberized Lamella in the Mestome Sheath of Wheat Leaves. Australian Journal of Botany 23: 783-794

Peterson CA, Emanuel ME, Wilson C. 1982. Identification of a Casparian Band in the Hypodermis of Onion and Corn Roots. Canadian Journal of Botany 60: 1529-1535

Peterson CA, Peterson RL, Robards AW. 1978. A Correlated Histochemical and Ultrastructural Study of the Epidermis and Hypodermis of Onion Roots. Protoplasma 96: 1-26

Pinot F, Benveniste I, Salaün JP, Durst F. 1998. Methyl Jasmonate Induces Lauric Acid omega-Hydroxylase Activity and Accumulation of *CYP94A1* Transcripts but does not affect Epoxide Hydrolase Activities in *Vicia sativa* Seedlings. Plant Physiology 118: 1481-1486

Pinot F, Benveniste I, Salaün JP, Loreau O, Noël JP, Schreiber L, Durst F. 1999. Production *in vitro* by the Cytochrome P450 CYP94A1 of Major C18 Cutin Monomers and Potential Messengers in Plant-Pathogen Interactions: Enantioselectivity Studies. Biochemical Journal 342: 27-32

Pinot F, Skrabs M, Compagnon V, Salaün JP, Benveniste I, Schreiber L, Durst F. 2000. omega-Hydroxylation of Epoxy- and Hydroxy-Fatty Acids by CYP94A1: Possible Involvement in Plant Defence. Biochemical Society Transactions 28: 867-870

Pollard M, Beisson F, Li Y, Ohlrogge JB. 2008. Building Lipid Barriers: Biosynthesis of Cutin and Suberin. Trends in Plant Science 13: 236-246

Pozuelo JM, Espelie KE, Kolattukudy PE. 1984. Magnesium Deficiency Results in Increased Suberization in Endodermis and Hypodermis of Corn Roots. Plant Physiology 74: 256-260

Ranathunge K, Schreiber L, Franke R. 2011. Suberin Research in the Genomics Era—New Interest for an Old Polymer. Plant Science 180: 399-413

Rawsthorne S. 2002. Carbon Flux and Fatty Acid Synthesis in Plants. Progress in Lipid Research 41: 182-196

Riley RG, Kolattukudy PE. 1975. Evidence for Covalently Attached *p*-coumaric acid and ferulic acid in cutins and suberins. Plant Physiology 56: 650-654

Samuels L, Kunst L, Jetter R. 2008. Sealing Plant Surfaces: Cuticular Wax Formation by Epidermal Cells. Anuual Review in Plant Biology 59: 683-707

Sauveplane V, Kandel S, Kastner PE, Ehlting J, Compagnon V, Werck-Reichhart D, Pinot F. 2009. *Arabidopsis thaliana* CYP77A4 is the First Cytochrome P450 Able to Catalyze the Epoxidation of Free Fatty Acids in Plants. The FEBS Journal 276: 719-735

Schreiber L, Franke R, Hartmann K. 2005. Wax and Suberin Development of Native and Wound Periderm of Potato (*Solanum tuberosum* L.) and its Relation to Peridermal Transpiration. Planta 220: 520-530

Schreiber L, Hartmann K, Skabs M, Zeier J. 1999. Apoplastic Barriers in Roots: Chemical Composition of Endodermal and Hypodermal Cell Walls. Journal of Experimental Botany 50: 1267-1280

Schreiber L. 2010. Transport Barriers made of Cutin, Suberin and Associated Waxes. Trends in Plant Science 15: 546-553

Serra O, Hohn C, Franke R, Prat S, Molinas M, Figueras M. 2010. A Feruloyl Transferase Involved in the Biosynthesis of Suberin and Suberin-associated Wax is Required for Maturation and Sealing Properties of Potato Periderm. The Plant Journal 62: 277-290

Serra O, Soler M, Hohn C, Sauveplane V, Pinot F, Franke R, Schreiber L, Prat S, Molinas M, Figueras M. 2009a. CYP86A33-Targeted Gene Silencing in Potato Tuber Alters Suberin Composition, Distorts Suberin Lamellae, and Impairs the Periderm's Water Barrier Function. Plant Physiology 149: 1050-1060

Serra O, Soler M, Hohn C, Franke R, Schreiber L, Prat S, Molinas M, Figueras M. 2009b. Silencing of *St*KCS6 in Potato Periderm Leads to Reduced Chain Lengths of Suberin and Wax Compounds and Increased Peridermal Transpiration. Journal of Experimental Botany 60: 697-707

Shiono K, Ando M, Nishiuchi S, Takahashi H, Watanabe K, Nakamura M, Matsuo Y, Yasuno N, Yamanouchi U, Fujimoto M, Takanashi H, Ranathunge K, Franke RB, Shitan N, Nishizawa NK, Takamure I, Yano M, Tsutsumi N, Schreiber L, Yazaki K, Nakazono M, Kato K. 2014. *RCN1/OsABCG5*, an ATP-Binding Cassette (ABC) Transporter, is Required for Hypodermal Suberization of Roots in Rice (*Oryza sativa*). The Plant Journal 80: 40-51

Soler M, Serra O, Molinas M, Huguet G, Fluch S, Figueras M. 2007. A Genomic Approach to Suberin Biosynthesis and Cork Differentiation. Plant Physiology 144: 419-431

Soliday CL, Dean BB, Kolattukudy PE. 1978. Suberization: Inhibition by Washing and Stimulation by Abscisic Acid in Potato Disks and Tissue Culture. Plant Physiology 61: 170-174

Soliday CL, Kolattukudy PE. 1977. Biosynthesis of Cutin ω-Hydroxylation of Fatty Acids by a Microsomal Preparation from Germinating *Vicia faba*. Plant Physiology 59: 1116-1121

Soliday CL, Kolattukudy PE. 1978. Midchain Hydroxylation of 16-Hydroxypalmitic Acid by the Endoplasmic Reticulum Fraction from Germinating *Vicia faba*. Archives of Biochemistry and Biophysics 188: 338-347

Soliday CL, Kolattukudy PE, Davis RW. 1979. Chemical and Ultrastructural Evidence that Waxes Associated with the Suberin Polymer Constitute the Major Diffusion Barrier to Water Vapor in Potato Tuber (*Solanum tuberosum* L.). Planta 146: 607-614

Suttle JC, Hultstrand JF. 1994. Role of Endogenous Abscisic Acid in Potato Microtuber Dormancy. Plant Physiology 105: 891-896

Tijet N, Helvig C, Pinot F, Le Bouquin R, Lesot A, Durst F, Salaün JP, Benveniste I. 1998. Functional Expression in Yeast and Characterization of a Clofibrate-Inducible Plant Cytochrome P-450 (CYP94A1) Involved in Cutin Monomers Synthesis. Biochemical Journal 332: 583-589

van Doorn WG, Stead AD. 1997. Abscission of flowers and floral parts. Journal of Experimental Botany 48: 821-837

Vishwanath SJ, Kosma DK, Pulsifer IP, Scandola S, Pascal S, Joubès J, Dittrich-Domergue F, Lessire R, Rowland O, Domergue F. 2013. Suberin-Associated Fatty Alcohols in *Arabidopsis*: Distributions in Roots and Contributions to Seed Coat Barrier Properties. Plant Physiology 163: 1118-1132

Vogt E, Schönherr J, Schmidt HW. 1983. Water Permeability of Periderm Membranes Isolated Enzymatically from Potato-Tubers (*Solanum tuberosum* L). Planta 158: 294-301

Walton TJ. 1990. Waxes, Cutin and Suberin. *In* Methods in Plant Biochemistry. Harwood and Boyer (eds), Academic Press, London. Volume 4, pp 105-158

Wang W, Tian S, Stark RE. 2011. Isolation and Identification of Triglycerides and Ester Oligomers from Partial Degradation of Potato Suberin. Journal of Agricultural and Food Chemistry 58: 1040-1045

Wellesen K, Durst F, Pinot F, Benveniste I, Nettesheim K, Wisman E, Steiner-Lange S, Saedler H, Yephremov A. 2001. Functional Analysis of the *LACERATA* Gene of *Arabidopsis* Provides Evidence for Different Roles of Fatty Acid ω-Hydroxylation

in Development. Proceedings of the National Academy of Sciences of the United States of America 98: 9694-9699

Werck-Reichhart D, Bak S, Paquette S. 2002. Cytochromes P450. The *Arabidopsis* Book 1:e0028: 1-28

Wiermann R, Ahlers F, Schmitz-Thom I. 2005. Sporopollenin. Biopolymers Online 1: 209-227

Wilmesmeier S, Wiermann R. 1995. Influence of EPTC (S-Ethyl-Dipropyl-Thiocarbomate) on the Composition of Surface Waxes and Sporopollenin Structure in *Zea mays*. Journal of Plant Physiology 146: 22-28

Xiao F, Goodwin SM, Xiao Y, Sun Z, Baker D, Tang X, Jenks MA, Zhou JM. 2004. *Arabidopsis CYP86A2* Represses *Pseudomonas syringae* Type III Genes and is Required for Cuticle Development. The EMBO Journal 23: 2903-2913

Xiong L, Zhu JK. 2003. Regulation of Abscisic Acid Biosynthesis. Plant Physiology 133: 29-36

Yadav V, Molina I, Ranathunge K, Castillo IQ, Rothstein SJ, Reed JW. 2014. ABCG Transporters are Required for Suberin and Pollen Wall Extracellular Barriers in *Arabidopsis*. The Plant Cell 26: 3569-3588

Yan B, Stark RE. 2000. Biosynthesis, Molecular Structure, and Domain Architecture of Potato Suberin: a 13C NMR Study using Isotopically Labeled Precursors. Journal of Agricultural and Food Chemistry 48: 3298-3304

Yang W, Bernards MA. 2006. Wound Induced Metabolism in Potato (*Solanum tuberosum* L.) Tubers: Biosynthesis of Aliphatic Domain Monomers. Plant Signaling and Behavior 1: 59-66

Yang W, Bernards MA. 2007. Metabolomic Profiling of Wound-Induced Suberization in Potato (*Solanum tuberosum* L.) Tubers. Metabolomics 3: 147-159

Yang WL, Pollard M, Li-Beisson Y, Beisson F, Feig M, Ohlrogge JB. 2010. A Distinct Type of Glycerol-3-Phosphate Acyltransferase with *sn*-2 Preference and Phosphatase Activity Producing 2-Monoacylglycerol. Proceedings of the National Academy of Sciences of the United States of America 107: 12040-12045

Yang WL, Simpson JP, Li-Beisson Y, Beisson F, Pollard M, Ohlrogge JB. 2012. A Land-Plant-Specific Glycerol-3-Phosphate Acyltransferase Family in *Arabidopsis*: Substrate Specificity, *sn*-2 Preference, and Evolution. Plant Physiology 160: 638-652

Yogendra KN, Kumar A, Sarkar K, Li Y, Pushpa D, Mosa KA, Duggavathi R, Kushalappa AC. 2015. Transcription Factor *St*WRKY1 Regulates Phenylpropanoid Metabolites Conferring Late Blight Resistance in Potato. Journal of Experimental Botany 66: 7377-7389

Zhang J, Jia W, Yang J, Ismail AM. 2006. Role of ABA in Integrating Plant Responses to Drought and Salt Stresses. Field Crops Research 97: 111-119

Chapter 2

Identification and Characterization of Suberin-Associated ω-Hydroxylases in *Solanum tuberosum* L. cv. Russet Burbank

2.1 Introduction

Suberin is a complex biopolymer composed of two domains, a poly-phenolic domain and a poly-aliphatic domain. Deposited in both a tissue-specific manner during development as well as in a cell-specific manner during stress (e.g., salt (Krishnamurthy et al., 2014) or wounding (Dean and Kolattukudy, 1976)), the primary functions of suberin are to prevent water loss and form a barrier against pathogen attack (Vishwanath et al., 2015). The poly-phenolic domain is primarily composed of hydroxycinnamic acids and their derivatives, synthesized through phenylpropanoid biosynthesis; while the poly-aliphatic domain is primarily composed of modified fatty acids and their derivatives, synthesized through fatty acid biosynthesis (reviewed in Bernards, 2002).

Through studying suberin formation in response to wounding, metabolomics research identified an immediate up-regulation of phenolic metabolism post-wounding. Hydroxycinnamic acids and their derivatives were subsequently deposited interior to the primary cell wall, anchored through cross-linkages to cell wall carbohydrates (Yan and Stark, 2000; Graça and Pereira, 2000; Serra et al., 2014). Continuous production and incorporation of phenolics over the first two days post-wounding created a matrix of

oxidatively cross-linked hydroxycinammic acids, amides and alcohols (Yang and Bernards, 2007; Graça et al., 2015). After two days post-wounding, a substantial shift of metabolism occurs in these cells (Yang and Bernards, 2007). Fatty acid biosynthesis is up-regulated resulting in the deposition of a predominately aliphatic domain interior to the phenolic domain. The C16 and C18 fatty acid monomers undergo either desaturation or elongation to form very long chain fatty acids (VLCFA), and both may be further oxidized prior to incorporation into the polymer (Yang and Bernards, 2006; Ranathunge et al., 2011; Li-Beisson et al., 2013).

An interesting challenge presents itself when studying suberin biosynthesis, due to the strict spatial and temporal regulation of products from two different major metabolic pathways: phenylpropanoid and fatty acid biosynthesis. These two primary metabolic pathways are involved in many other plant processes, thus understanding the complex regulation that leads to suberin deposition requires the identification and characterization of unique gene expression and products specific to suberin biosynthesis. When examining the aliphatic biochemical pathways leading to modified fatty acid production, 55% of wound-induced suberin monomers were ω-hydroxylated after desaturation or elongation (Holloway, 1983; Bernards, 2002). With the exception of cutin and sporopollenin, which are developmentally formed in green aerial tissues and pollen, respectively, ω-hydroxylated fatty acids are otherwise not found within the plant. Thus, a logical focal point of research is to characterize suberin-associated fatty acid ω-hydroxylases, an essential but also uncommon biochemical step in plants.

Based on the characterization of ω-hydroxylation reactions in plants, five different Cytochrome P450s (CYPs) subfamilies of ω-hydroxylases have been identified. CYPs are membrane-bound enzymes known to catalyze oxidation reactions through the reduction of NADH or NADPH (see Figure 1.2), with each subfamily specializing on a particular reaction and/or substrate. CYP86A, CYP86B, CYP94A, CYP77A and CYP704B are the five plant subfamilies of CYPs that are able to hydroxylate fatty acids on the ω-carbon. One by one, members of these subfamilies are being identified in a variety of model plants and their functions elucidated through forward or reverse genetic approaches paired with biochemical characterization.

The *CYP86A* subfamily in *Arabidopsis* contains five members, four of which are predominately localized to the green aerial plant tissues and have been implicated in cutin biosynthesis (Wellesen et al., 2001 (*CYP86A8*); Xiao et al., 2004 (*CYP86A2*)); one remaining protein is *At*CYP86A1 localized to root tissue and characterized as suberin-associated (Li et al., 2007; Hofer et al., 2008). T-DNA insertion mutants of *cyp86a1* (known as *horst* mutants; *hydroxylase of root suberized tissue*) showed significant reduction of suberin-associated ω-hydroxylated shorter chain fatty acids (<C20), indicating a role in suberin fatty acid oxidation (Hofer et al., 2008). Subsequently, a potato homolog of *CYP86A1* was identified and named *CYP86A33*, known in this thesis as *Solanum tuberosum Fatty Acid ω-Hydroxylase 1* (*FAωH1*). *FAωH1* down regulation, using RNAi gene silencing, reduced aliphatic suberin by 60%, with a substantial 70% reduction in C18:1 ω-hydroxylated fatty acids and 90% reduction in the subsequently oxidized C18:1 α-ω dioic acids (Serra et al., 2009a). However, functional characterization

of FAωH1 has not been reported, and there is no direct evidence of its ability to catalyze fatty acid ω-hydroxylation.

In 2009, another CYP86B *Arabidopsis* subfamily sharing only 45% identity with CYP86A's was identified to contain two ω-hydroxylases, CYP86B1 and CYP86B2. *CYP86B1* was demonstrated to be highly expressed in roots, specifically in sites of high developmental suberin production (Compagnon et al., 2009). Both T-DNA insertion mutants and RNAi silencing constructs of *cyp86b1* (named *ralph* mutants; *root aliphatic plant hydroxylase*) caused a significant reduction in C22 and C24 ω-hydroxylated fatty acids and α,ω dioic acids. In the place of these oxidized mid-chain fatty acids accumulating, the corresponding unmodified C22 and C24 fatty acids were deposited in the suberin polymer (Compagnon et al., 2009). To date, no functional characterization of the CYP86B1 or CYP86B2 enzymes has been completed.

Six members of the CYP94A subfamily have been identified from *Vicia sativa* and *Nicotiana tabacum*. Exhibiting differences in both reaction specificity and substrate preference, in addition to being absent from the *Arabidopsis* genome, CYP94A is a curious subfamily. CYP94A1 was functionally characterized from *Vicia* microsomes as an ω-hydroxylase capable of acting on a variety of substrates, including many cutin-specific monomers such as 9,10-epoxystearic and 9,10-dihydroxystearic acids (Tijet et al., 1998). CYP94A2 from *Vicia* is not a strict ω-hydroxylase, as *in vitro* experiments showed a shift from ω-hydroxylation to ω-1 hydroxylation in shorter chain fatty acids (Kahn et al., 2001). In *Nicotiana tabacum*, CYP94A5 was demonstrated to catalyze the ω-hydroxylation of C12 to C18 saturated and unsaturated fatty acids (Le Bouquin et al.,

2001). However, in contrast to the other plant ω-hydroxylase CYP subfamilies, CYP94A5 also catalyzed the formation of 9,10-epoxystearic-α,ω dioic acid from both 9,10-epoxystearic acid and ω-hydroxy-9,10-epoxystearic acid (Le Bouquin et al., 2001). Thus, CYP94A5 is capable of catalyzing multiple oxidation reactions on the terminal carbon of a fatty acid chain. Conversion of ω-hydroxy C16 and ω-oxo C16 fatty acids to C16 α,ω-dioic acid by an unknown NADP-dependent enzyme had been previously characterized using *Vicia faba* epidermal protein extracts (Kolattukudy et al., 1975). Given the results from CYP94A5, it is likely this unknown epidermal enzyme is a CYP94A subfamily member. As complete oxidation is necessary to produce α,ω dioic acids, present in both suberin and cutin, it is plausible that the CYP94A subfamily members may catalyze both the initial ω-hydroxylation as well as subsequent oxidation reactions in some plant species. However, *Arabidopsis* does contain α,ω dioic acids in both its suberin and cutin biopolymers, but does not contain any members of the CYP94A subfamily.

Functional characterization of the CYP77A subfamily began with two *Arabidopsis* members, CYP77A4 (Sauveplane et al., 2009) and CYP77A6 (Li-Beisson et al., 2009). Both CYP77A's were shown to ω-hydroxylate fatty acids ranging from C12-C18 in length, while CYP77A4 was also capable of epoxidation of these fatty acids (Sauveplane et al., 2009).While induced in both cutin and suberin-forming tissues as well as with jasmonic acid treatment, the role of the two identified potato homologs CYP77A19 and CYP77A20 has not been determined to date (Grausem et al., 2014).

Finally, functional characterization of CYP704B1 from *Arabidopsis* (Dobritsa et al., 2009) and CYP704B2 from rice (Li et al., 2010) demonstrated *in vitro* ω-

hydroxylation of C16 and C18 fatty acids. Developmentally, CYP704B1 and CYP704B2 both have specific expression patterns restricted to developing anthers. Similar in structure to suberin, sporopollenin is derived from both phenolic and fatty acid components that are polymerized to create the tough outer pollen wall (Scott, 1994; Wiermann et al., 2005). However, due to the site-specific transcription of the CYP704B subfamily, it is likely restricted to a role in outer pollen coat formation.

Identification and functional characterization of a suberin-associated ω-hydroxylase(s) in potato is the next step in further understanding deposition of this complex biopolymer. As more than 55% of suberin monomers undergo ω-hydroxylation, characterization of ω-hydroxylase(s) would provide an opportunity to explore potential regulatory hormones and/or factors using a single gene that must be coordinately regulated to the other suberin-associated processes. Incorporating a genetics study approach into the *Solanum tuberosum* model system will create an inducible study system to explore the more challenging aspects of suberin deposition, such as the coordinate regulation of both phenolic and aliphatic metabolism. The goal of this research was to identify and characterize suberin-associated ω-hydroxylase(s) in *Solanum tuberosum*. In addition, in-depth *in silico* analysis of the promoter regions of suberin-associated ω-hydroxylase was used, to understand more thoroughly the possibly regulators of ω-hydroxylase suberin-associated gene expression. Generation of a promoter deletion series spanning the 2 kb upstream region from the ω-hydroxylase start codon resulted in preliminary analysis of key regions of the promoter, which will be used in future studies.

2.2 Materials and Methods

2.2.1 *In silico Identification of Solanum tuberosum ω-Hydroxylases*

Screening of the *Solanum tuberosum* genome for *CYP86A*s, *CYP86Bs, CYP94As* and *CYP704Bs* was completed using previously characterized ω-hydroxylase sequences (Table 2.1). The *Solanum tuberosum* genome released by the Potato Genome Sequencing Consortium (PGSC)[1] is from the diploid variety Phureja (Visser et al., 2009). With a subset of available *CYP86A* and *CYP94A* cDNA sequences for a nucleotide BLAST search (BLASTn), a second database screening was completed of the Expressed Sequence Tag (EST) collection in the DFCI Potato Gene Index database[2], which is composed of a variety of compiled datasets with 62330 unique stress-induced ESTs for the tetraploid *Solanum tuberosum*.

Using MEGA 6[3], a phylogenetic cluster analysis was performed with 54 protein sequences to analyze ω-hydroxylase gene family members for functional prediction. For the purposes of this analysis, CYP94D1 and CYP704C1 ω-hydroxylases were included as subfamily outgroups, as well as CYP52A1 from fungi as an ω-hydroxylase outgroup. Also, the *Arabidopsis* CYP73A5 sequence was included as a plant-specific functional outgroup, as it is a cinnamic-4 hydroxylase. The phylogenetic tree was constructed using the Maximum Likelihood method by Poisson model using Bootstrap testing with 1000 replications. Nucleotide and protein sequence similarity and identity between candidate

---

1 Potato Genome Sequencing Consortium database: http://www.potatogenome.net

2 DFCI Potato Gene Index: http://compbio.dfci.harvard.edu/tgi/

3 MEGA 6 Freeware: http://www.megasoftware.net/mega.php

ω-hydroxylases were determined using Clustalω[4] to create a global alignment (Sievers et al., 2011).

4 Clustalω Freeware: http://www.clustal.org/omega/

Table 2.1: Functionally Characterized Plant CYP Sequences Utilized in Searching for Potato CYP Orthologs.
Each nucleotide sequence was used to BLASTn search the DFCI Potato Gene Indices and the *Solanum tuberosum* group Phureja genome (PGSC) database to identify putative CYP ω-hydroxylase candidates in potato.

Name	Species	EMBL No.	Reference
CYP86A1	*Arabidopsis thaliana*	P48422	Benveniste et al., 1998; Hofer et al., 2007
CYP86A2	*Arabidopsis thaliana*	O23066	Xiao et al., 2004
CYP86A8	*Arabidopsis thaliana*	O8O823	Wellesen et al., 2001
CYP94A1	*Vicia sativa*	O81117	Pinot et al., 1998; Tijet et al., 1998; Pinot et al., 2000, Benveniste et al., 2005
CYP94A2	*Vicia sativa*	P98188	Le Bouquin et al., 1999; Kahn et al., 2001
CYP94A5	*Nicotiana tabacum*	Q8W2N1	Le Bouquin et al., 2001
CYP86B1	*Arabidopsis thaliana*	Q9FMY1	Compagnon et al., 2009
CYP704B1	*Arabidopsis thaliana*	Q9C788	Dobritsa et al., 2009

2.2.2 *Cloning and Characterization of Putative ω-Hydroxylases in Solanum tuberosum cv. Russet Burbank*

2.2.2.1 Full-Length Sequencing of EST716349

Sequences obtained from the DFCI database contained contiguous sequences (contigs) created from multiple EST sequences for two full length *Solanum tuberosum* ω-hydroxylase candidates (*TC114700* and *TC120302*) and a single EST for the third candidate (*EST716349*). To determine the full-length cDNA sequence for this latter gene

from a single EST, both 5' and 3' Rapid Amplification of cDNA Ends (RACE) were performed. RNA was extracted from suberizing potato tissue three days post-wounding using hot phenol-chloroform treatment (Sambrook et al., 1989). Due to the abundance of starch in the tubers, three washes with phenol:chloroform 1:1 were performed. For a list of the primer sequences, please refer to Appendix 1. Products were electrophoresed on a 1.2% w/v agarose gel, extracted using Qiagen Gel Extraction kit and directly sequenced by Robarts Sequencing Facility (London, Canada).

To determine the 3' UTR of *EST716349*, first-strand cDNA was created using an oligo-dT Adaptor Primer (Invitrogen) and extended using Superscript^{TM}II RT. After degradation of RNA using RNaseH, the gene-specific primer (CYP94A7race3F) and universal adapter primer (Invitrogen) were used to amplify the 3' region using PCR. With this initial PCR reaction as a template, a second nested gene-specific primer (CYP94A7race3nestF) and universal adapter primer were used to re-amplify the 3' cDNA region, which was followed by electrophoresis, gel purification, and direct sequencing. The protocol was repeated to use the initial 500 bp sequence identified as a template for further 3'RACE. To construct the full length cDNA sequence, DNAman was used to align the overlapping cDNA sequences that resulted from 5' and 3' RACE.

2.2.2.2 Tissue-specific Expression of Putative ω-Hydroxylases

Tissue-specific expression of putative ω-hydroxylases was determined using primers designed for seven putative potato ω-hydroxylase candidates using unique exon-predicted regions where possible (Appendix 1). All primers were 18-24 bp in length

within a predicted DNA melting temperature (T_m) range of 50-66ºC and contained minimal predicted secondary structure (as predicted using DNAMAN; Lynnon Corporation, 2005). Each primer set was optimized for temperature, Mg^{2+} concentration and cycle number to produce a single product of expected size. PCR reactions were performed with a Biorad iCycler thermocycler and products electrophoresed on a 1.5% w/v agarose gel, stained for 40 minutes with 500 µM ethidium bromide and then destained for 5 minutes, followed by visualization under UV light using ChemiDoc XRS with Quantity One 1-D Analysis Software (BioRad).

To identify gene expression profiles of the ω-hydroxylase candidates, root, stem and leaf tissue were collected from *in vitro* grown potato plantlets (cv. Désirée) as well as throughout a 6-day time-course of wound-induced suberin deposition (cv. Russet Burbank). For Désirée potato plantlets, surface sterilized microtubers were grown under ambient light at 25ºC on MSMO media (Sigma M6899; pH 5.7 solidified with Gelzan™ CM (Sigma G1910). For Russet Burbank potatoes used in the suberin time-course, 3 month old potato tubers were wounded and incubated in the dark at 25ºC for a period of up to six days. The suberizing tuber layer was carefully removed from the tuber using a thin metal spatula to separate the newly produced outer phellem layers from the internal unsuberized tuber parenchyma. Collected tissue was flash-frozen in liquid nitrogen and stored at -80ºC until RNA was extracted using hot phenol-chloroform (Sambrook et al., 1989). Total RNA was treated with either TURBO DNase (Ambion) or DNaseI (Invitrogen) to remove any DNA contamination and spectrophotometrically quantified at 260 nm and 280 nm to determine concentration and purity of the RNA. cDNA synthesis

using Superscript^{TM}II RT (Invitrogen) was used to generate templates for semi-quantitative RT-PCR.

2.2.2.3 Cloning *FAωH1* Coding Region

CYP86A33 has been previously cloned (Serra et al., 2009). However, I simultaneously cloned the coding sequence of this gene from cv. Russet Burbank using a pair of primers based on the coding region of contig TC114700 from the DFCI Potato Gene Index database[5] (Appendix 1). The Russet Burbank cloned sequence is referred to as *FAωH1*. A 5' *Nco*I-*Bam*HI restriction enzyme site (5' CCATGG) and a 3' *Xba*I restriction enzyme site (5' TCTAGA) were incorporated to flank the cloned *FAωH1* sequence. Following PCR amplification with High Fidelity *Taq* Polymerase (Invitrogen), the product was electrophoresed on a 1% w/v agarose gel, extracted and then purified (Qiagen Gel Extraction kit). Subsequently, the *FAωH1* sequence was ligated overnight at 14ºC into a pGEM®-T Easy vector (Promega) and transformed into DH5α *E. coli* using a $CaCl_2$ heat-shock method (Sambrook et al., 1989). Transformed cells were selected on Luria-Bertani (LB: 10 g/L Bactotryptone, 5 g/L yeast extract, 10 g/L NaCl; for solid media add 15 g/L agar) with 100 μg/mL ampicillin for selection and grown overnight at 37ºC. Three single transformed colonies were selected for further analysis, yielding three independent clones that were double digested using BamHI and XbaI, then sequenced

[5] http://compbio.dfci.harvard.edu/tgi

(UWO Robarts Sequencing Facility). The *FAωH1* sequence from a single colony (pGEM13) was directionally sub-cloned using *Nco*I and *Xba*I restriction enzyme digests into pTRCHIS2B to incorporate a *myc* epitope tag and 6X HIS tag for recombinant protein expression (ThermoFisher Scientific; Figure 2.1). The vector pTRCHIS2B contains an IPTG-inducible promoter (p*TRC*) and an ampicillin antibiotic resistance gene. The final construct containing the *FAωH1* with C-terminal myc epitope tag and 6X HIS tag in pTRCHIS2B was named *FAωH1::HIS*.

a)

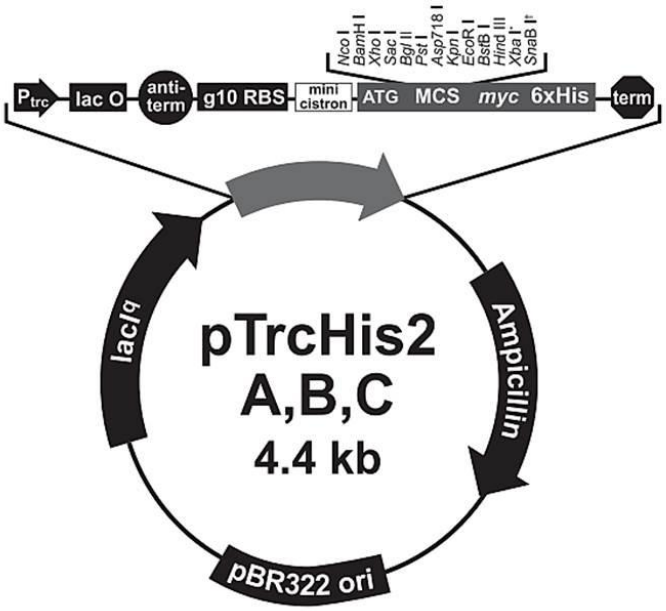

b) **pTrcHis2 B MCS**

```
                pTrcHis forward priming site
                RBS                                  Mini cistron                                  Nco I
                                                     RBS
361 AAAATTAAAG AGGTATATAT TA ATG TAT CGA TTA AAT AAG GAG GAA TAA ACC
                              Met Tyr Arg Leu Asn Lys Glu Glu *** 

    BamH I      Xho I Sac I Bgl II    Pst I Asp718 I Kpn I     EcoR I BstB I Hind III Xba I
413 ATG GATCCGAGCT CGAGATCTGC AGCTGGTACC ATATGGGAAT TCGAAGCTTT CTA
    Met
                myc epitope tag                                          Sal I
469 GAA CAA AAA CTC ATC TCA GAA GAG GAT CTG AAT AGC GCC GTC GAC CAT
    Glu Gln Lys Leu Ile Ser Glu Glu Asp Leu Asn Ser Ala Val Asp His
    ProBond™ binding domain
518 CAT CAT CAT CAT CAT TGA GTTTA
    His His His His His *** 
```

Figure 2.1: Cloning strategy for *FAωH1* coding region.
a) *p*TrcHis2B vector map (top) and pTrcHis2B polylinker (bottom) from Thermo-Scientific. *FAωH1* was cloned into pGEM®-T Easy with b) primers that included 5' *Nco*I-*Bam*HI site and 3'*XBa*I site prior to the stop codon. *FAωH1* was subcloned into *p*TrcHis2B with *Nco*I and *Xba*I, eliminating the stop codon and creating a fusion protein with *myc* epitope tags and 6X HIS tags. The tagged *FAωH1* sequence was expressed in BL21-A1 *E.coli* (Invitrogen).

2.2.3 *Functional Characterization of FAωH1*

2.2.3.1 Recombinant FAωH1 Protein Expression in BL21-A1 *E. coli*

FAωH1-TAG was transformed into *E.coli* BL21-A1 (Invitrogen) using a $CaCl_2$ heat-shock method (Sambrook et al., 1989). The BL21-A1 strain is specially designed for heterologous protein expression, containing a tightly controlled inducible system through T7 RNA polymerase expression under the control of an arabinose-inducible promoter. A single colony of transformed *FAωH1-TAG*: BL21-A1 was used to inoculate a 2 mL liquid starter culture grown overnight in selective media (LB with kanamycin (50 μg/mL); shaken at 190 rpm, 37ºC). The starter culture was used to inoculate a larger 10 mL culture in a 50 mL Erlenmeyer flask (1:100 dilution). Cultures were grown until mid-log phase with an OD_{600} of 0.4, where 1 mL of culture was removed as the uninduced control. *FAωH1::HIS p*rotein induction was done by the addition of L-arabinose and IPTG (final concentrations 0.2% w/v and 1 mM, respectively).

To determine the point of optimal FAωH1::HIS protein expression, 1 mL samples were taken every 2 hours for 10 hours post-induction. For screening purposes, dot blots were utilized to identify optimal expression conditions. To isolate the soluble protein from both induced and non-induced FAωH1::HIS BL21-A1 cultures' the cells were

harvested through centrifugation (5000 x g for 5 minutes at 4ºC). To prepare a crude protein extract, cellular membranes were disrupted using a lysis buffer (100 mM NaCl, 50 mM TRIS pH 8, 2 mM 6-aminocaproic acid, 0.1% DDM (n-dodecyl β-D-maltoside), 0.5 mg/mL lysozyme (chicken egg white, Sigma)). Samples were incubated on ice for 45 minutes then centrifuged to remove cellular debris (16000 x g for 10 minutes at 4ºC). Supernatant was transferred to a fresh vial, as it contained the soluble proteins including FAωH1::HIS. To determine the protein concentration of the crude extract, a Bradford assay was performed (Bio-Rad). To generate a standard curve of protein concentrations, a stock of 2 mg/mL bovine serum albumin (BSA) was used for a series of protein solutions with known concentrations ranging from 0.125 mg/mL to 2 mg/mL. To measure absorbance with a microplate reader (SpecraMax Gemini XPS, Molecular Devices, CA), 2 µL crude protein extract was added to 200 µL Bradford reagent and thoroughly mixed with 795 µL MQH_20 then transferred to a 96-well plate (Thermo-Scientific). Absorbance at 595 nm was measured after 5 minutes, and protein concentration determined using standard curve from BSA. Crude soluble protein extracts were stored at 4ºC until further use.

Dot blots were performed over the 10-hour post-induction timecourse using 10 µL of soluble protein extract, which was dispensed on 0.45 µm pore-size nitrocellulose membrane (Bio-Rad). For dot blots, 2 µL of soluble protein extract was applied to a nitrocellulose membrane for each condition including variations in induction time, temperature and IPTG concentration. The membrane was blocked from additional protein binding by washing with 5% w/v dry milk in TRIS buffered saline (TBS; 20 mM Tris-

HCl, 150 mM NaCl, pH 7.5) for 1 hour with gentle shaking. To remove excess milk proteins, membranes were washed three times for 5 minutes each with TBS containing 0.05% Tween 20 (referred to as TBS-T). Subsequently, the membrane was incubated with the primary antibody specific for the 6x His tag on FAωH1::HIS, a monoclonal anti-polyHIS (Sigma-Aldrich). Incubation with anti-poly HIS primary antibody was in a 1:5000 dilution in TBS for 1 hour with gentle shaking. To visualize the dot blot, membrane was incubated with 1 mL of Enhanced Chemiluminescent (ECL) reagent for 1 minute (Bio-Rad). After incubation, excess ECL solution was quickly discarded and membrane wrapped in Saran-wrap. In a dark room, X-ray film was placed in a cassette with the membrane and developed after 2 and 5 minute exposures.

Once the optimal time point of induced FAωH1::HIS expression was determined, visual confirmation of protein size and expression was done by separating proteins using SDS-PAGE followed by Western blotting. A 12% w/v, 0.75 mm thick polyacrylamide gel was prepared following standard protocols (Bio-Rad). To prepare protein samples, 25 µg of protein was removed from each crude cell extract and added to an equal volume of 2x protein sample buffer (2% w/v SDS, 20% v/v glycerol, 20 mM Tris-HCl, pH 6.8, 2 mM EDTA, 160 mM DTT, 0.1 mg/mL bromophenol blue dye). Samples were heated at 95ºC for 10 minutes prior to loading into the gel. Once samples were loaded into the wells, the gel was electrophoresed at 120 V for approximately 1 hour until the protein ladder was approaching the bottom of the gel. To visualize proteins from the crude extracts, gel was stained for 1 hour with Coomassie Brilliant Blue solution (Bio-Rad; 50% v/v methanol,

10% v/v glacial acetic acid) and destained overnight (40% methanol v/v and 10% v/v glacial acetic acid).

For Western Blotting, proteins separated through SDS-PAGE were transferred to nitrocellulose membrane for detection. The nitrocellulose membrane was placed directly on the SDS-PAGE gel and sandwiched between Whatman No.1 filter paper and thin sponges to create a stack. All air bubbles within the stack were removed by rolling a glass test tube over the stack repeatedly. The stack was then placed in a cassette and submerged in 1x transfer buffer (25 mM Tris, 190 mM glycine, 20% methanol) in an ice-chilled electrophoresis transfer tank. Transfer of proteins to the nitrocellulose membrane was done under 100 V current for 2 hours. Subsequently, the cassette was removed from the tank and the stack dismantled, with the nitrocellulose membrane being carefully placed on clean Whatman No.1 filter paper to allow it to dry. Once dry, the same protocol for blocking the membrane with milk protein, probing with antibodies and detecting using ECL was followed as described for the dot blots.

2.2.3.2 Biochemical Assay for ω-Hydroxylase Activity with *in vitro* FAωH1 Recombinant Protein

To determine recombinant FAωH1 protein function, an enzyme assay was designed to test the conversion of fatty acid substrates into ω-hydroxylated products for detection using Gas Chromatography-Mass Spectroscopy (GC-MS). As FAωH1 is a Cytochrome P450 protein, it requires an NADPH regenerating system to provide a continuous supply of reducing power as well as one or the other cytochrome P450

reductase to complete the oxidation reaction. WAT11 is a genetically engineered strain of *Saccharomyces cerevisiae* stably transformed with the *Arabidopsis* NADPH reductase (ATR1), which is expressed under galactose growth conditions (Urban et al., 1997). WAT11 was grown at 28ºC to a density of 7-8x 10^7 cells per mL with YPG media (5 g/L glucose; 10 g/L yeast extract; 10 g/L bactopeptone; 3% (by volume) ethanol. ATR1 expression was induced with YPL media (identical to YPG but with galactose (5 g/L) instead of glucose) until the culture reached a density of 2 x 10^8 cells per mL. Cells were harvested and microsomes prepared according to Pompon et al. (1996). Final microsomal preparations were resuspended in 100 mM KH_2PO_4 pH 7.4 with 20% v/v glycerol and diluted to 2.5 mg/mL microsomal protein.

To assay ω-hydroxylation activity, palmitic acid (C16) was chosen as the primary substrate as *in vivo* C16 is a prominent substrate during suberization. Within a 200 µL reaction volume, the following components were added in order: *E.coli* soluble protein extract in 100 mM KH_2PO_4 buffer pH 7, 50 µg WAT11 microsomal preparation (NADPH-regenerating system), 6.7 mM G-6-P (glucose-6-phosphate), 10 units G-6-P dehydrogenase (Sigma), 100 µM C16 palmitic acid, and 1 mM NADPH. Assays were run for 1 hour at 27ºC, and the reactions stopped using 100 µL of acetonitrile (containing 0.2% v/v acetic acid). A variety of both negative and positive control reactions were performed to ensure accurate results including: uninduced *E.coli* FAωH1::HIS protein (negative control), uninduced WAT11 microsomal preparation (negative control), no addition of NADPH (negative control), no addition of C16 substrate (negative control), and addition of NADPH reductase from rabbit replacing WAT11 microsomal preparation

(positive control). Products were detected using a Varian CP-3800 Gas Chromatograph equipped with two detectors, a flame ionization detector (GC-FID) and Saturn 220 ion trap Mass Spectrometer (GC-MS). Two CP-Sil 5 CB low bleed MS columns (WCOT silica 30 m x 0.25 mm ID) were used, with one column directed to the FID and the other column to the MS. The injector oven was set at 250ºC, and the FID oven was set at 300ºC. In splitless mode, 1 µL of sample was injected into each column, using high purity helium as the carrier gas (flow rate of 1 mL min^{-1}). Products were eluted with the following program: 70ºC held for 2 minutes, ramped to 200ºC at 40ºC min^{-1} and held for 2 minutes, ramped to 300ºC at 3ºC min^{-1} and held for 9.42 minutes for a total run time of 50 minutes.

2.2.4 *FAωH1 Promoter Cloning, in silico Analysis and Construction of FAωH1 Promoter Deletion Series*

2.2.4.1 Identification and Cloning of the *FAωH1* Promoter

To identify the 2 kb upstream region of *FAωH1* likely to contain the promoter elements, the *FAωH1* coding region sequenced from Russet Burbank was used to BLASTn search the Phureja genome database. After identifying the Phureja *FAωH1* ortholog, the 2 kb upstream sequence was isolated and utilized for primer design. Following the same cloning protocol as with the *FAωH1* coding sequence, the 2 kb upstream of the predicted translation start site for *FAωH1* was cloned from Russet Burbank into pGEM®-T Easy using primers based on the Phureja genome sequence

(Appendix 2). Twenty sequenced independent transformants from Russet Burbank were used for a multiple sequence alignment using DNAMAN.

2.2.4.2 *In silico* Analysis of Promoter Region for *FAωH1*

Two unique *FAωH1* alleles from Russet Burbank were further analyzed *in silico* to identify known promoter motifs for the 2 kb upstream sequence from the predicted translation start site using the PLACE (Plant Cis-Acting DNA Elements) database[6] (Higo et al., 1999) and the PlantCARE (Plant Cis-Acting Regulatory Element) database[7] (Lescot et al., 2002).

2.2.4.3 Construction of *FAωH1* Promoter Deletion Series

A promoter deletion series was designed with 12 forward primers, each one starting immediately downstream of an identified ABA-related promoter motif (Appendix 2). All forward primers incorporated a *Sal*I restriction enzyme site (5' GTCGAC) and were all designed to pair and amplify with a single reverse primer containing a *Bam*HI restriction enzyme site (5' GGATCC) positioned at the predicted translation start site of *FAωH1*. Starting from the 2 kb *FAωH1* cloned upstream sequence; progressively shorter upstream sequences were amplified, subcloned into pGEM®-T Easy, transformed into

[6] http://www.dna.affrc.go.jp/PLACE/
[7] http://bioinformatics.psb.ugent.be/webtools/plantcare/html/

DH5α *E. coli* and then sequenced. To generate each individual deletion construct in Russet Burbank, multiple clones for the removal of each ABA-related promoter motif were aligned to generate a consensus sequence. Subsequently, one clone with an exact sequence match to the consensus sequence was digested using *Sal*I and *Bam*HI, and electrophoresed to isolate and purify the promoter fragment before being directionally subcloned into pBI101 promoter expression construct (Clontech; Appendix 3 for vector map). These final 12 *promoterFAωH1::GUS* constructs were each transformed into DH5α *E. coli*, miniprepped and sequenced again to ensure proper frame for β-glucuronidase expression.

2.2.4.4 Generation of Transgenic Potato Hairy Roots and GUS Quantification Post-Treatment (Work Done by Anica Bjelica)

To generate transgenic hairy roots, the midribs of 4–5 week old *in vitro* grown potato leaves cv. Désirée were wounded with a scalpel previously dipped in a culture of transformed *Agrobacterium rhizogenes* LBA9402 harboring the appropriate promoter construct. Wounded and inoculated leaves were placed at room temperature on MSMO media (Sigma M6899), pH 5.7, containing 500 µg/mL cefotaxime and solidified with Gelzan™ CM (Sigma G1910). By three weeks post-inoculation, 20% to 30% of inoculated leaves had emerging hairy roots. Transgenic hairy roots containing a *promoterFAωH1::GUS* construct were selected on MSMO with kanamycin (50 µg/mL). To verify selection of transformed hairy roots, PCR genotyping was conducted on genomic DNA, using GUS specific primers with a predicted amplicon of 750 bp.

Three independent lines of each *promoterFAωH1::GUS* construct were exposed to 10^{-4} M ABA solution in Petri dishes for 4 hours. Excess ABA solution was blotted from the roots using sterile filter paper. As a control, the same treatment was performed with water. Roots were incubated for 2 and 4 days post-treatment prior to performing a quantitative GUS assay following Sprenger-Haussels and Weisshaar (2000). Soluble protein was extracted from 1–4 hairy root(s) (10–50 mg of tissue), and 50 µL of protein extract was mixed with 50 µL of GUS assay buffer (2 mM 4-methylumbelliferyl-β-D-glucuronide (4-MUG), 50 mM Na-phosphate, pH 7.0, 1 mM EDTA, 0.1% Triton X-100, 10 mM β-mercaptoethanol). Fluorescence of 4-methylumbelliferone (4-MU) was measured after 0, 30 and 60 minutes of incubation at 37ºC. For fluorescence measurements, 20 µL aliquots were mixed with 200 µL 0.2 M Na_2CO_3 and measured with excitation/emission wavelength of 365/455 nm on microplate reader (SpecraMax Gemini XPS, Molecular Devices, CA). GUS activity was calculated by determining ΔE_{455} over the 30–60 minute time interval and normalized to protein concentration (determined according to Bradford, 1976).

2.3 Results and Discussion

2.3.1 *In silico Search and Identification of CYP ω-Hydroxylase Sequences in Phureja Genome*

The first plant ω-hydroxylase reported was from the *Arabidopsis CYP86A* subfamily, *CYP86A1* (Benveniste et al., 1998). Identified through screening an EST database with non-plant ω-hydroxylase sequences, CYP86A1 was functionally characterized to have *in vitro* ω-hydroxylase active on saturated C12-C16 and unsaturated

C18 substrates (Benveniste et al., 1998). Subsequently, two other members of the *Arabidopsis* CYP86A subfamily were characterized, LACERATA (LCR*;* CYP86A8) and CYP86A2, both of which were implicated in cutin biosynthetic ω-hydroxylation (Wellesen et al., 2001; Xiao et al., 2004). From the *Arabidopsis* genome sequence release two additional members of the *CYP86A* gene family were identified (*CYP86A4* and *CYP86A7*).

A comprehensive study of *CYP86As* explored gene expression under a variety of conditions, including stress-induced and hormone-induced expression, which revealed distinct expression patterns for each *CYP86A* indicating very process-specific expression (Duan and Schuler, 2005). Functional characterization of *CYP86A1* revealed root-specific tissue expression, strongly localized to developmental deposition of suberin (Hofer et al., 2008). Therefore, CYP86A1 ortholog was the primary candidate for a suberin-associated ω-hydroxylase in potato.

2.3.1.1 Identification of *CYP86As*, *CYP86Bs*, *CYP94As* and *CYP704Bs* in *Solanum tuberosum* group Phureja Genome

Known *CYP86A, CYP86B, CYP94A* and *CYP704B* sequences from a variety of plant species were utilized to search the Phureja genome sequence, a diploid member of *Solanum tuberosum* species. Multi-gene families were identified for both *CYP86A* and *CYP94A* in Phureja, whereas *CYP86B* and *CYP704B* both revealed only a single candidate as a putative ortholog (Table 2.2). For *CYP86As*, three highly similar sequences to the *Arabidopsis* gene family were identified in the Phureja genome. The first candidate,

CYP86A33, had 86% amino acid similarity to CYP86A1, and shared a similar gene structure containing a single intron. The second candidate, CYP86A69, contained no introns and had 81% amino acid similarity to the protein CYP86A7. The third candidate, CYP86A68, contained no introns in the gene sequence and shared 80% amino acid similarity with CYP86A8. Between these three Phureja CYP86A sequences, there was 69-78% similarity in protein sequences. For the purposes of naming within this thesis: *CYP86A33* is *FAωH1*; *CYP86A69* is *FAωH2*; and *CYP86A68* is *FAωH3*.

Table 2.2: Putative ω-Hydroxylases Identified in Phureja Genome Sequence
Potato Genome Sequencing Consortium database was screened with functionally characterized ω-hydroxylase CYPs from four different subfamilies to identified putative orthologs in the Phureja genome. Clustalω pairwise comparison of each potato putative ortholog and the closest related functionally characterized ω-hydroxylase are listed (% identity/% similarity).

Name	Phureja Genome Accession No	Intron	Clustalω Pairwise Comparison
FAωH1/ CYP86A33	PGSC0003DMP400052827	339 bp	*At*CYP86A1: 73.5%/86.3%
FAωH2/ CYP86A69	PGSC0003DMP400021569	None	*At*CYP86A7: 67.9%/80.9%
FAωH3/ CYP86A68	PGSC0003DMP400068917	None	*At*CYP86A8: 70.0%/79.7%
FAωO1/ CYP94A26	PGSC0003DMP400032667	None	*Nt*CYP94A5: 82.5%/91.4%
FAωO2/ CYP94A24	PGSC0003DMP400054719	None	*Nt*CYP94A5: 83.4%/91.0%
FAωO3/ CYP94A25	PGSC0003DMP400013001	None	*Vs*CYP94A1: 51.6%/72.6%
*St*CYP704B	PGSC0003DMP400069225	None	*At*CYP704B1: 72.2%/79.2%
*St*CYP86B	PGSC0003DMP400018704	238 bp	*At*CYP86B1: 67.7%/77.6%

With respect to *CYP94As*, three Phureja candidates were identified as closely related to *Nicotiana tabacum* (tobacco) and *Vicia sativa* (spring vetch) genes. The first and second candidates, CYP94A26 and CYP94A24, shared 91% amino acid sequence similarity with tobacco CYP94A5 and CYP94A4, respectively. The final candidate, CYP94A25, was more distantly related with only 73% sequence similarity to CYP94A1 from spring vetch. None of the *CYP94A* nucleotide sequences contained introns, and this small multigene family had 76-86% similarity in protein sequences. For the purposes of this thesis: *CYP94A26* is *FAωO1*; *CYP94A24* is *FAωO2*; and *CYP94A25* is *FAωO3*.

A Phureja genome BLASTp search revealed a single putative ortholog for both CYP86B1 and CYP704B1 ω-hydroxylases. The single CYP86B Phureja putative ω-hydroxylase was identified and shared 78% sequence similarity CYP86B1 and contained one genomic intron of the approximately the same size. Phureja genome screening with CYP704B1 identified one candidate with 79% sequence similarity to CYP704B1. To date, neither potato *CYP86B* or *CYP704B* have been identified with a unique CYP number, and thus are referred to as *StCYP86B* and *StCYP704B*, respectively.

2.3.1.2 Phylogenetic Analysis of CYP ω-Hydroxylases in Plants

To explore the evolutionary relationships in an effort to predict function among gene family members as well as between orthologs of different plant species, 54 available plant ω-hydroxylase sequences were used for a phylogenetic analysis (Figure 2.2). Previous phylogenetic analysis of the *Arabidopsis CYP86A* subfamily identified *CYP86A1* as the original sequence that had undergone a duplication event, leading to *CYP86A7* (Duan and Schuler, 2005). Subsequently, three additional paralogs were generated in *Arabidopsis* through duplication, giving rise to *CYP86A8* followed by *CYP86A2* and *CYP86A4*.

FAωH1 grouped closely with *Arabidopsis* CYP86A1 and *Vitis vinifera* (wine grape) CYP86A30 (Figure 2.2), displaying high sequence similarity indicative of homology. Since the characterization of *CYP86A1* in *Arabidopsis*, other highly similar ω-hydroxylases in different species have also been characterized as suberin-associated (e.g. *CYP86A32* in *Quercus suber* (Soler et al., 2007) and *CYP86A33*/*FAωH1* in *Solanum*

tuberosum cv. Désirée (Serra et al., 2009a)). The two other CYP86A potato protein sequences, FAωH2 and FAωH3, grouped closely with the CYP86A7 and CYP86A8 groups characterized as cutin-associated in *Arabidopsis* (Wellesen et al., 2001; Xiao et al., 2004). Of the 23 CYP86A sequences included in this analysis, only three monocots from the Poales order were available including *Oryza sativa* (rice), *Zea mays* (corn) and *Triticum aestivum* (wheat). These multi-gene families separated into two small clusters, one closely related to a group of suberin-associated ω-hydroxylases while the other diverged early to form an outgroup consisting of the cutin-associated ω-hydroxylases. As monocots display numerous morphological differences from dicots, it is not surprising that they have genetically distinct protein sequences that form separate clusters (Judd et al., 2016). The CYP86B subfamily is a small subfamily with only five available sequences at this time, with the single rice CYP86B (monocot) sequence diverging from the rest. The potato CYP86B is most similar in sequence to the *Arabidopsis* CYP86B1, paralleling the findings of the CYP86A subfamily.

Figure 2.2: Phylogenetic Analysis of Plant CYP ω-Hydroxylases.
Maximum likelihood phylogenetic analysis using MEGA6 software of available ω-hydroxylase sequences from four different plant Cytochrome P450 Subfamilies including CYP86A, CYP86B, CYP94A and CYP704B. To differentiate between CYP subfamilies, CYP94D1 was included as an outgroup for CYP94A and CYP704C1 was included as an outgroup for CYP704B. CYP52A1 was included as a non-plant ω-hydroxylase outgroup and CYP73A5 (cinnamic 4-hydroxylase) was included as an CYP outgroup. All protein accession numbers are UniProt (http://www.uniprot.org/uniprot/) with the exception of *Solanum* sequences referring to the Potato Genome Sequencing Consortium (http://solanaceae.plantbiology.msu.edu/pgsc_download.shtml). At: *Arabidopsis thaliana* (thale cress); Ct: *Candida tropicalis* (yeast); Ga: *Gossypium arboreum* (tree cotton); Gm: *Glycine max* (soybean); Ml: *Maesa lanceolata* (false assegai tree); Mt: *Medicago truncatula* (barrel medic); Nt: *Nicotiana tabacum* (tobacco); Os: *Oryza sativa* (rice); Pg: *Picea glauca* (white spruce); Ph: *Petunia hybrida* (petunia); Pt: *Populus trichocarpa* (Western balsam poplar); Pp: *Physcomitrella patens* (moss); Qs: *Quercus suber* (cork oak); Sm: *Salvia miltiorrhiza* (Chinese sage); Smo: *Selaginella moellendorffii* (spikemoss); *Solanum tuberosum* (potato); Ta: *Triticum aestivum* (wheat); Vs: *Vicia sativa* (spring vetch). *Vitis vinifera* (wine grape), Zm: *Zea maize* (corn).

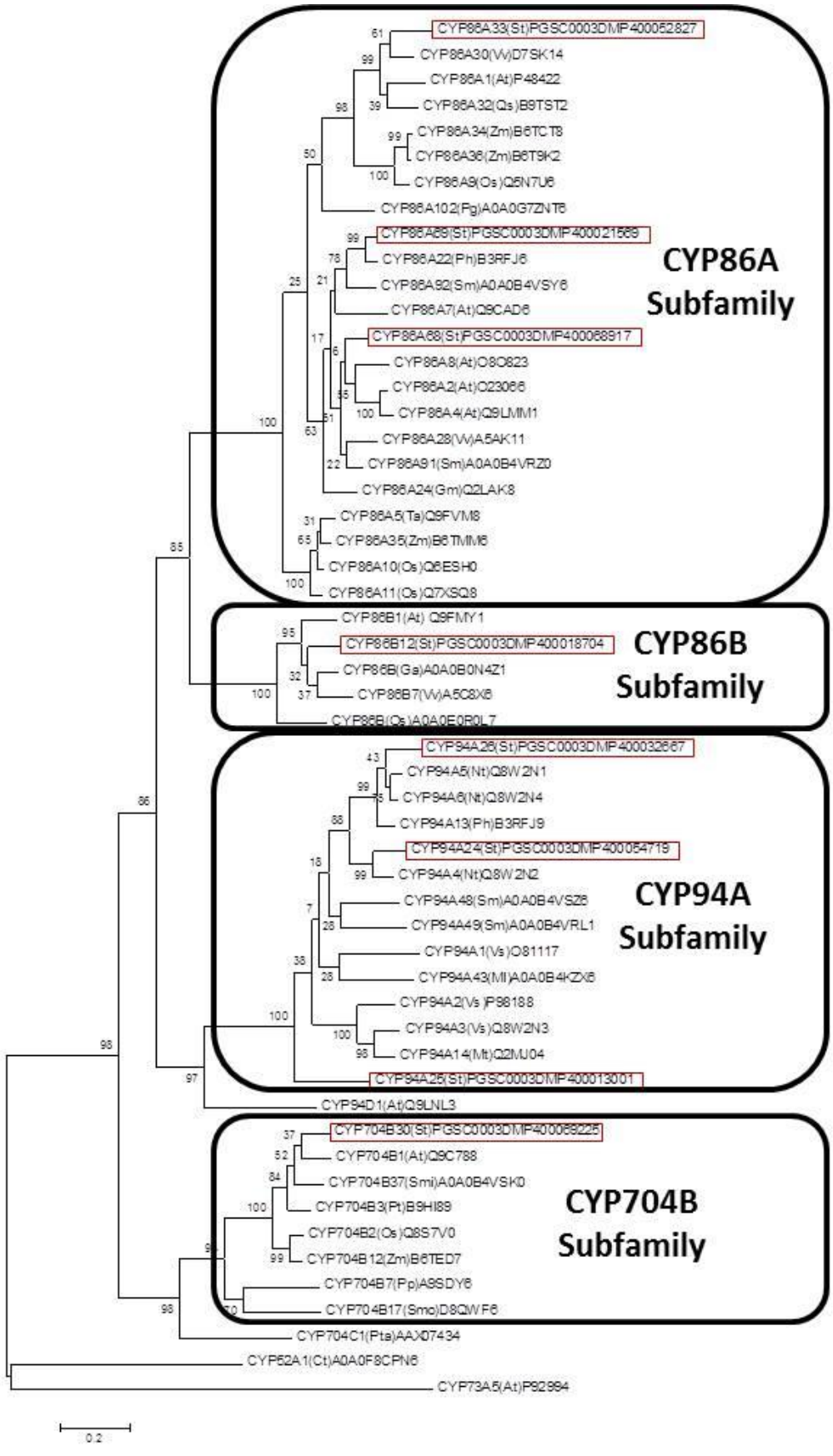
CYP86A33(St)PGSC0003DMP400052827
CYP86A30(Vv)D7SK14
CYP86A1(At)P48422
CYP86A32(Qs)B9TST2
CYP86A34(Zm)B6TCT8
CYP86A36(Zm)B6T9K2
CYP86A9(Os)Q5N7U6
CYP86A102(Pg)A0A0G7ZNT6
CYP86A69(St)PGSC0003DMP400021569
CYP86A22(Ph)B3RFJ6
CYP86A92(Sm)A0A0B4VSY6
CYP86A7(At)Q9CAD6
CYP86A68(St)PGSC0003DMP400068917
CYP86A8(At)O80823
CYP86A2(At)O23066
CYP86A4(At)Q9LMM1
CYP86A28(Vv)A5AK11
CYP86A91(Sm)A0A0B4VRZ0
CYP86A24(Gm)Q2LAK8
CYP86A5(Ta)Q9FVM8
CYP86A35(Zm)B6TMM6
CYP86A10(Os)Q6ESH0
CYP86A11(Os)Q7XSQ8
CYP86A Subfamily
CYP86B1(At) Q9FMY1
CYP86B12(St)PGSC0003DMP400018704
CYP86B(Ga)A0A0B0N4Z1
CYP86B7(Vv)A5C8X6
CYP86B(Os)A0A0E0R0L7
CYP86B Subfamily
CYP94A26(St)PGSC0003DMP400032667
CYP94A5(Nt)Q8W2N1
CYP94A6(Nt)Q8W2N4
CYP94A13(Ph)B3RFJ9
CYP94A24(St)PGSC0003DMP400054719
CYP94A4(Nt)Q8W2N2
CYP94A48(Sm)A0A0B4VSZ8
CYP94A49(Sm)A0A0B4VRL1
CYP94A1(Vs)O81117
CYP94A43(Ml)A0A0B4KZX6
CYP94A2(Vs)P98188
CYP94A3(Vs)Q8W2N3
CYP94A14(Mt)Q2MJ04
CYP94A25(St)PGSC0003DMP400013001
CYP94A Subfamily
CYP94D1(At)Q9LNL3
CYP704B30(St)PGSC0003DMP400069225
CYP704B1(At)Q9C788
CYP704B37(Smi)A0A0B4VSK0
CYP704B3(Pt)B9HI89
CYP704B2(Os)Q8S7V0
CYP704B12(Zm)B6TED7
CYP704B7(Pp)A9SDY6
CYP704B17(Smo)D8QWF6
CYP704B Subfamily
CYP704C1(Pta)AAX07434
CYP52A1(Ct)A0A0F8CPN6
CYP73A5(At)P92994
0.2

The CYP94A subfamily is notably absent from the majority of rosids, including *Arabidopsis*, as well as the monocots (Figure 2.2 and 2.3). As these plant species undergo suberization both developmentally and in response to wounding, CYP94As must not be essential for aliphatic polymer biosynthesis in all plant species. The 14 CYP94A sequences available for analysis included multi-gene families belonging to the core eudicots including both rosids (*Vicia sativa* (spring vetch), *Glycine max* (soybean)) and asterids (*Salvia miltiorrhiza* (Chinese sage), tobacco and potato). FAωO1 and FAωO2 sequences cluster with the closely-related asterid tobacco, whereas FAωO3 is evolutionarily distinct and more closely resembles CYP94A1 from the rosid spring vetch.

Eight sequences of the CYP704B subfamily were available to include in the phylogenetic analysis. The two monocot sequences, rice (CYP704B2) and corn (CYP704B12), clustered together within a monophyletic group. As seen within the CYP86A and CYP86B subfamilies, the potato CYP704B grouped closely with the *Arabidopsis* CYP704B1. As the *Arabidopsis CYP704B1* and rice *CYP704B2* have been characterized and are specifically expressed in anthers during flowering, it is unlikely that the ω-hydroxylase from this family is suberin-associated in potato. At this time, no further investigation into the *CYP704B* ω-hydroxylase subfamily was warranted.

The phylogenetic analysis of currently identified CYP sequences identified two interesting results. First, regarding the CYP86A subfamily, the three Phureja FAωH sequences subgrouped closely with all CYP86A *Arabidopsis* genes, indicating these genes may be homologous (share function through common descent) (Figure 2.3). As the *Arabidopsis* multi-gene family has been more extensively characterized than that of

potato, with CYP86A1 primarily associated with suberin deposition and the remaining CYP86A's associated with cutin deposition, these results indicate that further investigation of FAωH1 is warranted for understanding suberization. Second, regarding both subfamilies, questions remain as to how these two multi-gene ω-hydroxylase protein subfamilies arose in different plant lineages over evolutionary time. The CYP86A subfamily is widely distributed across all plant orders included in this analysis, including monocots and both Asterid and Rosid dicots. Although some of the species included in the CYP94A subfamily analysis are not present in the CYP86A, the genome sequences for these particular species are not publicly available at this time. However, other members of the same orders (e.g. Solanales or Fabales) have both CYP86A and CYP94A sequences (Figure 2.3). The CYP94A subfamily has not been identified in any monocot genome sequence to date, but is present in both the Rosid and the Asterid dicots. Multiple members of Solanales (Asterid), Lamiales (Asterid) and Fabales (Rosid) also contain CYP86As. As more genomes become publicly available, evidence of how and when the CYP94A subfamily arose within select orders of these two distinct plant lineages will become more evident.

2.3.1.3 Identification of Stress-Induced *CYP86A* and *CYP94A* Putative ω-Hydroxylases in *Solanum tuberosum* cultivars

Suberin deposition is triggered by many plant stresses, including drought, salt, cold, metals and anoxia (Enstone et al., 2003; Ranathunge et al., 2011). To investigate gene expression of the putative ω-hydroxylases induced by stress, *CYP86A* and *CYP94A*

genes were used to screen the Expressed Sequence Tag (EST) collection in the DFCI Potato Gene Index database. The DCFI database contained 62330 stress-induced ESTs

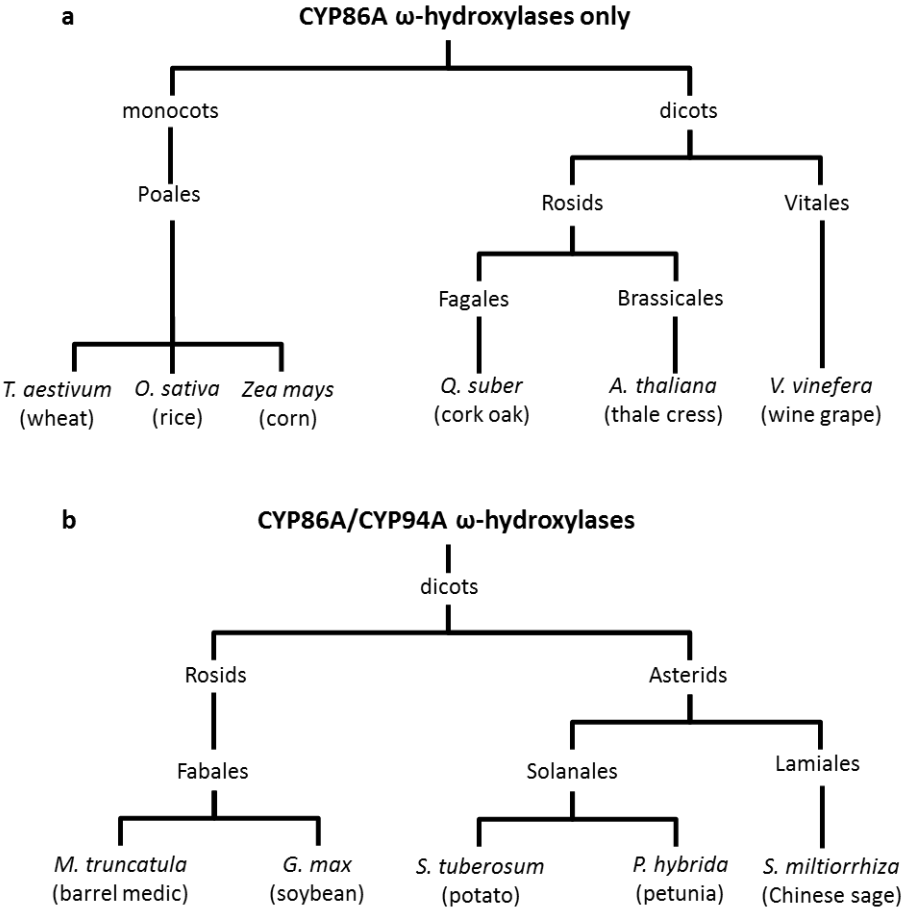

Figure 2.3: Schematic Representation of CYP86A and CYP94A Sequences Identified in Flowering Plants.

Phylogenetic tree representing the plant species with identified CYP86A and CYP94A putative ω-hydroxylases. a, the monocots and dicots orders with characterized species containing only CYP86A subfamily members; b, the Rosid and Asterid dicot orders with characterized species containing both CYP86A and CYP94A subfamily members. Plant classification follows Angiosperm Phylogeny Group IV (2016).

compiled from hundreds of independent research projects. At the time of this research, neither *CYP86B1* nor *CYP704B1* had been functionally characterized as ω-hydroxylases, so the focus remained on the multi-gene families. BLASTn searches identified three ω-hydroxylase candidates induced by stress. The first candidate was expressed under multiple conditions including abiotic stress, which through assembling seven ESTs formed a tentative contig (TC) of the full protein coding region called *TC114700*. *TC114700* was 1763 bp, with the translation start site 59 bp downstream from the transcription start site. The nucleotide coding region sequence differed by 15 nucleotides from the Phureja *FAωH1* sequence, and the predicted 521 amino acid sequence differed by only one amino acid (T→A at position 514).

The second candidate identified was *TC120302*, assembled from 12 ESTs that were expressed in multiple tissues as well as during pathogen infection. The *TC120302* sequence was 2032 bp and was identical to the *FAωH2* nucleotide sequence from the Phureja genome, with the corresponding 554 predicted amino acid sequence.

Finally, the third candidate identified was a single EST sequence, *EST716349*. Isolated from an abiotic stress cDNA library; *EST716349* was induced by either one or a combination of cold, heat, salt and drought stress. Although definitively a *CYP94A* subfamily member, the partial 760 bp sequence contained 24 single nucleotide polymorphisms relative to *FAωO1*. The *EST716349* predicted translation resulted in a 325 amino acid sequence with seven amino acid differences relative to FAωO1. However, it is notable that this was a single EST sequence so the complete sequence was unavailable for comparison.

2.3.2 *Cloning and Characterization of Putative ω-Hydroxylases FAωH1, FAωH2 and FAωO1*

2.3.2.1 Full Length Sequencing of EST716349

To determine the full length coding sequence of the CYP94A putative ω-hydroxylase from the single sequence EST716349, 5' and 3' RACE were performed. Using gene-specific primers, the 5' untranslated (UTR) region was amplified resulting in a short 39 bp fragment using potato cv. Russet Burbank as template DNA. Two successive rounds of 3'RACE identified 808 bp downstream of *ESTS716349* including 611 bp of coding region to the predicted stop codon and 197 bp of a 3'UTR including the poly-adenylation signal (Figure 2.4). Using DNAman to generate a pairwise sequence alignment between *FAωO1* from Russet Burbank with Phureja, the coding region sequence was similar with a total of 30 nucleotide differences resulting in 8 amino acid substitutions (Figure 2.5).

2.3.2.2 Tissue-Specific Expression Profiles of Putative ω-Hydroxylases

To further characterize the three stress-induced candidates (*FAωH1*, *FAωH2* and *FAωO1*), both tissue-specific and suberin-associated gene expression were measured. Using semi-quantitative RT-PCR, gene expression was determined for all three candidates in nine different plant tissues as well as during a 7-day timecourse of suberin deposition post-wounding (Figure 2.6). Semi-quantitative expression showed fairly widespread developmental expression of the putative ω-hydroxylases, with specific tissue-specific expression patterns for each gene family member. *FAωH1* was strongly

expressed in the roots, indicating *FAωH1* may be the potato ortholog of *CYP86A1*. No expression of *FAωH1* was evident in aerial tissues of the plant (Figure 2.6a). *FAωH1* also was strongly expressed during suberin deposition after 2 days post-wounding, and expression remained high throughout the 7-day timecourse (Figure 2.6b).

```
   1 AATATTTCAT TAATCAAATT CATAAATCTT GAAAAAAAAa tgacatttat agacttatta
  61 ctcttttgcc ttattccctt tctcttcatt ttcctcatca aattccaaaa aacaagaaaa
 121 aaccccattt catcaaatac taaaatacca aaatcatatc ctattattgg ttcttatttt
 181 tccatattag caaatcaaga acaaagaatt caatggatat ctgatattat ccttagcacc
 241 cctaaactta cttttactct aattcgaccc ctcaatttcc acacaatttt cactgccaat
 301 ccatctaatg ttcaacacat tctcaaaaca aacttccctg tttaccaaaa aggccataat
 361 tcaaattcta ctcttgctga tttccttagt aatggtattt tcaacgtcga tggcgatata
 421 tggaagtatc aacgacaagt tgctagccac gaattcaaca ctagatcatt acgaaaattc
 481 gttgaatctg tagttgatat tgaggtctct gaacgtttaa ttcccatact cgctaatgct
 541 gctgctgaga aaaaagttgt tgatattcaa gacattttac aaagatttgc atttgataac
 601 atttgtaaaa ttgcatttgg atttgatcca gagtatttgt taccaaacct gcctgaagca
 661 gaattcgcgg tagcatttga agattgcgtt agattaagta gtgaaagatt cattcttcct
 721 tatccgttga tttggaaaat taaacgtgtt ttcggtattg gttcagagaa gaaattacga
 781 attgcagttg aaaaagtacg tgaattcgcg aaaaaaatag tgagggagaa acagagggag
 841 ttgaatgaga agtcatcgtt ggattcagct gatttgttgt cgagattttt gagtactggt
 901 cattctgatg aagatttcgt tgttgatata gtgataagtt ttaTTTTGGC AGGACGTGAC
 961 ACGACTTCAG CTGCATTGAC ATGGTTTTTC TGGTTGATTT CGAAGAATCC AGAGGCGGAA
1021 TCTGAAATAT TAAAAGAAAT TGGGGAGAAA GAAGAAGATG TTTTAATGCG ATATGATGAA
1081 GTAAAAAACA TGATGTATAC TCATGCTTCA CTTTGTGAAA GCATGAGGTT TTATCCTCCG
1141 GTACCAATGG ATTCGAAGGA AGCAGTTAAA GATGATGTAT TGCCTGATGG TACATTTGTG
1201 AAGAAGGGGA CGAGGGTGAC TTATCATCCT TACGCAATGG GAAGATCAGA GGAGATTTGG
1261 GGAGAAGATT GGGCGGAATT CAAGCCAGAG AGATGGTTGA ATAAGGATGA AATGACGGGG
1321 AATTGGATGT TTGTAGGAAA AGATGCATTC ACATATCCTG TTTTTCAAGC AGGACCGCGA
1381 GTTTGTTTAG GGAAAGAAAT GGCGTTTTTG CAAATGAAGA GGGTGGTAGC TGGTGTTTTG
1441 CAGCGGTTTA AGGTGGTTCC GGTGGCGGAG AAAGGGGTGG AGCCGATGTT TATATCGTAT
1501 TTGACGGCCA AGATGAAAGG AGGTTTCCCT GTTACTATTG AGGAAAGGAT GTAGGAGTAG
1561 TAGTCTCATG AACAAAATGT CAAAAAACAA GTTTATTGTG TGTGTTTTTA GATTATTTGC
1621 TTTTTGATAA TTGATTTGTA GTAATGATTG TATTAATTAT TGATGAGTAT ATTGTTTTTC
1681 TAATAATCAT CGTTTTTTTT TACATCGAGT TATATATGAT TTCTCTTTGA AATTATCAAA
1741 AAAAAAAAAA AA
```

Figure 2.4: Full Length Transcript Sequence of *FAωO1* from cv. Russet Burbank. Full-length cDNA sequence obtained from 5'and 3' RACE using *EST716349* as a template. *EST716349* sequence shown in small letters; results from 5'and 3' RACE shown in capital letters within boxes. Predicted coding region shown with translation start codon at 39 bp and predicted stop codon at 1552 bp shown (bolded and underlined).

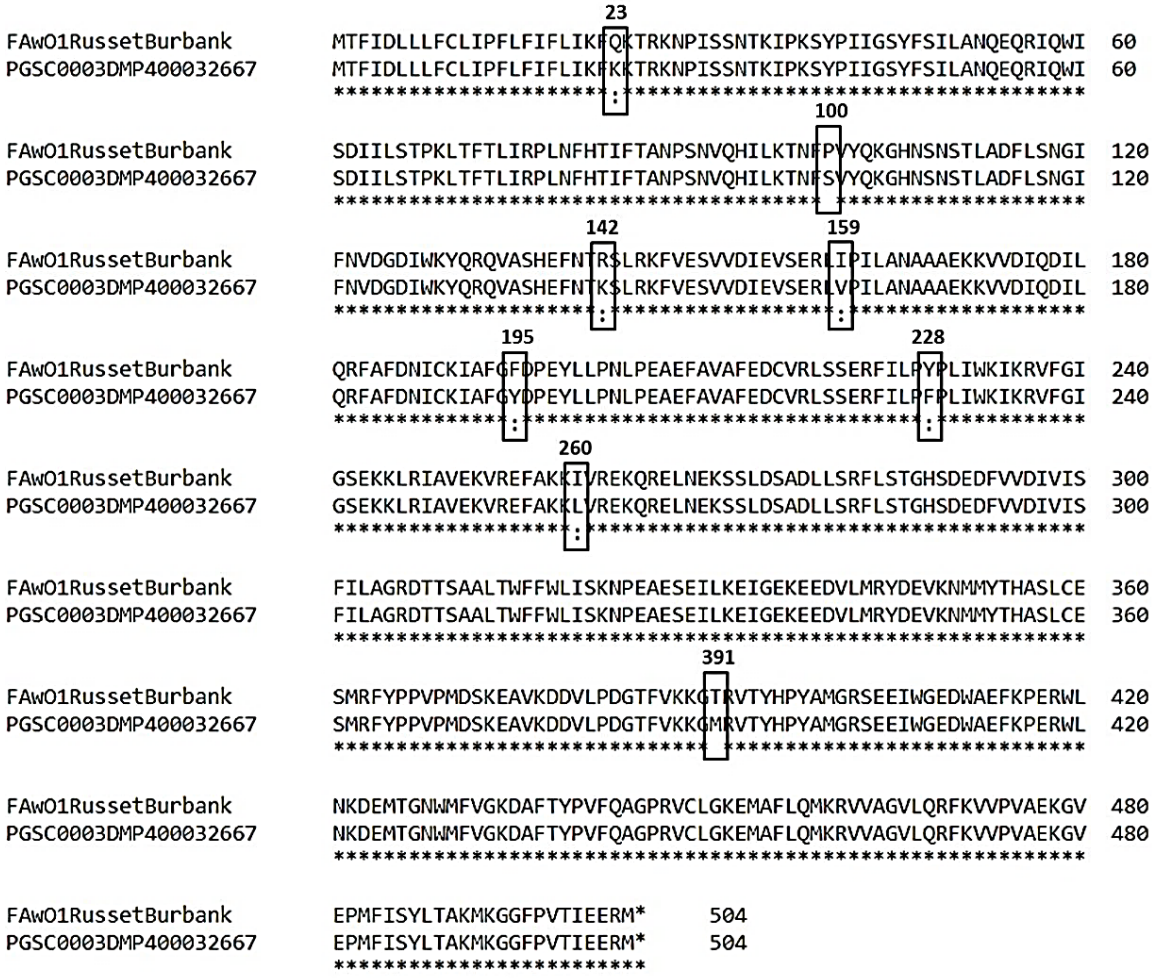

Figure 2.5: Pairwise Protein Sequence Alignment of FAωO1 from cv. Russet Burbank and Group Phureja.
Complete sequences of FAωO1 from potato cv. Russet Burbank and putative ω-hydroxylase CYP94A26 were aligned using Clustalω (global alignment). Eight amino acid substitutions are present (shown in boxes) when comparing these two *Solanum tuberosum* sequences from cv. Russet Burbank and group Phureja. Conservative amino acid substitutions are shown with ":" symbol; non-conservative substitutions have no symbol beneath (sites 100 and 391).

In contrast to *FAωH1*, both *FAωH2* and *FAωO1* were highly expressed only in green aerial tissue of the plant (including stems, young leaves, mature leaves, closed flowers, open flowers and fruits; Figure 2.6a). As these tissues form cuticles, it is likely that these two genes are associated with production of cutin aliphatic monomer synthesis.

In addition, *FAωO1* was expressed in all tissues tested, indicating it may not be specific to a particular biopolymer formation (e.g. suberin, cutin or sporopollenin). This is an interesting finding as *FAωO1* orthologs are not found in all plants; as previously mentioned the *CYP94A's* have been found only in select rosid and asterid orders, and thus would not be expected to be the primary enzyme driving ω-hydroxylation during the formation of fundamental plant biopolymers. During suberin deposition post-wounding, both *FAωH2* and *FAωO1* were expressed later in the timecourse (day 3 and day 4, respectively; Figure 2.6b).

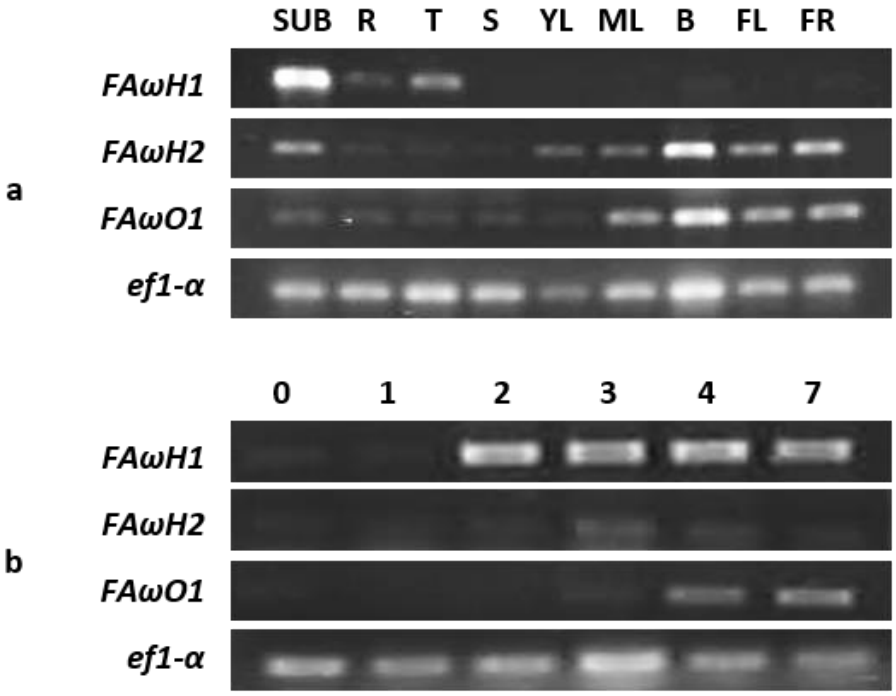

Figure 2.6: Semi-Quantitative RT-PCR Analyses of Developmental and Suberin-Induced Expression of *FAωH1*, *FAωH2* and *FAωO1*.
a, Tissue-specific developmental gene expression examined in nine tissues collected from field-grown potato plants (cv. Russet Burbank) for *FAωH1*, *FAωH2* and *FAωO1*. SUB (wound-induced suberin), R (roots), T (immature tubers), S (stem), YL (young leaves), ML (mature leaves), B (immature flower buds), FL (open flowers), FR (immature fruits). Semi-QT PCR control reactions used a housekeeping gene (ef-1α). b, Suberin-specific gene expression examined over a 7-day timecourse post-wounding from 6-month old potato tubers (cv. Russet Burbank) for *FAωH1*, *FAωH2* and *FAωO1*. Tissue was briefly

washed in sterile water prior to 25^{o}C incubation post-wounding for the duration of the timecourse until collection. Numeric labels refer to number of days post-wounding that tissue was collected (i.e., time zero labelled is 0).

Suberin-associated ω-hydroxylase *CYP86A1* from *Arabidopsis* had localized tissue expression to the root system, as it is strongly expressed during development in suberizing cell types (Hofer et al., 2008). Phylogenetic analysis showed that one of the stress-induced candidates, FAωH1, has a high degree of sequence similarity to CYP86A1, implying homology (refer to Figure 2.2).

Paired with the strong expression pattern from *FAωH1*, expression of the *FAωH2* and *FAωO1* during suberin deposition indicates that there may be functional redundancy or monomer specificity in the role of each ω-hydroxylase. However, based on their tissue-specific expression predominately in cuticle forming cells and their delayed expression during suberization post-wounding, FAωH2 and FAωO1 are not likely the primary ω-hydroxylase(s) driving aliphatic monomer modification in wound-induced suberin. Therefore, the gene expression profile of *FAωH1* suggests that it is the strongest candidate for a potato suberin-associated ω-hydroxylase.

2.3.2.3 Cloning *FAωH1* Coding Region

After demonstrating *FAωH1*expression in roots and wounded tuber tissue, the next step was to clone and sequence of the Russet Burbank *FAωH1* allele to characterize the role of *FAωH1* in suberin biosynthesis. Comparison of available orthologous potato alleles, including the Burbank *FAωH1* allele, the Désirée *FAωH1* allele (B9TST1, Serra et al., 2009) and the Phureja *FAωH1* allele (PGSC0003DMP400052827, PGSC 2011),

indicated two site-specific changes in amino acid sequences (Figure 2.7). At site 87, cv. Désirée has a non-conserved missense substitution from a cysteine to arginine. The second substitution, at site 514 near the C-terminal end, was specific to Phureja resulting in a conserved nonpolar change from threonine to alanine. Neither substitution is within the highly conserved regions of CYP450 sequence (Figure 2.7). The first conserved CYP motif, I-helix, is the CYP oxygen binding and activation motif (A/G-G-X-E/D-T-T/S) (Nelson and Werck-Reichhart, 2011; Chen et al., 2014). The second conserved CYP motif, labelled heme motif, is the heme-binding domain and the most highly conserved

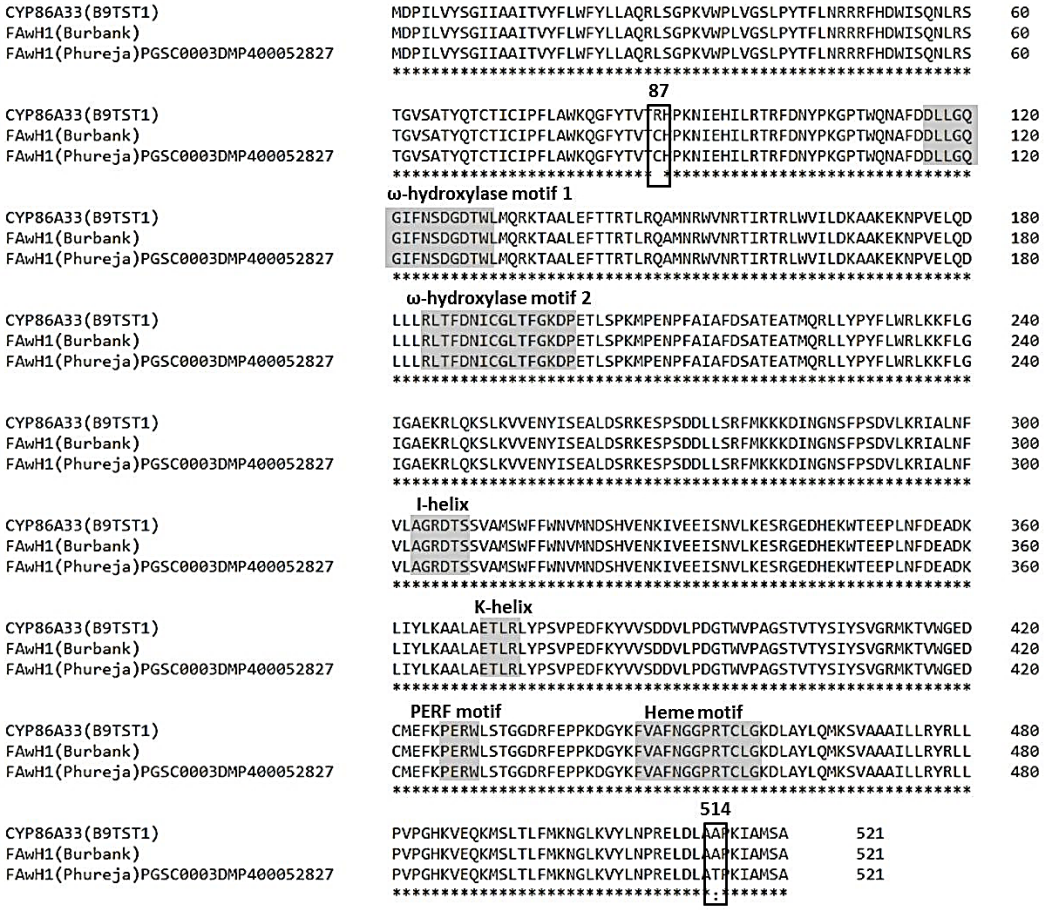

Figure 2.7: Sequence Alignments of Three FAωH1 *Solanum tuberosum* Alleles from Different Potato Cultivars

FAωH1 protein sequences were compared from two different potato cultivars and a group, including cv. Russet Burbank (tetraploid, dark brown skin, white flesh), cv. Désirée (tetraploid, red skin, light yellow flesh) and group Phureja (diploid, fingerling elongated tubers). Sites 87 and 514 (black box) indicated non-conserved amino acid positions in the potato ω-hydroxylase sequences. Conserved motifs (light grey boxes) include CYP-specific sequences (I-helix, K-helix, PERF motif and Heme-motif) as well as two CYP ω-hydroxylase-specific motifs.

element in this protein family (F-X-X-G-X-R-X-C-X-G). The third conserved CYP motif, PERF, is the cysteine heme-iron binding motif (either PERF or P-X-R-X). Finally, the fourth conserved CYP motif, the K-helix, is required for proper enzyme function (E-X-X-R) (Nelson and Werck-Reichhart, 2011). Two ω-hydroxylase-specific binding motifs, labelled ω-hydroxylase motif 1 and 2, are specific to the insertion of molecular oxygen on the ω-carbon (G-X-G-I-F-X-X-X-G-X-X-W and R-L-T-F-D-N-I-C-G-L-T-F-G-K-D-P, respectively; Werck-Reichhart et al., 2002). Overall, analysis of these three CYP sequences indicated an extremely high level of sequence conservation between different potato cultivars or groups. *Solanum tuberosum* L. contains many different cultivars (also referred to as varieties). Phureja was originally classified as a separate species, *Solanum phureja*, which was re-classified as a group within *Solanum tuberosum* once molecular biology was incorporated into flowering plants classification (Angiosperm Phylogeny Group, 1998). Phureja is technically not a cultivar but not genetically distinct enough to be considered a separate species. The highly conserved ω-hydroxylase sequence from these three morphologically distinct potatoes implies shared function of FAωH1 between all cultivars and groups. All the major protein domains required for ω-hydroxylase function are identical, with only two amino acid substitutions occurring outside of these highly conserved regions distinguishing the three homologs. Based on these results, conclusions regarding ω-hydroxylation from one potato cultivar may be safely applied to

another cultivar, which is useful as, globally, many suberin researchers choose to experiment on different potato cultivars.

2.3.3 *Functional Characterization of* FAωH1

2.3.3.1 Recombinant FAωH1 Protein Expression in BL21-A1 *E. coli*

The next step was the characterization of FAωH1, and indeed confirmation of its function as an ω-hydroxylase, through recombinant FAωH1 expression followed by an *in vitro* assay. FAωH1 was subcloned into an *E.coli* expression vector pTRCHIS2B (referred to as FAωH1::TAG) and transformed into a specialized strain of *E.coli* BL21-A1. As CYP450 proteins are known to be challenging to obtain as functional proteins *in vitro*, BL21-A1 was chosen for tightly controlled expression as it is engineered for inducible expression under control the arabinose promoter (*ara*BAD). In addition, BL21-A1 is deficient in *Ion* and OmpT proteases to reduce heterologous protein degradation. Induced expression of FAωH1::TAG in BL21-A1 initially resulted in large quantities of soluble protein. Total soluble protein fractions ranged in concentration from 2-2.5 mg/mL of protein, which contained induced protein of approximately 62 kDa (Figure 2.8a). Western blot analysis confirmed a single band of induced FAωH1 protein contained within the soluble protein extract (Figure 2.8b).

2.3.3.2 Biochemical Assay for ω-Hydroxylase Activity with *in vitro* FAωH1 Recombinant Protein

Recombinant FAωH1::TAG protein was isolated from *E. coli* using a lysis buffer, and the soluble crude protein was isolated and quantified using a Bradford assay. To assay ω-hydroxylase activity, WAT11 microsomal preparations containing the *Arabidopsis* NADPH-reductase were added to the reaction to provide the necessary

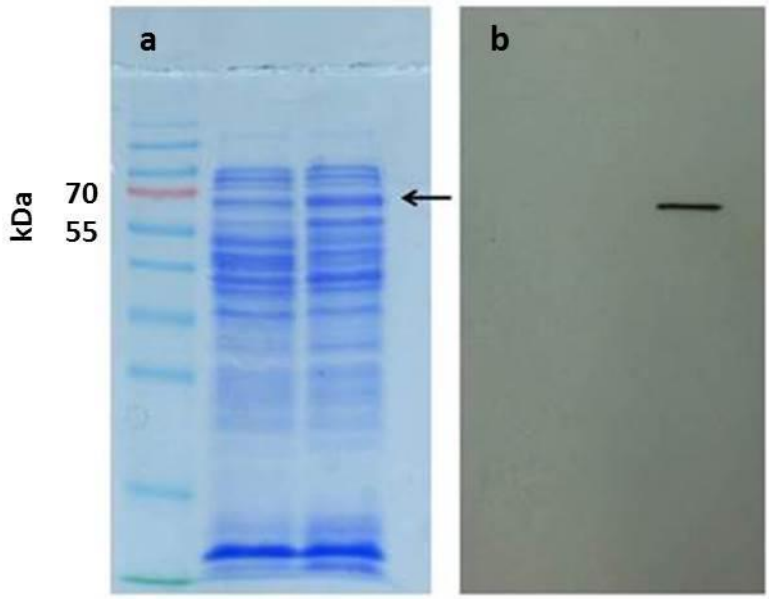

Figure 2.8: Visualization of Induced FAωH1::HIS expression in BL21-A1 *E. coli*. a, SDS-PAGE separation of soluble protein extract from uninduced FAωH1::TAG cultures (middle lane) and induced FAωH1::TAG protein cultures (right lane). The PageRuler Prestained Protein ladder (Thermo Scientific, left lane)) marks the 70 kDa (red protein band) and 55 kDa (blue band below red) size protein bands. Black arrow indicates induced FAωH1 protein of approximately 62 kDa. b, Western blot of SDS-PAGE using anti-HIS primary antibody specific to 6x HIS tag of FAωH1::TAG for visualization. No signal detected from the protein marker or uninduced protein cultures (middle lane), with a strong single band present within the induced FAωH1::TAG *E.coli* cultures.

reduction required for CYP ω-hydroxylation (Urban et al., 1997). To ensure this mechanism of CYP regeneration was functional, a positive control using rabbit liver NADPH reductase was also tested (Table 2.3). In both cases conversion of C16 palmitate into C16 ω-hydroxypalmitate occurred, with a higher amount of conversion using the WAT11 regeneration system containing a plant-specific NADPH reductase. A full suite of negative controls reactions were tested to ensure conversion occurred only in the presence of induced, functional FAωH1::TAG protein (see Table 2.3). The substrate palmitate was chosen as it is a major ω-hydroxylated product in suberin biosynthesis. Palmitate is easily soluble in the phosphate buffer and has a commercially available ω-

Table 2.3: Enzymatic Assay Reactions for *in vitro* ω-Hydroxylase Functional Characterization.
Suite of reactions to assay *in vitro* activity of FAωH1 through measuring the conversion of C16 palmate to C16 ω-hydroxypalmitate using GC-FID and GC-MS. Induced refers to induced *in vitro* FAωH1 protein expression controlled through activation of the promoter. Uninduced refers to *E.coli* and WAT11 yeast systems containing the construct without activation of the promoter controlling the gene of interest. Boiled refers to induced FAωH1 *in vitro* protein that was boiled for 10 minutes prior to enzymatic assay. n/d refers to no detectable GC ω-hydroxypalmitate product peak. The rabbit NADPH reductase was used as a positive control for activity in the WAT11 microsomal preparations containing ATR1 NADPH reductase from *Arabidopsis*.

***E.coli* protein**	**WAT11 microsomal preparation**	**NADPH (mM)**	**NADPH regenerating system**	**C16 substrate (mM)**	**GC Area Peak Count (kcount)**
Induced	Induced	1	WAT11	0.1	550
Induced	----	1	Rabbit NADPH Reductase	0.1	175
Induced	----	1	----	0.1	n/d
Induced	Uninduced	1	----	0.1	n/d
Uninduced	Induced	1	WAT11	0.1	n/d
Boiled	Induced	1	WAT11	0.1	n/d
Induced	Induced	----	WAT11	0.1	n/d
Induced	Induced	1	WAT11	-----	n/d

hydroxylated standard (16-hydroxypamitate). After substrate addition, assays were incubated and the final products detected using GC-MS. Using fatty acid standards, the conversion of C16 palmitate to C16 ω-hydroxypalmitate was demonstrated (Figure 2.9 c). In all negative control reactions, no conversion occurred (Figure 2.9a). In the positive control reaction, rabbit liver NADPH reductase facilitated the conversion of palmitate to ω-hydroxypalmitate with a small peak of 175 kcounts. With respect to the uninduced FAωH1::TAG cultures, like the negative controls there was no conversion of palmitate. However, the induced FAωH1::TAG showed clear conversion of palmitate to ω-

hydroxypalmitate resulting in a peak of 550 kcounts in the presence of WAT11 NADPH reductase (Figure 2.9b, d).

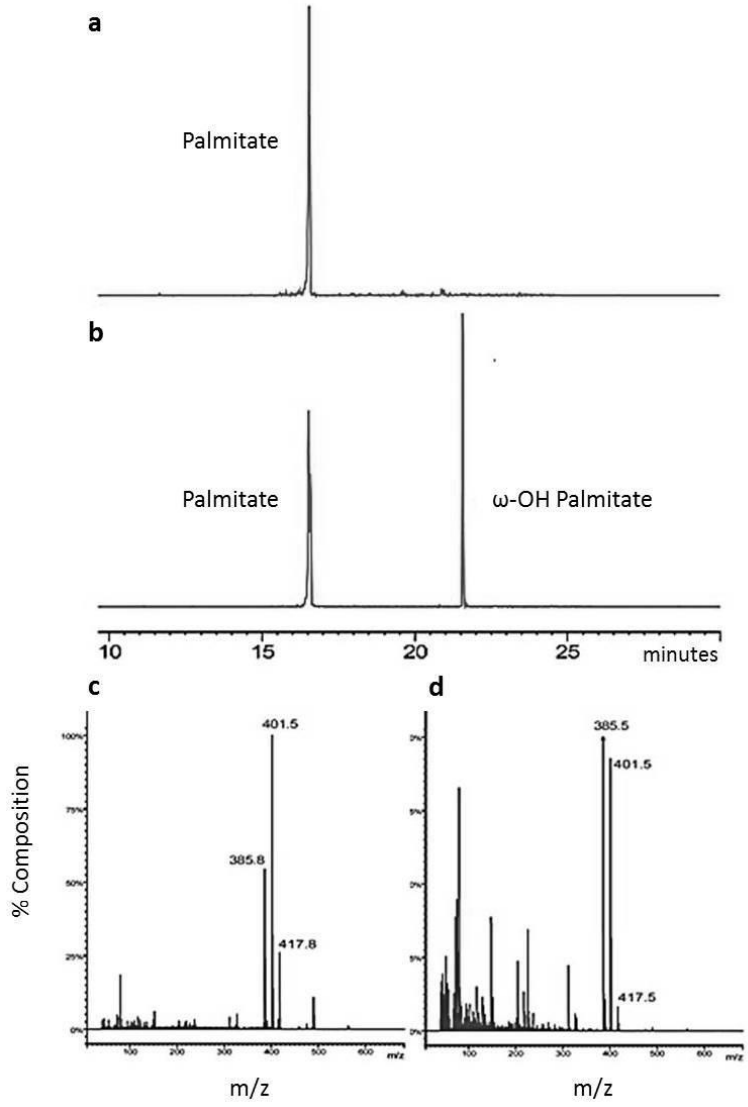

Figure 2.9: Functional Characterization of *in vitro* FAωH1 ω-Hydroxylation with C16 Palmitate.

Enzymatic conversion of C16 palmitate to C16 ω-OH palmitate by the addition of recombinant FAωH1 protein during assay. a, Negative control reaction using boiled soluble protein extract from induced FAωH1::TAG *E.coli*; b, experimental assay containing soluble protein extract from induced FAωH1::TAG *E.coli* cultures showing the conversion of C16 palmitate substrate into C16 ω-OH palmitate product; c, mass spectrum of authentic C16 ω-OH palmitate standard, as the TMS ester-TMS ether; and d, corresponding mass spectrum of the main product peak at ~ 22.5 min in panel b.

Recombinant FAωH1::TAG was initially successfully assayed for ω-hydroxylase activity using C16 palmitate as a substrate (Table 2.3 and Figure 2.9). However, in all subsequent replicates of induced BL21-A1 FAωH1::TAG cultures the recombinant protein formed insoluble inclusion bodies, which could no longer be isolated from the soluble protein. Many different growth conditions including media formulation, shaker speed, incubation time and temperature were modified through trial and error, including the addition of 5-aminolevulinic acid (ALA) as a supplement for CYPs. As previously mentioned, CYPs are known as challenging recombinant protein expression targets; and specifically FAωH1 recombinant expression was previously attempted but unsuccessful (Serra et al., 2009). Subsequently, the FAωH1::TAG sequence was subcloned into a pYeDP60 *Saccharomyces cerevisiae* (yeast) expression vector to utilize a second expression system, but this also did not result in functional FAωH1 protein (data not shown).

Since recombinant expression of FAωH1::TAG was not reproducible, due to recombinant protein forming inclusion bodies in all subsequent protein extracts, C16 palmitate was the only substrate tested with FAωH1::TAG. However, there are many substrates that may be the preferred substrates for ω-hydroxylases, which will need to be explored in the future. Fatty acids are generated through fatty acid biosynthesis in the plastid, and are exported to the cytoplasm and activated to fatty acyl-CoA thioesters (Vishwanath et al., 2015). CYP86A22 (from petunia) is active with both saturated and unsaturated acyl-CoA substrates in petunia, while it does not readily use free fatty acids as substrates (Han et al., 2010). RNA*i* suppression of *CYP86A22* resulted in a complete

reduction of 18:1 ω-hydroxy fatty acids, which normally dominate stigma fatty acids (Han et al., 2010). In previous functional characterization of the *Arabidopsis* CYP86A

subfamily, free fatty acids ranging from C12-C18:1 have been used as substrates (Benveniste et al., 1998, Rupasinghe et al., 2007). Although it is recognized that longer chain fatty acids may also be preferred substrates, solubility becomes an issue as the hydrocarbon chain length increases. The preferred substrate for CYP86A1 was C16 and C18:1, while the enzyme was also active in ω-hydroxylating C18:2, C14 and C12 (Benveniste et al., 1998). Subsequently, an in-depth protein structure and function analysis across all *At*CYP86A's confirmed these findings (Rapasinghe et al., 2007). In both studies, CYP86A1 was unable to metabolize saturated C18 (stearic acid) *in vitro* (Benveniste et al., 1998; Rapasinghe et al., 2007). The next step in characterization was to examine *in vivo* the role of CYP86A1, using T-DNA insertion lines of *cyp86a1/horst* mutants (Hofer et al., 2008). ω-Hydroxylation of longer chain fatty acids (≥C20) was unaffected in *cyp86a1/horst* mutants, whereas saturated C16 as well as saturated and unsaturated C18 ω-hydroxylation was significantly reduced (Hofer et al., 2008). Thus, saturated C18 ω-hydroxylation results were inconsistent between *in vitro* and *in vivo*. *In vivo* saturated C18 ω-hydroxylated products were reduced whereas *in vitro* saturated C18 was not able to catalyze ω-hydroxylation (Benveniste et al., 1998; Rapasinghe et al., 2007; Hofer et al., 2008). This inconsistency indicates that either *in situ* elements are required for saturated C18 ω-hydroxylation or saturated C18 ω-hydroxylated products may be the result of elongation from ω-hydroxylated C16 acyl-CoAs. Consistent with the latter hypothesis, ω-hydroxylated C16 has been demonstrated *in vitro* as a substrate for LACs (Schnurr et al., 2004). Taken together, CYP86A1 is presumed to prefer C16 and C18 fatty acids as substrates. At this time the preferred form of the substrate, whether free fatty acids or acyl-fatty acids, or if ω-hydroxylation occurs predominately on C16 which

through FAE is elongated to C18 remains unknown. Therefore, the preferred substrates by ω-hydroxylases remain unknown and, due to challenges in both recombinant protein expression and substrate solubility, it remains a challenging area of research.

2.3.3.3 Complementation Analysis of *Arabidopsis cyp86a1/horst* Mutants with *StFAωH1*

While the *in vitro* recombinant protein FAωH1 enzyme assay provided direct evidence of ω-hydroxylase activity, a full characterization of the substrate preference was not attained. Using the cloned *St*FAωH1 coding sequence described above, Anica Bjelica (technician in Bernards' laboratory) designed a complementation experiment using the *Arabidopsis* T-DNA insertion mutant line *cyp86a1/horst*. These *cyp86a1*/*horst* mutants exhibited a significant reduction in suberin aliphatic monomers including ω-hydroxylated fatty acids less than C20, which indicated that CYP86A1 has a chain length specificity (Hofer et al., 2008). Complementation analysis with the *Arabidopsis* CYP86A1 was able to reconstitute normal monomer ω-hydroxylation. The cloned Burbank *FAωH1* coding region, driven by the *Arabidopsis CYP86A1* promoter partially complemented the *Arabidopsis cyp86a1/horst* mutant, resulting in reconstituting C16 and C18:1 ω-hydroxylated fatty acids (Bjelica et al., 2016; Appendix 4). These complementation results confirm that the Burbank FAωH1 functions *in vivo* as an ω-hydroxylase active on palmitate, which was established through the *in vitro* recombinant FAωH1 enzyme assay.

2.3.4 *FAωH1 Promoter Cloning, in silico Analysis and Construction of FAωH1 Promoter Deletion Series*

2.3.4.1 Identification and Cloning of the *FAωH1* Promoter from cv. Russet Burbank

FAωH1 has been demonstrated through this work to be a suberin-associated fatty acid ω-hydroxylase, as it displayed strong wound-induced gene expression during the induction of aliphatic suberin metabolism as well as converted C16 palmitate to C16 ω-OH palmitate. The focus of this chapter was to identify and characterize a unique and specific suberin-associated gene. The combination of *FAωH1*'s root-specific developmental expression and post-wounding induction indicate that *FAωH1* is a suberin-associated ω-hydroxylase, and provides an excellent model gene for future work to begin exploring the regulation of aliphatic suberin biosynthesis.

Wounding activates many metabolic pathways simultaneously, as was illustrated by a survey of 8200 *Arabidopsis* genes with changes in gene expression for over 600 transcripts in response to wounding (Cheong et al., 2002). To begin exploring the complex regulation necessary to co-ordinate wound-induced suberin biosynthesis, characterization of the *FAωH1* promoter would provide an opportunity to identify key regulatory elements. To determine the *FAωH1* promoter region sequence, the Phureja genome database was mined to identify the upstream 2 kb from the *FAωH1* translation start site. Forward and reverse primers were designed to PCR amplify the 2 kb upstream of the translation start site of the *FAωH1* coding region in cv. Russet Burbank. Twenty randomly chosen *E. coli* colonies containing the 2 kb promoter region in pGEM®-T Easy

were independently sequenced and then compared through a multiple sequence alignment. Two different alleles of *FAωH1* promoter were identified in Russet Burbank, whereas the Phureja genome was generated from an artificially created doubled monoploid so it contains only one allele.

The first promoter allele, P1, was 2056 bp in length and present in 12 of the 20 sequenced clones (Appendix 5a). The second allele, P2, was 2073 bp in length and present in the remaining eight sequenced clones (Appendix 5b). All sequenced clones were aligned using a Clustalω global alignment, generating a consensus sequence for each promoter allele. The two alleles P1 and P2 were 89.6% identical in nucleotide sequence with 194 bp differences identified by pairwise sequence alignment (Appendix 6).

2.3.4.2 *In silico* Analysis of Promoter Region for *FAωH1*

Using the PLACE database (Higo et al., 1999), each allele was screened for cis-acting regulatory elements to elucidate how the P1 and P2 promoters regulate *FAωH1* transcription. Both alleles contained 404 common motifs at the same location spanning the 2 kb promoter region, with many transcription factors and common cis-regulatory elements being identified such as TATA boxes, DOF transcription factor binding sites (DOFCOREZM) and CAAT boxes(CAATBOX1) (Appendices 7a and 7b). The P1 allele contained 94 individual promoter motifs not found in P2; and vice versa P2 allele contained 121 individual promoter motifs not present in P1. Many of these individual motifs were present in both promoters; however, they differed significantly in sequence

location and copy number between alleles. Although the promoter region is under less stringent selection pressure to maintain its sequence than the coding region, it was surprising that these two promoter alleles differed in 20% of their motif locations (Table 2.4). Yet only one coding sequence for *FAωH1* was cloned from Russet Burbank, indicating strong selection pressure to maintain the protein coding region of the *FAωH1* alleles.

Identification and characterization of wound-inducible genes, such as *win1* and *wun1*, have provided the opportunity to determine the promoter motifs required for wound-induced expression (Logemann and Schnell, 1989; Stanford et al., 1989). From these analyses and the study of pathogen-induced gene expression, the W-box cis-element ((T)TGAC(C/T)) has been identified and shown to be a binding site for the WRKY-family of transcription factors (Rushton et al., 1996; Du and Chen, 2000, Hahn et al., 2013). WRKY proteins are a large family with a conserved WRKYGQK sequence and a DNA-binding domain active in regulating plant defense responses and development (Rushton et al., 1996; Johnston et al., 2002; Eulgem, 2006; Pandey and Somssich, 2009). A WRKY transcription factor from *Medicago truncatula* has been shown to induce phenolic accumulation in transgenic tobacco lines, indicating a role in regulating phenylpropanoid biosynthesis (Naoumkina et al., 2008). P1 and P2 *in silico* analysis identified WBOX elements in both alleles (Table 2.4). Wound-inducible *FAωH1*expression was demonstrated using β-glucuronidase expression with only the first 263 bp of the P2 promoter sequence upstream from the translation start site, indicating this is the minimal promoter required for wound-responsive expression (Lee, 2010). The

FAωH1 P1 and P2 promoter alleles both contain many WRKY/WBOX, 11 and 12 motifs, respectively (Table 2.4). Wounding quickly induces suberin biosynthesis in plants,

Table 2.4: P1 and P2 *FAωH1* Predicted Promoter Elements Related to Developmental and Wound-Induced Suberin Formation through *in silico* Analysis. PLACE scan of previously characterized promoter elements related to root-specific expression, wound-induced expression and ABA-responsive elements. Motif name refers to the published name for the promoter binding site; allele refers to identification of the motif on one or both of the promoters alleles (P1 and/or P2), sequence location identifies location on the motif on the + or – strand of the DNA with upstream location relative to the translation start site; signal sequence refers to the DNA sequencing of the promoter binding site or motif; associated factors and functions identifies other closely related sequences and functional characterization of these elements.

Motif Name	Allele	Location (bp) (+/- strand)	Signal Sequence	Associated Factors and Functions
WRKY710S	P2	-255	TGAC	**WBOXATNPR1** (TTGAC): binding site for SA-induced WRKY transcription factor **WBOXNTCHN48** (CTGACY): Elicitor-responsive element **WBOXHVIS01** (TGACT): binding element **WBOXNTERF3** (TGACY): responsive to wounding WBOX's also known to be responsive to ABA
	P1/P2	+334/337		
	P1/P2	+496/509		
	P1/P2	-950/966		
	P1/P2	-1101/1118		
	P1/P2	+1159/1169		
	P1/P2	-1325/1338		
	P1	+1634		
	P1/P2	-1643/1660		
	P1/P2	+1742/1760		
	P1/P2	+1772/1789		
	P2	+1941		
	P1/P2	-2051/2068		

ROOTMOTIFTAPOX1	P1/P2 P1/P2 P1/P2 P1/P2 P1/P2 P1/P2 P1 P1/P2 P1/P2 P1 P1/P2 P1/P2 P1/P2 P1/P2 P1/P2	-114/107 +388/394 +430/436 +454/467 +533/546 -534/547 -611/629 +662 +947/963 +1330/1343 -1359 -1458/1475 -1532/1549 -1651/1668 -1663/1680 -1669/1686	ATATT	Root-specific element from rolD gene
OSE1ROOTNODULE	P1/P2 P1/P2 P1 P1/P2	+734/750 -797/813 +1080 -1952/1968	AAAGAT	Activated in the infected cells of root nodules in *Vicia faba*
ACGTATERD1	P1 P1/P2 P1/P2 P1 P1/P2	+/-138 +/-289/291 +/-953/969 +/-1249 +/-1740/1758	ACGT	**ABRERATCAL** (MACGYGB) **ABRELATERD1** (ACGTG) **ACGTCBOX** (GACGTC) Etiolation-induced; dehydration; ABA-related
MYB1AT	P1 P1 P2 P2 P1 P1/P2	+34 +266 -460 -561 +838 +1540/1557	WAACCA	Dehydration-responsiveness; ABA-related
MYBCORE	P1/P2 P1/P2 P1/P2	-209/202 -910/926 -1225/1235	CNGTTR	Drought and ABA Expression
MYBGAHV	P1/P2	+843/859	TAACAAA	
MYBST1	P1/P2 P2	-475/491 +1654	GGATA	
MYBPZM	P1/P2	+700/716	CCWACC	Developmentally upregulated by ABA

MYCCONSENSUSAT or EBOXBNNAPA	P1/P2 P1/P2 P1/P2 P1 P2 P1/P2	+/-460/473 +/-675/691 +/-986/1003 +/-1170 +/-1390 +/-1746/1764	CANNTG	**MYCATERD22** (CACATG): MYC binding site, ABA and dehydration **MYCATERD1** (CATGTG): MYC binding site, ABA and dehydration
DPBFCOREDCDC3	P1 P2	+399 +1391	ACACNNG	ABA-regulated
LTRECOREATCOR15	P1/P2 P2	+867/883 -1466	CCGAC	Downregulated by ABA (various stresses)
RYREPEATBNNAPA	P1/P2 P1/P2	+780/796 -782/798	CATGCA	ABA-related; required for seed specific expression
TBOXATGAPB	P1/P2 P1	-257/259 -1769	ACTTTG	Upregulated by ABA and light

with phenolic gene expression evident within 3 hours (Kumar et al., 2010). However, there must be an additional regulatory factor blocking WRKY/WBOX sites at the time of wounding as *FAωH1* expression is not upregulated until 48 hours post-wounding (Figure 2.6b).

Root-specific *FAωH1* gene expression was demonstrated using semi-quantitative RT-PCR (Figure 2.4a). Both P1 and P2 promoter alleles contain numerous copies of the root-specific promoter motif ROOTMOTIFAPOX1 (ATATT), 16 and 14, respectively (Table 2.4). Identified from the rolD gene, ROOTMOTIFAPOX1 is expressed in the root elongation zone and vasculature (Elfmayan and Tepfer, 1995). A cluster of ROOTMOTIFAPOX1 occurs within 630 bp of the translation start site for *FAωH1* for both P1 and P2, with seven motifs present in each promoter. A second root-specific promoter element set, OSE1ROOTNODULE and OSE2ROOTNODULE, were also

present in multiple copies and have been attributed to root-specific expression during infection (Table 2.5; Veiweg et al., 2004). In *Arabidopsis*, the suberin-associated *CYP86A1* ω-hydroxylase is the only *CYP86A* gene characterized by root-specific expression. Therefore, the specificity of tissue expression may be used in the future as a tool for easy identification of the suberin-associated ω-hydroxylases in other species.

Table 2.5: *FAωH1* P1 Promoter Deletion Series with Systematic Removal of ABRE-like Elements
Twelve promoter deletion constructs were created through the systematic removal of sequence upstream of chosen ABRE-like promoter motifs. Sequences were PCR amplified and subcloned into pBI101 promoter expression vector to drive β-glucuronidase expression. Constructs 1, 5, 9 and 11 were utilized in preliminary promoter characterization by Anica Bjelica (Bjelica et al., submitted).

No.	Motif Name	Site	Signal Sequence
1.	MYB1AT	+266	WAACCA (AAACCA)
2.	DPBFCOREDCDC3	+399	ACACNNG (ACACCG)
3.	MYCCONSENSUSAT or EBOXBNNAPA (MYCCONS)	+/-460	CANNTG (CAAATG)
4.	MYCCONSENSUSAT or EBOXBNNAPA (MYCATERD1 + strand; MYCATRD22 - strand)	+/-675	CANNTG (+ CATGTG; -CACATG)
5.	RYREPEATBNNAPA	+/-782	CATGGCA
6.	MYBIAT	+828	WAACCA (AAACCA)
7.	LTRECOREATCOR15	+867	CCGAC
8.	MYCCONSENSUSAT or EBOXBNNAPA (MYCATERD1 + strand; MYCATRD22 - strand)	+/-986	CANNTG (+ CATGTG; -CACATG)
9.	MYCCONSENSUSAT or EBOXBNNAPA	+/-1170	CANNTG (CATTTG)
10.	MYBIAT	+/-1540	WAACCA (AAACCA)
11.	MYCCONSENSUSAT or EBOXBNNAPA (MYCATERD1 + strand; MYCATRD22 - strand)	+/-1764	CANNTG (+/- CATATG)
12.	FULL P1 PROMOTER	2056	

In addition to identifying both wound-inducible and root-specific motifs, stress responsive promoter elements are also an important area of focus in understanding the regulation of suberin biosynthesis. Cis-elements including ABA-Response Elements (ABREs; (PyACGTGG/TC)), MYB and MYC sites all have been functionally characterized as transcriptional elements responsive to ABA. Within suberin biosynthesis, the phenolic enzyme Phenylalanine Ammonia Lyase (PAL) has been demonstrated to be regulated in part by ABA (Bray, 1994; Giraudat et al., 1994; Busk and Pages, 1998; Kumar et al., 2010). Drought, salt-stress and wounding have also been demonstrated to effect ABA biosynthesis through transcriptional regulation, indicating the cross-talk that occurs between different stress pathways (Xiong and Zhu, 2003; Suttle et al., 2013).

Over three decades ago, wound-induced aliphatic suberin deposition in Russet Burbank potato tubers was found to be upregulated with the application of exogenous ABA (Soliday et al., 1978; Cottle and Kolattukudy 1982). Recently there has been significant progress in understanding the ABA signaling pathway, which has unveiled an "ABA signalosome" (Umezawa et al., 2010). Environmental signals trigger ABA to bind soluble PYR/PYL/RCAR receptors, causing SnRK2 protein kinase to be released from PPC2 protein phosphatase's negative regulation allowing phosphorylation of downstream factors such as AREB/ABF transcription factors and membrane proteins involving ion channels (Ma et al., 2009; Park et al., 2009; Umezawa et al., 2009). AREB/ABF transcription factors subsequently bind ABRE (ABA-responsive elements) and ABRE-like cis-elements to induce metabolic shifts in response to the original environmental stress (Umezawa et al., 2010). ABRE and ABRE-like elements are conserved cis-

elements that control gene expression by basic-domain leucine zipper (bZIP)-type transcription factors (Uno et al., 2000). Interestingly, WRKY transcription factors have also been reported to have a significant role in regulating ABA-responsive genes, suggesting that WRKY signaling may be connected to the ABA signaling pathway involving SnRKs (Jiang and Yu, 2009; Ren et al., 2010; Shang et al., 2010).

The *in silico* analysis of both *FAωH1* promoter alleles identified many ABA-like response elements including 13 MYB binding sites (MYB1AT, MYBCORE, MYBGAHV, MYBST1, MYBPZM), 13 WRKY/WBOX elements (WRKY710S, WBOXATNPR1, WBOXNTCHN48, WBOXHVIS01, WBOXNTERF3), 6 MYC (mycorrhiza) binding sites (MYCCONSENSUSAT or EBOXBNNAP, MYCATERD22, MYCATERD1), 5 ACGT-containing ABREs (ACGTATERD1, ABRERATICAL, ABRELATEDERD1, ACGTCBOX), and 4 stress responsive elements also known to be responsive to ABA (LTRECOREATCOR15, TBOXATGAPB, DPBFCOREDCDC3, RYREPEATBNNAPA) (Table 2.4). Careful analysis revealed the presence of a total 41 ABA responsive elements within the 2 kb of both the P1 and P2 promoter regions. One cluster of these elements accounted for a third of the total ABA responsive elements, and spanned from 200-600 bp upstream of the translation start site (Table 2.4). Clustering of ABA responsive elements suggests that these regions may contain a combination of regulatory elements that are critical to transcriptional activation or repression.

2.3.4.3 Construction of *FAωH1* Promoter Deletion Series

To determine if ABA responsive elements were critical to the induction of *FAωH1* post-wounding, a promoter deletion series was designed to remove previously characterized ABA response elements (Table 2.5). As two promoter alleles were identified in Russet Burbank, which had 89.6% sequence identity, the P1 promoter allele was chosen to generate the deletions series (referred to as P1). Twelve constructs of increasing size were created and subcloned into a pBI101 promoter expression vector for expression analysis. For the purpose of this analysis, the upstream 2 kb of sequence relative to the translation start site is referred to as the promoter, although other regulatory elements effecting transcription may be found outside this region.

Of the 12 constructs created, four were chosen for preliminary analysis using promoter::GUS fusions in transgenic hairy roots. Hairy roots are caused through infection of plant tissue with *Agrobacterium rhizogenes*, resulting in a DNA transfer from the bacterium, which causes prolific adventitious root formation (Willmitzer et al., 1982). Hairy roots provide an excellent model system of stable transformation resulting in root production that is inducible from any plant tissue (Makhzoum et al., 2012). Comparative analysis of hairy roots to normal developmentally produced roots in soybean has demonstrated that hairy-root suberin is very similar to wild-type, with the same composition of aliphatic suberin monomer classes in both tissues (Sharma, 2012). Therefore, using *A. rhizogenes* to transfer promoter expression vectors provides a stable transformation system for testing the *FAωH1* promoter expression.

Transgenic hairy roots were generated by introduction of the four *promoterFAωH1::GUS* constructs (plus empty vector control) into *A. rhizogenes* strain LBA9402 and used for inoculation of potato leaf tissue by Anica Bjelica (Bjelica et al.,

submitted). Treatment of transformed potato leaf tissue with ABA or water followed by GUS quantification 2 and 4 days post-treatment yielded no difference between treatments for a given construct. However, analysis of GUS expression from the four transgenic promoter constructs in hairy roots revealed significant variations in the level of *FAωH1* promoter activity based on promoter length (Figure 2.10). As each transformant in this study was from an independent transformant line, biological variation contributed to the high level of variation found in the GUS expression data. The longest P1 promoter sequence (1764 bp) induced measurable expression with its GUS expression set to a value of 1. All other constructs yielded higher expression, which is expressed relative to the 1764 bp P1 sequence. Two of the other tested P1 promoter constructs, 1170 and 266 bp, did not drive significantly increased GUS expression relative to the longest P1 sequence tested. Therefore, the first 266 bp upstream contains the critical regulatory sites necessary for *FAωH1* upregulation in response to water or ABA treatment. Interestingly, expression of GUS under the control of the 782 bp P1 promoter sequence yielded the highest expression of GUS.

The first 266 bp of the P1 promoter, that drove the same expression level as the 1764 bp sequence, contained multiple elements responsive to dehydration and ABA (refer to Table 2.5; MYBCORE, two MYBIAT, ACGTATERD1 and TBOXATGAPB). Cross-talk between abiotic stress response pathways makes it very challenging to elucidate regulatory mechanisms. Many wounding-inducible genes have also been previously shown to be induced by water stress, implying that dehydration may regulate response to mechanical wounding (Reymond et al., 2000). In addition, genes sensitive to touch are also involved in the mechanical wound response, and are upregulated quickly post-

wounding with phenolic metabolism (Reymond et al., 2000). ABA is tightly linked to gene expression in many drought or high-salinity genes, with an *Arabidopsis* microarray study finding that half of the genes induced by dehydration also are induced by ABA

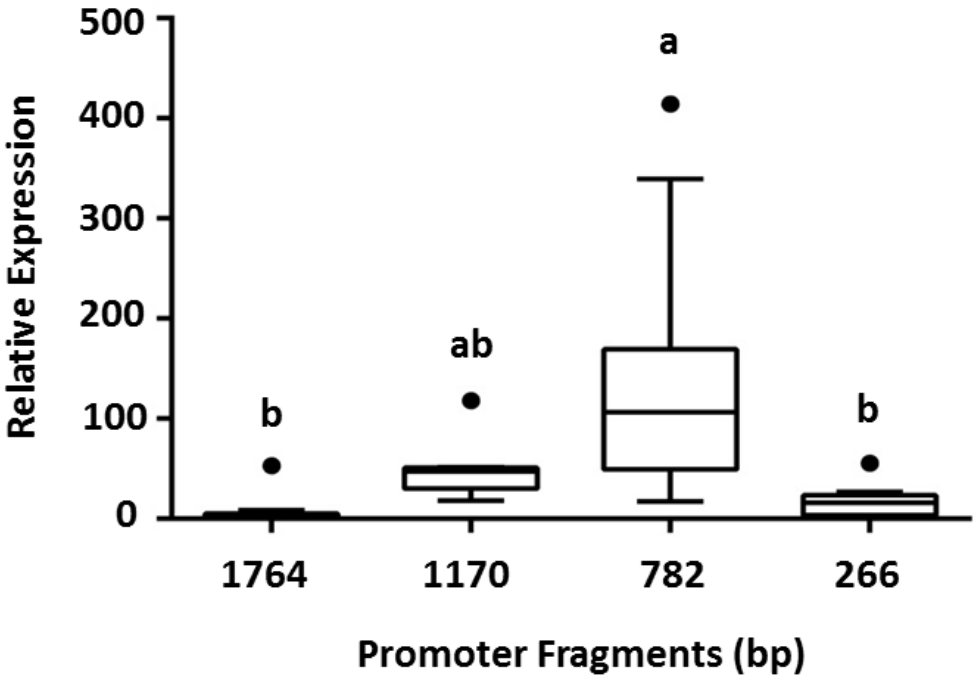

Figure 2.10: *β*-Glucuronidase Expression Driven by Russet Burbank *FAωH1* Promoter Deletion Series.
Four *promoterFAωH1::GUS* constructs of varying lengths were tested to investigate the GUS expression driven by P1 promoter sequences in response to wounding. Quantitative GUS assays were carried out using total protein extracts from tissue samples from hairy roots transformed with one of four *promoterFAωH1::GUS* constructs (plus an empty vector control). GUS activity was calculated and normalized to protein concentration. After correction for background fluorescence (from empty vector controls), GUS expression data were normalized to the level of expression in samples from full promoter constructs. Data are combined for all treatments (water and ABA), according to P1 promoter construct. Boxes labeled with the same letter denote expression levels not significantly different based on Welch's ANOVA followed by Games-Howell post-hoc test (p=0.05). Figure modified from Bjelica et al., submitted.

(Seki et al., 2002). In the short 266 bp P1 promoter construct, ABA-dependent transcription could be initiated through MYBCORE and MYBIATs (for ABA-dependent

and ABA-independent pathway review, see Yamaguchi-Shinozaki and Shinozaki, 2006). Although the ABA-treated hairy roots had higher GUS expression, there was no statistical difference between treatments for any of the constructs. This result would indicate that either the manipulation of the hairy roots for experimentation is enough to induce expression, perhaps through the touch response or stress due to the 4 hour incubation treatment, or that the ABA effect occurred at a different time post-treatment and was missed by this analysis.

Increased expression from the 782 bp P1 promoter construct coincided with the inclusion of an area of rich in ABRE-responsive elements (refer to Table 2.4 and Appendix 7a). Further experimentation including a more detailed promoter expression study would need to be done to determine if the increased GUS activity from this construct was due to the addition of regulatory enhancers related to ABA or wound-specific cis-elements. Also, it is unclear if the lower expression of the two longer constructs is due to the presence of unidentified transcriptional repressor binding sites.

2.4 Summary

Characterization of ω-hydroxylases in potato involved four CYP450 subfamilies, including *CYP86A, CYP86B, CYP94A* and *CYP704B.* Suberin is deposited both during development in a cell-specific manner as well as through induction by abiotic stress. To aid in identifying a suberin-associated ω-hydroxylase, the DCFI database of ESTs generated from abiotic stress treatment was screened using functionally characterized *CYP86A* and *CYP94A* subfamily members. Of the three candidates identified, transcription of *FAωH1* exhibited both root-specific expression as well as strong

induction two days post-wounding during suberin formation. Functional characterization of recombinant FAωH1 enzyme *in vitro* provided direct evidence of the conversion of C16 palmitate to C16 ω-hydroxypalmitate, confirming its role as an ω-hydroxylase. In addition, Anica Bjelica used the cv. Russet Burbank *FAωH1* coding region to complement the *Arabidopsis cyp86a1/horst* mutant showing *in vivo* ω-hydroxylation of C16 and C18:1 fatty acids during wound-induced suberization. Taken together, FAωH1 has been proven to be a suberin-associated ω-hydroxylase.

To begin to explore the regulation of *FAωH1*, an *in silico* analysis of the 2 kb promoter region from Phureja genome identified numerous motifs that had been characterized to induce root-specific expression, wound-induced expression and ABA-induced expression. Subsequent cloning and sequencing of the *FAωH1* promoter region from cv. Russet Burbank identified two different alleles with 89.6% sequence identity. One of these two alleles, P1, was chosen to construct a promoter deletion series to begin to characterize the *FAωH1* promoter region. In addition, Bernards' laboratory technician Anica Bjelica transformed four of the *FAωH1* promoter deletion constructs into *A. rhizogenes* to generate transgenic hairy root cultures. Interestingly, the mid-sized 782 bp *promoterFAωH1::GUS* constructs exhibited higher GUS expression than both the shorter and longer constructs. Future work will be to continue characterizing the regulation of *FAωH1* through promoter deletion constructs as well as to determine the major factors contributing to induction during suberin biosynthesis.

References

Angiosperm Phylogeny Group. 1998. An Ordinal Classification for the Families of Flowering Plants. Annals of the Missouri Botanical Garden 85: 531-553

Angiosperm Phylogeny Group. 2016. An Update of the Angiosperm Phylogeny Group Classification for the Orders and Families of Flowering Plants: APG IV. Botanical Journal of the Linnean Society doi:10.1111/boj.12385

Benveniste I, Tijet N, Adas F, Philipps G, Salaün JP, Durst F. 1998. *CYP86A1* from *Arabidopsis thaliana* Encodes a Cytochrome P450-dependent Fatty Acid omega-Hydroxylase. Biochemical and Biophysical Research Communications 243: 688-693

Benveniste I, Bronner R, Wang Y, Compagnon V, Michler P, Schreiber L, Salaün JP, Durst F, Pinot F. 2005. *CYP94A1*, a Plant Cytochrome P450-catalyzing Fatty Acid omega-Hydroxylase, is Selectively Induced by Chemical Stress in *Vicia sativa* Seedlings. Planta 221: 881-890

Bernards, MA. 2002. Demystifying Suberin. Canadian Journal of Botany 80: 227-240

Bray, EA. 1994. Alterations in Gene Expression in Response to Water Deficit. *In* Stress-Induced Gene Expression in Plants. Basra (ed), Harwood Academic, Amsterdam. pp 1-23

Busk PK, Pages M. 1998. Regulation of Abscisic Acid-Induced Transcription. Plant Molecular Biology 37: 425-435

Bjelica A, Haggitt ML, Woolfson KN, Lee D, Makhzoum AB, Bernards MA. 2016. Fatty Acid ω-Hydroxylases from *Solanum tuberosum*. Accepted providing revisions to Plant Cell Reports

Chen X, Want T, Lv B, Li J, Luo L, Lu S, Zhang X, Ma H, Ming F. 2014. The *NAC* Family Transcription Factor *OsNAP* Confers Abiotic Stress Response through the ABA Pathway. Plant and Cellular Physiology 55: 604-619

Cheong YH, Chang HS, Gupta R, Wang X, Zhu T, Luan S. 2002. Transcriptional Profiling Reveals Novel Interactions Between Wounding, Pathogen, Abiotic Stress, and Hormonal Responses in *Arabidopsis*. Plant Physiology 129: 661-677

Compagnon V, Diehl P, Benveniste I, Meyer D, Schaller H, Schreiber L, Franke R, Pinot F. 2009. *CYP86B1* is Required for Very Long Chain omega-Hydroxyacid and alpha, omega-Dicarboxylic Acid Synthesis in Root and Seed Suberin Polyester. Plant Physiology 150: 1831-1843

Cottle W, Kolattukudy PE. 1982. Abscisic Acid Simulation of Suberization. Plant Physiology 70: 775-780

Dean BB, Kolattukudy PE. 1976. Synthesis of Suberin during Wound-healing in Jade Leaves, Tomato Fruit, and Bean Pods. Plant Physiology 58: 411-416

Dobritsa AA, Shrestha J, Morant M, Pinot F, Matsuno M, Swanson R, Møller BL, Preuss D. 2009. *CYP704B1* is a Long-chain Fatty Acid omega-Hydroxylase Essential for Sporopollenin Synthesis in Pollen of *Arabidopsis*. Plant Physiology 151: 574-589

Du L, Chen Z. 2000. Identification of Genes Encoding Receptor-like Protein Kinases as Possible Targets of Pathogen- and Salicylic Acid-Induced *WRKY* DNA-Binding Proteins in *Arabidopsis*. The Plant Journal 24: 837-847

Duan H, Schuler MA. 2005. Differential Expression and Evolution of the *Arabidopsis CYP86A* Subfamily. Plant Physiology 137: 1067-1081

Elfmayan T, Tepfer M. 1995. Evaluation in Tobacco of the Organ Specificity and Strength of the *rolD* Promoter, Domain A of the 35S Promoter and the 35S2 Promoter. Transgenic Research 4: 388-396

Enstone DE, Peterson CA, Ma F. 2003. Root Endodermis and Exodermis: Structure, Function, and Response to the Environment. Journal of Plant Growth Regulation 21: 335-351

Euglem T. 2006. Dissecting the *WRKY* Web of Plant Defense Regulators. Public Library of Science (PLoS) Pathogen 2: e126

Giraudat J, Parcy F, Bertauche N, Gosti F, Leung J, Morris PC, Bouvier-Durand M, Vartanian N. 1994. Current Advances in Abscisic Acid Action and Signaling. Plant Molecular Biology 26: 1557-1577

Graça J, Cabral V, Santos S, Lamosa P, Serra O, Molinas M, Schreiber L, Kauder F, Franke R. 2015. Partial Depolymerization of Genetically Modified Potato Tuber Periderm Reveals Intermolecular Linkages in Suberin Polyester. Phytochemistry 117: 209-219

Graça J, Pereira H. 2000. Methanolysis of Bark Suberins: Analysis of Glycerol and Acid Monomers. Phytochemical Analysis 11: 45-51

Grausem B, Widemann E, Verdier G, Nosbusch D, Aubert Y, Beisson L, Schreiber L, Franke R, Pinot F. 2014. CYP77A19 and CYP77A20 Characterized from *Solanum tuberosum* Oxidize Fatty Acids *in vitro* and Partially Restore the Wild Phenotype in an *Arabidopsis thaliana* Cutin Mutant. Plant, Cell and Environment 37: 2102-2115

Hahn A, Kilian J, Mohrholz A, Ladwig F, Peschke F, Dautel R, Harter K, Berendzen KW, Wanke D. 2013. Plant Core Environmental Stress Response Genes are Systemically Coordinated during Abiotic Stress. International Journal of Molecular Sciences 14: 7617-7641

Holloway PJ. 1983. Some Variations in the Composition of Suberin from the Cork Layers of Higher-Plants. Phytochemistry 22: 495-502

Higo K, Ugawa Y, Iwamoto M, Korenaga T. 1999. Plant Cis-Acting Regulatory DNA Elements (PLACE) database: 1999. Nucleic Acids Research 27: 297-300

Höfer R, Briesen I, Beck M, Pinot F, Schreiber L, Franke R. 2008. The *Arabidopsis* Cytochrome P450 *CYP86A1* encodes a Fatty Acid omega-Hydroxylase Involved in Suberin Monomer Biosynthesis. Journal of Experimental Botany 59: 2347-2360

Jiang W, Yu D. 2009. *Arabidopsis WRKY2* Transcription Factor Mediates Seed Germination and Post-Germination Arrest of Development by Abscisic Acid. BioMed Central Plant Biology 9: 96

Johnson R, Wagner R, Verhey SD, Walker-Simmons MK. 2002. The ABA-Responsive Kinase PKABA1 Interacts with a Seed-Specific ABA Response Element Binding Factor, TaABF, and Phosphorylates TaABF Peptide Sequences. Plant Physiology 130: 837-846

Judd WS, Campbell CS, Kellog KA, Stevens PG, Donoghue MJ. 2016. Plant Systematics: A Phylogenetic Approach. 4th Ed. Sunderland, Massachusetts Sinauer Associates.

Kahn RA, Le Bouquin R, Pinot F, Benveniste I, Durst F. 2001. A Conservative Amino Acid Substitution Alters the Regiospecificity of CYP94A2, a Fatty Acid Hydroxylase from the Plant *Vicia sativa*. Archives of Biochemistry and Biophysics 391: 180-187

Kolattukudy PE. 1975. Biochemistry of Cutin, Suberin and Waxes, the Lipid Barriers on Plants. *In* Recent Advances in the Chemistry and Biochemistry of Plant Lipids. Galliard and Mercer (eds), Academic Press, New York. pp 203-246

Krishnamurthy P, Jyothi-Prakash PA, Qin L, He J, Lin Q, Loh C-S, Kumar PP. 2014. Role of Root Hydrophobic Barriers in Salt Exclusion of a Mangrove Plant *Avicennia officinalis*. Plant, Cell and Environment 37: 1656-1671

Kumar GN, Lulai EC, Suttle JC, Knowles NR. 2010. Age-induced Loss of Wound-Healing Ability in Potato Tubers is Partly Regulated by ABA. Planta 232: 1433-1445

Le Bouquin R, Pinot F, Benveniste I, Salaün JP, Durst F. 1999. Cloning and Functional Characterization of *CYP94A2*, a Medium Chain Fatty Acid Hydroxylase from *Vicia sativa*. Biochemical and Biophysical Research Communications 261: 156-162

Le Bouquin R, Skrabs M, Kahn R, Benveniste I, Salaün JP, Schreiber L, Durst F, Pinot F. 2001. *CYP94A5*, a New Cytochrome P450 from *Nicotiana tabacum* is able to Catalyze the Oxidation of Fatty Acids to the omega-Alcohol and to the Corresponding Diacid. European Journal of Biochemistry 268: 3083-3090

Lee DPN. 2010. Promoter Analysis of Potato (*Solanum tuberosum*) *Fatty Acid ω-Hydroxylase 1* (*FAωH1*). MSc Thesis, University of Western Ontario, Canada

Lescot M, Déhais P, Thijs G, Marchal K, Moreau Y, Van D Peer Y, Rouzé P, Rombauts S. 2002. PlantCARE, a Database of Plant Cis-Acting Regulatory Elements and a Portal to Tools for *in silico* Analysis of Promoter Sequences. Nucleic Acids Research 30: 325-327

Li Y, Beisson F, Koo AJ, Molina I, Pollard M, Ohlrogge J. 2007. Identification of Acyltransferases Required for Cutin Biosynthesis and Production of Cutin with Suberin-like Monomers. Proceedings of the National Academy of Sciences of the United States of America 104: 18339-18344

Li H, Pinot F, Sauveplane V, Werck-Reichhart D, Diehl P, Schreiber L, Franke R, Zhang P, Chen L, Gao Y, Liang W, Zhang D. 2010. Cytochrome P450 Family Member *CYP704B2* Catalyzes the {omega}-Hydroxylation of Fatty Acids and is Required for Anther Cutin Biosynthesis and Pollen Exine Formation in Rice. The Plant Cell 22: 173-190

Li-Beisson Y, Pollard M, Sauveplane V, Pinot F, Ohlrogge J, Beisson F. 2009. Nanoridges that Characterize the Surface Morphology of Flowers Require the Synthesis of Cutin Polyester. Proceedings of the National Acacdemy of Sciences of the United States of America 106: 22008-22013

Li-Beisson Y, Shorrosh B, Beisson F, Andersson MX, Arondel V, Bates PD, Baud S, Bird D, Debono A, Durrett TP, Franke RB, Graham IA, Katayama K, Kelly AA, Larson T, Markham JE, Miquel M, Molina I, Nishida I, Rowland O, Samuels L, Schmid KM, Wada H, Welti R, Xu C, Zallot R, Ohlrogge J. 2013. Acyl-Lipid Metabolism. The *Arabidopsis* Book 11: e0161. pp 24

Logemann J, Schnell J. 1989. Nucleotide Sequence and Regulated Expression of a Wound-Inducible Potato Gene (*wun1*). Molecular and General Genetics 219: 81-88

Ma Y, Szostkiewicz I, Korte A, Moes D, Yang Y, Christmann A, Grill E. 2009. Regulators of PP2C Phosphatase Activity Function as Abscisic Acid Sensors. Science 324: 1064-1068

Mackenzie F, Boa AN, Diego-Taboada A, Atkin SL, Sathyapalan T. 2015. Sporopollenin, the least known yet toughest natural biopolymer. Frontiers in Materials 2: 66

Makzoum AB, Sharma P, Bernards MA, Trémouillaux-Guiller J. 2012. Hairy Roots: An Ideal Platform for Transgenic Plant Production and Other Promising Applications. *In* Phytochemicals, Plant Growth, and the Environment. Gang (ed), Springer, New York. pp 95-142

Molina I, Li-Beisson Y, Beisson F, Ohlrogge JB, Pollard M. 2009. Identification of an *Arabidopsis* Feruloyl-Coenzyme A Transferase Required for Suberin Synthesis. Plant Physiology 151: 1317-1328

Naoumkina M, He X, Dixon R. 2008. Elicitor-Induced Transcription Factors for Metabolic Reprogramming of Secondary Metabolism in *Medicago truncatula*. BioMed Central Plant Biology 8: 132

Nelson D, Werck-Reichhart D. 2011. A P450-Centric View of Plant Evolution. The Plant Journal for Cell and Molecular Biology 66: 194-211

Pandey SP, Somssich IE. 2009. The Role of *WRKY* Transcription Factors in Plant Immunity. Plant Physiology 150: 1648-1655

Park SY, Fung P, Nishimura N, Jensen DR, Fujii H, Zhao Y, Lumba S, Santiago J, Rodrigues A, Chow TF, Alfred SE, Bonetta D, Finkelstein R, Provart NJ, Desveaux D, Rodriguez PL, McCourt P, Zhu JK, Schroeder JI, Volkman BF, Cutler SR. 2009. Abscisic Acid Inhibits Type 2C Protein Phosphatases via the PYR/PYL Family of START Proteins. Science 324: 1068-1071

Pinot F, Benveniste I, Salaün JP, Durst F. 1998. Methyl Jasmonate Induces Lauric Acid omega-Hydroxylase Activity and Accumulation of *CYP94A1* Transcripts but does not affect Epoxide Hydrolase Activities in *Vicia sativa* Seedlings. Plant Physiology 118: 1481-1486

Pinot F, Benveniste I, Salaün JP, Loreau O, Noël JP, Schreiber L, Durst F. 1999. Production *in vitro* by the Cytochrome P450 *CYP94A1* of Major C18 Cutin Monomers and Potential Messengers in Plant-Pathogen Interactions: Enantioselectivity Studies. Biochemical Journal 342: 27-32

Pinot F, Skrabs M, Compagnon V, Salaün JP, Benveniste I, Schreiber L, Durst F. 2000. omega-Hydroxylation of Epoxy- and Hydroxy-Fatty Acids by *CYP94A1*: Possible Involvement in Plant Defence. Biochemical Society Transactions 28: 867-870

Pompon D, Louerat B, Bronine A, Urban P. 1996. Yeast Expression of Animal and Plant P450s in Optimized Redox Environments. Methods in Enzymology 272: 51-64

Ranathunge K, Schreiber L, Franke R. 2011. Suberin Research in the Genomics Era- New Interest for an Old Polymer. Plant Science 180: 399-413

Ren X, Chen Z, Liu Y, Zhang H, Zhang M, Liu Q, Hong X, Zhu JK, Gong Z. 2010. *ABO3*, a *WRKY* Transcription Factor, Mediates Plant Responses to Abscisic Acid and Drought Tolerance in *Arabidopsis*. The Plant Journal for Cell and Molecular Biology 63: 417-429

Reymond P, Weber H, Damond M, Farmer EE. 2000. Differential Gene Expression in Repsonse to Mechanical Wounding and Insect Feeding in *Arabidopsis*. The Plant Cell 12: 707-719

Rupasinghe SG, Duan H, Schuler MA. 2007. Molecular Definitions of Fatty Acid Hydroxylases in *Arabidopsis thaliana*. Proteins 68: 279-293

Rushton PJ, Torres JT, Parniske M, Wenert P, Hahlbrock K, Somssich IE. 1996. Interaction of Elicitor-Induced DNA-Binding Proteins with Elicitor Response Elements in the Promoters of Parsley *PR1* Genes. The EMBO Journal 15: 5690-5700

Sambrook J, Fritschi EF, Maniatis T. 1989. Molecular Cloning: A Laboratory Manual. Cold Spring Harbor Laboratory Press, New York. pp 362-364

Sauveplane V, Kandel S, Kastner PE, Ehlting J, Compagnon V, Werck-Reichhart D, Pinot F. 2009. *Arabidopsis thaliana* CYP77A4 is the First Cytochrome P450 Able to Catalyze the Epoxidation of Free Fatty Acids in Plants. The FEBS Journal 276: 719-735

Schnurr J, Shockey J, Browse J. 2004. The Acyl-CoA Synthetase Encoded by *LACS2* is Essential for Normal Cuticle Development in *Arabidopsis*. The Plant Cell 16: 629-642

Scott RJ. 1994. Pollen Exine—the Sporopollenin Enigma and the Physics of Pattern. *In* Molecular and Cellular Aspects of Plant Reproduction. Scott and Stead (eds), Acaedemy Press, London. pp 49-81

Serra O, Soler M, Hohn C, Sauveplane V, Pinot F, Franke R, Schreiber L, Prat S, Molinas M, Figueras M. 2009. *CYP86A33*-Targeted Gene Silencing in Potato Tuber Alters Suberin Composition, Distorts Suberin Lamellae, and Impairs the Periderm's Water Barrier Function. Plant Physiology 149: 1050-1060

Serra O, Chatterjee S, Figueras M, Molinas M, Stark RE. 2014. Deconstructing a Plant Macromolecular Assembly: Chemical Architecture, Molecular Flexibility, and Mechanical Performance of Natural and Engineered Potato Suberins. Biomacromolecules 15: 799-811

Sharma, P. 2012. Hairy Roots as a Model to Investigate the Role of Suberin in the *Phytophthora sojae*-soybean pathosystem. Electronic Thesis and Dissertation Repository 677. pp 38

Shang Y, Yan L, Liu ZQ, Cao Z, Mei C, Xin Q, Wu FQ, Wang XF, Du SY, Jiang T, Zhang XF, Zhao R, Sun HL, Liu R, Yu YT, Zhang DP. 2010. The Mg-chelatase H subunit of *Arabidopsis* antagonizes a group of *WRKY* transcription repressors to relieve ABA-responsive genes of inhibition. The Plant Cell 22: 1909-1935

Sievers F, Wilm A, Dineen D, Gibson TJ, Karplus K, Li W, Lopez R, McWilliam H, Remmert M, Söding J, Thompson JD, Higgins DJ. Fast, Scalable Generation of High-Quality Protein Multiple Sequence Alignments using ClustalOmega. Molecular Systems Biology 7: 539

Soler M, Serra O, Molinas M, Huguet G, Fluch S, Figueras M. 2007. A Genomic Approach to Suberin Biosynthesis and Cork Differentiation. Plant Physiology 144: 419-431

Soliday CL, Kolattukudy PE. 1978. Midchain Hydroxylation of 16-Hydroxypalmitic Acid by the Endoplasmic Reticulum Fraction from Germinating *Vicia faba*. Archives of Biochemistry and Biophysics 188: 338-347

Sprenger-Haussels M, Weisshaar B. 2000. Transactivation Properties of Parsley Proline-Rich *bZIP* Transcription Factors. The Plant Journal 22: 1-8

Stanford A, Bevan M, Northcote D. 1989. Differential Expression within a Family of Novel Wound-Induced Genes in Potato. Molecular and General Genetics 215: 200-208

Suttle JC, Lulai EC, Huckle LL, Neubauer JD. 2013. Wounding of Potato Tubers Induces Increases in ABA Biosynthesis and Catabolism and Alters Expression of ABA Metabolic Genes. Journal of Plant Physiology 170: 560-566

Tijet N, Helvig C, Pinot F, Le Bouquin R, Lesot A, Durst F, Salaün JP, Benveniste I. 1998. Functional Expression in Yeast and Characterization of a Clofibrate-Inducible Plant Cytochrome P-450 (*CYP94A1*) Involved in Cutin Monomers Synthesis. Biochemical Journal 332: 583-589

Umezawa T, Sugiyama N, Mizoguchi M, Hayashi S, Myouga F, Yamaguchi-Shinozaki K, Ishihama Y, Hirayama T, Shinozaki K. 2009. Type 2C Protein Phosphatases Directly Regulate Abscisic Acid-Activated Protein Kinases in *Arabidopsis*. Proceedings of the National Academy of Sciences of the United States of America 106: 17588-17593

Umezawa T, Nakashima K, Miyakawa T, Kuromori T, Tanokura M, Shinozaki K, Yamaguchi-Shinozaki K. 2010. Molecular Basis of the Core Regulatory Network in ABA Responses: Sensing, Signaling and Transport. Plant and Cell Physiology 51: 1821-1839

Uno Y, Furihata T, Abe H, Yoshida R, Shinozaki K, Yamaguchi-Shinozaki K. 2000. *Arabidopsis* Basic Leucine Zipper Transcription Factors Involved in an Abscisic Acid-Dependent Signal Transduction Pathway under Drought and High-Salinity Conditions. Proceedings of the National Academy of Sciences of the United States of America 97: 11632-11637

Urban P, Mignotte C, Kazmaier M, Delorme F, Pompon D. 1997. Cloning, Yeast Expression, and Characterization of the Coupling of Two Distantly Related *Arabidopsis thaliana* NADPH-Cytochrome P450 Reductases with P450 *CYP73A5*. The Journal of Biological Chemistry 272: 19176-19186

Vieweg MF, Frühling M, Quandt HJ, Heim U, Bäumlein H, Pühler A, Küster H, Andreas MP. 2004. The Promoter of the Vicia faba L. Leghemoglobin Gene *VfLb29* is Specifically Activated in the Infected Cells of Root Nodules and in the Arbuscule-Containing Cells of Mycorrhizal Roots from Different Legume and Nonlegume Plants. Molecular Plant-Microbe Interactions 17: 62-69

Vishwanath SJ, Delude C, Domergue F, Rowland O. Suberin: Biosynthesis, Regulation, and Polymer Assembly of a Protective Extracellular Barrier. Plant Cell Reports 34: 573-586

Wellesen K, Durst F, Pinot F, Benveniste I, Nettesheim K, Wisman E, Steiner-Lange S, Saedler H, Yephremov A. 2001. Functional Analysis of the *LACERATA* Gene of *Arabidopsis* Provides Evidence for Different Roles of Fatty Acid ω-Hydroxylation in Development. Proceedings of the National Academy of Sciences of the United States of America 98: 9694-9699

Werck-Reichhart D, Bak S, Paquette S. 2002. Cytochromes P450. The *Arabidopsis* Book 9:e0144 1-28

Wiermann R, Ahlers F, Schmitz-Thom I. 2005. Sporopollenin. Biopolymers Online 1: 209-227

Willmitzer L, Sanchez-Serrano J, Buschfeld E, Schell J. 1982. DNA from *Agrobacterium rhizogenes* is transferred to and expressed in axenic hairy root plant tissues. Molecular Genetics and Genomics 186: 16-22

Xiao F, Goodwin SM, Xiao Y, Sun Z, Baker D, Tang X, Jenks MA, Zhou JM. 2004. *Arabidopsis CYP86A2* Represses *Pseudomonas syringae* Type III Genes and is Required for Cuticle Development. The EMBO Journal 23: 2903-2913

Xiong L, Zhu JK. 2003. Regulation of Abscisic Acid Biosynthesis. Plant Physiology 133: 29-36

Xu X, Pan S, Cheng S, Zhang B, Mu D, Ni P, Zhang G, Yang S, Li R, Wang J, Orjeda G, Guzman F, Torres M, Lozano R, Ponce O, Martinez D, De la Cruz G, Chakrabarti SK, Patil VU, Skryabin KG, Kuznetsov BB, Ravin NV, Kolganova TV, Beletsky AV, Mardanov AV, Di Genova A, Bolser DM, Martin DM, Li G, Yang Y, Kuang H, Hu Q, Xiong X, Bishop GJ, Sagredo B, Mejia N, Zagorski W, Gromadka R, Gawor J, Szczesny P, Huang S, Zhang Z, Liang C, He J, Li Y, He Y, Xu J, Zhang Y, Xie B, Du Y, Qu D, Bonierbale M, Ghislain M, Herrera Mdel R, Giuliano G, Pietrella M, Perrotta G, Facella P, O'Brien K, Feingold SE, Barreiro LE, Massa GA, Diambra L, Whitty BR, Vaillancourt B, Lin H, Massa AN, Geoffroy M, Lundback S, DellaPenna D, Buell CR, Sharma SK, Marshall DF, Waugh R, Bryan GJ, Destefanis M, Nagy I, Milbourne D, Thomson SJ, Fiers M, Jacobs JM, Nielsen KL, Sonderkaer M, Iovene M, Torres GA, Jiang J, Veilleux RE, Bachem CW, de Boer J, Borm T, Kloosterman B, van Eck H, Datema E, Hekkert BL, Goverse A, van Ham RC, Visser RG. 2011. Genome Sequence and Analysis of the Tuber Crop Potato. Nature 475: 189-195

Yan B, Stark RE. 2000. Biosynthesis, Molecular Structure, and Domain Architecture of Potato Suberin: a 13C NMR Study using Isotopically Labeled Precursors. Journal of Agricultural and Food Chemistry 48: 3298-3304

Yang W, Bernards MA. 2007. Metabolomic Analysis of Wound-Induced Suberization in Potato (*Solanum tuberosum* L.) Tubers. Metabolomics 3: 147-159

Chapter 3

Effect of Abscisic Acid on Wound-Induced Suberin Deposition in *Solanum tuberosum* L. cv. Russet Burbank

3.1 Introduction

Complex cross-talk between plant hormones drives normal plant growth and development, as well as initiates biotic and abiotic stress responses. Each of the hormone classes and/or types[8] has been found to play a unique role in a variety of plant processes, but the complexity of their interactions hinders the full understanding of their individual regulatory roles. For example, the regulation of cellular response to wounding involves four major hormones: salicylic acid, jasmonates, ethylene and abscisic acid (ABA) (Savatin et al., 2014). Teasing apart the individual post-wounding roles of each hormone has arisen from more than 60 years of plant research. Changes in hormone concentrations occur rapidly post-wounding, and are presumed to function as a signaling response to initiate sealing the wound site (Lulai and Suttle, 2004; Lulai et al., 2011, Boher et al., 2013). However, the fundamental understanding of how these hormones work either individually or synergistically to initiate and sustain gene expression that drives the wound response is still unknown.

---

[8] Auxins, cytokinins, gibberelins, ethylene, ABA (abscisic acid), jasmonates, salicylic acid, brassinosteroids and peptide hormones

In response to a wounding event, the cells surrounding a wound site synthesize and deposit the complex biopolymer called suberin. The function of suberin is to seal the tissues at the wound site, providing protection from water loss and invading pathogens (Vishwanath et al., 2015). The regulation of wound-induced suberin biosynthesis and deposition has been difficult to investigate due to the complexity of the biopolymer itself and the variety of plant processes activated upon wounding (Vishwanath et al., 2015).

Suberin biosynthesis requires the coordination of two major plant metabolic pathways, phenylpropanoid biosynthesis and fatty acid biosynthesis, yielding phenolic and aliphatic monomers, respectively, that are polymerized to form suberin (Bernards, 2002). The phenolic monomers include hydroxycinnamic acids, amides and esters while the aliphatic monomers consist of fatty acids, alcohols, ω-hydroxy fatty acids and α,ω dioic acids. More than 80 enzymatic reactions are required for the production of phenolic and aliphatic monomers alone, prior to their transport and incorporation interior to the cell wall. Once at the site of incorporation, monomers may be esterified together through functional groups to create an insoluble matrix (insolubles) or freely incorporated without becoming covalently-linked to create the waxes (solubles) associated with the polymer (Li-Beisson et al., 2013; Vishwanath et al., 2015).

Wound-induced suberization involves two stages, first the formation of the closing layer followed by development of the wound periderm (Lulai and Neubauer, 2014). The closing layer is formed during the first 7 days in parenchyma cells surrounding the wound site, to provide an initial barrier at the wound site against water loss and pathogen attack. Subsequently, the wound periderm is formed over the next 40 days from newly developed meristematic tissue called the phellogen, which deposits

structured rows of phellem to provide a more substantial and long-term barrier. Due in part to the complexity of suberin biosynthesis and deposition, which requires tight regulation both spatially and temporarily of individual genes as well as entire biosynthetic pathways, hormone regulation of these processes has not been thoroughly investigated to date.

Previous research indicates ABA has a primary role in maintaining water balance in the plant, as it has been demonstrated to affect drought (Shinozaki and Yamaguchi-Shinozaki, 2007) and salt stress responses (Wang et al., 2015) as well as aquaporin gene expression contributing to stomatal closure (Grondin et al., 2015). In the context of aliphatic suberin biosynthesis, ABA plays a role in upregulation of 18:1 ω-hydroxy fatty acids and α, ω-dioic acids (Soliday et al., 1978), as well as to impact the functionality of the suberin barrier in potato tubers as measured by the resistance of water vapour diffusion across wounded surface tissue (Cottle and Kolattukudy, 1982). In a follow up study to this early work, Lulai et al. (2008) wounded potato tuber tissue and treated it with ABA as well as fluridone (FD), a carotenoid biosynthesis inhibitor that blocks the production of precursors to ABA biosynthesis (see Figure 3.1). Using a qualitative study based on histochemical staining and subsequent microscopy, the effect of ABA application and FD inhibition of ABA biosynthesis was explored. Both decreased accumulation of aliphatic and phenolic components and as well as a significantly increased water loss post-wounding resulted from treatment with FD (Lulai et al., 2008). However, there has been no quantitative study to determine the scope of ABA's effect on the initiation of suberization or to begin to elucidate ABA's regulatory involvement in the

many biosynthetic pathways required to generate modified phenolic and aliphatic monomers for suberin.

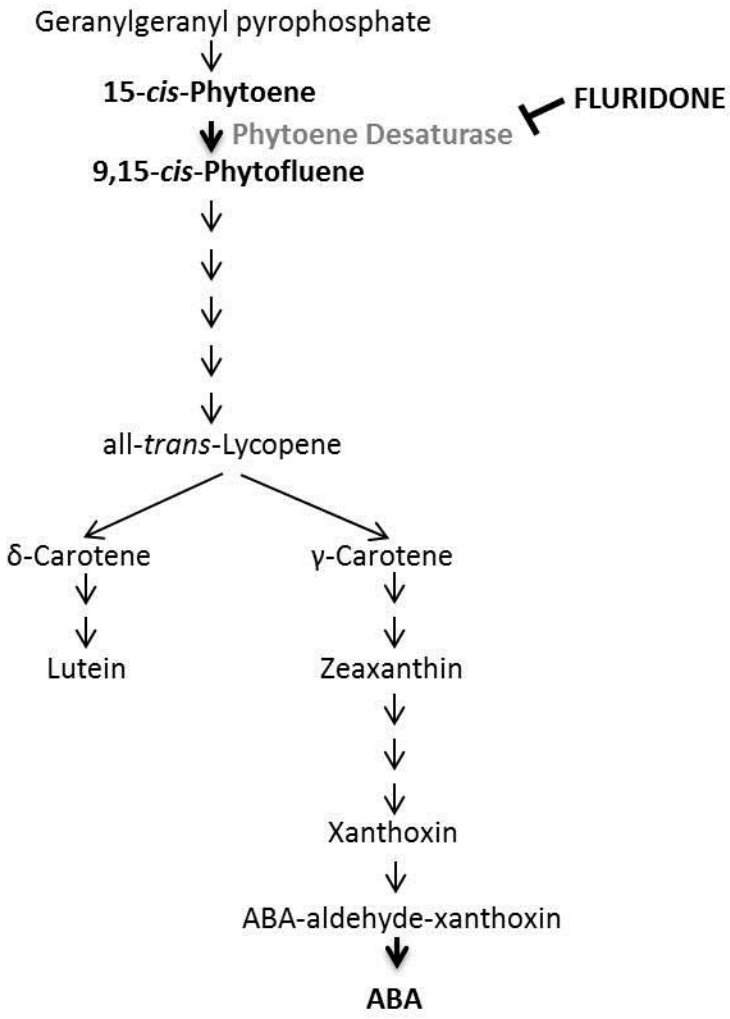

Figure 3.1 Simplified carotenoid biosynthetic pathways leading to ABA biosynthesis. Geranylgeranyl pyrophosphate is used to generate 15-*cis*-phytoene that is subsequently desaturated to produce 9,15-*cis*-phytoene by the enzyme phytoene desaturase. Treatment of tissue with fluridone severely inhibits phytoene desaturase, resulting in an absence of carotenoid biosynthesis as well as the production of ABA.

From the characterization of *Solanum tuberosum* Russet Burbank *Fatty Acid ω-Hydroxylase 1* (*FAωH1*) wound-induced gene expression, it was determined that initiation of gene expression matched temporally with the upregulation of aliphatic

metabolism two days post-wounding (refer to Figure 2.6b). *In silico* analysis of the 2 kb upstream *FAωH1* promoter region uncovered an interesting finding, as there were 41 ABA-like responsive elements relative to only a handful of other hormone-related promoter motifs (refer to Table 2.4 and Appendices 7a and 7b). The prevalence of ABA-related motifs indicates a strong role for ABA in *FAωH1* gene regulation. Regulation of the fatty acid ω-hydroxylation is important during suberization, as more than 55% of aliphatic suberin monomers undergo this oxidation prior to incorporation into the suberin biopolymer (Holloway, 1983, Bernards, 2002). Kumar et al. (2010) recently established that application of exogenous ABA enhanced PAL1 transcription, part of phenolic suberin biosynthesis. In addition, the interplay between ABA and salicylic acid in regulation of feruloyl-CoA transferase (FHT) also confirms a role for ABA in regulating aliphatic suberin biosynthesis (Boher et al., 2013). Thus, ABA is a strong candidate for the role as master regulator, coordinating both phenolic and aliphatic biosynthetic genes to produce suberin.

With a recent resurgence of interest in suberin in plant research as well as sequencing of the *Phureja* genome (an ancestral diploid parent of *S. tuberosum;* Xu et al., 2011), many key suberin-associated genes in potato have now been identified and functionally characterized (Vishwanath et al., 2015). In this study, the expression profiles of five previously characterized suberin-associated genes were investigated as well as the *Solanum tuberosum CYP86A* and *CYP94A* multi-gene subfamilies. For suberin-associated genes, three of the chosen genes had been previously characterized in *Solanum tuberosum* (*FAωH1 (CYP86A33)* from Chapter 2 of this thesis and Serra et al., 2009a; *KCS6* from Serra et al., 2009b; *PAL1* from Kumar et al., 2010). The other two genes were identified

through *in silico* analysis of the Phureja genome based on sequence similarity to previously characterized *Arabidopsis* orthologs (*FHT* from Serra et al., 2010; *CYP86B1* from Compagnon et al., 2009, Molina et al., 2009).

Each suberin-associated gene in this study was strategically included as they represent key reactions in the production of suberin. Initiation of suberin monomer deposition begins with phenolics, with PAL1 catalyzing the production of trans-cinnamic acid, representing the first step in suberin-associated metabolism from the phenylpropanoid pathway (Bernards, 2002). As a proxy for the shift from phenolic to aliphatic metabolism, FHT has been characterized to act as a bridge conjugating ferulic acid with ω-hydroxyacids and alcohols (Gou et al., 2009; Molina et al., 2009; Serra et al., 2010; Boher et al., 2013). Within aliphatic metabolism, KCS6 has been established as a suberin-associated keto-acyl synthase, involved in fatty acid elongation (Serra et al., 2009b). And finally, as the majority of aliphatic monomers undergo ω-hydroxylation prior to incorporation, both FAωH1 and CYP86B1 characterized suberin-associated fatty acid ω-hydroxylases were included (Chapter 2; Serra et al., 2009a; Compagnon et al., 2009, Molina et al., 2009). The potato CYP subfamilies are putative ω-hydroxylases and/or ω-oxidases (refer to Chapter 2), and the extent of the different gene family members involvement in suberization had not been explored. These uncharacterized *CYP86A* and *CYP94A* gene families were all identified through *in silico* analysis of the Phureja genome database.

This study was designed to coordinate the effects of FD and ABA treatement on both the expression profiles of suberin-associated genes with changes in the identity and quantity of aliphatic suberin monomers. Thus, the goals of the present research were two-

fold: first, to investigate role of ABA in regulation of these suberin-associated genes, and second, to identify the metabolic changes in wound-induced aliphatic suberin biosynthesis and deposition after treatment with ABA and FD.

3.2 Materials and Methods

Eight month old *Solanum tuberosum* cv. Russet Burbank tubers were surface-sterilized in 20% v/v bleach for 20 minutes, transferred to a laminar flow cabinet, washed thoroughly with sterilized distilled water (dH_2O), and sectioned into 2 cm thick slices. Slices were subdivided into three treatments: (1) dH_2O -washed control, (2) 10^{-4} M FD, and (3) both 10^{-4} M ABA and 10^{-4} M FD. Previous studies had determined 10^{-4} M ABA to be the optimal concentration for exogenous application during suberin formation (Soliday et al., 1978; Cottle and Kolattukudy, 1982). Tuber slices were rinsed briefly in dH_2O to remove excess starch then incubated 4 hours in 1 L of treatment solution. FD and ABA (100mM) were dissolved in dimethyl sulfoxide (DMSO) and diluted with dH_2O to the final concentration (10^{-4} M). DMSO was added to 0.1% v/v in the dH_2O control treatment. The treatment solutions were exchanged for fresh solutions at the mid-point of the incubation. Tuber slices were rinsed and placed upright in a sterile Magenta box on a 1 cm elevated mesh platform covering a wetted No.1 Whatman paper (to maintain a high humidity environment). All treatments were incubated in the dark at 28ºC for 1 to 14 days; with day 0 replicates being processed immediately after treatment (at 4 hours post-wounding).

To harvest tissue, the 1 cm thick tuber slices were sampled perpendicular to the cut faces with a No. 9 copper cork borer (VWR). Using a razor blade, the top and bottom tissue of the resulting tuber cylinders were quickly excised to create 1-2 mm thick tuber

discs. For each time-point, 12 tuber discs from the same tuber slice were pooled to create one sample, with three different sample replicates collected per treatment/timepoint. The 12 individual tuber discs from each sample replicate were randomly subdivided into: (1) 4-disc individual replicate for ABA quantification; (2) 4-disc pooled treatment/timepoint sample for RNA extraction; and (3) 4-disc individual replicate for aliphatic monomer composition analysis. All harvested tissue was quickly subdivided, flash frozen with liquid N_2 and stored at -80ºC until processed.

3.2.1 *ABA Quantification with LC-MS*

Extraction of ABA was done for all individual replicates throughout the 14-day treatment time-course and quantified using LC-MS (Liquid Chromatography with Mass Spectroscopy). Frozen 4-disc replicates were ground to a fine powder under liquid N_2 with a mortar and pestle and aliquoted into 1 g subsamples. To each sample, 5 mL ice-cold 90% v/v methanol containing 0.1% v/v acetic acid was added as well as 20 µL of each ABA-D_4 standard (2.5 µg/mL). Tissue was incubated with occasional stirring for five minutes, and then transferred to 15 mL centrifuge tube. The mortar and pestle were washed three times with 3 mL ice-cold 90% v/v methanol with 0.1% v/v acetic acid solution, which was added to the initial 5 mL extraction. Samples were centrifuged at 12000 x g for 10 minutes, and supernatant transferred to 25 mL round-bottom flasks to evaporate solvent under vacuum at 40ºC using a roto-evaporator (Buchi, Switzerland). When less than 1.5 mL liquid extract remained, samples were transferred to 1.5 mL microcentrifuge tubes and centrifuged at 15000 x g for 5 minutes. Supernatant was transferred for analysis to a LC vial containing a micro-volume insert (Agilent). For LC-

MS analysis, 100 µL sample were injected onto a Zorbax C-18 column (3.0 x 50 mm, 1.8 µm; Agilent Technologies, USA) attached to an Agilent 1260 LC system and eluted with the following solvent gradient (solvent A = 0.1% v/v formic acid in Milli-Q H_2O; solvent B = 0.1% v/v formic acid in 90% v/v acetonitrile); start condition, 20% v/v B in A, followed by a three step gradient to 60% v/v B in A over 4.5 minutes, 80% v/v B in A over 3 minutes and finally 100% B over 2.5 minutes. After 2 minutes at 100% B, the initial conditions were restored over 1 minute followed by a 7 minute equilibration before the next sample was injected. The solvent flow rate was 0.3 mL/min. Compounds were detected by UV absorbance (240 nm) and ESI-TOF-MS in negative ion mode. The ESI-TOF parameters were: drying gas at 350ºC, 10 mL/min; nebulizer at 45 PSI; Vcap at 4000 V; Fragmentor at 150 V. Spectra were collected at 1.03/sec (9729 transients/spectrum) in the 100-1000 m/z range. Reference mass solution (112.985587 m/z and 1033.988109 m/z) were infused constantly via a second nebulizer at 15 psi. ABA ($[M-H]^-$ = 263.1289) was quantified using the ABA-D_4 ($[M-H]^-$ = 267.1540) peak area as an internal calibration standard, using Agilent Mass Hunter Qualitative Analysis software (V B05) (Agilent Technologies, USA).

3.2.2 *Semi-Quantitative RT-PCR for Suberin-Associated Gene Expression*

Roots, leaves, tuber periderm and tuber parenchyma tissue from *S. tuberosum* plants grown in the lab under ambient light in Promix soil were harvested, flash frozen in liquid N_2 and stored at -80ºC. These four tissues in addition to the individual replicates from the ABA/FD experimental timecourse previously collected and flash frozen were used for RNA extraction using hot phenol-chloroform (Sambrook et al., 1989). To

remove any DNA contamination, RNA was treated with DNaseI (Invitrogen) and quantified spectrophotometrically at 260 nm and 280 nm to determine concentration and purity of the RNA. cDNA synthesis using the Superscript™II RT kit (Invitrogen) generated templates for semi-quantitative RT-PCR. Primers were designed for five suberin-associated potato genes as well as the *CYP86A* and *CYP94A* ω-hydroxylase multi-gene families to determine tissue-specific gene expression (Table 3.1). All primers were 18-24 bp in length within a predicted DNA melting temperature (T_m) range of 50-66ºC and contained minimal predicted secondary structure (as predicted using DNAMAN; Lynnon Corporation, 2005). Using a Biorad iCycler thermocycler, PCR was performed on suberin and leaf control cDNA templates using suberin-associated gene primers as well as a housekeeping control gene *ef1-α* (Nicot et al., 2005). To optimize primers, multiple reactions spanning temperature and Mg^{2+} concentrations were used to determine ideal conditions to produce a single product of expected size. PCR products were loaded into a 1% to 1.2% agarose gel containing 2.5 µM ethidium bromide to stain PCR products (agarose dissolved using heat in 1X Tris-Acetate-EDTA (TAE) buffer with ethidium bromide subsequently added) and electrophoresed at 100 mV. PCR products were visualized using ChemiDoc XRS with Quantity One 1-D Analysis software (BioRad). After choosing ideal temperature and salt concentrations, the semi-QT cycle number was optimized for each primer set to determine the exponential growth cycle number. Bands were quantified using Quantity One 1-D Analysis software (BioRad) and plotted to determine the cycle corresponding with exponential amplification of template, which was identified and used for semi-quantitative RT-PCR expression analysis.

Table 3.1: Primer Sequences and Conditions for Semi-Quantitative RT-PCR of cv. Russet Burbank Suberin-Associated *CYP86A* and *CYP94A* ω-hydroxylases.
Primers used to amplify individual suberin-associated genes in different plant tissues and throughout the ABA/FD experimental timecourse.

Gene	Primer Name: Sequence	Product size (bp)	T_m (^oC)
PAL1	PAL1F: 5'GCGATTTTCGCTGAAGTG	596	54
	PAL1R: 5'TCTTGCTCGGCACTCTGA		
FHT	StFHTex1ex2F: 5'TCACTATGCAAGGAACAATCAC	385	50
	StFHTex2R: 5'GTATTATCACCAATATCCTCTATG		
KCS6	StKCS6ex1ex2F: 5'TCTGCACAAATTTGGTAACACATC	200	57
	StKCS6ex2R: 5'TCTGGGATGAACACTGGGT		
FAωH1 (*CYP86A33*)	TC114700PotF: 5'TTTCCTTTTATCTCCTAGCAC	750	54
	TC114700PotR: 5'TAAATCATCTGATGGACTTTCC		
StCYP86B	StCYP86B1ex1F: 5'TTGTCACTCCCACGCTTGTA	495	53
	StCYP86B1ex1ex2R: 5'CAACTCTTTGTGATCAACTG		
FAωH2 (*CYP86A69*)	TC120302PotF: 5'CAACGGGTATGATGATTGTAGC	950	57
	TC120302PotR: 5'TCTCGGGTTCAAGCTGACAAGC		
FAωH3 (*CYP86A68*)	StCYP86A68FAωH3F: 5'AATCTCCGTGCGTGTGGT	600	57
	StCYP86A68FAωH3R: 5'TTCCAAGCCCAAGCCATT		
FAωO1 (*CYP94iA26*)	EST716349PotF: 5'ATTCGACCCCTCAATTTCCAC	600	54
	EST716349PotR: 5'CTCCCTCTGTTTCTCCCTC		
FAωO2 (*CYP94A24*)	StCYP94A24FAωO2F: 5'TTATTTATTGCCATCTCTACCAC	500	50
	StCYP94A24FAωO2R: 5'CAAAGTGAAGCGTGTGTG		

Gene	Primer Name: Sequence	Product size (bp)	T_m (^oC)
FAωO3 (*CYP94A25*)	StCYP94A25FAωO3F: 5'TCCCGTCCCTGTTGATAC	385	53
	StCYP94A25FAωO3R: 5'GCTCCTCACCTTCATCCA		
ef1-α	EF1-ALPHA400F: 5'TCACTGCCCAGGTCATCATC	400	57
	EF1-ALPHA400R: 5'GGAACACCAGCATCACACTG		

For determining expression patterns for suberin-associated genes and *CYP86A* and *CYP94A* subfamilies, root, leaf, periderm and parenchyma as well as ABA/FD-treated tuber tissue were used. To enable normalization of gene expression with *ef1-α* for each treatment/time point, each PCR mastermix contained cDNA for one treatment/time point, PCR buffer, $MgCl_2$, dH_2O, dNTPs and *Taq* polymerase (Invitrogen). The mastermix was thoroughly mixed and aliquoted for the addition of each suberin-associated gene forward and reverse primers. Thus, each treatment/time point sample could be normalized because it contained the exact same amount of cDNA as the housekeeping control.

To normalize samples to the housekeeping control, using Quantity One 1-D Analysis software (BioRad) each band of fluorescence representing *ef1-α* expression was quantified using a defined area for each treatment/time point (e.g. W0, W1, W2). To correct for background fluorescence, the fluorescence of an equivalent area was taken from an empty gel lane and subtracted from the band fluorescence. For each suberin-associated gene from the same cDNA mastermix, band fluorescence was measured where detectable and background fluorescence subtracted. To normalize expression relative to the housekeeping gene *ef1-α*, expression data for each treatment/time point from the suberin-associated genes was expressed as a number relative to *ef1-α*.

To normalize within the three technical replicates for each suberin-associated gene to explore the relative expression between treatments and time points, for which absolute fluorescence values may differ depending on the UV exposure time, one treatment/time point sample with clearly visible expression was chosen and its value set to 1 in all replicates. All other treatment/time point fluorescence values were divided by this chosen sample fluorescence and expressed relative to that value.

For each set of technical replicates relating to a particular gene, the normalized values for each treatment/time point were evaluated using a Levene's test for equal variance. In cases where ½ limit of detection was used for values, unequal variance relative to technical replicate variance of measured samples was common. If equal variance occurred between treatments, then a 1-way ANOVA followed by a Tukey HSD post-hoc test determined differences in expression between treatments. If unequal variance was present in the replicates, then a Welch's ANOVA was performed followed by a Games-Howell post-hoc test to determine differences. All statistical tests were evaluated at $P \leq 0.05$.

3.2.3 *Aliphatic Monomer Separation, Identification and Quantification with GC-FID and GC-MS*

Each ABA/FD treatment sample was ground to a fine powder in liquid N_2 with a mortar and pestle, transferred to a pre-weighed cellulose extraction thimble (Whatman Ltd., England), and placed in a 10 mL beaker containing 2:1 chloroform/methanol solution. Thimbles were placed in micro-soxhlet extractors, and using medium heat to sustain a light boil the samples underwent three solvent extractions. The first two

extractions were completed with 50 mL of 2:1 chloroform:methanol over 3 hours each, followed by a final overnight extraction using 50 mL of chloroform.

3.2.3.1 Soluble Monomer Extraction and Sample Preparation

Soluble extracts were retained, pooled and subsequently the volume was reduced under vacuum to 1 mL in a round-bottom flask using a rotary evaporator (Buchi, Switzerland). Remaining solvent was transferred to a 4 mL glass vial with three chloroform washes from the flask, and dried under a stream of N_2 gas. The dried soluble residue was trans-esterified using 500 µL acidic methanol (2 M MeOH/HCl; Supelco/Sigma-Aldrich, USA) by incubating tightly-closed vials for 2 hours in an 80ºC water bath. Vials were cooled to room temperature and the reaction stopped with 1 mL NaCl-saturated water. Carefully, 10 µL of 1 mg mL^{-1} triacontane was added as an internal standard prior to extracting the hydrolysate three consecutive times with 1 mL hexane each time (shaken vigorously). With a clean 4 mL glass vial, any residual water in the pooled hexane extracts was removed with anhydrous Na_2SO_4. The soluble extract was transferred to a fresh 2 mL glass vial and dried using N_2 gas. The soluble residue was resuspended in 50 µL of pyridine (Sigma Aldrich) and 50 µL 99% bis(trimethylsilyl)trifluoroacetamide (BSTFA) + 1% trimethylsilyl (TMS; Supelco/Sigma Aldrich) for derivatization at 70ºC for 40 minutes in a water bath. Finally, the derivatized sample was transferred to a GC vial containing a micro-volume insert (Agilent) for GC-MS analysis (see Section 2.3.3).

3.2.3.2 Insoluble Monomer Extraction and Sample Preparation

Insoluble extracts contained in the cellulose extraction thimbles were dried at room temperature prior to weighing. From these samples, a sub-sample ranging from 15-35 mg of tissue was transferred into 4 mL glass vials for depolymerization of insoluble aliphatic suberin. The insoluble samples were depolymerized and the resulting aliphatic monomers extracted and derivatized following the same protocol as for the soluble extraction (section 3.2.3.1), beginning with trans-esterification using acidic methanol.

3.2.3.3 GC-MS Quantification

Analysis of methyl ester and TMS ether derivatives used a Varian CP-3800 Gas Chromatograph equipped with two detectors, a flame ionization detector (GC-FID) and Varian MS220 ion trap Mass Spectrometer (GC-MS). As the GC contained two detectors, it had a pair of CP-Sil 5 CB low bleed MS columns (WCOT silica 30 m x 0.25 mm ID) with one column directed to the FID and the other to the MS. The injector oven was set at 250ºC, and the FID oven was set at 300°C. In splitless mode, 1 µL of sample was injected into each column and the monomers eluted with the following program: 70ºC held for 2 minutes; ramped to 200ºC at 40ºC min^{-1} and held for 2 minutes; ramped to 300ºC at 3ºC min^{-1} and held for 9.42 minutes for a total run time of 50 minutes. The carrier gas was high purity helium with a flow rate of 1 mL min^{-1}. Monomers were identified based on their electron-impact MS spectra (70eV, m/z 40 – 550). Suberin-associated monomers were quantified from the GC -FID chromatograms, and normalized to the triacontane internal standard.

3.2.3.4 Data Analysis, Normalization and Statistical Assessment for Aliphatic Suberin Monomers Quantified by GC-MS

Data analysis of aliphatic monomers combined GC-MS for aliphatic monomer identification and GC-FID to quantify the compounds of interest. Previous analysis of known aliphatic standards provided a basis for the retention profile and times, which enabled confident identification of eluted compounds from the MS chromatogram (Table 3.2). With the corresponding FID chromatogram, areas from manually assigned peaks were recorded and normalized using the internal standard for each sample. In the case of C22 compounds, co-elution of contaminating peaks required a selected ion search for both C22 and contaminating compounds to generate a proportion of peak area associated with the target C22 compound.

Calculating monomer abundance required normalization using the internal standard triacontane (C30 alkane). Standard curves from different chemical classes were utilized to convert the sample area values from FID chromatograms into sample concentrations, to determine the nmol per sample (fatty acids: $y=2591x - 6976$; primary alcohols: $y= 3356x - 7393$; ω-OH fatty acids $y= 2908x - 7056$). The fatty acid standard curve was used as an estimate for 2-OH C24 and α,ω dioic acids. The suberin-enriched surface area of potato samples was calculated from the diameter of the No. 9 cork borer used for standardized sectioning multiplied by the number of tissue slices used for the extraction. Monomer quantities for each individual compound were expressed in nmol cm^{-2}. In samples that had no detectable MS signature for a particular compound, a value of 250 area counts (half the limit of detection) was recorded. In samples that had

Table 3.2: Targeted Identification of Suberin-Associated Fatty Acids, Fatty Alcohols, ω-Hydroxy Fatty Acids and α,ω Dioic Acids using Mass Spectroscopy
Compounds listed in the order of elution from GC-MS after methanolic HCl treatment followed by TMS derivitization. The major fragment masses listed identify the characteristic signatures associated with each compound and chain length. FAME: fatty acid methyl ester (CH3 bonded to O in α-COOH); FA-TMS ester: fatty acid TMS ester (TMS bonded to O in α-COOH); alcohol TMS ether (TMS bonded to O in α-CH_2O); dimethyl ester (CH3 bonded to both the α-COOH and ω-COOH).

Compound	Structure	Mass Ion Signature
Palmitic acid	C16:0 FAME	270, 227, 143, 87
Ferulic Acid	Ferulic acid TMS ester	280, 265, 250
Palmityl alcohol	C16:0H TMS ether	299
16:0 membrane	C16:O FA-TMS ester	328, 313, 129, 117
Stearic acid	C18:0 FAME	298, 255, 143, 87
Stearyl alcohol	C18:OH TMS Ether	327
18:1 membrane	C18:1 FA-TMS ester	354, 339, 129, 117
C16 α,ω-dioic acid	C16 dimethyl ester	283, 241, 209, 112, 98
18:0 membrane	C18:0 FA-TMS ester	356, 341, 129, 117
ω-OH palmitic acid	C16:0 ω-OH M ester/TMS ether	343, 327, 311
Arachidic acid	C20 FAME	326, 283, 143, 87
Arachidyl alcohol	C20:OH TMS ether	355
C18:1 α,ω-dioic acid	C18:1 dimethyl ester	340, 309, 290, 276, 98
ω-OH oleic acid	C18:1 ω-OH M ester/TMS ether	384, 369, 353, 337
Behenic acid	C22 FAME	354, 311, 143, 87
Behenyl alcohol	C22:OH TMS ether	383
ω-OH arachidic acid	C20 ω-OH M ester/TMS ether	399, 383, 367
Lignoceric acid	C24 FAME	382, 339, 143, 87
Lignoceryl alcohol	C24:OH TMS ether	411
ω-OH behenic acid	C22 ω-OH M ester/TMS ether	442, 427, 411, 395
2-OH lignoceric acid	C24:OH M ester/TMS ether	470, 455, 427, 411
Cerotic acid	C26 FAME	410, 367, 143, 87
Ceryl alcohol	C26:OH TMS ether	439
ω-OH lignoceric acid	C24 ω-OH M ester/TMS ether	470, 455, 439, 423
Montanic acid	C28:FAME	438, 395, 143, 87
Montanyl alcohol	C28:OH TMS ether	467
ω-OH cerotic acid	C26 ω-OH M ester/TMS ether	498, 483, 467, 451

detectable MS signatures for a particular compound but no distinct peak was present in the chromatogram (signal to noise ratio less than 3:1), these compounds also had a value of 250 counts recorded but were noted as “trace” values. Error associated with the GC-MS detection was determined from a calibration of C18, C20 and C22 fatty acid methyl

esters (FAMES) ranging from 0.5-45 ng μL^{-1}. To account for typical variability in sample detection, the GC-MS variance was calculated from standard curves and incorporated into the ½ detection limit average resulting in the final sample estimations for no detection or trace amounts.

Statistical analysis of soluble and insoluble datasets was done using SPSS Statistics (IBM, v.19). A two-way Analysis of Variance (ANOVA) for total aliphatics was performed using treatment (water, FD, ABA/FD) and time (days: 0, 1, 2, 3, 4, 6) at $P \leq 0.05$. Due to interaction, a one-way ANOVA analysis was performed to determine the main effects of each treatment and evaluated at $P \leq 0.05$ for: total aliphatics, each compound class (fatty acids, primary alcohols, ω-OH fatty acids, α,ω dioic acids), and each chain length with the classes (ranging from C16-C28). In cases where ½ limit of detection was used for values, unequal variance relative to biological variance of measured samples was common. In cases where the Levene's test for unequal variance showed significant difference (evaluated at $P \leq 0.05$), a Welch 1-way ANOVA for unequal variance followed by Games-Howell post-hoc test was done in place of the typical 1-way ANOVA with Tukey HSD post-hoc test. Effects with $P \leq 0.05$ were reported as statistically significant.

3.3 Results and Discussion

3.3.1 *Quantification of ABA Concentration in Tubers Post-wounding*

To ensure that FD treatment was an effective inhibitor of *de novo* ABA biosynthesis, as well as to determine the duration of FD treatment effect, ABA levels were quantified from the wounded potato tuber tissue using LC-MS. Tubers from each

treatment/time point replicate included in the FD/ABA post-wounding treatment study were measured for ABA content. Subsequently, the levels of ABA in these samples were correlated with results from semi-quantitative gene expression and aliphatic monomer analysis studies, to determine the effects of ABA on suberin biosynthesis.

Previous studies that quantified ABA post-wounding in tubers found an initial drop of ABA from steady state levels occurs within 24 hours post-wounding, followed by re-establishment of the steady state level 4-6 days post-wounding (Lulai et al., 2008; Kumar et al., 2010). In this study, this pattern of change in ABA accumulation post-wounding was replicated as ABA concentration initially dropped 85% within 24 hours post-wounding from an average of 85 ng/g FW to 15 ng/g FW (Figure 3.2). This dramatic drop in ABA was due to increased catabolism, with ABA metabolized into phaseic acid and subsequently dihydrophaseic acid quickly over the first 24 hours post-wounding (Suttle et al., 2013). Subsequently, ABA concentration in the tissue increased averaging 100 ng/g FW between day 3 and 4 post-wounding. The increase in ABA was due to substantial upregulation of ABA metabolism, which was derived from carotenoid biosynthesis (Nambara and Marion-Poll, 2005). Finally, ABA levels slightly declined to a new steady state level of an average of 70 ng/g FW between day 6 and day 14.

FD-treated tubers exhibited a similar initial ABA concentration as the water controls at time zero (4 hours post-wounding). Subsequently, the ABA levels dropped within the first 24 hours in the tuber tissue, resulting in a 90% reduction from the initial ABA level by two days post-wounding. There was no significant recovery of ABA from this drop throughout the 14 day timecourse. *De novo* ABA biosynthesis in the control

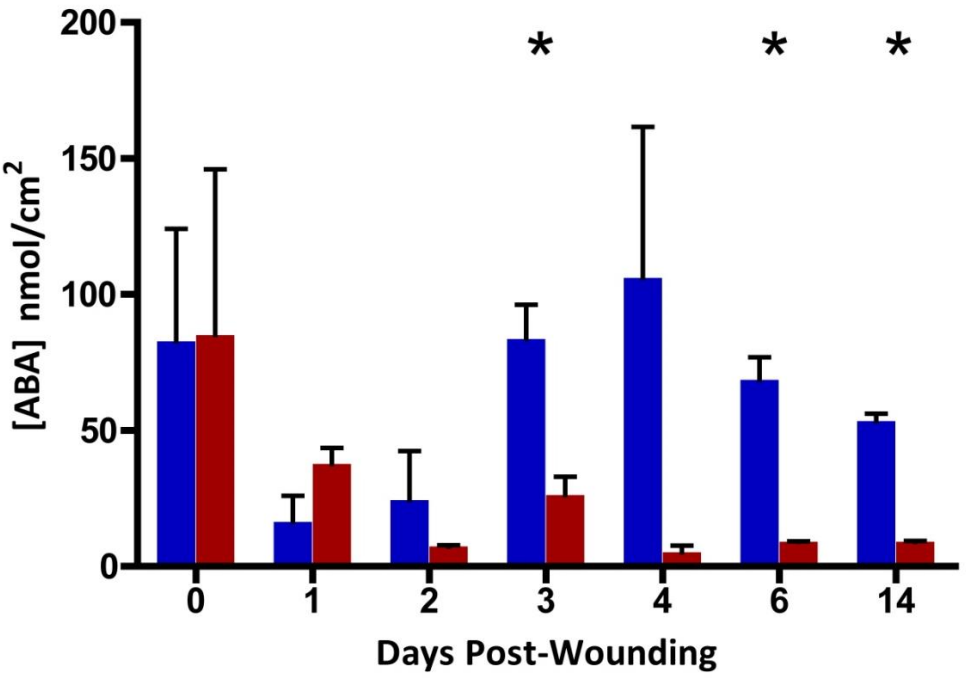

Figure 3.2: Post-wounding Quantification of ABA in Potato Tubers
ABA concentration was measured in potato tubers post-wounding in water-treated control (blue bars), FD-treated (red bars) and exogenous ABA/FD-treated (data not shown). Data quantified using LC-MS. Statistically significant differences ($p \leq 0.05$) shown between two treatments with two replicates per treatment. Data represented by mean ± standard deviation, n=3.

tubers resulted in the re-establishment of ABA concentrations, whereas FD-treated tubers could not produce the ABA precursors necessary for *de novo* biosynthesis and therefore could not replace lost ABA. ABA levels remained almost completely abolished for the remainder of the 14 day timecourse, indicating a long term effect of FD. FD treatment has been previously shown to inhibit phytoene desaturase, which catalyzes the production of ABA precursors (refer to Figure 3.1, Gamble and Mullet, 1986). With respect to ABA in wounded potato tuber tissue, FD application acts as an effective suppressor of *de novo* ABA biosynthesis throughout the formation of the suberized closing layer.

In the ABA/FD treatment, exogenous ABA was readily taken up by the wounded tuber tissue, with levels reaching 3000 ng/g FW in the tissue by day 1 post-wounding. ABA levels remained at this concentration throughout the entire 14 day timecourse (data not shown). Although FD has inhibited *de novo* biosynthesis of ABA, the exogenous supply of ABA was effectively taken up by the wounded tissue.

3.3.2 *Effect of ABA and FD on Gene Expression Profiles for Suberin-Associated Genes in Potato*

The effect of ABA on suberization was initially investigated over 35 years ago, with experiments measuring the effect of ABA post-wounding on water permeability and C18:1 dioic acid accumulation post-wounding in tubers (Soliday et al., 1978; Cottle and Kolattukudy, 1982). The mechanism(s) of ABA's effect were not further investigated until Lulai et al. (2008) re-visited this research. Lulai et al. (2008) provided qualitative evidence using histochemical staining techniques for aliphatic and phenolic domains that *de novo* ABA biosynthesis was necessary for proper suberin monomer accumulation. However, there was no in-depth look at the types of monomers affected by the inhibition of *de novo* ABA biosynthesis, whether it was a global decrease in synthesis or specific to a particular class of monomers.

To begin exploring the role of ABA in regulation of monomer production, the first step was to investigate transcription initiation using different treatment conditions. To determine if ABA regulates gene expression for select suberin-associated genes, semi-quantitative RT-PCR was performed using nucleic acids extracted from exogenous ABA and/or FD-treated potato tubers post-wounding. RNA was extracted and cDNA prepared

from each ABA and/or FD sample, as well as the water control, to give a comprehensive expression profile for each selected gene.

3.3.2.1 *PAL1* Transcription Profile in Response to ABA/FD Treatment

The reaction catalyzed by PAL1 is the first committed step in the phenylalanine pathway, which converts L-phenylalanine to ammonia and trans-cinnamic acid. Regarding *PAL1* transcriptional regulation, previous studies have shown induced expression post-wounding, typically peaking after 12-24 hours before dropping to a steady state expression level (Kumar et al., 2010). In addition, Lulai et al. (2008) showed that PAL1 activity was moderately attenuated by FD treatment, but not abolished. Regarding ABA transcriptional regulation, exogenous ABA application has been previously shown to boost *PAL1* transcript levels in wound-healing tubers (Kumar et al., 2010). However, no previous investigation included exploring the impact on *PAL1* transcription of removing *de novo* ABA biosynthesis, to determine whether it was the process of ABA biosynthesis or the presence of ABA causing differential expression.

Expression of *PAL1* in the water control remained fairly constant throughout the timecourse, with a slightly higher expression at the initial timepoint (Figure 3.3). Expression was beginning to increase at the day 6 timepoint, consistent with previous semi-QT RT-PCR results (Kumar et al., 2010). With the application of FD, expression rose on day 1 before dropping again to a steady state level of expression similar to the water controls. ABA/FD-treated tubers showed the expression as FD treatment alone, indicating that exogenous ABA did not affect *PAL1* gene expression. Kumar et al. (2010) investigated the application of exogenous ABA without FD, and found *PAL1* expression

to be increased over the 6 day timecourse, reaching maximal expression on day 4. Another study of *PAL1* transcription in response to wounding by the same researchers showed *PAL1* expression to increase steadily post-wounding in controls, reaching a sustained maximal level from day 3 through 28 post-wounding (Lulai and Neubauer, 2014). Therefore, at this time no conclusions can be made on the effect of ABA on *PAL1* transcription. However, ABA still must play a role in phenylpropanoid biosynthesis. PAL1 enzyme activity was significantly increased by the application of exogenous ABA (Cottle and Kolattukudy, 1982; Lulai et al., 2008; Kumar et al., 2010), and FD inhibition significantly decreased PAL1 activity at day 1 post-wounding. Further investigations into the effect of ABA are required to elucidate the action of ABA or ABA biosynthesis in phenolic regulation.

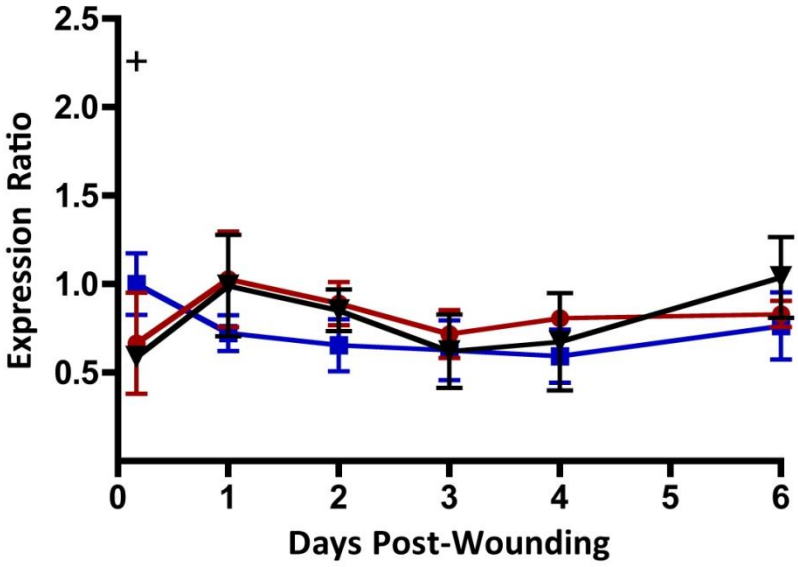

Figure 3.3: Effect of Exogenous ABA and FD Treatment on *PAL1* Transcription in Wounded Potato Tubers over 6 Days.
Squares are water controls, circles are FD treatment, and triangles are exogenous ABA/FD treatment. Statistically significant differences ($p \leq 0.05$) shown between three treatments (+ between water and ABA). Data represented by mean ± standard deviation, n=3.

3.3.2.2 *FHT* Transcription Profile in Response to ABA/FD Treatment

Linking phenylpropanoid metabolism and aliphatic metabolism, *FHT* uses feruloyl-CoA as an acyl donor to C16 ω-OH palmitic acid and primary alcohols (Serra et al., 2010). Potato *FHT* expression knockdown tubers showed an altered suberin composition with over 70% reduction in ferulic acid and 18:1 ω-hydroxy fatty acids. In addition, the quantity of soluble waxes doubled and the composition shifted with significantly increased free C22-C28 fatty acids and primary alcohols while C25-C27 alkanes decreased (Serra et al., 2010).

FHT expression in the water controls showed the same profile as previously published qPCR expression post-wounding (Lulai and Neubauer, 2014), with a delay in expression of 1-2 days relative to unwashed wounded tissue. Water-washing tissue after wounding has reproducibly been shown to delay aliphatic deposition in suberization (Soliday et al., 1976, Cottle and Kolattukudy 1982), which was necessary in the experimental design to mimic treatment with FD and ABA solutions. As with the qPCR result, no expression of *FHT* was detected immediately post-wounding on day 0. In the water control, induction occurred between day 2 and day 3 and was sustained at a high level throughout the remainder of the timecourse (Figure 3.4). The FD treatment completely abolished the induction of *FHT* at day 3, with no gene expression detectable throughout the 6-day timecourse. However, in contrast to the FD treatment, the application of exogenous ABA with FD initiated a sustained early upregulation of *FHT* expression evident by day 1. With the ABA/FD treatment, by day 2 the *FHT* expression level rose to a comparable expression level as the water control after initiation on day 3. Therefore, as exogenous ABA application results in premature transcription initiation as

well as re-constitutes abolished expression in FD treated tubers, ABA plays a clear role in the transcriptional regulation of *FHT*.

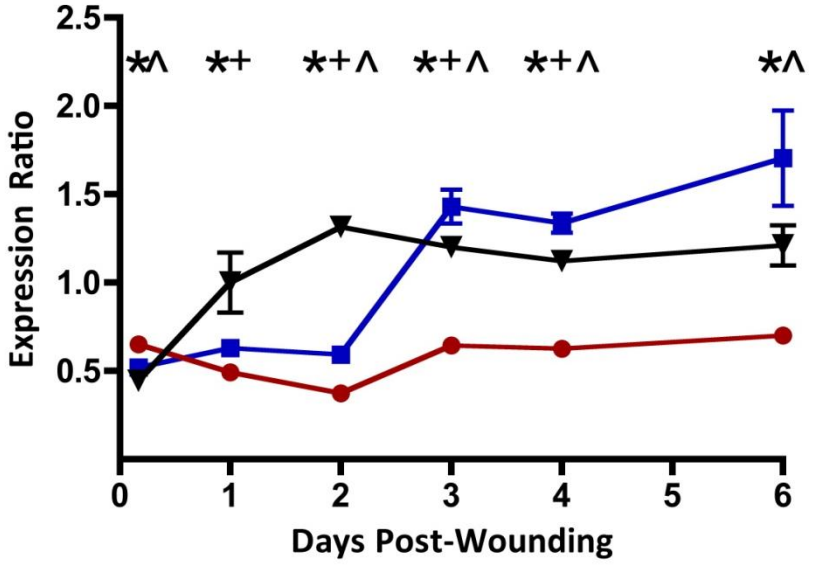

Figure 3.4: Effect of Exogenous ABA and FD Treatment on *FHT* Transcription in Wounded Potato Tubers over 6 Days.
Squares are water controls, circles are FD treatment, and triangles are exogenous ABA/FD treatment. Statistically significant differences ($p \leq 0.05$) shown between three treatments (^ between water and FD; + between water and ABA, * between ABA and FD). Data represented by mean ± standard deviation, n=3.

3.3.2.3 *KCS* Transcription Profile in Response to ABA/FD Treatment

Critical to the elongation of fatty acids that are subsequently modified and incorporated into aliphatic suberin, *KCS6* has been demonstrated as part of the suberin-specific elongation process in a potato (Serra et al., 2009b). KCS6 is a β-ketoacyl-CoA synthase, which is a condensing enzyme of the fatty acid elongase (FAE) complex essential for production of very long-chain fatty acids (VLCFAs) greater than C18. Downregulation of *KCS6* expression results in decreased C26 fatty acid elongation, affecting only VLCFAs ≥C28 resulting in the accumulation of shorter chain fatty acids (Serra et al., 2009b).

Similar to *FHT*, the *KCS6* water control show transcription upregulation by 3 days post wounding. Expression remained constant throughout the remainder of the timecourse, reaching a maximal level by day 6 (Figure 3.5). With FD treatment, transcription initiation was abolished throughout the timecourse. Exogenous ABA with FD treatment resulted in a premature upregulation of gene expression beginning by day 1, reaching a maximal level by day 2 which was sustained throughout the timecourse. As with *FHT*, *KCS6* was clearly transcriptionally regulated in part by ABA, as the addition of exogenous ABA resulted in premature upregulation while the inhibition of *de novo* ABA biosynthesis resulted in a corresponding abolishment of transcriptional initiation.

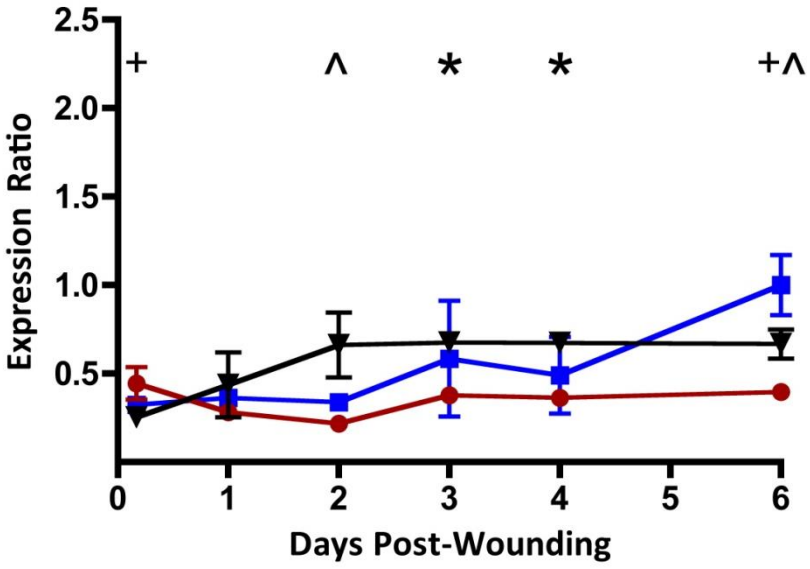

Figure 3.5: Effect of Exogenous ABA and FD Treatment on *KCS* Transcription in Wounded Potato Tubers over 6 Days.
Squares are water controls, circles are FD treatment, and triangles are exogenous ABA/FD treatment. Statistically significant differences ($p \leq 0.05$) shown between three treatments (^ between water and FD; + between water and ABA, * between ABA and FD). Data represented by mean ± standard deviation, n=3.

3.3.2.4 *CYP86A33* and *StCYP86B* Transcription Profiles in Response to ABA/FD Treatment

Hydroxylation of the terminal methyl group (ω-hydroxylation) is catalyzed by five Cytochrome P450 subfamilies in plants: *CYP86A*, *CYP86B*, *CYP94A*, *CYP77A* and *CYP704B*. *FAωH1* and *CYP86B1* are fatty acid ω-hydroxylases involved in suberin biosynthesis (Chapter 2 of this thesis; Serra et al., 2009a; Compagnon et al., 2009; Molina et al., 2009). Fatty acids or fatty acyl Co-A's are hydroxylated to C16:0 and C18:1 ω-hydroxy fatty acids, which can be subsequently oxidized into α,ω-dioic acids. *FAωH1* (*CYP86A33)* RNA*i* knockdown results in a 60% reduction in both total suberin as well as glycerol content; and more specifically a 70% and 90% reduction in 18:1 ω-hydroxy fatty acids and α,ω-dioic acids, respectively (Serra et al., 2009a). However, investigation into members of a gene family often reveals redundant gene expression patterns, adding to the complexity of identifying gene function. In the case of *FAωH1 (CYP86A33)*, complete RNAi knockdowns did not completely abolish ω-hydroxylated monomer production for suberization, indicating redundancy in the pathway (Serra et al., 2009a). While *FAωH1* (*CYP86A33)* affects shorter chain ω-hydroxylation, in *Arabidopsis* the reduction of *CYP86B1* transcription resulted in nearly eliminating the mid-chain C22 and C24 ω-hydroxy fatty acids production (Compagnon et al., 2009).

FAωH1 expression in the water controls replicated the qPCR expression with no detectable expression initially post-wounding, with a strong induction by day 3 post-wounding and expression remaining high throughout day 6 (Figure 3.6). FD treatment abolished *FAωH1* expression throughout the timecourse, completely suppressing the induction of transcription between day 2 and day 3 post-wounding. The addition of exogenous ABA complemented the FD treatment and restored transcriptional upregulation of *FAωH1*, but resulted in significantly earlier initiation relative to the water

controls beginning by day 1. Exogenous ABA/FD treatement caused *FAωH1* to reach a maximal expression level by day 2, a full day earlier than the water controls, and remain high throughout the timecourse.

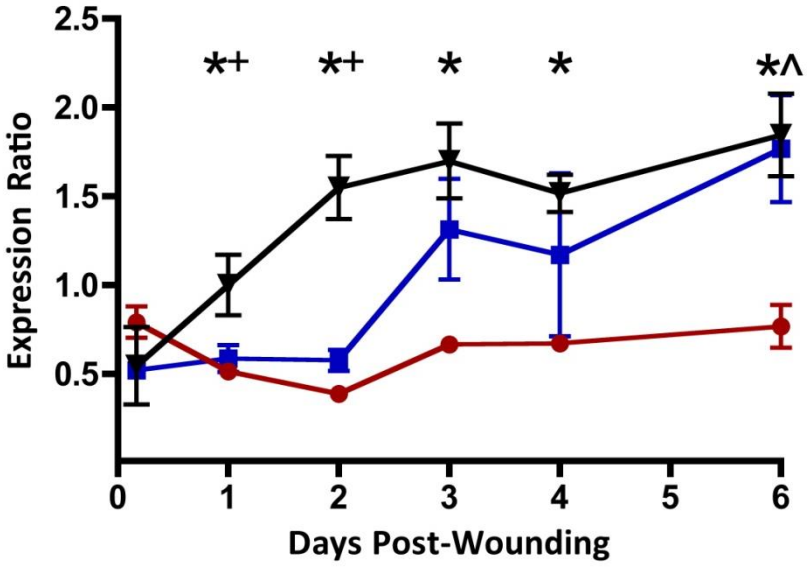

Figure 3.6: Effect of Exogenous ABA and FD Treatment on *FAωH1* Transcription in Wounded Potato Tubers over 6 Days.
Squares are water controls, circles are FD treatment, and triangles are exogenous ABA/FD treatment. Statistically significant differences ($p \leq 0.05$) shown between three treatments (^ between water and FD; + between water and ABA, * between ABA and FD). Data represented by mean ± standard deviation, n=3.

Expression of *StCYP86B* was not detectable throughout day 1 and 2 post-wounding in the water controls, with significant upregulation by day 3 which remained high throughout day 6 (Figure 3.7). However, in contrast to *FAωH1*, *StCYP86B* expression was induced by both FD and ABA/FD treatment by day 1 post-wounding. Although FD induced transcription by day 1 post-wounding, it did not sustain expression throughout the timecourse. Exogenous ABA/FD treatment resulted in a strong and sustained induction of *StCYP86B* throughout the timecourse. Therefore, the removal of *de novo* ABA biosynthesis established early induction of *StCYP86B*, whereas the application

of exogenous ABA was required for sustained expression. This result indicates that ABA may regulate transcription through two separate mechanisms: first, through the action of *de novo* ABA biosynthesis potentially involving products of the carotenoid pathway, and second, through the cellular concentration of ABA *in planta*.

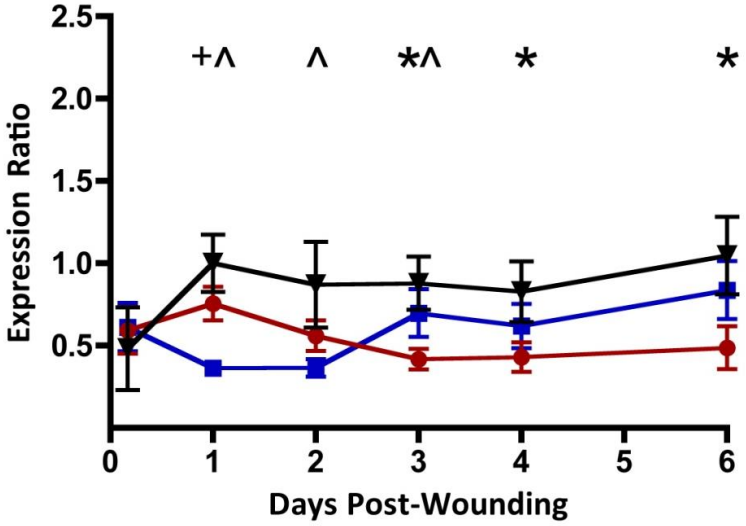

Figure 3.7: Effect of Exogenous ABA and FD Treatment on *StCYP86B* Transcription in Wounded Potato Tubers over 6 Days.
Squares are water controls, circles are FD treatment, and triangles are exogenous ABA/FD treatment. Statistically significant differences ($p \leq 0.05$) shown between three treatments (^ between water and FD; + between water and ABA, * between ABA and FD). Data represented by mean ± standard deviation, n=3.

3.3.2.5 *CYP86A* and *CYP94A* Multi-gene Families Transcription Profiles in Response to ABA/FD Treatment

In silico analysis of the *S. tuberosum* group Phureja potato genome identified two other *CYP86A* subfamily members, *CYP86A69* (*FAωH2*) and *CYP86A68* (*FAωH3*) (see Chapter 2, Table 2.2). Expression of the *FAωH2* water controls was undetectable throughout the 6 day timecourse (Figure 3.8). FD treatment resulted in variable low expression at day 0 post-wounding, with no further detectable expression throughout the 6 day timecourse. Exogenous ABA with FD did initiate transcription on day 1, albeit at a

low level, but *FAωH2* expression was not sustained throughout the timecourse. Therefore, *FAωH2* was not strongly induced during suberization and ABA does not sustain gene expression, but may be transiently upregulated through increased ABA concentration.

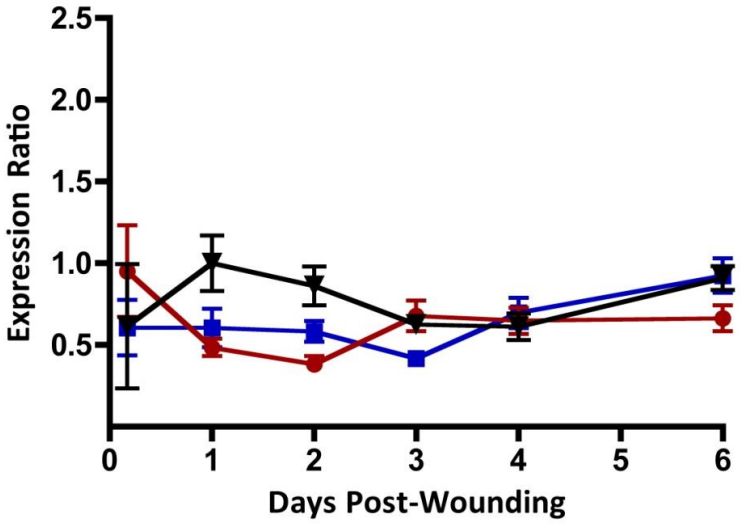

Figure 3.8: Effect of Exogenous ABA and FD Treatment on *FAωH2* Transcription in Wounded Potato Tubers over 6 Days.
Squares are water controls, circles are FD treatment, and triangles are exogenous ABA/FD treatment. Statistically significant differences ($p \leq 0.05$) shown between three treatments (∧ between water and FD; + between water and ABA, * between ABA and FD). Data represented by mean ± standard deviation, n=3.

Expression of *FAωH3* in the water controls was also not detectable throughout the timecourse. This finding indicated that in the multi-gene *CYP86A* subfamily, the dominant suberin-associated ω-hydroxylase was *CYP86A33/FAωH1*. FD treatment initiated transcription by day 1 post-wounding, but did not result in sustained expression. Exogenous ABA/FD treatment was able to both initiate and sustain expression of *FAωH3* throughout the 6 day timecourse (Figure 3.9).

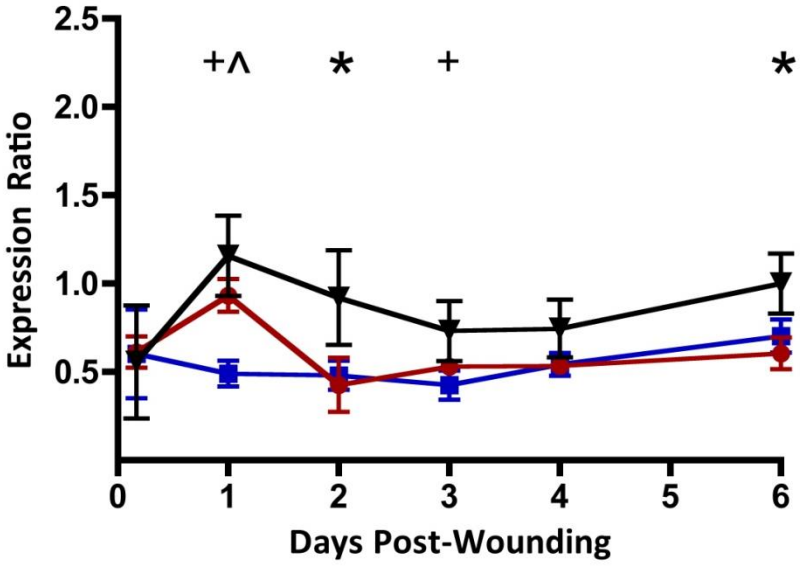

Figure 3.9: Effect of Exogenous ABA and FD Treatment on *FAωH3* Transcription in Wounded Potato Tubers over 6 Days.
Squares are water controls, circles are FD treatment, and triangles are exogenous ABA/FD treatment. Statistically significant differences ($p \leq 0.05$) shown between three treatments (^ between water and FD; + between water and ABA, * between ABA and FD). Data represented by mean ± standard deviation, n=3.

The *CYP94A* subfamily has been characterized as ω-oxidases, capable of catalyzing both ω-hydroxylation as well as the subsequent oxidation reactions to produce α,ω dioic acids (Tijet et al., 1998; Le Bouquin et al., 2001). Although members of this CYP family have been functionally characterized *in vitro* (Tijet et al., 1998; Pinot et al., 1999; Le Bouquin et al., 1999, 2001), there has been no investigation to their role *in planta*. The *CYP94A* subfamily in *S. tuberosum* contains three members: *CYP94A26* (*FAωO1*), *CYP94A24* (*FAωO2*) and *CYP94A25* (*FAωO3*). *FAωO1* in water controls showed expression at day 0 (4 hours post-wounding), which by day 1 had dropped to undetectable levels throughout day 6. FD treatment resulted in the same pattern of *FAωO1*expression as the water controls, indicating that *de novo* ABA biosynthesis does not have a role in *FAωO1* regulation. Exogenous ABA with FD resulted in a significant

delay in the drop of *FAωO1*expression, sustaining expression through day 1 and dropping to non-detectable levels by day 2. However, a second initiation of expression was visible in the *FAωO1* ABA/ FD treatment as expression was detectable on again on day 6, which differed from the water controls. Therefore, increased ABA concentration can initiate *FAωO1* transcription.

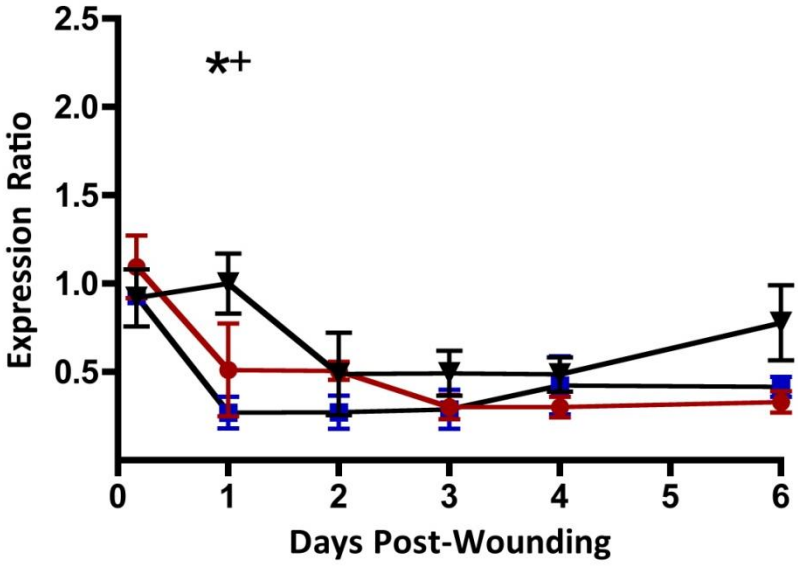

Figure 3.10: Effect of Exogenous ABA and FD Treatment on *FAωO1* Transcription in Wounded Potato Tubers over 6 Days.
Squares are water controls, circles are FD treatment, and triangles are exogenous ABA/FD treatment. Statistically significant differences ($p \leq 0.05$) shown between three treatments (^ between water and FD; + between water and ABA, * between ABA and FD). Data represented by mean ± standard deviation, n=3.

The second member of the *CYP94A* subfamily, *FAωO2*, had no detectable expression result from any treatment during the timecourse (data not shown). The third member of this subfamily, *FAωO3*, had the same expression pattern as *FAωO1* in the water controls (Figure 3.11). FD treatment significantly delayed the drop in expression, as it was still detectable by day 1. Exogenous ABA with FD resulted in the same delay as FD alone, with expression being sustained through day 1 and dropping by day 2.

However, as with *FAωO1*, there was a second increase in expression detected at day 6 with the increased ABA concentration, indicating that ABA can upregulate gene expression of *FAωO3*.

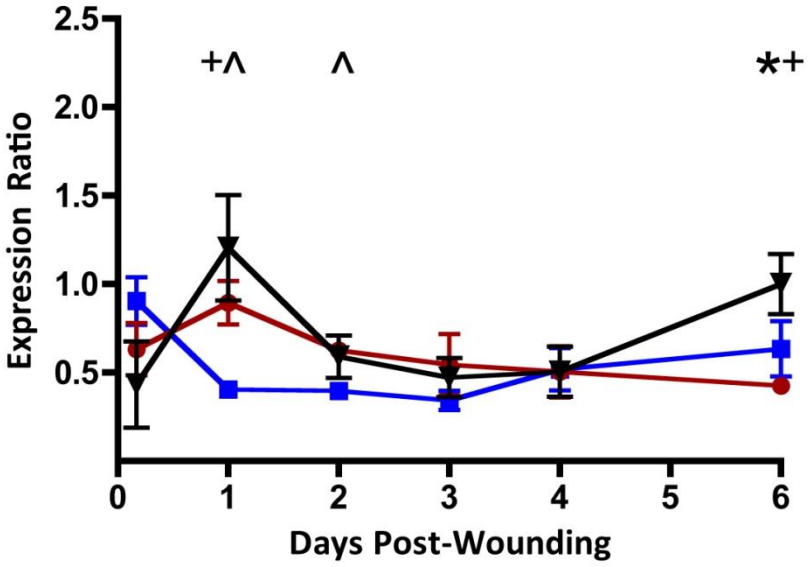

Figure 3.11: Effect of Exogenous ABA and FD Treatment on *FAωO3* Transcription in Wounded Potato Tubers over 6 Days.
Squares are water controls, circles are FD treatment, and triangles are exogenous ABA/FD treatment. Statistically significant differences ($p \leq 0.05$) shown between three treatments (^ between water and FD; + between water and ABA, * between ABA and FD). Data represented by mean ± standard deviation, n=3.

3.3.2.6 General Effects of ABA and FD on Gene Expression in Potato

Previous investigations of ABA effects post-wounding have focused on using exogenous ABA application to dramatically increase tissue concentrations, but cannot distinguish between the effects of ABA biosynthesis and the presence of ABA. The FD treatment investigated the role of post-wounding, *de novo* ABA formation, as FD inhibits the production of precursors necessary for ABA biosynthesis resulting in the strong reduction of *de novo* synthesis. The exogenous ABA with FD treatment served two purposes. First, to explore if exogenous ABA could rescue FD phenotypes, indicating FD

treatment effects were due to the absence of ABA. And second, to determine if the presense of ABA was directly or indirectly involved in the regulation of suberin-associated gene expression.

After analyzing the detailed expression results for each of the nine genes, three overall patterns emerged from the data. The time points chosen for this experiment do not provide the fine detail necessary to investigate the early induction post-wounding, over the first 24 hours, but were selected to focus on the effects of FD and ABA on gene expression during suberization of the initial closing layer. The two treatments chosen, FD alone and exogenous ABA with FD, were used to examine the effects on initiation, sustainment and/or timing of suberin-associated gene expression. The sample tissue utilized for RNA isolation in this transcription study was also quantified for ABA levels. FD-treated tissue was demonstrated to have minimal ABA accumulation throughout the 6 days, while exogenous ABA application was shown to dramatically increase ABA levels above that in the water controls (Figure 3.2).

The first major trend evident from FD treatment was that removal of *de novo* ABA biosynthesis induced transcription for some genes, including *PAL1*, *StCYP86B*, *FAωH3* and *FAωO3*. For these four genes, increased expression on day 1 occurred in both FD and ABA/FD treatments relative to the water controls. Exogenous ABA application did not rescue the FD phenotype during these early time points. There are two possible reasons why exogenous ABA was unable to rescue this FD phenotype: either the process of *de novo* ABA biosynthesis was necessary for transcriptional regulation; or FD may be causing another indirect effect unrelated to ABA resulting in the FD phenotype, as FD acts as a inhibitor upstream of ABA biosynthesis. A more detailed timecourse over

the first 48 hours post-wounding was necessary to determine the early effects on transcription for these genes, preferably with a more specific inhibitor of ABA biosynthesis.

FD has been shown to attenuate PAL1 enzyme activity (Lulai et al., 2008), and the expression data from this study demonstrated that FD effects *PAL1* gene expression at a transcriptional level. The FD effect on *PAL1* appears to be transient; as FD treatment does not differ from the control treatment after day 2 (Figure 3.3). Thus, there was only a small window of time after wounding that *de novo* ABA biosynthesis may upregulate *PAL1* transcription. This FD transient upregulation was also evident in the *StCYP86B*, *FAωH3* and *FAωO3* expression patterns. FD-treated tubers had no induction of *PAL1*, *FAωH3*, *FAωO1* and *FAωO3* expression after day 2, which was the same as the water controls for these four genes (Figures 3.3, 3.9-3.11). However, regarding *StCYP86B* and the remaining genes investigated, FD-induced suppression of gene expression was evident after day 2 was sustained throughout the closing layer suberization; with suppression of gene expression past the third day through to the sixth day relative to the water controls (Figures 3.4-3.8). Therefore, removal of *de novo* ABA biosynthesis does result in no detectable gene expression in all nine genes after the first 48 hours post-wounding.

The second major trend evident from FD treatment was that removal of *de novo* ABA biosynthesis by FD treatment inhibited transcription initiation, which could be recovered either partially or fully with exogenous ABA application. Recovery was evident in the previously characterized suberin-associated aliphatic genes (*FHT*, *KCS*, *FAωH1* and *StCYP86B*) as well as the uncharacterized *FAωH2* and *FAωO1* (Figures

3.4-3.8, 3.10). The exogenous ABA with FD recovers transcription levels similar to the water controls after day 3. In contrast, the FD alone treatment for these samples results in no detectable gene expression. Thus, the recovery of the FD phenotype with exogenous ABA application clearly indicated a regulatory role for the presence of ABA in aliphatic biosynthesis.

The third major trend evident from exogenous ABA application was that high concentrations of ABA could prematurely initiate and in some cases also sustain transcription of aliphatic genes. Exogenous ABA application resulted in the upregulation of *FHT*, *KCS*, *FAωH1*, *FAωO1* and *FAωH2* expression by day 2 post-wounding, which did not occur in the water control (Figures 3.4-3.6, 3.8, 3.10). *FHT*, *FAωH1* and *KCS*, three previously characterized suberin-associated genes, all show increased expression close to the maximal level by day 2 post-wounding. In contrast, the water controls show initiated and sustained expression by day 3, a full day later. *FHT*, *FAωH1* and *KCS* all exhibited sustained expression from day 2 through day 6, at comparable levels to the water controls once initiated. FD treatment alone initiated no transcription from day 2 through day 6 from these same genes. Thus, exogenous ABA treatment both initiated and sustained expression with *FHT*, *KCS* and *FAωH1*; with the premature initiation beginning two days earlier compared to the water controls (Figures 3.4-3.6). Regarding *FAωH2* and *FAω01*, previously uninvestigated members of the *CYP86A* and *CYP94A* subfamilies, respectively, exogenous ABA application resulted in transient upregulation of expression by day 1, but this was not sustained as expression dropped below detectable levels by day 3 (Figures 3.8 and 3.10). Water controls for *FAωH2* and *FAω01* both had no detectable expression after day 1 of the closing layer formation. As *FAωH2* and *FAω01* are both

putative ω-hydroxylases, but are not induced in the controls throughout suberization, they likely act in other plant biopolymer formation such as cutin or sporopollenin. Interestingly, ABA does have the ability to upregulate their expression indicating a potential regulatory role in those processes as well.

As mentioned previously during the discussion of ABA concentrations post-wounding (see Section 3.1), post-wounding ABA concentrations decreased dramatically within the first 24 hours. As *de novo* synthesis began to reestablish ABA, by day 3 post-wounding the concentrations of ABA have returned to the initial concentration prior to wounding. Over the following three days, ABA concentrations transiently increased and decreased as it began to reach and maintain a new steady state. In this experiment, adding exogenous ABA to the system at the time of wounding as well as an inhibitor of *de novo* ABA biosynthesis enabled the discernment of ABA concentration effects versus ABA *de novo* synthesis effects. More experimentation such as an ABA pulse/chase study, which would allow tracking of the exogenous ABA application, will be needed to identify the role of ABA in aliphatic regulation. However, this was the first evidence that multiple suberin-associated genes including *FHT*, *KCS* and *FAωH1* are hormonally upregulated by ABA, indicating broad global control within aliphatic transcriptional.

3.3.3 *Effect of ABA and FD Treatment on Aliphatic Suberin Monomer Composition in Potato Post-wounding*

To begin to explore the more global effect of ABA in the regulation of aliphatic suberin biosynthesis, an in-depth quantitative chemical analysis of suberin-associated fatty acids, fatty alcohols, ω-hydroxylated and α,ω dioic acids was undertaken. The goal

was to understand the effects of FD and exogenous ABA treatment on the accumulation of both soluble waxes and insoluble aliphatics. Soluble waxes are composed of non-covalently linked compounds freely extracted from the suberized tissue with chloroform and methanol, whereas insoluble aliphatics are polymerized compounds extracted through trans-esterification reactions using methanolic-HCl. Previously the Bernards' lab group has investigated the metabolome of phenolic and aliphatic suberization during normal tuber wound healing, tracking the accumulation of both soluble and insoluble compounds (Yang and Bernards 2006, 2007). Yang and Bernards identified two important results: first, that there was a large metabolic shift in aliphatic metabolism between day 2 and day 3 post-wounding that resulted in the accumulation of insoluble aliphatic monomers throughout the rest of suberin closing layer formation (Yang and Bernards, 2007); and second, that there was no large overall accumulation of soluble aliphatics during the process of suberization (Yang and Bernards, 2006). When aliphatic metabolism is upregulated during suberization, the first step in the biosynthetic pathway is to form the free fatty acids. C16 and C18:1 fatty acids may be subsequently activated to fatty thioesters (fatty acyl CoAs) and undergo one of two developmental fates. They may be either desaturated followed by ω-hydroxylation, of which a proportion are further oxidized to α,ω dioic acids; or elongated to form VLCFAs, frequently undergoing subsequent reduction to primary alcohols or oxidation to ω-hydroxy fatty acids and α,ω dioic acids (Yang and Bernards, 2006). Thus, when looking at suberin metabolism as a whole, the production and incorporation of shorter chain fatty acid monomers is anticipated first; while modified or longer chain fatty acids would be slightly delayed through additional biosynthetic elongation steps.

3.3.3.1 Total Soluble and Insoluble Aliphatic Quantification Post-wounding

To begin to understand the effects of FD and exogenous ABA treatment on suberization, the water controls provided an important baseline for normal suberin development post-wounding. Total soluble aliphatics monomers remain fairly constant throughout the 14 day timecourse, with no significant accumulation of aliphatics. In the water controls, soluble aliphatic compound accumulation for the majority of monomers rose over the first three days, then dropped at day 4, and recovered from day 6 to day 14 (Figure 3.12a). FD treatment resulted in 34.6% lower solubles on day 2, as well as a 29.3% lower accumulation at the day 6 relative to the water controls. However, the overall total soluble accumulation at day 14 was the same in the FD treatment and water controls, indicating these were transient effects. Exogenous ABA with FD did not rescue the FD phenotype on day 2, which exhibited the same drop in solubles as the FD treatment alone. As ABA did not rescue the FD phenotype on two days post-wounding, *de novo* ABA biosynthesis must be directly or indirectly have induced higher levels of aliphatic monomer synthesis in the water controls. In contrast to FD, exogenous ABA/FD treatment did result in an altered phenotype later in the timecourse. With exogenous ABA, total solubles began to accumulate to greater levels by day 4 post-wounding. This differed from both the controls and FD treatment, both of which had a significant drop in monomer levels on day 4, 54.5% and 52.6%, respectively. From day 4, the ABA-treated tissue showed a continued accumulation in solubles, resulting in a 270% rise between day 4 and 14. Thus, exogenous ABA both diminished the drop in total soluble aliphatic pools at day 4 as well as increased the total soluble accumulation throughout the 14 day timecourse. Therefore, ABA concentration must play a regulatory role in soluble aliphatic

compound accumulation, which could be a result of increased monomer production or decreased transport from soluble pools for incorporation into the suberin biopolymer.

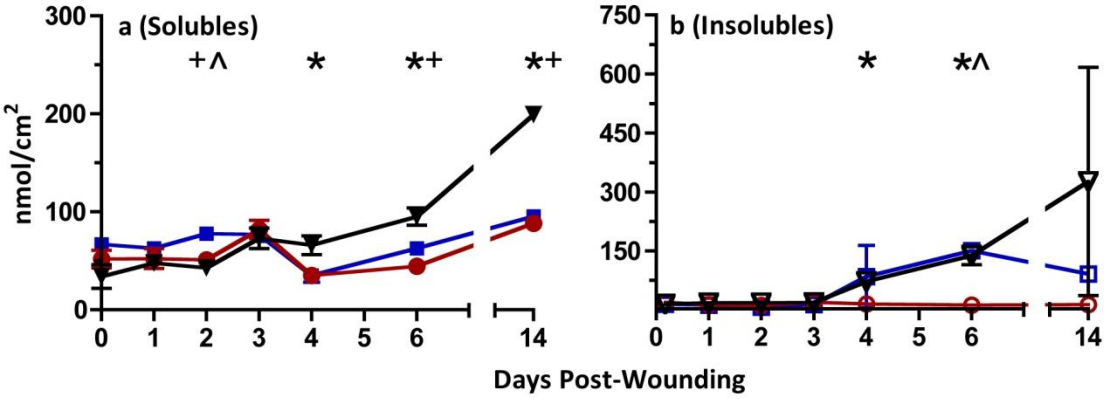

Figure 3.12: Effect of Exogenous ABA and FD treatment on Total Aliphatic Monomer Accumulation in Wounded Potato Tubers over 14 days
a, Total aliphatic soluble wax monomer accumulation of fatty acids, fatty alcohols, ω-OH fatty acids and α, ω dioic acids. b, Total aliphatic insoluble monomer accumulation of fatty acids, fatty alcohols, ω-OH fatty acids and α, ω dioic acids. Squares are water controls, circles are FD treatment, and triangles are exogenous ABA/FD treatment. Closed symbols represent soluble aliphatic waxes, open symbols represent insoluble aliphatics. Statistically significant differences ($p \leq 0.05$) shown between three treatments (^ between water and FD; + between water and ABA, * between ABA and FD). Data represented by mean ± standard deviation, n=3.

Total insoluble aliphatic accumulation in water controls began to increase between day 3 and day 4 post-wounding, showing significant accumulation by day 6 timecourse as monomers are covalently linked to the biopolymer (Figure 3.12b). FD treatment caused a significant phenotype with little to no accumulation of aliphatics in suberin over the 14 day timecourse. Exogenous ABA recovered the FD phenotype, restoring aliphatic accumulation from day 3 through 14.

Based on the analysis of total soluble and total insoluble monomer accumulation, there was a significant effect with both FD and exogenous ABA treatments. Therefore, a more thorough analysis of both monomer class (fatty acids, primary alcohols and ω-

hydroxylated fatty acids) and chain length (C16-C28) was necessary to further understand the effect of exogenous ABA and FD treatment have on monomer production and deposition.

3.3.3.2 Soluble Monomer Analysis of Suberin Aliphatics

3.3.3.2.a Soluble Fatty Acid Quantification

Starting with the soluble free fatty acids, potato aliphatic suberin normally contains chain lengths ranging from C20-C28. When examining the water controls for total fatty acid accumulation, there was a notable drop at day 4, evident to some extent in all fatty acid chain lengths (Figure 3.13). By day 6, the soluble fatty acid pools in the water controls show recovery and then stabilize to presumably a new steady state level. The only exception of this was C28, where continued accumulation of C28 fatty acids occurred over the day 3 levels into day 14 (Figure 3.13e). FD treatment did not create a dramatic soluble fatty acid phenotype relative to the water controls, with two notable treatment effects occurring. The first was a slight delay in recovery of free fatty acids after the day 4 drop in soluble pools, which was especially evident in longer chain fatty acids on day 6 (Figure 3.13e-f). By day 14, the concentrations of shorter and mid-chain free fatty acids (C20-C24) are not significantly different in the FD treatment than from the water controls (Figure 3.13a-c). However, longer chain C26 and C28 fatty acids do not re-establish soluble fatty acid levels and have a significantly lower accumulation by day 14 (Figure 3.13e).

Exogenous ABA application with FD creates a strong soluble fatty acid phenotype. With the FD/ABA treatment, total free fatty acids increased significantly from day 4 through 14 when compared to FD-treated tubers or water controls (Figure 3.13). Therefore, there was a significant regulatory component of ABA concentration in sustaining fatty acid biosynthesis or accumulation in the soluble pool. As all chain lengths do show significant accumulation differences by day 14, the effect of ABA was not limited to only one chain length of free fatty acids. However, it is notable that the shorter and mid-chain fatty acids (C20, C22 and C24) showed an earlier increase of fatty acid soluble pools by day 4, whereas the longer chain fatty acids (C26 and C28) are delayed and differ from the water controls only after day 6 (Figure 3.13a-e).

3.3.3.2.b Soluble Primary Alcohol Quantification

Soluble primary alcohols accumulated similarly to soluble fatty acids (compare Figure 3.13f and 3.14h). As with free fatty acids, the water controls exhibited a drop in soluble pools between day 3 and day 4, which by day 14 had recovered to initial steady state levels in the shorter and mid-chain lengths (Figure 3.14a-d). The longer chain fatty alcohols, C24-C28, continued to accumulate beyond their initial levels between day 6 and 14 (Figure 3.14e-g). FD treatment resulted in a similar profile of soluble alcohol accumulation to the water controls. However, FD treatment prevented accumulation of the longer chain C24-C28 primary alcohols later in the timecourse, indicating *de novo* ABA biosynthesis may directly or indirectly regulate soluble alcohol production or incorporation. Additionally, FD treatment created a notable phenotype of the short-chain C16 soluble alcohols. (Note the scale of C16 primary alcohols, as it was a very small

proportion of suberin-associated monomers.) Day 2 levels in the FD treatment were reduced, and did not recover throughout the timecourse (Figure 3.14a). Thus, there was a distinct chain length specific effect of FD on the primary alcohols, with the short chain phenotype especially evident at day 3 and day 14 when the mid- and longer chain alcohols increase the accumulation of the soluble alcohol pool (compare Figure 3.14a-b to c-g).

Exogenous ABA with FD resulted in an increased accumulation of all primary alcohols chain lengths except C16 relative to water controls. Especially evident with C20 and C28 alcohol chain lengths, at day 4 there was a difference between ABA/FD and water controls or FD treatment (Figures 3.14c and f). All chain lengths except C16 and C22 showed increased accumulation of soluble alcohols by day 14. Although exogenous ABA was able to transiently recover the day 2 phenotype in C16-OH, this recovery was short lived as there was no spike in accumulation of C16 soluble pools at day 3 or by day 14, which was present in the water controls (Figure 3.14a). The C22-OH data did not follow the same trend relative to the C20 or C24 alcohols, and it is possible that this was due to co-elution of another peak at the same retention time as the C22 alcohol, which interfered with quantitation. Treatment of the GC-MS data required a selected ion search to estimate the proportion of the C22-OH peak composed of the alcohol versus the contaminating compound, and thus the quantification of this particular alcohol chain length should be interpreted with caution.

3.3.3.2.c Soluble ω-OH Fatty Acid and α,ω-Dioic Acid Quantification

For ω-hydroxylated fatty acids, there was a remarkably different accumulation pattern in the soluble pools between short- and mid- to long-chain ω-hydroxylated fatty acids. C16 and C18:1 ω-OH's as well as C18:1 α,ω-dioics had negligible soluble pools until day 3, when an accumulation of products in the soluble pools was evident (Figures 3.15 a-b and 3.16). Soluble C16 and C18:1 ω-hydroxylated fatty acids peaked by day 6, and then declined back to a negligible level by day 14. In contrast, C20-C26 ω-OH fatty acids maintain their initial soluble pool concentrations over the first 3 days post-wounding, before substantially droping by day 4 in the water controls (Figure 3.15 c-f). C20-24 ω-OH's subsequently recovered to initial levels by day 14; whereas C26 ω-OH recovered faster peaking at day 6, similar to the short chain ω-hydroxylated monomers.

For the ω-hydroxylated fatty acids with soluble pools that rose day 4 through day 6, including C16, C18:1 and C26, FD treatment completely abolished this initiation of monomer accumulation (Figure 3.15 a, b and f and 3.16). Conversely, in the mid-chain C20-24 ω-OH's FD treatment resulted in a transient decrease in soluble ω-hydroxylated fatty acid accumulation at day 2, but had no impact from day 4 through 6 relative to the controls.

Exogenous ABA application resulted in recovery of the FD phenotype at day 6 for the three affected chain lengths, C16, C18:1 and C26 ω-OH's (Figure 3.15 a, b, f and 3.16). In particular, a significant chain length effect was present for C18:1 ω-OH, as there was a 167% greater accumulation in the soluble pool relative to the water control (Figure 3.15b). Whereas shorter chain C16 and C18:1 ω-OH monomers had greater accumulation

at day 6, the mid- and longer chain C22-C26 monomers accumulate significantly larger soluble pools at day 14 (Figure 3.15 d-f). In both cases, a significant difference was evident at the time of maximal accumulation in the soluble pool.

3.3.3.3 Insoluble Monomer Analysis of Suberin Aliphatics

3.3.3.3.a Insoluble Fatty Acid Quantification

Investigating the insoluble aliphatic accumulation included the monomers assumed to have passed through the soluble pool that are incorporated into the biopolymer through ester linkages, resulting in a 3-D insoluble matrix. Water controls began to incorporate fatty acids into the biopolymer between day 3 and day 4, which steadily accumulated through the remainder of the 14 day timecourse (Figure 3.17). FD treatment prevents the incorporation of aliphatics into the suberin macromolecule, and was effective throughout the 14 day timecourse with only C20 fatty acids beginning to show a small accumulation by day 14 (Figure 3.17 a-e). Exogenous ABA with FD treatment resulted in the recovery of fatty acid incorporation into the suberin macromolecule, indicating that the removal of *de novo* ABA biosynthesis resulted in a loss of polymerization. In addition, exogenous ABA application resulted in a significant transient increase in fatty acid incorporation two days post-wounding, and this effect was chain length specific and only present for the mid-chain C20 and C22 fatty acids (Figure 3.17 a, b).

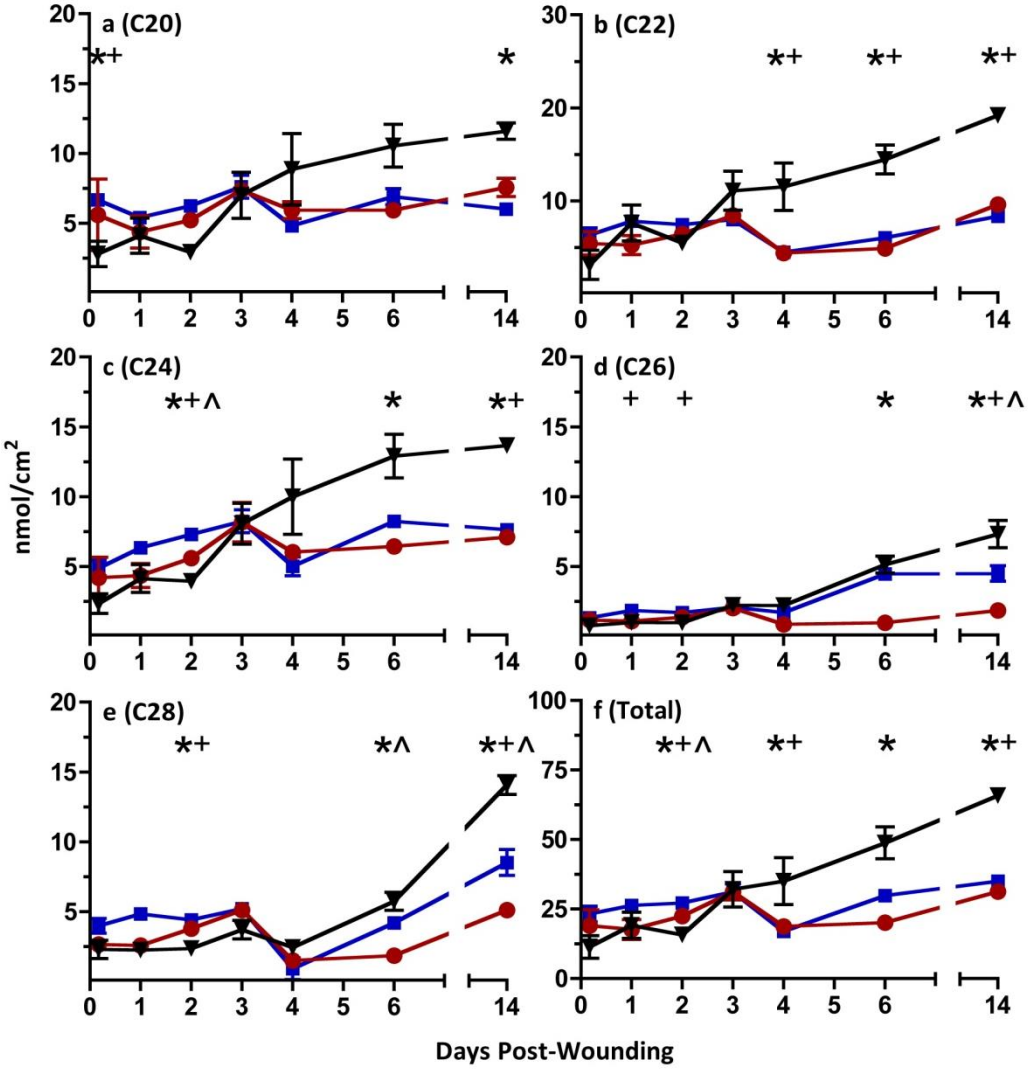

Figure 3.13: Effect of Exogenous ABA and FD treatment on Soluble Fatty Acid Accumulation in Wounded Potato Tubers over 14 days
a, C20; b, C22; c C24; d, C26; e, C28; and f, total fatty acids (C20-C28). Squares are water controls, circles are FD treatment, and triangles are exogenous ABA/FD treatment. Statistically significant differences ($p \leq 0.05$) shown between three treatments (∧ between water and FD; + between water and ABA, * between ABA and FD). Data represented by mean ± standard deviation, n=3.

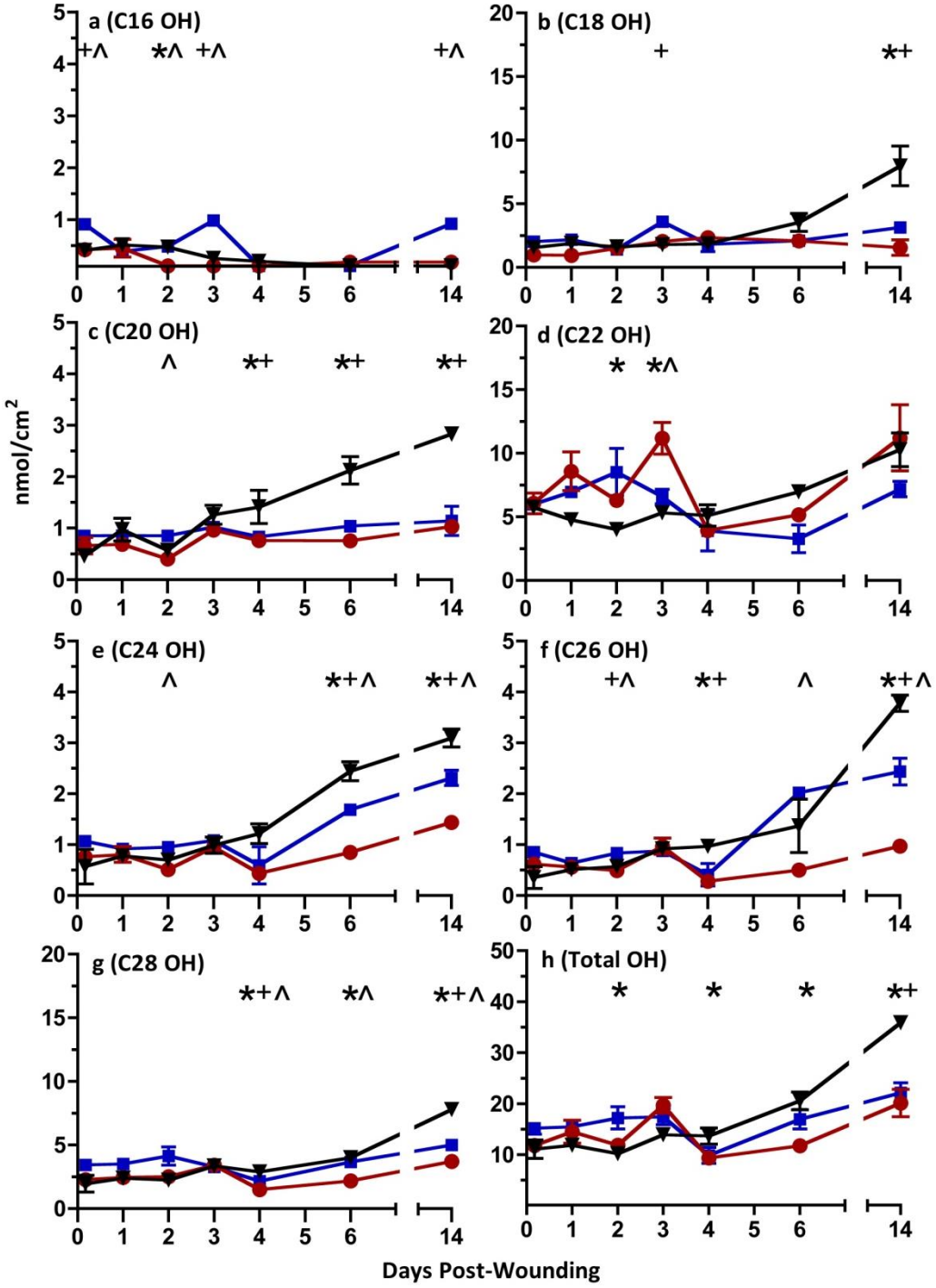

Figure 3.14: Effect of Exogenous ABA and FD treatment on Soluble Fatty Alcohol Accumulation in Wounded Potato Tubers over 14 days

a, C16; b, C18; c, C20; d, C22; e, C24; f, C26; g, C28; h, total fatty alcohols (C16-C28). Squares are water controls, circles are FD treatment, and triangles are exogenous ABA/FD treatment. Statistically significant differences ($p \leq 0.05$) shown between three treatments (∧ between water and FD; + between water and ABA, * between ABA and FD). Data represented by mean ± standard deviation, n=3.

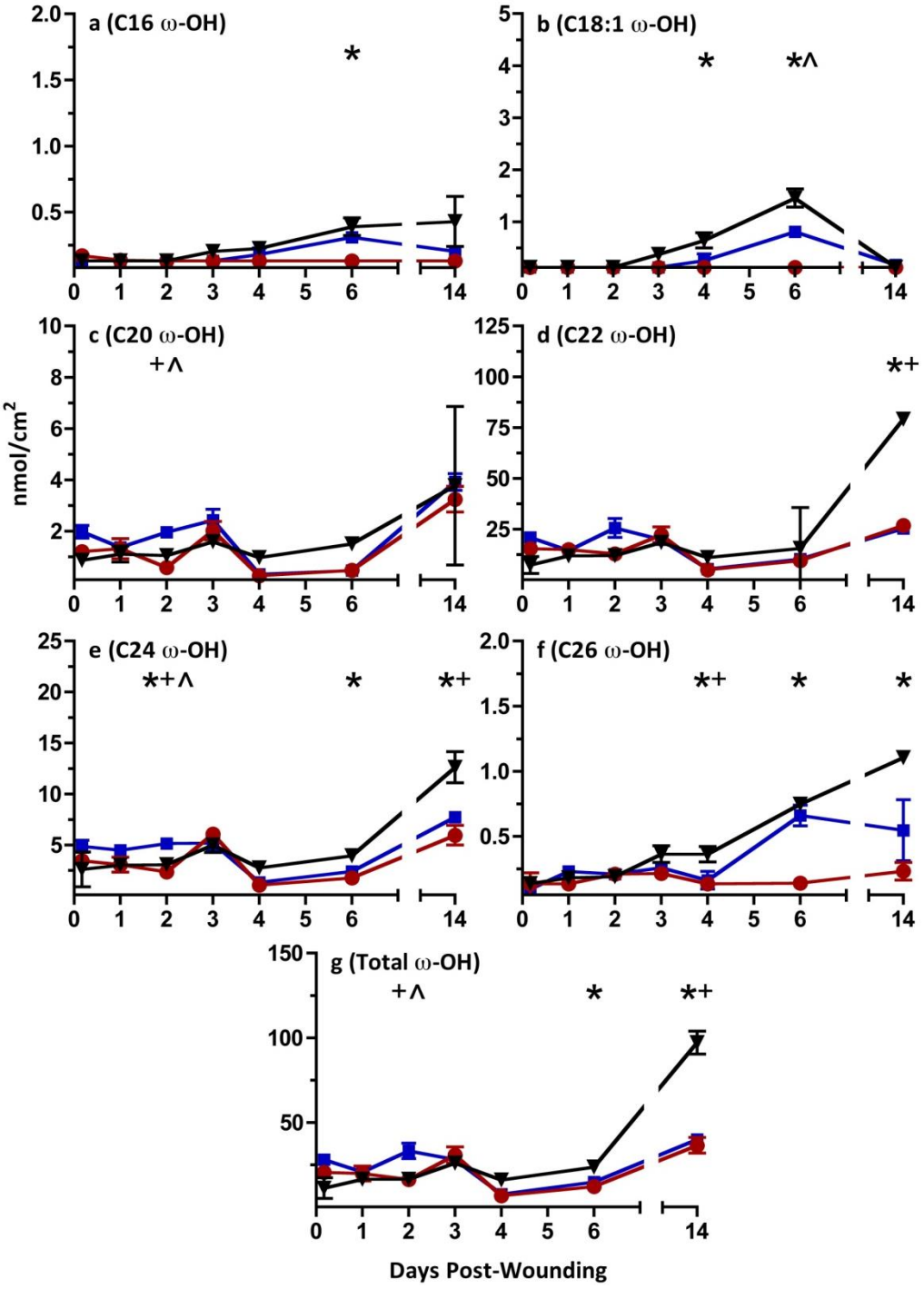

Figure 3.15: Effect of Exogenous ABA and FD treatment on Soluble ω-Hydroxylated Fatty Acid Accumulation in Wounded Potato Tubers over 14 days
a, C16; b, C18:1; c, C20; d, C22; e, C24; f, C26; g, total ω-OH fatty acids (C16-C26). Squares are water controls, circles are FD treatment, and triangles are exogenous ABA/FD treatment. Statistically significant differences ($p \leq 0.05$) shown between three treatments (∧ between water and FD; + between water and ABA, * between ABA and FD). Data represented by mean ± standard deviation, n=3.

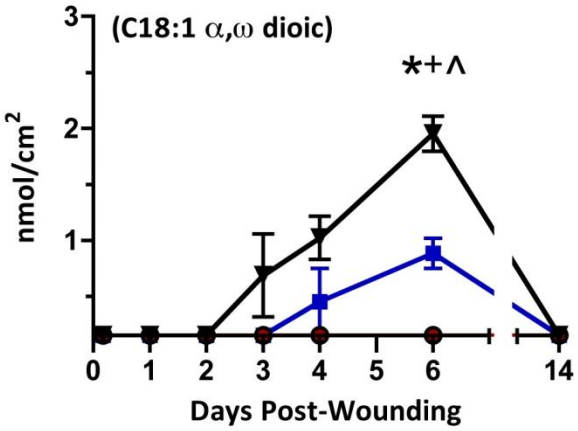

Figure 3.16: Effect of Exogenous ABA and FD treatment on Soluble C18:1 α, ω-Dioic Acid Accumulation in Wounded Potato Tubers over 14 days
Squares are water controls, circles are FD treatment, and triangles are exogenous ABA/FD treatment. Statistically significant differences ($p \leq 0.05$) shown between three treatments (^ between water and FD; + between water and ABA, * between ABA and FD). Data represented by mean ± standard deviation, n=3.

3.3.3.3.b Insoluble Primary Alcohol Quantification

For primary alcohol incorporation, similar accumulation patterns occurred as with the insoluble fatty acids (Figure 3.18). Primary alcohol incorporation began between day 3 and day 4 in the water controls, and continued to accumulate through day 14 post-wounding. FD treatment eliminated the incorporation of primary alcohols into the biopolymer, with no accumulation throughout the 14 days. (Note the large error bars in C26-OH samples at day 6, which were caused by a single large value). Exogenous ABA application with FD resulted in the recovery of the normal accumulation from day 3 onward. As seen with the C20 and C22 fatty acids, the corresponding primary alcohols also have a transient upregulation of aliphatic incorporation by day 2, which was not present in the water controls (Figure 3.18 c and d).

3.3.3.3.c Insoluble ω-OH Fatty Acid and α,ω-Dioic Acid Quantification

Regarding ω-hydroxylated fatty acids, as with the insoluble fatty acids and primary alcohols, the accumulation of ω-hydroxylated fatty acids started between day 3 and day 4 in the water controls, and a continued rise in throughout the 14 days (Figures 3.19 and 3.20). FD treatment inhibited the incorporation of monomers into the suberin biopolymer, with only a slight accumulation by day 14 in the shortest chain C16 ω-OH fatty acid (Figure 3.19a). The control phenotype was recovered by addition of exogenous ABA, which resulted in a normal accumulation throughout the timecourse (Figure 3.19 a-f). Although not statistically significant, as seen with fatty acids and primary alcohols there were transient early accumulations present by day 2 for the short and mid-chain ω-OH fatty acids, including C16, C20, C22 and C24 (Figure 3.19 a, c-f). The further oxidized α,ω-dioic acids show the same patterns of accumulation, including the corresponding C16 α,ω-dioic acid by day 2 (Figure 3.20a).

3.4 Summary

After analyzing the detailed monomer accumulation in both soluble and insoluble suberin aliphatics, several interesting patterns emerged from treatment with FD and exogenous ABA. Analyzing the initial days post-wounding, an FD effect was evident at day 2 in soluble pools of total fatty acids, total fatty alcohols and total ω-hydroxylated fatty acids. At this time point, the water controls showed no reduction of soluble monomers where FD-treatment did reduce these aliphatics in both FD and ABA/FD-treated tubers (Figures 3.13f, 3.14h, 3.15g). The FD inhibition of soluble pool levels was

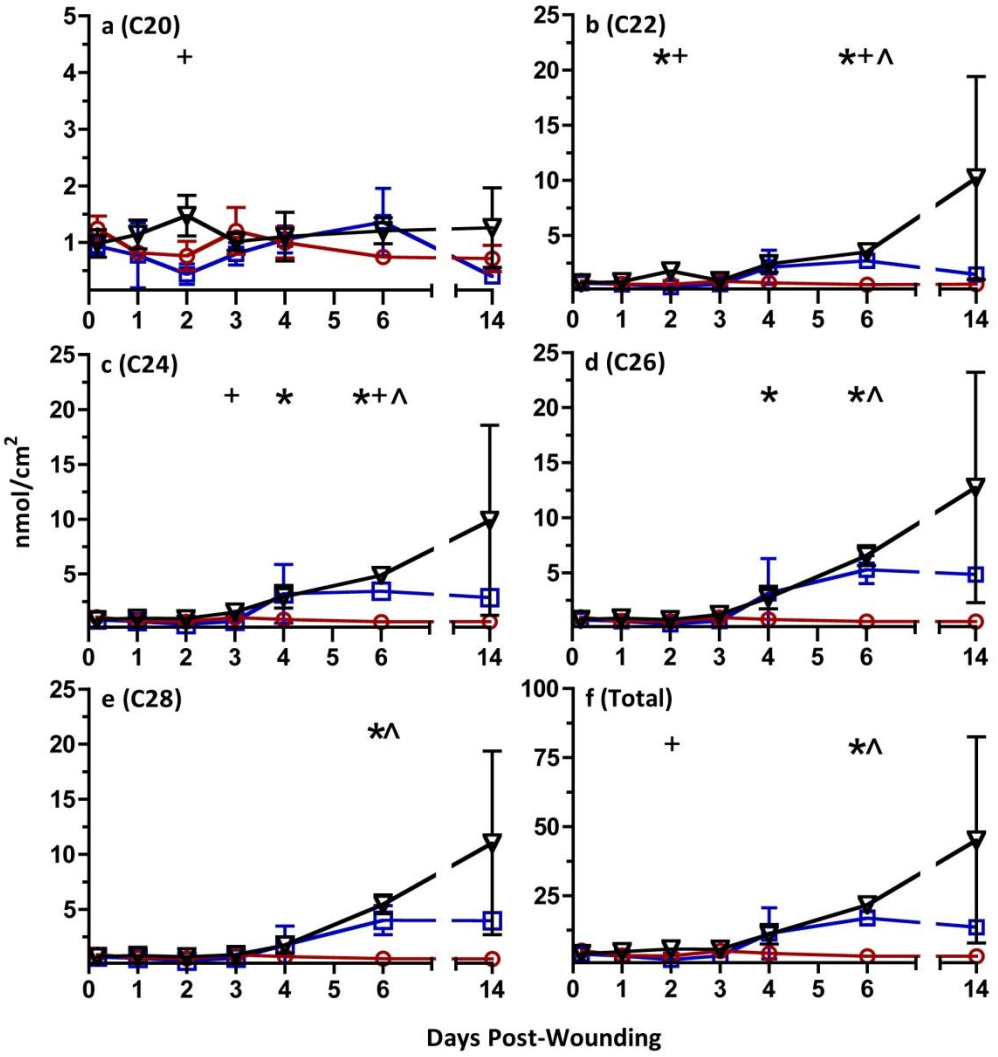

Figure 3.17: Effect of Exogenous ABA and FD treatment on Insoluble Fatty Acid Accumulation in Wounded Potato Tubers over 14 days

a, C20; b, C22; c, C24; d, C26; e, C26; and f, total fatty acids (C20-C28). Squares are water controls, circles are FD treatment, and triangles are exogenous ABA/FD treatment. Statistically significant differences ($p \leq 0.05$) shown between three treatments (^ between water and FD; + between water and ABA, * between ABA and FD). Data represented by mean ± standard deviation, n=3.

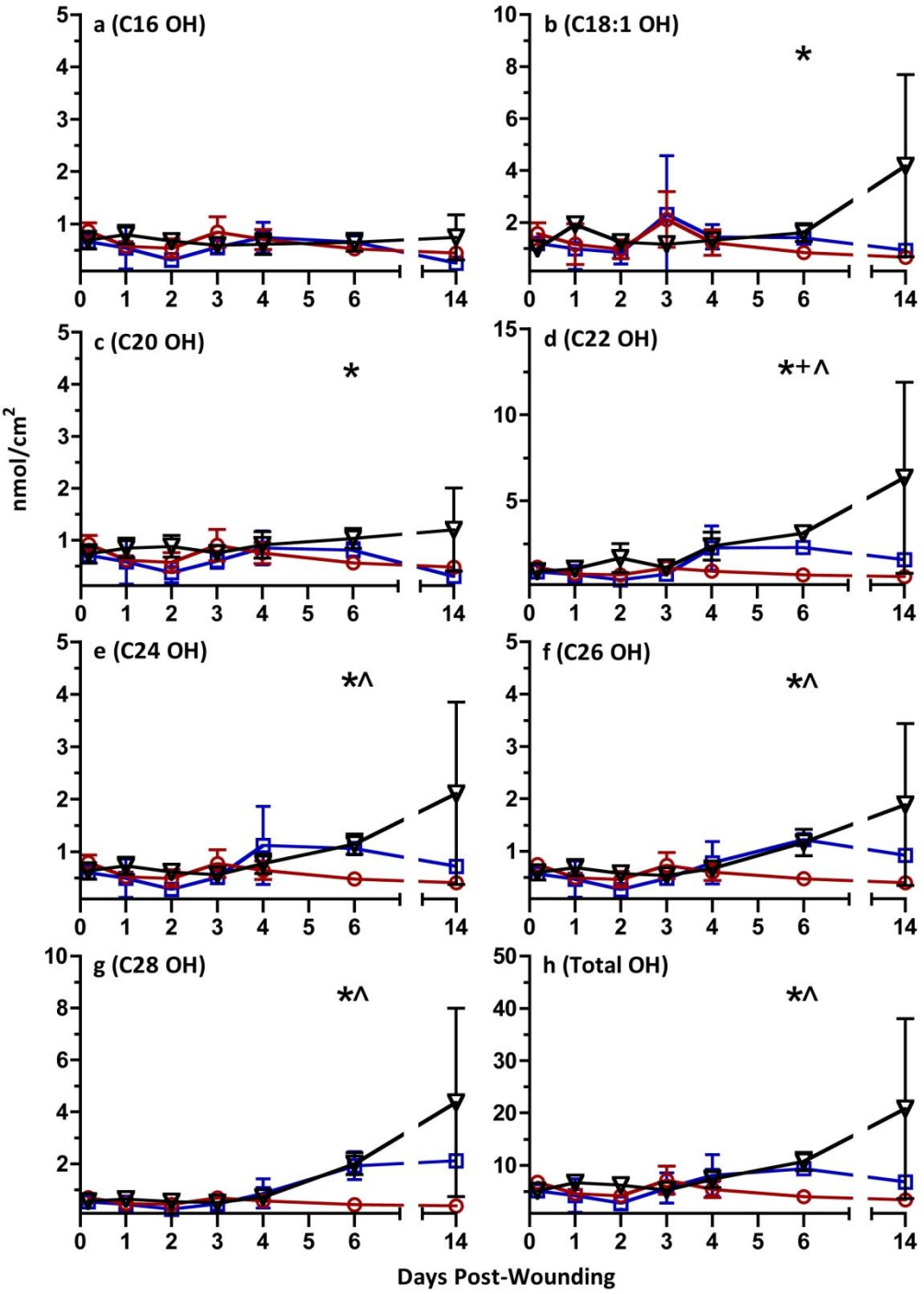

Figure 3.18: Effect of Exogenous ABA and FD treatment on Insoluble Fatty Alcohols Accumulation in Wounded Potato Tubers over 14 days
a, C16; b, C18; c, C20; d, C22; e, C24; f, C26; g, C28; h, total fatty acids (C16-C28). Squares are water controls, circles are FD treatment, and triangles are exogenous ABA/FD treatment. Statistically significant differences ($p \leq 0.05$) shown between three treatments (^ between water and FD; + between water and ABA, * between ABA and FD). Data represented by mean ± standard deviation, n=3.

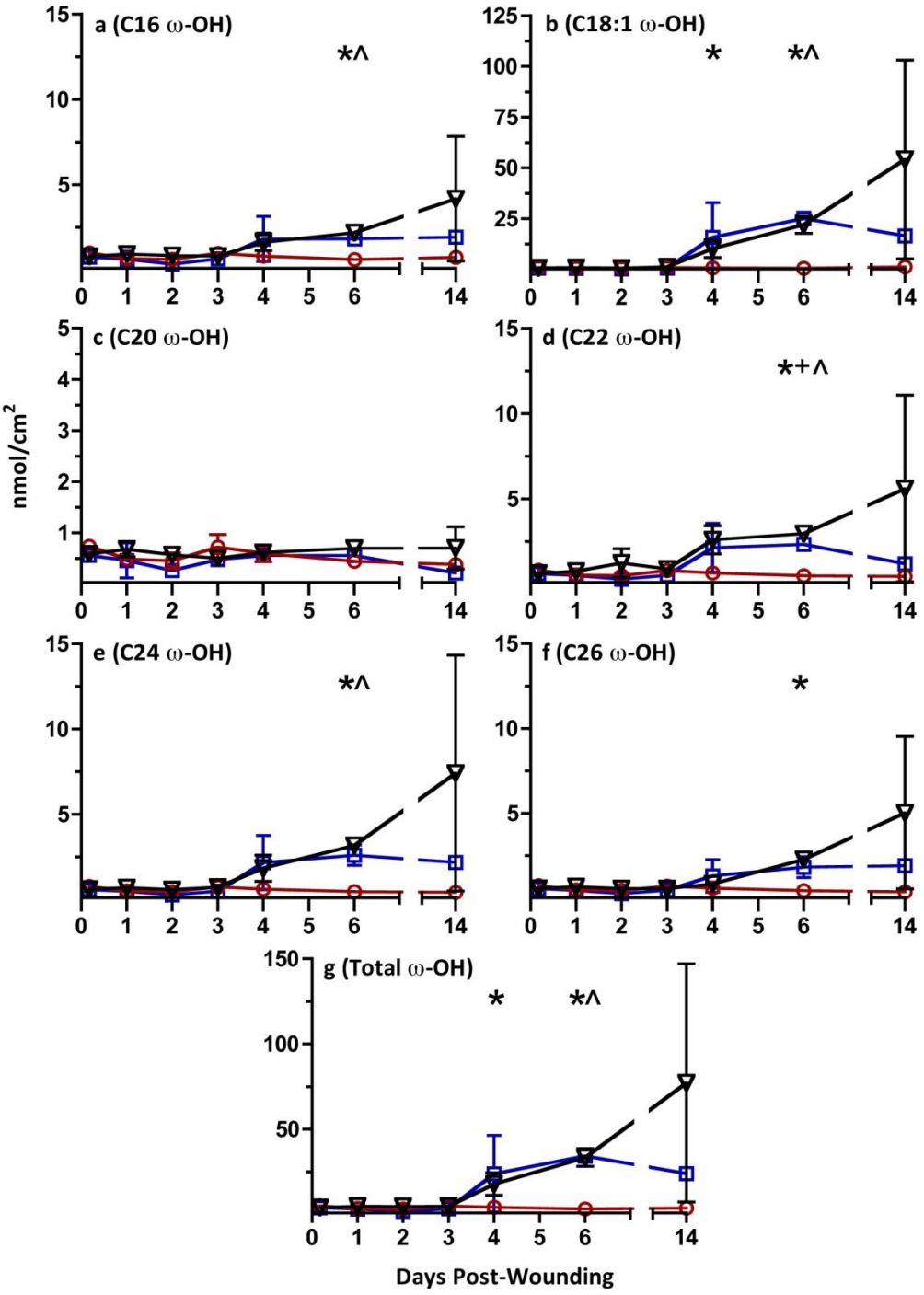

Figure 3.19: Effect of Exogenous ABA and FD treatment on Insoluble ω-OH Fatty Acid Accumulation in Wounded Potato Tubers over 14 days
a, C16; b, C18:1; c, C20; d, C22; e, C24; f, C26; g, total ω-OH fatty acids (C16-C26). Squares are water controls, circles are FD treatment, and triangles are exogenous ABA/FD treatment. Statistically significant differences ($p \leq 0.05$) shown between three treatments (^ between water and FD; + between water and ABA, * between ABA and FD). Data represented by mean ± standard deviation, n=3.

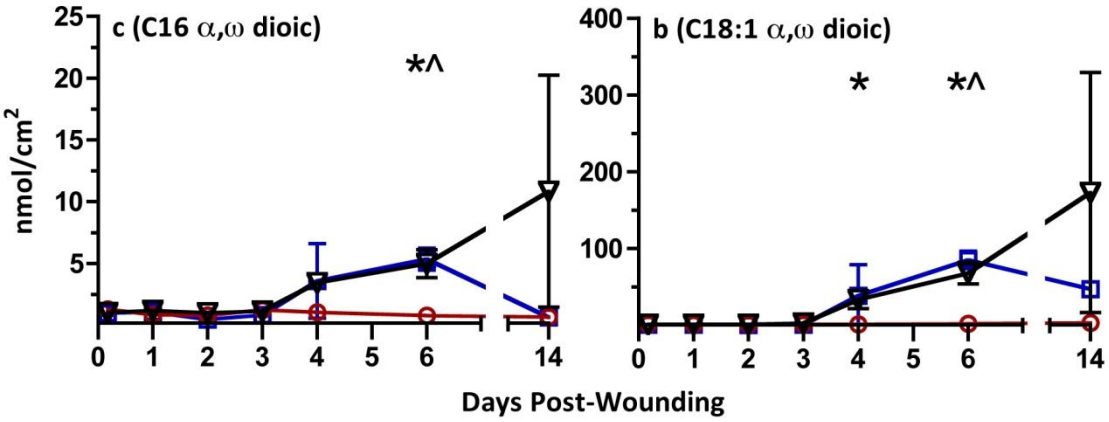

Figure 3.20: Effect of Exogenous ABA and FD treatment on Insoluble α, ω-Dioic Acid Accumulation in Wounded Potato Tubers over 14 days
a, C16; b, C18:1. Squares are water controls, circles are FD treatment, and triangles are exogenous ABA/FD treatment. Statistically significant differences ($p \leq 0.05$) shown between three treatments (^ between water and FD; + between water and ABA, * between ABA and FD). Data represented by mean ± standard deviation, n=3.

transient as FD and ABA/FD-treated tubers mirrored the water controls by day 3 post-wounding. As both FD and ABA/FD-treatments inhibited soluble accumulation relative to water controls at 2 days post-wounding, *de novo* ABA biosynthesis had a regulatory role in soluble monomer production. Interestingly, suberin-associated gene expression over the first 2 days post-wounding was not induced in the water controls and FD-treated tubers, while a transient up-regulation was present in the ABA/FD-treated tubers (Figures 3.4-3.7). Logically, increased suberin-associated gene expression should result in increased accumulation of soluble aliphatic monomers, but exogenous ABA upregulation of suberin aliphatic biosynthesis genes did not result in greater monomer accumulation. However, as insoluble monomers are shuttled through the soluble pool prior to incorporation, increased aliphatics may accumulate in either. When analyzing the insolubles over the first 2 days post-wounding, C20-C22 fatty acid monomer accumulation reflected the gene expression patterns with a transient upregulation in exogenous ABA/FD-treated tubers. Although the accumulation of insoluble C20 and C22

fatty acids was the only statistically significant result, the trend was also present in the primary alcohols and ω-hydroxylated products (Figures 3.17 a-b, f; 3.18 c-d; 3.19 c-d). Thus, prior to day 3 post-wounding, soluble accumulation does not correspond to aliphatic suberin-associated gene expression whereas insoluble accumulation did reflect aliphatic suberin-associated gene expression. As the soluble pool must be passed through by monomers for incorporation into the insoluble matrix, these results together indicated that ABA-induced monomer production was shuttled straight through the soluble pool and incorporated directly into the insoluble biopolymer. Therefore, inhibition of *de novo* biosynthesis prior to day 3 post-wounding prevented soluble accumulation. Exogenous ABA application facilitated a transient increase of insoluble monomer incorporation, likely due to increased transcription of suberin-associated genes which resulted in increased overall monomer production.

Analysis of the later period of closing layer formation and into wound periderm formation, a substantially different effect of exogenous ABA and FD treatment was present. FD treatment did not significantly alter the soluble accumulation after day 4 post-wounding; whereas the addition of exogenous ABA did cause a significantly greater soluble accumulation (Figures 3.13f, 3.14h, 3.15g). The accumulation of solubles in the ABA/FD treatment could have been the result of an increased influx into the soluble pool or a decreased efflux due to hinder incorporation into the suberin biopolymer. Exogenous ABA did not significantly increase gene expression from water controls after day 3 post-wounding; indicating that transcript levels for these enzymes did not increase production capacity of soluble monomers (Figures 3.4-3.7). FD treatment abolished suberin-associated aliphatic gene expression over the first 6 days post-wounding, but relative to

water controls the FD treatment did not significantly alter the total soluble accumulation in suberin for most monomer classes (Figures 3.13f, 3.14h, 3.15g). Thus, aliphatic monomer production and modification was likely not the point of regulation for soluble monomer accumulation. As with earlier in the wound-healing process, accumulation of insoluble monomers after day 4 corresponds to suberin-associated gene expression (Figures 3.17f, 3.18h, 3.19g). Insoluble aliphatic incorporation was almost completely inhibited throughout the 14 days post-wounding, with no suberin-associated gene expression occurring in the FD treatment. Exogenous ABA application did not significantly increase insoluble incorporation relative to water controls after day 4, which also exhibited no difference in gene expression from the water controls after day 4. Therefore, after day 4 a lack of *de novo* ABA biosynthesis resulted in a lack of insoluble incorporation into the biopolymer, even though soluble monomer levels were comparable between FD treatment and water controls.

A clear and substantial temporal change in responsiveness to ABA occurred around day 3 post-wounding (Figure 3.21). First, decreasing *de novo* ABA biosynthesis prior to day 3 post-wounding resulted in decreased soluble accumulation, contrasting post-day 3 where *de novo* ABA biosynthesis did not impact soluble accumulation. Second, increasing ABA concentration through exogenous application prior to day 3 post-wounding resulted in no change in soluble accumulation, contrasting with the post-day 3 increase in ABA concentration which did result in increased soluble accumulation. Insoluble accumulation of aliphatics was almost completely inhibited with FD throughout

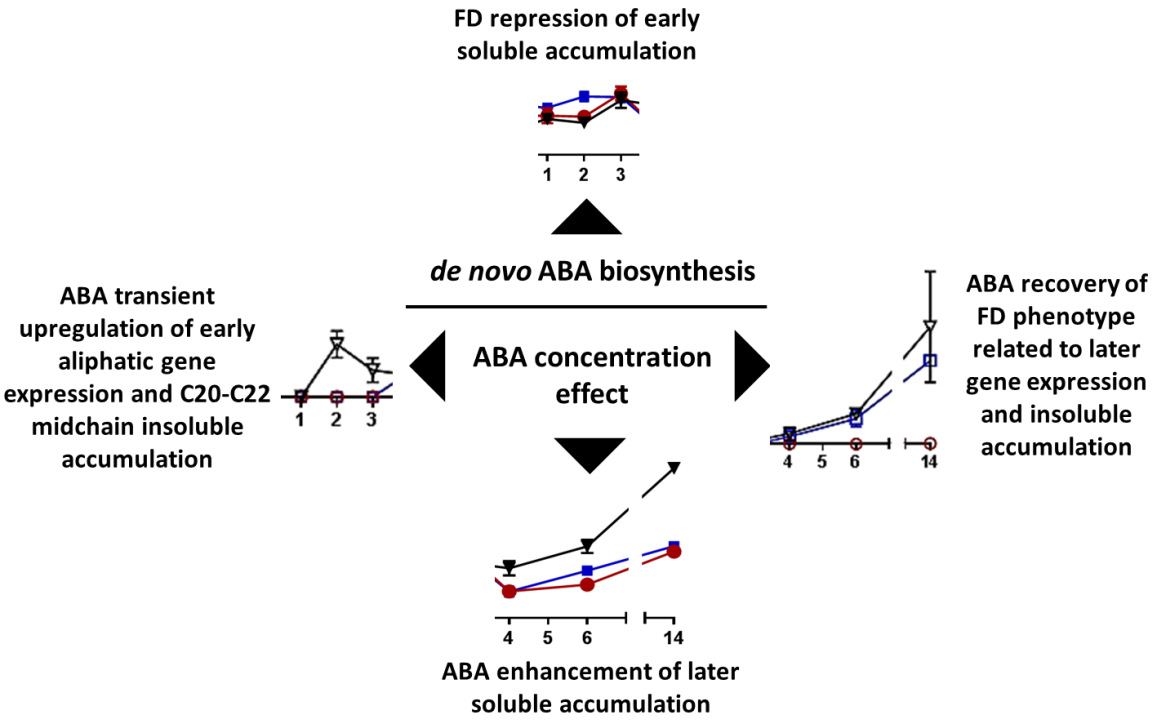

Figure 3.21: Summary of ABA Regulatory Effects on Suberin-Associated Gene Expression and Soluble and Insoluble Aliphatic Monomer Initiation and Accumulation.
Squares are water controls (blue), circles are FD treatment (red), and triangles are exogenous ABA/FD treatment (black). Data graphs were chosen as representative of general trends.

the 14 day timecourse, but the FD phenotype was rescued by exogenous ABA application indicating *de novo* ABA biosynthesis did not regulate insoluble incorporation. Overall, these results demonstrated that *de novo* ABA biosynthesis may have an early impact on soluble pools, timed when aliphatic gene regulation was normally upregulated to begin incorporation of aliphatics into the suberin macromolecule, but does not impact the overall accumulation of soluble pools. ABA concentration may have a later impact on soluble pools, as increased accumulation occurs after day 4 when there was no FD phenotype. ABA concentration also clearly regulated insoluble accumulation, as exogenous ABA rescued the FD phenotype throughout the timecourse. In addition,

exogenous ABA transiently increased the monomer incorporation by day 2 post-wounding, indicating a temporal regulatory role as well. Gene expression of suberin-associated genes with ABA/FD treatment was closely correlated to insoluble accumulation, demonstrating that transcription and monomer incorporation are under the same regulatory control. Further studies such as a pulse/chase ABA experiment will be needed to determine the regulation of soluble accumulation, and to determine why sustained accumulation of solubles occurs after day 4 with exogenous ABA application.

Diverging from the overall trends identified with FD and ABA/FD treatment in this study, two chain-length specific effects were observed. The first involved short-chain ω-hydroxylated fatty acids, because C16 and C18:1 ω-OH fatty acids and C18:1 α,ω-dioic acids showed a unique pattern of soluble accumulation with exogenous ABA treatment. For these shorter chain monomers, accumulation in the soluble pool rose between day 3 and day 6 to a maximal point, before decreasing back to a steady state level by day 14 (Figures 3.15 a-b, 3.16). Soluble monomer accumulation of these short-chain ω-hydroxylated fatty acids was also present in the water controls, but to a lesser extent. No accumulation of ω-hydroxylated soluble monomers occurred in the FD-treated tubers between days 4 to 14. While exogenous ABA did lead to a greater accumulation of these compounds in the soluble pools between day 4 and day 6, for the ω-hydroxylated monomers this increased flux far exceeded the initial steady state levels and was transient, declining back to initial levels by day 14. Thus, there is a differential accumulation effect from exogenous ABA in short-chain ω-hydroxylated fatty acids versus the rest of the soluble fatty acids and fatty acid derivatives.

The second observable chain-length effect involved longer chain C26-C28 fatty acids, fatty alcohols and ω-hydroxylated fatty acids. For these longer chain monomers, accumulation in the FD-treated soluble pool was repressed whereas the amounts of these compounds rose in water controls between day 4 and day 14 to a maximal point (Figures 3.13 d-e, 3.14 f-g, 3.15f). As ABA/FD treatment resulted in over-accumulation of soluble monomers over this time period, it appeared that longer chain soluble monomer accumulation was more sensitive to the lack of ABA than are shorter chain lengths.

In conclusion, this was the first quantitative study that comprehensively examined the process of suberization from gene expression through soluble and insoluble aliphatic incorporation into the biopolymer. ABA has been found to be a strong, potentially global regulator of these processes, impacting transcription of key genes and subsequent accumulation of soluble aliphatic compounds and their incorporation into the suberin matrix. Both the concentration of ABA and *de novo* biosynthesis of ABA appear to play a role in the regulation of aliphatic suberin biosynthesis, with a temporal shift around day 3 post-wounding from an early effect to a later effect. ABA itself, however, was not the master regulator of the entire process, as reduction of ABA in the FD treatment does not abolish soluble monomer accumulation. Therefore, ABA was a major regulator for suberin-associated gene expression and downstream insoluble aliphatic monomer accumulation, but another factor played a role in regulating the soluble aliphatic accumulation.

References

Bernards, MA. 2002. Demystifying Suberin. Canadian Journal of Botany 80: 227-240

Boher P, Serra O, Soler M, Molinas M, Figueras M. 2013. The Potato Suberin Feruloyl Transferase *FHT* which Accumulates in the Phellogen is Induced by Wounding and Regulated by Abscisic and Salicylic Acids. Journal of Experimental Botany 64: 3225-3236

Compagnon V, Diehl P, Benveniste I, Meyer D, Schaller H, Schreiber L, Franke R, Pinot F. 2009. *CYP86B1* is Required for Very Long Chain omega-Hydroxyacid and alpha, omega-Dicarboxylic Acid Synthesis in Root and Seed Suberin Polyester. Plant Physiology 150: 1831-1843

Cottle W, Kolattukudy PE. 1982. Abscisic Acid Simulation of Suberization. Plant Physiology 70: 775-780

Gamble PE, Mullet JE. 1986. Inhibition of Carotenoid Accumulation and Abscisic Acid Biosynthesis in Fluridone-Treated Dark-Grown Barley. European Journal of Biochemistry 160: 117-121

Gou JY, Yu XH, Liu CJ. 2009. A Hydroxycinnamoyltransferase Responsible for Synthesizing Suberin Aromatics in *Arabidopsis*. Proceedings of the National Academy of Sciences of the United States of America 106: 18855-18860

Grondin A, Rodrigues O, Verdoucq L, Merlot S, Leonhardt N, Maurel C. 2015. Aquaporins Contribute to ABA-Triggered Stomatal Closure through OST1-Mediated Phosphorylation. The Plant Cell 27: 1945-1954

Holloway PJ. 1983. Some Variations in the Composition of Suberin from the Cork Layers of Higher-Plants. Phytochemistry 22: 495-502

Kumar GN, Lulai EC, Suttle JC, Knowles NR. 2010. Age-induced Loss of Wound-Healing Ability in Potato Tubers is Partly Regulated by ABA. Planta 232: 1433-1445

Le Bouquin R, Pinot F, Benveniste I, Salaün JP, Durst F. 1999. Cloning and Functional Characterization of CYP94A2, a Medium Chain Fatty Acid Hydroxylase from *Vicia sativa*. Biochemical and Biophysical Research Communications 261: 156-162

Le Bouquin R, Skrabs M, Kahn R, Benveniste I, Salaün JP, Schreiber L, Durst F, Pinot F. 2001. CYP94A5, a New Cytochrome P450 from *Nicotiana tabacum* is Able to Catalyze the Oxidation of Fatty Acids to the omega-Alcohol and to the Corresponding Diacid. European Journal of Biochemistry 268: 3083-3090

Li-Beisson Y, Shorrosh B, Beisson F, Andersson MX, Arondel V, Bates PD, Baud S, Bird D, Debono A, Durrett TP, Franke RB, Graham IA, Katayama K, Kelly AA,

Larson T, Markham JE, Miquel M, Molina I, Nishida I, Rowland O, Samuels L, Schmid KM, Wada H, Welti R, Xu C, Zallot R, Ohlrogge J. 2013. Acyl-Lipid Metabolism. The *Arabidopsis* Book 11: e0161. pp 24

Lulai E, Huckle L, Neubauer J, Suttle J. 2011. Coordinate Expression of *AOS* Genes and JA Accumulation: JA Is Not Required for Initiation of Closing Layer in Wound Healing Tubers. Journal of Plant Physiology 168: 976-982

Lulai EC, Neubauer JD. 2014. Wound-Induced Suberization Genes are Differentially Expressed, Spatially and Temporally, During Closing Layer and Wound Periderm Formation. Postharvest Biology and Technology 90: 24-33

Lulai EC, Suttle JC. 2004. The Involvement of Ethylene in Wound Induced Suberization of Potato Tuber (*Solanum tuberosum* L.): A Critical Assessment. Postharvest Biology and Technology 34: 105-112

Lulai EC, Suttle JC, Pederson SM. 2008. Regulatory Involvement of Abscisic Acid in Potato Tuber Wound-Healing. Journal of Experimental Botany 59: 1175-1186

Molina I, Li-Beisson Y, Beisson F, Ohlrogge JB, Pollard M. 2009. Identification of an *Arabidopsis* Feruloyl-Coenzyme A Transferase Required for Suberin Synthesis. Plant Physiology 151: 1317-1328

Nambara E, Marion-Poll A. 2005. Abscisic Acid Biosynthesis and Catabolism. Annual Review of Plant Biology 56: 165-186

Nicot N, Hausman J-F, Hoffmann L, Evers D. 2005. Housekeeping Gene Selection for Real-Time RT-PCR Normalization in Potato during Biotic and Abiotic Stress. Journal of Experimental Botany 285: 1-8

Pinot F, Benveniste I, Salaün JP, Loreau O, Noël JP, Schreiber L, Durst F. 1999. Production *in vitro* by the Cytochrome P450 CYP94A1 of Major C18 Cutin Monomers and Potential Messengers in Plant-Pathogen Interactions: Enantioselectivity Studies. Biochemical Journal 342: 27-32

Sambrook J, Fritschi EF, Maniatis T. 1989. Molecular Cloning: A Laboratory Manual. Cold Spring Harbor Laboratory Press, New York. pp 362-364

Savatin EV, Gramegna G, Modesti V, Cervone F. 2014. Wounding in the Plant Tissue: The Defense of a Dangerous Passage. Frontiers in Plant Science 5: 470

Serra O, Hohn C, Franke R, Prat S, Molinas M, Figueras M. 2010. A Feruloyl Transferase Involved in the Biosynthesis of Suberin and Suberin-Associated Wax is Required for Maturation and Sealing Properties of Potato Periderm. The Plant Journal 62: 277-290

Serra O, Soler M, Hohn C, Sauveplane V, Pinot F, Franke R, Schreiber L, Prat S, Molinas M, Figueras M. 2009a. *CYP86A33*-Targeted Gene Silencing in Potato Tuber Alters Suberin Composition, Distorts Suberin Lamellae, and Impairs the Periderm's Water Barrier Function. Plant Physiology 149: 1050-1060

Serra O, Soler M, Hohn C, Franke R, Schreiber L, Prat S, Molinas M, Figueras M. 2009b. Silencing of *StKCS6* in Potato Periderm Leads to Reduced Chain Lengths of

Suberin and Wax Compounds and Increased Peridermal Transpiration. Journal of Experimental Botany 60: 697-707

Shinozaki K, Yamaguchi-Shinozaki K. 2007. Gene Networks Involved in Drought Stress Response and Tolerance. Journal of Experimental Botany 58: 221-227

Soliday CL, Dean BB, Kolattukudy PE. 1978. Suberization: Inhibition by Washing and Stimulation by Abscisic Acid in Potato Disks and Tissue Culture. Plant Physiology 61: 170-174

Tijet N, Helvig C, Pinot F, Le Bouquin R, Lesot A, Durst F, Salaün JP, Benveniste I. 1998. Functional Expression in Yeast and Characterization of a Clofibrate-Inducible Plant Cytochrome P-450 (CYP94A1) Involved in Cutin Monomers Synthesis. Biochemical Journal 332: 583-589

Vishwanath SJ, Kosma DK, Pulsifer IP, Scandola S, Pascal S, Joubès J, Dittrich-Domergue F, Lessire R, Rowland O, Domergue F. 2013. Suberin-Associated Fatty Alcohols in *Arabidopsis*: Distributions in Roots and Contributions to Seed Coat Barrier Properties. Plant Physiology 163: 1118-1132

Wang T, Tohge T, Ivakov AA, Mueller-Roeber B, Fernie AR, Mutwil M, Schippers JHM, Persson S. 2015. Salt-Related MYB1 (SRM1) Coordinates Abscisic Acid Biosynthesis and Signaling During Salt Stress in *Arabidopsis*. Plant Physiology 169: 1027-1041

Xu X, Pan S, Cheng S, Zhang B, Mu D, Ni P, Zhang G, Yang S, Li R, Wang J, Orjeda G, Guzman F, Torres M, Lozano R, Ponce O, Martinez D, De la Cruz G, Chakrabarti SK, Patil VU, Skryabin KG, Kuznetsov BB, Ravin NV, Kolganova TV, Beletsky AV, Mardanov AV, Di Genova A, Bolser DM, Martin DM, Li G, Yang Y, Kuang H, Hu Q, Xiong X, Bishop GJ, Sagredo B, Mejia N, Zagorski W, Gromadka R, Gawor J, Szczesny P, Huang S, Zhang Z, Liang C, He J, Li Y, He Y, Xu J, Zhang Y, Xie B, Du Y, Qu D, Bonierbale M, Ghislain M, Herrera Mdel R, Giuliano G, Pietrella M, Perrotta G, Facella P, O'Brien K, Feingold SE, Barreiro LE, Massa GA, Diambra L, Whitty BR, Vaillancourt B, Lin H, Massa AN, Geoffroy M, Lundback S, DellaPenna D, Buell CR, Sharma SK, Marshall DF, Waugh R, Bryan GJ, Destefanis M, Nagy I, Milbourne D, Thomson SJ, Fiers M, Jacobs JM, Nielsen KL, Sonderkaer M, Iovene M, Torres GA, Jiang J, Veilleux RE, Bachem CW, de Boer J, Borm T, Kloosterman B, van Eck H, Datema E, Hekkert BL, Goverse A, van Ham RC, Visser RG. 2011. Genome Sequence and Analysis of the Tuber Crop Potato. Nature 475: 189-195

Yang W, Bernards MA. 2006. Wound Induced Metabolism in Potato (*Solanum tuberosum* L.) Tubers: Biosynthesis of Aliphatic Domain Monomers. Plant Signaling and Behavior 1: 59-66

Yang W, Bernards MA. 2007. Metabolomic Analysis of Wound-Induced Suberization in Potato (*Solanum tuberosum* L.) Tubers. Metabolomics 3: 147-159

Chapter 4

Suberin-Associated ω-Hydroxylation and ABA Regulation of Suberin Aliphatic Biosynthesis

4.1 Analysis of Past and Current Work

Suberin is a defense biopolymer in plants that is pre-formed in specialized cells during development as well as induced by biotic and abiotic stressors including wounding. As suberin functions both to prevent water loss and pathogen attack, a quantitative reduction of suberin deposition has been correlated to a decreased field tolerance against pathogens (Thomas et al., 2007) and increased water permeability (Schreiber et al., 2005). To develop crops that are resistant to biotic and abiotic stressors without becoming more dependent upon chemical pesticides, suberin biosynthesis has become an area of focused plant research. Over the past 10 years, the molecular tools available for research using plants have allowed researchers to identify the major suberin-associated genes for the production of the aliphatic domain within suberin. When suberin research was first initiated 40 years ago, *Solanum tuberosum* cv. Russet Burbank was chosen as the model system as tubers provided a large wound-inducible surface for biosynthesis and potatoes are clonally propagated producing identical genotypes. Both native periderms and wound-induced periderms of potato suberin have been extensively chemically characterized (e.g., Riley and Kolattukudy, 1975; Holloway, 1983, Neubauer et al., 2013). The completion of the *Arabidopsis* genome sequencing (2000) led to the

development of many molecular tools for plant research. However, for use as a suberin model system it remained challenging to work with as its small plant size has little developmental deposition or surface area available for wound-induced suberin production (Franke et al., 2012). Sequencing of the potato genome (2011) has led to the first opportunity to study the genetic regulation of wound-inducible suberin biosynthesis, with relative ease, with corresponding quantitative chemical analysis of aliphatic monomers produced.

Regarding aliphatic monomer production in potato, the major classes of suberin-associated compounds are fatty acids, fatty alcohols, ω-hydroxylated fatty acids and α,ω-dioic acids (Kolattukudy et al., 1976; Yang and Bernards, 2006; Schreiber, 2010). These aliphatics are incorporated into the suberin biopolymer in one of two forms, either as free monomers (termed solubles) or as cross-linked (esterified) monomers (termed insolubles). The soluble and insoluble monomers originate from fatty acid biosynthesis in the plastid, which produces C16:0 and C18:1 fatty acids that are exported to the cytoplasm where they are destined for one of two metabolic fates: (1) saturated fatty acids may undergo elongation to form very long chain fatty acids (VLCFA) ranging from C20-28, which can be further modified by reduction, decarboxylation, and/or oxidation; or (2) desaturated fatty acids that are oxidized to form ω-hydroxy fatty acids and α,ω-dioic acids (Yang and Bernards, 2006). To date, suberin-associated genes have been identified in potato (*St*) for many of these reactions including fatty acid ω-hydroxylation (*StCYP86A33/FAωH1* (Chapter 2 of this thesis; Serra et al., 2009a)), fatty acid elongation (*StKCS6;* Serra et al., 2009b), and insoluble incorporation of ω-hydroxylated fatty acids and primary alcohols via esterification to feruloyl-CoA (*StFHT;* Serra et al., 2010; Boher et al., 2013).

One of the major enzymatic reactions during the formation of aliphatic suberin monomers is ω-hydroxylation, as 55% of monomers undergo this modification (Yang and Bernards, 2006). The ω-oxidation of fatty acids is critical to formation of the macromolecular structure. Fatty acids with functional groups at each end of the molecule enable the ester linkages to form with glycerol, ferulates and hydroxycinnamates, resulting in the production of a 3-dimensional biopolymer (Graça and Pereira, 2000; Graça et al., 2015). At the beginning of this project, no suberin-associated ω-hydroxylases had been characterized in any plant. The identification and functional characterization of a suberin-associated ω-hydroxylase in potato was the primary goal of this research project, as well as investigating the regulation of its expression and activity. The ω-hydroxylation reaction is restricted in plants to the production of three spatially separate biopolymers: cutin, sporopollenin and suberin. Thus, the first step was to identify ω-hydroxylase(s) expressed developmentally in roots or induced by wounding. *FAωH1*, *FAωH2* and *FAωO1* were identified by searching an abiotic stress EST database, with cutin-associated *Arabidopsis* ω-hydroxylases as model genes to guide the homology search. Cloning and gene expression analysis indicated *FAωH1* was strongly expressed in roots during development as well as induced by wounding, establishing itself as a strong candidate for a suberin-associated ω-hydroxylase. At the same time, a research group from Spain cloned, sequenced and published the identity of *CYP86A33* from cv. Désirée, which was the homolog to FAωH1 (Serra et al., 2009a). Serra et al. (2009a) characterized *CYP86A33* as a fatty acid ω-hydroxylase based on RNA*i*-mediated gene silencing, which dramatically reduced the ω-hydroxylated monomers incorporated in the suberin biopolymer. However, due to an inability to produce functional recombinant CYP86A33 protein they could not functionally characterize the enzyme directly *in vitro*.

Simultaneously, production of recombinant protein for FAωH1 was being pursued in Bernards' laboratory. Functional characterization of FAωH1 proved challenging due to solubility issues with FAωH1, resulting in C16 palmitate being the only substrate assayed with recombinant FAωH1 protein. However, ω-hydroxylation of C16 palmitate to C16 ω-hydroxypalmitate confirmed that *in vitro* FAωH1 was an ω-hydroxylase capable of metabolizing fatty acid substrates. Further confirmation of *in situ* FAωH1 activity by lab colleague Anica Bjelica utilized the cloned potato *FAωH1* sequence to complement an *Arabidopsis cyp86a1/horst* ω-hydroxylase mutant (Bjelica et al., submitted). Together, these findings demonstrate conclusively that FAωH1 is a potato suberin-associated ω-hydroxylase.

Characterization of the potato suberin-associated ω-hydroxylase *FAωH1* created an opportunity to study suberin regulation and biosynthesis using an inducible system. As suberin monomers are derived from two major metabolic pathways, fatty acid biosynthesis and phenylpropanoid biosynthesis, most suberin-associated enzymatic reactions are also active during normal primary metabolism in plants. Suberization requires tightly controlled spatial and temporal activation of these two different metabolic pathways. Consequently, past research to investigate potential regulators of suberin biosynthesis has been scarce. Soliday et al. (1978) tested for hormonal control of suberization, using diffusion resistance as a proxy for development of biopolymer formation. Of the four hormones tested, ABA increased the diffusion resistance significantly earlier post-wounding by 3 days, but did not change the final diffusion resistance of the closing layer. Soliday et al. (1978) proposed that ABA formation post-wounding led to the activation of a water soluble Suberin-Inducing Factor (SIF)

responsible for inducing suberin biosynthesis. Subsequently, Cottle and Kolattukudy (1982) demonstrated that both phenolic and aliphatic monomer accumulation was enhanced with exogenous ABA application. The investigation into ABA's regulatory role in suberization was not re-visited until over 25 years later, when Lulai et al. (2008) used exogenous ABA and FD application to show that both ABA concentration and *de novo* ABA biosynthesis impacted phenolic and aliphatic accumulation during suberization. Lulai et al. (2008) relied on a qualitative technique of phenolic autofluorescence and histochemical staining of aliphatic-associated components to estimate the amount of suberization during closing layer formation. No investigation of ABA's regulatory role in class and chain-length specific monomer formation during suberization was done at that time.

This study is the first comprehensive quantitative analysis of the effect of both pre-existing (endogenous) ABA concentration and wound-induced *de novo* ABA biosynthesis on the major classes of suberin-associated aliphatic monomers. To evaluate the complex metabolic regulation required for aliphatic monomer production, critical fatty acids and modified fatty acids were monitored in this study. I found that ABA has both class-specific and chain-length specific regulatory effects in suberin aliphatics. Unexpectedly, a temporal sensitivity to ABA differed between the accumulation of soluble and insoluble monomers. These accumulations differed from early to later closing layer formation with the inhibition of *de novo* ABA biosynthesis or application of exogenous ABA. All esterified insoluble monomers must pass through the soluble monomer pool before incorporation into the suberin macromolecule. Whereas exogenous ABA had no early effect on soluble accumulation, there was a transient increase of 3.75-6

fold by day 2 of insoluble accumulation of C20 and C22 fatty acids, respectively. Therefore, the increased ABA concentration resulted in a direct increase in monomer biosynthesis and esterification or polymerization. Over the same time period, suberin-associated gene expression also was transiently upregulated with all classes of fatty acid monomer production enhanced. However, these effects were temporary and after day 4 post-wounding a new ABA phenotype developed. The accumulation of insolubles mirrored water controls from day 4 onward, while the soluble accumulation began to increase significantly past control levels. Therefore, while exogenous ABA resulted in increased insoluble accumulation early in the closing layer formation, it resulted in increased soluble accumulation later in closing layer formation and into wound periderm formation. Therefore, there is another level of regulation governing the incorporation into the biopolymer that is temporally affected by ABA.

To determine the role of ABA formation in the regulation of suberization, a potent inhibitor of an ABA precursor production called fluridone (FD) was applied to wounded potato tubers. The majority of FD phenotypes in the wounded tubers were rescued through application of exogenous ABA, indicating it was the presence of ABA and not the actual biosynthesis of ABA that regulated these processes. These results corroborated a previous qualitative study, which characterized the aliphatic histochemical staining of ABA and ABA/FD treatments as similar which indicated that aliphatic biosynthesis increased with exogenous ABA regardless of *de novo* synthesis inhibition (Lulai et al., 2008). However, one consequence of FD treatment was not overcome by exogenous ABA application in this study. Specifically, during early closing layer formation, prior to day 3, water controls showed an accumulation of soluble monomers that did not occur in either

the FD or ABA/FD treatments. Lack of recovery of soluble accumulation with exogenous ABA indicated that *de novo* ABA biosynthesis was important for soluble accumulation. Therefore, this present study identified regulatory mechanisms involving both ABA presence and the spatio-temporal appearance of ABA through biosynthesis.

With the completion of this suberin study on closing layer formation post-wounding, a new understanding of the many points of ABA regulation within the complex biopolymer formation has emerged. From the level of transcription to metabolite formation to monomer incorporation, ABA is clearly a positive regulator for many aspects of suberin formation. As *PAL1* gene expression was not significantly affected by FD or ABA, a comprehensive sister study of phenolic metabolism was completed (Haggitt et al., in preparation), which showed no major impact of FD or ABA on phenolic metabolism or bioaccumulation of soluble polar suberin monomers. Therefore, both phenolic and aliphatic suberin metabolism are not coordinately regulated by ABA and there must be another master regulator involved, which is a major finding.

Regarding exogenous ABA application, it was remarkable to see a coordinated effect between aliphatic gene transcription and insoluble monomer accumulation in aliphatic suberin. Both *FHT* and *FAωH1* transcription was initiated by day 1, increasing through day 2 before the water controls were initiated on day 3. The same trend was present for insoluble C20 and C22 fatty acids, primary alcohols and ω-hydroxy fatty acids as well as C16 ω-hydroxy fatty acids and α,ω-dioic acids. However, a corresponding trend was not seen in the soluble pools. With *in silico* analysis having identified over 40 individual ABA-related promoter motifs in the 2 kb upstream of *FAωH1*, this study confirmed through semi-QT RT-PCR that ABA is a transcriptional regulator of *FAωH1*

gene expression. As ABA is also required for all insoluble monomer incorporation during closing layer formation, it clearly controls multiple regulatory points during suberization.

4.2 Future Directions for Suberin Research

4.2.1 *The Age of Genetics and High-Throughput Sequencing*

With the release of the potato genome sequence, the use of bioinformatics data from techniques such as RNAseq in combination with *in silico* promoter analyses will quicken the pace of suberin research and understanding the global regulation of suberin-associated gene expression. In this study, developmental and post-wounding expression of *FAωH1*, *FAωH2* and *FAωO1* was investigated prior to the release of the Phureja genome sequence. Semi QT-RT PCR of two stress-induced *CYP86A's* revealed *FAωH1* expression in roots, tubers and post-wounding in suberizing tissue whereas *FAωH2* was predominately in green tissues including leaves, immature fruits and flowers with moderate expression post-wounding (Figure 2.6). This indicated that *FAωH1* was a strong candidate as a suberin-associated ω-hydroxylase compared to the other CYP86A stress-induced candidate. Subsequently, the analysis of the *FAωH1* promoter region after the release of the Phureja genome (2011) identified extensive promoter motifs correlated with root expression, wound-induction and ABA-like responsive elements (Appendices 7a and 7b). Identification of the many ABA-like responsive elements led me to revisit ABA as a regulator of transcription, not only for *FAωH1* but also other suberin-associated genes that had been identified. Although this research followed a linear progression from sequence identification to functional characterization to the final exploration of ABA as a master regulator of soluble and insoluble aliphatic monomer production, the ability to

make these connections is now plausible in a fraction of the time. For instance, two years after the publication of the Phureja genome, the incorporation of RNAseq data occurred for many gene sequences. A simple BLASTp of the Phureja genome with another ω-hydroxylase sequence would now quickly identify the eight potato candidates. In addition, examination of the RNAseq data would identify likely candidates for the ω-hydroxylase expressed in the specific pattern indicating a role in suberization. In comparing *FAωH1* and *FAωH2* candidates now using the PGSC database, RNAseq data indicates that *FAωH1* is most strongly expressed tubers, periderm, roots and upon application of 50 μM ABA for 24 hours; whereas *FAωH2* is most strongly expressed in stems, stolons, flowers, leaves and immature fruits but also exhibits high expression upon application of ABA. Full examination of the RNAseq data indicates *FAωH1* is also induced by 150 mM NaCl, 10 μM BAP, 10 μM IAA, 260 μM mannitol, drought stress and pathogenic challenge. Thus, *FAωH1* expression mirrors what would be expected from a suberin-associated gene responsive to abiotic and biotic stress. The power of high-throughput sequencing will dramatically increase the speed of research, as analysis of differential gene expression under multiple conditions is now readily available. By providing researchers with the tools to make more educated hypotheses, which then can be verified using laboratory methods, the trial-and-error method required in the past for many research projects will no longer be necessary.

Shifts in metabolism require differential gene expression, regulated through transcription factors binding to cis-elements in the promoter. When investigating processes that drive significant shifts in metabolism, such as wound-healing, the amount of data collected with new molecular techniques can be daunting. For example, a survey

of 8200 *Arabidopsis* genes identified changes in expression for over 600 genes in response to wounding, including many MYB- and WRKY-like transcription factors (Cheong et al., 2002). *In silico* promoter analysis provides a powerful tool to identify potential regulators of gene expression, so that researchers may make informed choices about where to focus their efforts. Continued use of promoter deletion series, such as the one generated during this research project, will allow testing of key promoter motifs to determine those that significantly impact gene expression (Table 2.5). As researchers continues to expand our understanding of the regulation of gene expression, it is important to be mindful that this is the first level of regulation. Partnering gene or protein expression studies with measuring the actual outputs of the target metabolic pathway is critical, as the metabolome determines the phenotype of the organism.

The next logical step moving forward in suberin research is to unite the field in the development and use of Phureja as a diploid model organism. Previous research has already demonstrated its viability as a transformation system (e.g., Morris et al., 2006; Ducreux et al., 2008; Campbell et al., 2015). With the sequenced genome and RNAseq resources as well as a tuber forming model system that produces genetically identical tubers with large areas available for wounding, it is the ideal model system. Many research groups are currently using different tetraploid cultivars of potato, which complicates genetic experimentation. At this time there are fewer than 30 research groups globally focused on characterization of suberin-associated processes, so this is the ideal time for a universal shift to the diploid Phureja.

4.2.2 *Exploring the Role of ABA and Identifying the Master Regulator of Suberin*

Exploring the effect of ABA on suberin-associated gene expression with the corresponding targeted metabolite analysis of both soluble and insoluble suberin monomers demonstrated the clear role of transcriptional regulation in suberization. In addition to the future identification and characterization of more suberin-associated genes, the next wave of suberin research will focus on the transcription factors that regulate suberin-associated gene expression. Abe et al. (1997, 2003) previously characterized an *Arabidopsis* transcription factor, *MYB2*, which is induced by ABA biosynthesis in response to dehydration or salt stress and functions as a transcriptional activator for many ABA-responsive genes. In terms of promoter elements, DRE/CRT (Li et al., 2014) and ABRE (Nakashima and Yamaguchi-Shinozaki, 2010) are well-characterized cis-acting promoter elements involved in stress-induced gene expression. In this thesis, the inhibition of *de novo* ABA biosynthesis by FD resulted in a phenotype that lacked accumulation of aliphatic monomers in the suberin biopolymer (Figure 3.12b). The strong FD phenotype became evident when the accumulation of ABA normally would occur, 3 days post-wounding (Figure 3.2). This finding corroborates to previous work with drought and salinity stress responses, which identified that ABA-responsive elements (ABREs) function later in the stress response after the accumulation of ABA through *de novo* biosynthesis (Nakashima and Yamaguchi-Shinozaki, 2010). The early stress response in plants has been attributed to transcription factors that bind DRE/CRT cis-elements, with the upstream regulators of these transcription factors still unknown (Li et al., 2014). Recently, Kosma et al. (2014) identified another *Arabidopsis* MYB transcription factor, MYB41, which when overexpressed resulted in ectopic suberin formation and upregulation of all known suberin-associated genes. MYB41 specifically induces suberin in response to abiotic stress, and does not regulate gene expression during

developmental suberin deposition (Kosma et al., 2014). Thus, it appears that there are regulatory differences governing developmental suberin deposition and stress-induced suberin deposition, adding another layer of complexity to the regulation of suberin biosynthesis.

Another direction of future research will be to elucidate the complex regulation between different plant hormones and how they may synergistically or antagonistically act during development and in response to stress. Recently, Barberon et al. (2016) identified ethylene as a negative regulator of suberin development in roots, with application over 24 hours resulting in a 40% reduction in total root suberin. ABA and ethylene were used to demonstrate how suberin deposition differs to enhance the plant's response to various nutrient deficiencies, indicating an advantage in some circumstances to decreasing suberin deposition. Further studies to explore the role of plant hormones and interplay between them are necessary to understand the complex regulation of suberin deposition.

Although it is clear that ABA plays a major role in the regulation of suberin biosynthesis, further research is required to elucidate its exact roles. Tracer experiments using deuterated ABA application at the site of wounding will enable researchers to track the metabolic fate of ABA, and may be utilized up to 3 days post-wounding prior to the formation an effective suberin barrier. To identify the master regulator required to co-ordinate the phenolic and aliphatic metabolism both spatially and temporally, the primary goal will be to tease apart the regulators of ABA biosynthesis. This task will be no small undertaking, as ABA is involved in regulating many different biological processes.

However, understanding the complex regulation and identifying the master regulator of suberin biosynthesis will be the driving force of suberin research in the future.

References

Abe H, Yamaguchi-Shinozaki K, Urao T, Iwasaki T, Hosokawa D, Shinozaki K. 1997. Role of *Arabidopsis* MYC and MYB Homologs in Drought- and Abscisic Acid-Regulated Gene Expression. The Plant Cell 9: 1859-1868

Abe H, Urao T, Ito T, Seki M, Shinozaki K, Yamaguchi-Shinozaki K. 2003. *Arabidopsis* AtMYC2 (bHLH) and AtMYB2 (MYB) Function as Transcriptional Activators in Abscisic Acid Signaling. The Plant Cell 15: 63-78

Barberon M, Vermeer JEM, De Bellis D, Wang P, Naseer S, Andersen TG, Humbel BM, Nawrath C, Takano J, Salt DE, Geldner N. 2016. Adaptation of Root Function by Nutrient-Induced Plasticity of Endodermal Differentiation. Cell 164: 447-459

Bjelica A, Haggitt ML, Woolfson KN, Lee D, Makhzoum AB, Bernards MA. 2016. Fatty Acid ω-Hydroxylases from *Solanum tuberosum*. Accepted providing revisions to Plant Cell Reports

Boher P, Serra O, Soler M, Molinas M, Figueras M. 2013. The Potato Suberin Feruloyl Transferase *FHT* which Accumulates in the Phellogen is Induced by Wounding and Regulated by Abscisic and Salicylic Acids. Journal of Experimental Botany 64: 3225-3236

Campbell R, Morris WL, Mortimer CL, Misawa N, Ducreux LJM, Morris JA, Hedley PE, Fraser PD, Taylor MA. 2015. Optimising Ketocarotenoid Production in Potato Tubers: Effect of Genetic Background, Transgene Combinations and Environment. Plant Science 234: 227-237

Cheong YH, Change HS, Gupta R, Wang X, Zhu T, Luan S. 2002. Transcriptional Profiling Reveals Novel Interactions between Wounding, Pathogen, Abiotic Stress, and Hormonal Responses in *Arabidopsis*. Plant Physiology 129: 661-677

Cottle W, Kolattukudy PE. 1982. Abscisic Acid Simulation of Suberization. Plant Physiology 70: 775-780

Ducreux LJM, Morris WL, Prosser IM, Morris JA, Beale MH, Wright F, Shepherd T, Bryan GJ, Hedley PE, Taylor MA. 2008. Expression Profiling of Potato Germplasm Differentiated in Quality Traits Leads to the Identification of Candidate Flavour and Texture Genes. Journal of Experimental Botany 59: 4219-4231

Franke RB, Dombrink I, Schreiber L. 2012. Suberin goes genomics: use of a short living plant to investigate a long lasting polymer. Frontiers in Plant Science 3: 1-8

Graça J, Pereira H. 2000. Methanolysis of Bark suberins: Analysis of Glycerol and Acid Monomers. Phytochemical Analysis 11: 45-51

Graça J, Cabral V, Santos S, Lamosa P, Serra O, Molinas M, Schreiber L, Kauder F, Franke R. 2015. Partial Depolymerization of Genetically Modified Potato Tuber Periderm Reveals Intermolecular Linkages in Suberin Polyester. Phytochemistry 117: 209-219

Haggitt ML, Woolfson KN, Zhang Y, Kachura A, Bjelica A, Bernards MA. Differential Regulation of Polar and Non-Polar Metabolism During Wound-Induced Suberization in Potato (*Solanum tuberosum*) tubers. In preparation for submission to The Plant Cell

Holloway PJ. 1983. Some Variations in the Composition of Suberin from the Cork Layers of Higher-Plants. Phytochemistry 22: 495-502

Kolattukudy PE, Croteau R, Buckner JS. 1976. The Biochemistry of Plant Waxes. *In* Chemistry and Biochemistry of Natural Waxes. Kolattukudy (ed), American Elsevier, New York. pp 289-347

Kosma DK, Murmu J, Razeq FM, Santos P, Bourgault R, Molina I, Rowland O. 2014. *AtMYB41* activates ectopic suberin synthesis and assembly in multiple plant species and cell types. The Plant Journal 80: 216-229

Li C, Yue J, Wu X, Xu C, Yu J. 2014. An ABA-Responsive DRE-Binding Protein Gene from *Setaria italica, SiARDP*, the Target Gene of SiAREB, Plays a Critical Role Under Drought Stress. Journal of Experimental Botany 65: 5415-5427

Lulai EC, Suttle JC, Pederson SM. 2008. Regulatory Involvement of Abscisic Acid in Potato Tuber Wound-Healing. Journal of Experimental Botany 59: 1175-1186

Morris WL, Ducreux LJ, Fraser PD, Millam S, Taylor MA. 2006. Engineering Ketocarotenoid Biosynthesis in Potato Tubers. Metabolic Engineering 8: 253-263

Nakashima K, Yamaguchi-Shinozaki K. 2010. Promoters and Transcription Factors in Abiotic Stress-Responsive Gene Expression. *In* Abiotic Stress Adaptation in Plants. Pareek, Sopory, Bohnert and Govindjee (eds), Springer, Netherlands. pp 199-216

Neubauer JD, Lulai EC, Thompson AL, Suttle JC, Bolton MD, Campbell LG. Molecular and Cytological Aspects of Native Periderm Maturation in Potato Tubers. Journal of Plant Physiology 170: 413-423

Nelson D, Werck-Reichhart D. 2011. A P450-Centric View of Plant Evolution. The Plant Journal 66:194-211

Riley RG, Kolattukudy PE. 1975. Evidence for Covalently Attached *p*-coumaric acid and ferulic acid in cutins and suberins. Plant Physiology 56: 650-654

Schreiber L, Franke R, Hartmann K. 2005. Wax and Suberin Development of Native and Wound Periderm of Potato (*Solanum tuberosum* L.) and its Relation to Peridermal Transpiration. Planta 220: 520-530

Schreiber L. 2010. Transport Barriers made of Cutin, Suberin and Associated Waxes. Trends in Plant Science 15: 546-553

Serra O, Hohn C, Franke R, Prat S, Molinas M, Figueras M. 2010. A Feruloyl Transferase Involved in the Biosynthesis of Suberin and Suberin-associated Wax is Required

for Maturation and Sealing Properties of Potato Periderm. The Plant Journal 62: 277-290

Serra O, Soler M, Hohn C, Sauveplane V, Pinot F, Franke R, Schreiber L, Prat S, Molinas M, Figueras M. 2009a. CYP86A33-Targeted Gene Silencing in Potato Tuber Alters Suberin Composition, Distorts Suberin Lamellae, and Impairs the Periderm's Water Barrier Function. Plant Physiology 149: 1050-1060

Serra O, Soler M, Hohn C, Franke R, Schreiber L, Prat S, Molinas M, Figueras M. 2009b. Silencing of *St*KCS6 in Potato Periderm Leads to Reduced Chain Lengths of Suberin and Wax Compounds and Increased Peridermal Transpiration. Journal of Experimental Botany 60: 697-707

Soliday CL, Kolattukudy PE. 1978. Midchain Hydroxylation of 16-Hydroxypalmitic Acid by the Endoplasmic Reticulum Fraction from Germinating *Vicia faba*. Archives of Biochemistry and Biophysics 188: 338-347

Thomas R, Fang X, Ranathunge K, Anderson TR, Peterson CA, Bernards MA. 2007. Soybean root suberin: anatomical distribution, chemical composition, and relationship to partial resistance to Phytophthora sojae. Plant Physiology 144: 299-311

Yang W, Bernards MA. 2006. Wound Induced Metabolism in Potato (*Solanum tuberosum* L.) Tubers: Biosynthesis of Aliphatic Domain Monomers. Plant Signaling and Behavior 1: 59-66

Appendix 1: Custom Designed Primer Sequences for ω-Hydroxylase Amplification. Primers for 5' and 3' RACE of EST716349; tissue-specific expression of all ω-hydroxylases; and cloning of FAωH1 coding region. Semi QT RT-PCR refers to the technique of semi-quantitative RT-PCR.

Target Gene PCR Reaction	**Primer Name: Sequence**	**T_m ºC**
FAωO1 5' RACE	CYP94A7race5outR: (gene-specific primer 1) 5'GCAAGAGTAGAATTTGAATTATGG	60
	CYP94A7race5nestR: (nested gene-specific primer 2) 5'GTGGAAATTGAGGGGTCGAAT	66
FAωO1 3' RACE (first 500 bp)	CYP94A7race3F: (gene-specific primer) 5'GATTGCGTTAGATTAAGTAGTG	55
	CYP94A7race3nestF: (re-amplification primer) 5'GTGAGGGAGAAACAGAGGGAG	64
FAωO1 3' RACE 2 (downstream 3'-sequence)	CYP94A7race3F2: (gene-specific primer) 5'CGGGGAATTGGATGTTTGTTGG	66
	CYP94A7race3nestF2: (re-amplification) 5'GTGAGGGAGAAACAGAGGGAG	60
TC114700 (*FAωH1* contig) Semi-QT RT-PCR	TC114700PotF: 5'TTTCCTTTTATCTCCTAGCAC	57
	TC114700PotR: 5'TAAATCATCTGATGGACTTTCC	59
TC120302 (*FAωH2* contig) Semi-QT RT-PCR	TC120302PotF: 5'CAACGGGTATGATGATTGTAGC	63
	TC120302PotR: 5'TCTCGGGTTCAAGCTGACAAGC	70
EST716349 (*FAωO1* EST) Semi-QT RT-PCR	EST716349PotF: 5'ATTCGACCCCTCAATTTCCAC	66
	EST716349PotR: 5'CTCCCTCTGTTTCTCCCTC	60
ef1-α (control gene) Semi-QT RT-PCR	ef1-alpha 400F: 5'TCACTGCCCAGGTCATCATC	66
	Ef1-alpha 400R: 5'GGAAACACCAGCATCACACTG	66
Cloning of *FAωH1* coding region	FAωH1pYES2NTF: 5'AAGCTTACCATGGATCCTATACT	59
	FAωH1pYES2NTR: 5'TCTAGACGCAGACATAGCAATC	61
	FAωH1pTRCHIS2R: 5'TCTAGAGCAGACATAGCAATC	56

Appendix 2: Primer Sequences for Cloning and Construction of the *FAωH1* Promoter Deletion Series.

Primers used for cloning the full length coding region and systematic deletion of ABRE-like promoter motifs to generate a deletion series for functionally characterizing the *FAωH1* promoter activation and repression. Forward deletion series primers contain a 5'*Sal*I site (GTCGAC) and the reverse deletion primer has a 5'*Bam*HI site (GGATCC) for directional cloning into pBI101 (Appendix 3).

Cloning Reactions	**Primer Name: Sequence**	**T_m (ºC)**
Cloning *FAωH1* upstream promoter region (2 kb)	FAωH1-2051PROMF: 5'GGGGACAAGTTTGTACAAAAAAGCAGGC TYYAAGTGTCATTTAA	82
	FAωH1+9PROMR: 5'GGGGACCACTTTGTACAAGAAACTGGGTY AGGATCCATTTTG	83
Forward *FAωH1* deletion series	P1P2-2056PROMF: 5'GTCGACAAGTGTCATTTAAATTGG	63
	P1P2-1739MYCONS1F: 5'GTCGACACGTGTACATTTATTTGTT	63
	P1P2-1534MYBIAT1F 5'GTCGACCCAATATAAATTAGAGTTTAATT	62
	P1-1164MYCONS2F: 5'GTCGACCTTAATGACATTCTAATTTC	62
	P1-980MYCAT1F: 5'GTCGACCCAAAACCGTAATTAGTA	64
	P1P2-862LTRECOR1F: 5'GTCGACCTCTAAAAGGGTTAAATTTTA	63
	P1-838MYBIAT2F: 5'GTCGACCCAATTTAAGTAGGTTGTT	64
	P1P2-777RYREP1F: 5'GTCGACGCAGAAACTAAACCTTTT	65
	P1-676MYCATCONS2F: 5'GTCGACTTGTGTGAAACTTCATATTT	63
	P1-460MYCONS4F: 5'GTCGACCACCTGATATTATTTTCA	63
	P1-393DPBF1F: 5'GTCGACGATAGATATTGAACAAACA	63
	P1-262MYBIAT3F: 5'GTCGACCAAAGCAAAGTTAGTAAAGT	63
Reverse *FAωH1* deletion series	P1P1FAωH1PROMR: 5'GGATCCTTTGAAAAAATTGTTTCTCT	64

Appendix 3: pBI101 β-Glucuronidase Expression Vector for *FAωH1* Promoter Deletion Series.

Twelve *FAωH1* promoter sequences of decreasing length were PCR amplified with primers designed for directional cloning into pBI101. PCR products were cloned into pGEM®-T Easy, sequenced and then cloned into pBI101 using 5'*Sal*I and 3'*Bam*HI sites. *FAωH1* translation start codon had been removed and the β-glucuronidase translation start site was 18 bp downstream of the 3' end of *FAωH1* promoter. Vector map from Tiandz (China, URL: http://www.tiandz.com/product/2733.html).

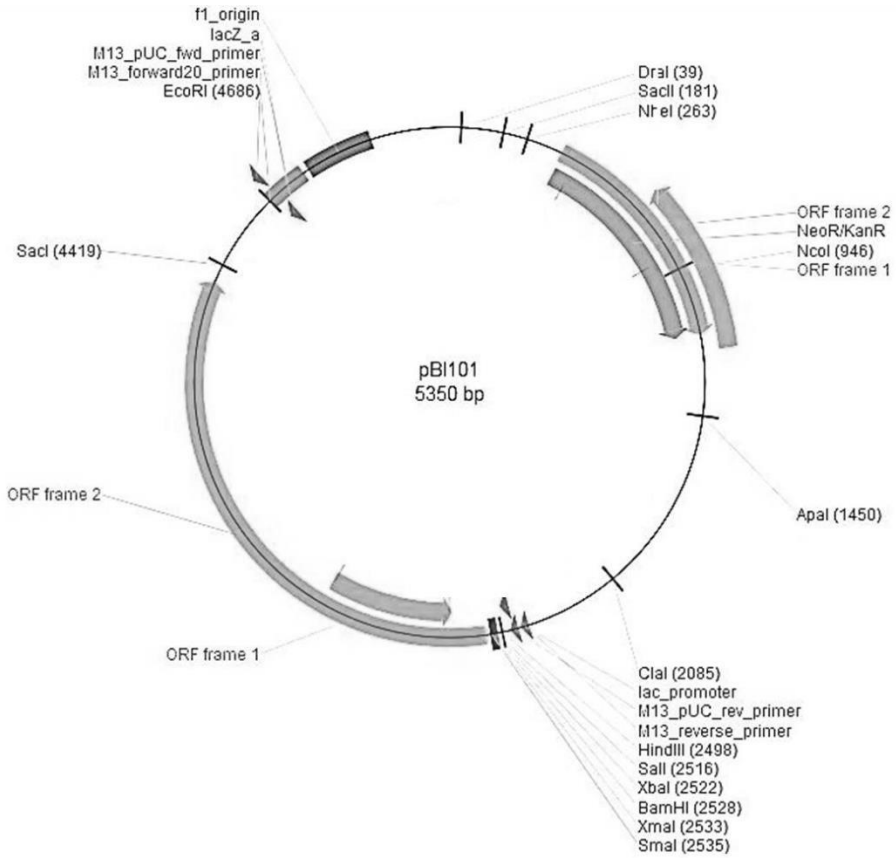

Appendix 4: Complementation Analysis of *cyp86a1/horst* Mutant with *FAωH1* under Control of *Arabidopsis* CYP86A1 Promoter

Homozygous lines of the *Arabidopsis* CYP86A1 mutant *horst-1* were transformed with constructs containing either AtCYP86A1 or StCYP86A33, both under the control of the *Arabidopsis* CYP86A1 promoter. Selected lines were grown in hydroponics, and the aliphatic suberin profiles of their roots measured using a no-extraction protocol based on methanolic-HCl depolymerization and GC-MS analysis (Frederic Domergue, CNRS, Bordeaux, personal communication). Wild type *Arabidopsis* plants (ecotype Columbia) were used as a control for "normal" *Arabidopsis* root aliphatic suberin. a, Total ω-hydroxy fatty acids (16:0, 18:1, 20:0, 22:0); b, Total ω-oxidized aliphatics (ω-hydroxy- and α,ω-dioic acids); c, Chain length distribution of ω-hydroxy- and α,ω-dioic acids isolated from *Arabidopsis* roots. In panel a and b, bars labeled with the same letter were not significantly different based on ANOVA followed by Tukey's post-hoc test ($p<0.05$). For panel c, bars labeled with the same letter, within each group, were not significantly different based on ANOVA followed by Tukey's post-hoc test ($p<0.05$). Figure from Bjelica et al., submitted.

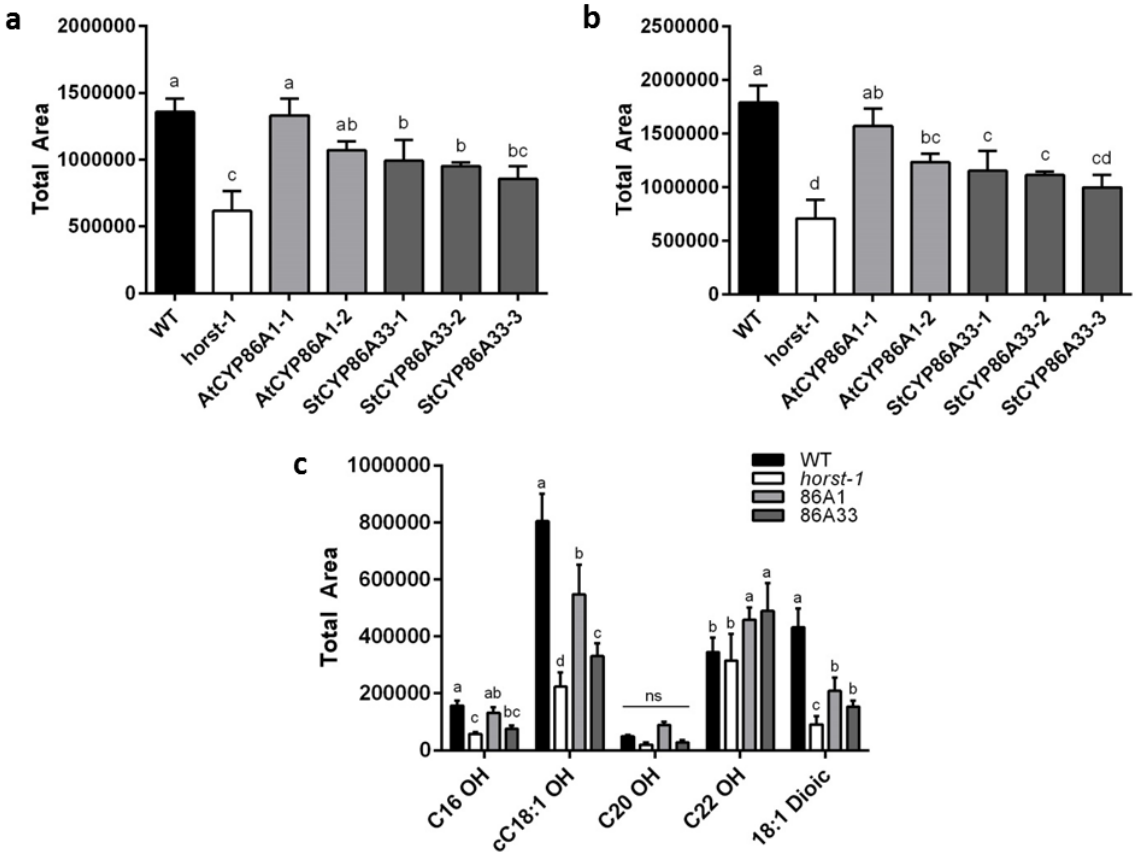

Appendix 5a: *FAωH1* P1 Promoter Allele Sequence (2056 bp)
Sequence begins at 2056 bp upstream from the translation start site. Each line represents 60 bp of sequence.

AAGTGTCATTTAAATTGGGACAAAAAAAGTACGAAGTTGTAGTTATTATTCTTTTTCTTT
CGGCTATTCCATCCTTCTCCATACACATTTTTCTTTTTAGTATATCTTTAAAAGAAAATG
ATACATTTTCTTAGACAAATACCTAATAACTCTTTTATTGGGCTTCATAAATTCAAGCCT
TCCAATCCTTATAGAATCGTTTTTCAAGGATTTGGAGCAAAGCCTTATTTCTCAACAAAG
CTAAACCGATTCCGAACTACTAATAGCTTAATTAGTGATGTGTTGACAAAGTGGAGAGAC
GGCTCTTAACATATGACGTGTACATTTATTTGTTCAATTTTATACAGATTTAGGTGTCTA
ATTTGCATACTTGGGAAATTTACTCAAATATAAATATAGAGCTAAATATAATGTCATTGG
ATGACTACTTAATTGGACCCTTTTATTGGGCTGTAAATAAACTGCGGTGTTGAACTGGAC
CTGAATTTCCAGTCCAGGCCAGCTTAAGCCTGCTGAAACCACCAATATAAATTAGAGTTT
AATTAGATAGTTCGGTTCCTTCCACGAGGTCTCAAATTCTAATTTTTGGAAATGGAAAAT
ATGTTTGTTGGAGCATTGCCCCTAGAAATAGTCTCTGCTTTGCGCAAATTCAAATTTAGT
AGGACTCTAATACAAATACTAGACGCATGGTAAAAAAATATATATAAATTAGAGTGTACA
CATATATATTGTCAAAGAAATTTTTACACTATGAAACAATCTGGCATGAACTGTTTCCTT
TGCAGTATTAATTAGAAGTTTCTTATACGTCCAATTAAATTTTGATGTAATAACAGGATT
AGTTATGGAAACAATGTATTCTAACATGTTTAAGTATATGGTGATCATTTGCTTAATGAC
ATTCTAATTTCTAATGTCGTAAGTTGCAGCTAATGCCTTTATAATACTACAAAAGTCAAG
GTTGTTGTAAATCACAAAGATTTTCTTAAGAAAGAGTTAAAAGCAGGAAAAGTTGGAGGT
AAAAGGTGGTATTCTATGTGTCTCTATTTCTTGCTTGGGAAGACTTTCCCATGTGCCAAA
ACCGTAATTAGTACCGTGGAACGACGTCATATTTAATTAGAGGTTTGGAGTTATGTACCT
ATTAGTAACAGTGTATCGAAAGCAAAAACTATTATTTATCTCTACAAACCGACCTCTAAA
AGGGTTAAATTTTAACAAAACCAATTTAAGTAGGTTGTTTTTTAAAGCTTCTAATTTAAT
CTTTCTAATCTTCTGCATGCAGAAACTAAACCTTTTAGAGTAGTTTTCCAGATTTTGGAG
AAAAGATGTATTTCTCAACACAGCTAAACCGATTCCCAACCACTCCCCACTTCTTCTGCT
CATGTGAAACTTCATATTTTTTGTTTTTTTTTTAAATTTTTATTTATTATGTTTGGTCGA
GGAAAATATGCATTATCTTCCATTTTTCTCTTCTTAGATAACAATTTACATAGTTAATCT
AAGAAGAAAGAATAAGATGTAAATATTTATTTGTATCAAGGACTTTAATTACTTAATTAT
GACCTAAAGAAAACAAATTATATCCTAATCCTGAACAAATGATATTATTTTCAAATTGAT
AGTATATATTATGAATAATGTCTAGAATACGAAAAAACACCCGATAGATATTGAACAAAC
AAATAACTTATTAAACAAGTTTAAAATTTGTATAAAGTACATGACCTAAGTTTTAAAAAA
AATTAACGCATAAGTGAATTCATGAGACGTGTACAAATTATATGAAGCTAAACCAAAGCA
AAGTTAGTAAAGTTTTCGTAAGAAAATTCATTACATTAATTCCTATCAACCGAATAAGGA
CCTTCTTTCTTTAATTTCTTTCATAAGTTATAAAAATTCTCAACAACTCTCTCCTAAACG
TTTCCTTTAATACATTCTACAAATATATATATATATATATAAACCTTACTCTCCCCTCTT
CCATATAACACATTCATTCTCTTTTCCTCTCTACTTCACTTAAACCAAAAAAAAAAAGAG
AAACAATTTTTTCAAA

Appendix 5b: *FAωH1* P2 Promoter Allele Sequence (2073 bp)
Sequence begins at 2073 bp upstream from the translation start site. Each line represents 60 bp of sequence.

AAGTGTCATTTAAATTGGGACAAAAAAAAGTAAGAAGTTGTAGTTATGATTCTTTTTCTT
TCGGCTATTCCATCCTTCTCCATACAAATTTTTCTTTTTAGTATATCTTTAAAAGAAAAT
GATACATTTCTTGACAAATACCTAGTAACTCTTTTATTGGGCTTCATAAATTCAAGCCTT
CCAATCCTTATAGAATCGTTTTTCAAGGATTTGGAGCAAAGCCTTATTTCTCAACAAAGC
TAAACCGATTCCGAACTACTAATAGCTTAATTAGTGATGTGTTGACAAACTGGAGAGACG
GCTCTTAACATATGACGTGTACATTTATTTGTTTAATTTTATACATATTTAAATGTCTAA
TTGTGCATACTCGGGAAATTTACTCAAATATAAATATAGAGCTAAATATAATGTCATTGG
ATAACTACTTAATTGGACCTTTTTATTGGGCTGTAAATAAACTGCGGTGTTGAACTGGAC
CTGAATTTCCAGTCCAAGCCAGCTTAAGCCTGCTGAAACCACCAATATAAATTAGAGTTT
AATTAGATAGTTCAGCACCTTCCACGAGGTCTCATATTCGAATTTTTGGAAATGGAAAAT
ATGTTTGTCGGAGCATTGCCCTAGAAATAGTCTTCGCAGTGCGCAAATCCAAATATAGTA
GGACCCTAATACAAATATTGGACACATGGTAAAAAAATCAAAGAAGTACATAACTTAGAG
TGTACACATATATTGTCAAAGAAGTTTTATACACTATGAAACAATCTGGCATGAACTGTA
TTTCCTTTGCAGTATTAATTAGAAGTTTCTTATACCTCCAATTAAATTTTGATGTAATAA
CAGGATTAGTTATGGAAATAATGTATTCTAACATGTTTAAGTATATGGTGATGATTTGCT
TAATGACATTCTAATGTTGTAAGTTGCAGCTAATGCCTTTATAATACTACAAAAGTCAAG
GTTGTTGTAAATCACATAGATTTTCTTTAAAACGAGCTAAAAGCAGGAAAAGTTGGAGGT
AAAAGGTTGTATTGTGTGTGTCTCTATTTCTTGCTTGGGAAGACTTCCCCATGTGCCAAA
ACCGTAATTAGTTACCGTGGAACGACGTCATATTTAATTAGATGTTTTGAGTTATGTACC
TATTGGTAACAGTATATCGAAAGCAAAAACTATTATTTATCTCTACAAACCGACCTCTAA
AAGGGTTAAATTTTAACAAAATCAATTTAAGTATGTTGTTTTTTAAAGCTTCTAATTTAA
TCTTTCTAATCTACTGCATGCAGAAACTAAACCTTTTAGAATAGTTTTCCAGATTTTGGA
GAAAAGATGTATTTCTCAACACAGCTAAACCGATTCCCAACCACTCCCCACTTCTTCTGC
TCATGTGAAACTTTCTATTTTTATTTTTATTTTACTTTTTATTTATTATAATTGATCGCG
GAAAATATATATTAGAGTATGTTCCATTTTTCTCTTCTTAGATAACTATTTACATGGTTA
ATCTAAGAAAAAAGAGTAAGATGTAAATATTTTTTTGTATCAAGGACTTTAATTACTTAA
TTATGACCTAAAGAAAGCAAATTATATCCTAATACTGAGCAAATGATATTTTTGGTTATT
TTCAAATTCATAGTATATATTATGAATTATGTCTGGAATACGAAAAAACAGCCAATAGAT
ATTGAACAAACAAATAATTGATTAAATAAGTTTAAAATTTGTATCAAGTACTACATGACC
AAATTTTTAAAAAAATTGTAACGCACAAGAAAATTCATGAAACGTGTACAAATTATATGA
AGCTAAAGCAAAGCAAAGTCAGTAAAGTTTTCGTAAGAAAATTAATAAAATTCATTACAT
TAATTCCTATCAACCGAATAAGGACCTTCTTTCTTTAATTTCTTTCATAAGTTATAAAAA
TTCTCAACAACTCTCTCCTAAACCTTTCCTTTAATACATTCTACAAATATATATATATAA
ACCTTACTCTCCCCTCTTCCATATAGCACATTCATTCTCTTTTCATCTCTACTTCACTTA
AACAAAAAAAAAAAGAGAAACAATTTTTTCAAA

Appendix 6: *FAωH1* P1 and P2 Promoter Sequence Alignment

Two *FAωH1* promoter alleles cloned from potato cv. Russet Burbank compared in a global sequence alignment performed by Clustalω. * signifies an identical nucleotide in a particular position; - indicates a gap required within the global sequence alignment.

```
P1Burbank       AAGTGTCATTTAA-ATTGGGACAAAAAAAAGTACGAAGTTGTAGTTATTATTCTTTTTCTT    59
P2Burbank       AAGTGTCATTTAAATTGGGACAAAAAAAAGTAAGAAGTTGTAGTTATGATTCTTTTTCTT    60
                *************  * **   ********** ************** ************

P1Burbank       TCGGCTATTCCATCCTTCTCCATACACATTTTTCTTTTTAGTATATCTTTAAAAGAAAAT    119
P2Burbank       TCGGCTATTCCATCCTTCTCCATACAAATTTTTCTTTTTAGTATATCTTTAAAAGAAAAT    120
                ************************** ***********************************

P1Burbank       GATACATTTTCTTAGACAAATACCTAATAACTCTTTTATTGGGCTTCATAAATTCAAGCC    179
P2Burbank       GATACATTTC--TTGACAAATACCTAGTAACTCTTTTATTGGGCTTCATAAATTCAAGCC    178
                *********   * ************ ***********************************

P1Burbank       TTCCAATCCTTATAGAATCGTTTTTCAAGGATTTGGAGCAAAGCCTTATTTCTCAACAAA    239
P2Burbank       TTCCAATCCTTATAGAATCGTTTTTCAAGGATTTGGAGCAAAGCCTTATTTCTCAACAAA    238
                ************************************************************

P1Burbank       GCTAAACCGATTCCGAACTACTAATAGCTTAATTAGTGATGTGTTGACAAAGTGGAGAGA    299
P2Burbank       GCTAAACCGATTCCGAACTACTAATAGCTTAATTAGTGATGTGTTGACAAACTGGAGAGA    298
                ************************************************* ********

P1Burbank       CGGCTCTTAACATATGACGTGTACATTTATTTGTTCAATTTTATACAGATTTAGGTGTCT    359
P2Burbank       CGGCTCTTAACATATGACGTGTACATTTATTTGTTTAATTTTATACATATTTAAATGTCT    358
                ********************************** ********** *****  *****

P1Burbank       AAT-TTGCATACTTGGGAAATTTACTCAAATATAAATATAGAGCTAAATATAATGTCATT    418
P2Burbank       AATTGTGCATACTCGGGAAATTTACTCAAATATAAATATAGAGCTAAATATAATGTCATT    418
                ***  ******** ************************************************

P1Burbank       GGATGACTACTTAATTGGACCCTTTTATTGGGCTGTAAATAAACTGCGGTGTTGAACTGG    478
P2Burbank       GGATAACTACTTAATTGGACCTTTTTATTGGGCTGTAAATAAACTGCGGTGTTGAACTGG    478
                **** ***************** ****************************************

P1Burbank       ACCTGAATTTCCAGTCCAGGCCAGCTTAAGCCTGCTGAAACCACCAATATAAATTAGAGT    538
P2Burbank       ACCTGAATTTCCAGTCCAAGCCAGCTTAAGCCTGCTGAAACCACCAATATAAATTAGAGT    538
                ****************** ****************************************

P1Burbank       TTAATTAGATAGTTCGGTTCCTTCCACGAGGTCTCAAATTCTAATTTTTGGAAATGGAAA    598
P2Burbank       TTAATTAGATAGTTCAGCACCTTCCACGAGGTCTCATATTCGAATTTTTGGAAATGGAAA    598
                *************** *  ***************** **** ******************

P1Burbank       ATATGTTTGTTGGAGCATTGCCCCTAGAAATAGTCTCTGCTTTGCGCAAATTCAAATTTA    658
P2Burbank       ATATGTTTGTCGGAGCATTGCCC-TAGAAATAGTCTTCGCAGTGCGCAAATCCAAATATA    657
                ********** ************ ************  **  ********* ***** **

P1Burbank       GTAGGACTCTAATACAAATACTAGACGCATGGTAAAAAAATATATATA-------AATTA    711
P2Burbank       GTAGGACCCTAATACAAATATTGGACACATGGTAAAAAAATCAAAGAAGTACATAACTTA    717
                ******* ************ * *** **************  *   *       * ***

P1Burbank       GAGTGTACACATATATATTGTCAAAG-AAATTTTTACACTATGAAACAATCTGGCATGAA    770
P2Burbank       GAGTGTACACA--TATATTGTCAAAGAAGTTTTATACACTATGAAACAATCTGGCATGAA    775
                ***********  ************* *  *** **************************

P1Burbank       --CTGTTTCCTTTGCAGTATTAATTAGAAGTTTCTTATACGTCCAATTAAATTTTGATGT    828
P2Burbank       CTGTATTTCCTTTGCAGTATTAATTAGAAGTTTCTTATACCTCCAATTAAATTTTGATGT    835
                   * ********************************** ******************

P1Burbank       AATAACAGGATTAGTTATGGAAACAATGTATTCTAACATGTTTAAGTATATGGTGATCAT    888
```

```
P2Burbank       AATAACAGGATTAGTTATGGAAATAATGTATTCTAACATGTTTAAGTATATGGTGATGAT     895
                ********************** ********************************** **

P1Burbank       TTGCTTAATGACATTCTAATTTCTAATGTCGTAAGTTGCAGCTAATGCCTTTATAATACT     948
P2Burbank       TTGCTTAATGACATTCTA-------ATGTTGTAAGTTGCAGCTAATGCCTTTATAATACT     948
                ******************       **** ******************************

P1Burbank       ACAAAAGTCAAGGTTGTTGTAAATCACAAAGATTTTCTTAAGAAAGAGTTAAAAGCAGGA    1008
P2Burbank       ACAAAAGTCAAGGTTGTTGTAAATCACATAGATTTTCTTTAAAACGAGCTAAAAGCAGGA    1008
                **************************** ********** * ** *** ***********

P1Burbank       AAAGTTGGAGGTAAAAGGTGGTATTCTATGTGTCTCTATTTCTTGCTTGGGAAGACTTTC    1068
P2Burbank       AAAGTTGGAGGTAAAAGGTTGTATTGTGTGTGTCTCTATTTCTTGCTTGGGAAGACTTCC    1068
                ****************** ***** * ****************************** *

P1Burbank       CCATGTGCCAAAACCGTAATTAG-TACCGTGGAACGACGTCATATTTAATTAGAGGTTTG    1127
P2Burbank       CCATGTGCCAAAACCGTAATTAGTTACCGTGGAACGACGTCATATTTAATTAGATGTTTT    1128
                ********************** ***************************** ****

P1Burbank       GAGTTATGTACCTATTAGTAACAGTGTATCGAAAGCAAAAACTATTATTTATCTCTACAA    1187
P2Burbank       GAGTTATGTACCTATTGGTAACAGTATATCGAAAGCAAAAACTATTATTTATCTCTACAA    1188
                **************** ******** ***********************************

P1Burbank       ACCGACCTCTAAAAGGGTTAAATTTTAACAAAACCAATTTAAGTAGGTTGTTTTTTAAAG    1247
P2Burbank       ACCGACCTCTAAAAGGGTTAAATTTTAACAAAATCAATTTAAGTATGTTGTTTTTTAAAG    1248
                ********************************** *********** **************

P1Burbank       CTTCTAATTTAATCTTTCTAATCTTCTGCATGCAGAAACTAAACCTTTTAGAGTAGTTTT    1307
P2Burbank       CTTCTAATTTAATCTTTCTAATCTACTGCATGCAGAAACTAAACCTTTTAGAATAGTTTT    1308
                ********************** ************************** *******

P1Burbank       CCAGATTTTGGAGAAAAGATGTATTTCTCAACACAGCTAAACCGATTCCCAACCACTCCC    1367
P2Burbank       CCAGATTTTGGAGAAAAGATGTATTTCTCAACACAGCTAAACCGATTCCCAACCACTCCC    1368
                ************************************************************

P1Burbank       CACTTCTTCTGCTCATGTGAAACTTCATATTTTTTGTTTTTTTTTTAAATTTTTATTTAT    1427
P2Burbank       CACTTCTTCTGCTCATGTGAAACTTTCTATTTTTTATTTTTATTTTACT--TTTTATTTAT    1426
                ************************  *******  **** ****     **********

P1Burbank       TATGTTTGGTCGAGGA-----AAATATGCATTATCTTCCATTTTTCTCTTCTTAGATAAC    1482
P2Burbank       TATAATTGATCGCGGAAAATATATATTAGAGTATGTTCCATTTTTCTCTTCTTAGATAAC    1486
                ***  *** *** ***      *   *  * *** **************************

P1Burbank       AATTTACATAGTTAATCTAAGAAGAAAGAATAAGATGTAAATATTTATTTGTATCAAGGA    1542
P2Burbank       TATTTACATGGTTAATCTAAGAAAAAAGAGTAAGATGTAAATATTTTTTTGTATCAAGGA    1546
                 ******** ************* ***** **************** **************

P1Burbank       CTTTAATTACTTAATTATGACCTAAAGAAAACAAATTATATCCTAATCCTGAACAAATGA    1602
P2Burbank       CTTTAATTACTTAATTATGACCTAAAGAAAGCAAATTATATCCTAATACTGAGCAAATGA    1606
                ****************************** **************** **** *******

P1Burbank       TATTA-------TTTTCAAATTGATAGTATATATTATGAATAATGTCTAGAATACGAAAA    1655
P2Burbank       TATTTTTGGTTATTTTCAAATTCATAGTATATATTATGAATTATGTCTGGAATACGAAAA    1666
                ****       ********** ****************** ****** ***********

P1Burbank       AACACCCGATAGATATTGAACAAACAAATAACTTATTAAACAAGTTTAAAATTTGTATAA    1715
P2Burbank       AACAGCCAATAGATATTGAACAAACAAATAATTGATTAAATAAGTTTAAAATTTGTATCA    1726
                **** ** ********************** * ****** ***************** *

P1Burbank       AGTACATGACCTA----AGTTTTAAAAAAAATTAACGCATAAGTGAATTCATGAGACGTG    1771
P2Burbank       AGTACTACATGACCAAATTTTTAAAAAAATTGTAACGCACAAGAAAATTCATGAAACGTG    1786
```

```
                ******   *          *** ******   ******* ***  ********* *****

P1Burbank       TACAAATTATATGAAGCTAAACCAAAGCAAAGTTAGTAAAGTTTTCGTAAGAAAA-----     1826
P2Burbank       TACAAATTATATGAAGCTAAAGCAAAGCAAAGTCAGTAAAGTTTTCGTAAGAAAATTAAT     1846
                ******************** *********** *********************

P1Burbank       ----TTCATTACATTAATTCCTATCAACCGAATAAGGACCTTCTTTCTTTAATTTCTTTC     1882
P2Burbank       AAAATTCATTACATTAATTCCTATCAACCGAATAAGGACCTTCTTTCTTTAATTTCTTTC     1906
                    ************************************************************

P1Burbank       ATAAGTTATAAAAATTCTCAACAACTCTCTCCTAAACGTTTCCTTTAATACATTCTACAA     1942
P2Burbank       ATAAGTTATAAAAATTCTCAACAACTCTCTCCTAAACCTTTCCTTTAATACATTCTACAA     1966
                ************************************ *********************

P1Burbank       ATATATATATATATATATAAACCTTACTCTCCCCTCTTCCATATAACACATTCATTCTCT     2002
P2Burbank       ATATATA------TATATAAACCTTACTCTCCCCTCTTCCATATAGCACATTCATTCTCT     2020
                *******      ********************************* **************

P1Burbank       TTTCCTCTCTACTTCACTTAAACCAAAAAAAAAAAAGAGAAACAATTTTTTCAAAGGATCC     2062
P2Burbank       TTTCATCTCTACTTCACTTAAACAAAAAAAAAAAAGAGAAACAATTTTTTCAAAATGGATC     2080
                **** ****************** **********    **  * *****  *** *   *

P1Burbank       -       2062
P2Burbank       C       2081
```

Appendix 7a: *In silico* Analysis of *FAωH1* P1 Promoter Sequence

List of promoter motifs identified by PLACE scan. Location (Loc.) given is 5' upstream of the translation start site on the coding strand (e.g. location of 1 would be 2056 bp upstream of the translation start site). Strand refers to the + or – orientation of the motif. Signal sequence is the consensus sequence attributed to the specific motif. Site # refers to the reference number for further information from the PLACE database. Grey represents promoter deletion series ABA-related elements; green represents other ABA-related elements; yellow represents wound-related elements; blue represents root-specific elements.

Factor or Site Name	Loc. (Str.) Signal Sequence	Site #
CACTFTPPCA1	2 (-) YACT	S000449
BIHD1OS	4 (+) TGTCA	S000498
WRKY71OS	5 (-) TGAC	S000447
CAATBOX1	14 (-) CAAT	S000028
CCAATBOX1	14 (-) CCAAT	S000030
DOFCOREZM	26 (+) AAAG	S000265
CACTFTPPCA1	28 (-) YACT	S000449
CURECORECR	29 (-) GTAC	S000493
CURECORECR	29 (+) GTAC	S000493
POLASIG3	45 (-) AATAAT	S000088
-10PEHVPSBD	47 (+) TATTCT	S000392
DOFCOREZM	51 (-) AAAG	S000265
GT1CONSENSUS	52 (-) GRWAAW	S000198
GT1GMSCAM4	52 (-) GAAAAA	S000453
POLLEN1LELAT52	54 (-) AGAAA	S000245
DOFCOREZM	57 (-) AAAG	S000265
LTRE1HVBLT49	58 (-) CCGAAA	S000250
NAPINMOTIFBN	82 (+) TACACAT	S000070
GT1CONSENSUS	88 (-) GRWAAW	S000198
GT1GMSCAM4	88 (-) GAAAAA	S000453
POLLEN1LELAT52	90 (-) AGAAA	S000245
DOFCOREZM	93 (-) AAAG	S000265
CACTFTPPCA1	99 (-) YACT	S000449
GATABOX	103 (-) GATA	S000039
NODCON1GM	104 (-) AAAGAT	S000461
OSE1ROOTNODULE	104 (-) AAAGAT	S000467
DOFCOREZM	106 (-) AAAG	S000265
TAAAGSTKST1	106 (-) TAAAG	S000387
DOFCOREZM	111 (+) AAAG	S000265
POLLEN1LELAT52	113 (+) AGAAA	S000245
GT1CONSENSUS	114 (+) GRWAAW	S000198
GATABOX	120 (+) GATA	S000039

GT1CONSENSUS	125 (-) GRWAAW	S000198
POLLEN1LELAT52	127 (-) AGAAA	S000245
CPBCSPOR	143 (-) TATTAG	S000491
NODCON2GM	150 (+) CTCTT	S000462
OSE2ROOTNODULE	150 (+) CTCTT	S000468
DOFCOREZM	152 (-) AAAG	S000265
POLASIG1	154 (-) AATAAA	S000080
CAATBOX1	157 (-) CAAT	S000028
CCAATBOX1	157 (-) CCAAT	S000030
SITEIIATCYTC	159 (+) TGGGCY	S000474
CCAATBOX1	182 (+) CCAAT	S000030
CAATBOX1	183 (+) CAAT	S000028
ARR1AT	184 (-) NGATT	S000454
BOXIINTPATPB	191 (+) ATAGAA	S000296
ARR1AT	195 (-) NGATT	S000454
GT1CONSENSUS	200 (-) GRWAAW	S000198
GT1GMSCAM4	200 (-) GAAAAA	S000453
ARR1AT	208 (+) NGATT	S000454
DOFCOREZM	219 (+) AAAG	S000265
TATABOX5	225 (+) TTATTT	S000203
POLLEN1LELAT52	228 (-) AGAAA	S000245
RAV1AAT	233 (+) CAACA	S000314
DOFCOREZM	237 (+) AAAG	S000265
ARR1AT	247 (+) NGATT	S000454
CACTFTPPCA1	258 (+) YACT	S000449
CPBCSPOR	260 (-) TATTAG	S000491
CACTFTPPCA1	274 (-) YACT	S000449
GTGANTG10	275 (+) GTGA	S000378
RAV1AAT	281 (-) CAACA	S000314
WBOXATNPR1	283 (+) TTGAC	S000390
BIHD1OS	284 (-) TGTCA	S000498
WRKY71OS	284 (+) TGAC	S000447
TBOXATGAPB	287 (-) ACTTTG	S000383
DOFCOREZM	288 (+) AAAG	S000265
CACTFTPPCA1	290 (-) YACT	S000449
SURECOREATSULTR11	296 (+) GAGAC	S000499
NODCON2GM	303 (+) CTCTT	S000462
OSE2ROOTNODULE	303 (+) CTCTT	S000468
EBOXBNNAPA	310 (-) CANNTG	S000144
CATATGGMSAUR	310 (-) CATATG	S000370
MYCCONSENSUSAT	310 (-) CANNTG	S000407
EBOXBNNAPA	310 (+) CANNTG	S000144
CATATGGMSAUR	310 (+) CATATG	S000370

MYCCONSENSUSAT	310 (+) CANNTG	S000407
HEXMOTIFTAH3H4	314 (-) ACGTCA	S000053
ASF1MOTIFCAMV	314 (+) TGACG	S000024
TGACGTVMAMY	314 (+) TGACGT	S000377
WRKY71OS	314 (+) TGAC	S000447
ACGTATERD1	316 (-) ACGT	S000415
ABRELATERD1	316 (+) ACGTG	S000414
ACGTATERD1	316 (+) ACGT	S000415
TOPOISOM	318 (+) GTNWAYATTNATNNG	S000112
CURECORECR	320 (-) GTAC	S000493
CURECORECR	320 (+) GTAC	S000493
L1BOXATPDF1	321 (-) TAAATGYA	S000386
CARGCW8GAT	323 (-) CWWWWWWWWG	S000431
CARGCW8GAT	323 (+) CWWWWWWWWG	S000431
POLASIG1	325 (-) AATAAA	S000080
TATABOX5	326 (+) TTATTT	S000203
INRNTPSADB	333 (+) YTCANTYY	S000395
CAATBOX1	335 (+) CAAT	S000028
ARR1AT	346 (+) NGATT	S000454
CACTFTPPCA1	368 (+) YACT	S000449
GT1CONSENSUS	374 (+) GRWAAW	S000198
CACTFTPPCA1	381 (+) YACT	S000449
ROOTMOTIFTAPOX1	387 (-) ATATT	S000098
SEF1MOTIF	389 (-) ATATTTAWW	S000006
TATABOX2	389 (+) TATAAAT	S000109
ROOTMOTIFTAPOX1	393 (-) ATATT	S000098
ROOTMOTIFTAPOX1	405 (-) ATATT	S000098
BIHD1OS	412 (+) TGTCA	S000498
WRKY71OS	413 (-) TGAC	S000447
CAATBOX1	416 (-) CAAT	S000028
CCAATBOX1	416 (-) CCAAT	S000030
WBOXHVISO1	422 (+) TGACT	S000442
WRKY71OS	422 (+) TGAC	S000447
WBOXNTERF3	422 (+) TGACY	S000457
CACTFTPPCA1	426 (+) YACT	S000449
CAATBOX1	432 (-) CAAT	S000028
CCAATBOX1	432 (-) CCAAT	S000030
PYRIMIDINEBOXOSRAMY1A	439 (+) CCTTTT	S000259
DOFCOREZM	440 (-) AAAG	S000265
POLASIG1	442 (-) AATAAA	S000080
CAATBOX1	445 (-) CAAT	S000028
CCAATBOX1	445 (-) CCAAT	S000030
SITEIIATCYTC	447 (+) TGGGCY	S000474

TATABOX5	455 (-) TTATTT	S000203
POLASIG1	456 (+) AATAAA	S000080
RAV1AAT	468 (-) CAACA	S000314
EECCRCAH1	483 (+) GANTTNC	S000494
GT1CONSENSUS	485 (-) GRWAAW	S000198
MYB1AT	516 (+) WAACCA	S000408
CCAATBOX1	522 (+) CCAAT	S000030
CAATBOX1	523 (+) CAAT	S000028
ROOTMOTIFTAPOX1	524 (-) ATATT	S000098
TATABOX2	526 (+) TATAAAT	S000109
POLASIG2	538 (-) AATTAAA	S000081
GATABOX	546 (+) GATA	S000039
SURECOREATSULTR11	569 (-) GAGAC	S000499
CARGCW8GAT	579 (-) CWWWWWWWWG	S000431
CARGCW8GAT	579 (+) CWWWWWWWWG	S000431
SEF4MOTIFGM7S	582 (+) RTTTTTR	S000103
GT1CONSENSUS	588 (+) GRWAAW	S000198
GT1CONSENSUS	594 (+) GRWAAW	S000198
GT1CONSENSUS	595 (+) GRWAAW	S000198
ROOTMOTIFTAPOX1	598 (-) ATATT	S000098
AACACOREOSGLUB1	603 (-) AACAAAC	S000353
RAV1AAT	606 (-) CAACA	S000314
CAATBOX1	615 (-) CAAT	S000028
E2FCONSENSUS	615 (+) WTTSSCSS	S000476
POLLEN1LELAT52	624 (+) AGAAA	S000245
SURECOREATSULTR11	631 (-) GAGAC	S000499
DOFCOREZM	638 (-) AAAG	S000265
ERELEE4	647 (+) AWTTCAAA	S000037
CACTFTPPCA1	658 (-) YACT	S000449
CPBCSPOR	667 (-) TATTAG	S000491
CACTFTPPCA1	677 (+) YACT	S000449
S1FBOXSORPS1L21	687 (+) ATGGTA	S000223
GT1CONSENSUS	689 (+) GRWAAW	S000198
ROOTMOTIFTAPOX1	697 (-) ATATT	S000098
TATAPVTRNALEU	701 (-) TTTATATA	S000340
TATABOX4	701 (+) TATATAA	S000111
TATABOX2	703 (+) TATAAAT	S000109
CACTFTPPCA1	713 (-) YACT	S000449
CURECORECR	716 (-) GTAC	S000493
CURECORECR	716 (+) GTAC	S000493
NAPINMOTIFBN	717 (+) TACACAT	S000070
ROOTMOTIFTAPOX1	726 (+) ATATT	S000098
CAATBOX1	728 (-) CAAT	S000028

BIHD1OS	730 (+) TGTCA	S000498
WBOXATNPR1	731 (-) TTGAC	S000390
WRKY71OS	731 (-) TGAC	S000447
DOFCOREZM	734 (+) AAAG	S000265
POLLEN1LELAT52	736 (+) AGAAA	S000245
SEF4MOTIFGM7S	740 (+) RTTTTTR	S000103
CACTFTPPCA1	747 (+) YACT	S000449
CCA1ATLHCB1	755 (+) AAMAATCT	S000149
CAATBOX1	757 (+) CAAT	S000028
ARR1AT	758 (-) NGATT	S000454
-300ELEMENT	777 (-) TGHAAARK	S000122
DOFCOREZM	778 (-) AAAG	S000265
PROLAMINBOXOSGLUB1	778 (-) TGCAAAG	S000354
CACTFTPPCA1	784 (-) YACT	S000449
TATABOX3	786 (+) TATTAAT	S000110
POLLEN1LELAT52	799 (-) AGAAA	S000245
ACGTATERD1	807 (-) ACGT	S000415
ACGTATERD1	807 (+) ACGT	S000415
CCAATBOX1	811 (+) CCAAT	S000030
CAATBOX1	812 (+) CAAT	S000028
POLASIG2	813 (+) AATTAAA	S000081
MYBCORE	831 (-) CNGTTR	S000176
ARR1AT	836 (+) NGATT	S000454
CAATBOX1	852 (+) CAAT	S000028
-10PEHVPSBD	857 (+) TATTCT	S000392
CACTFTPPCA1	873 (-) YACT	S000449
GTGANTG10	881 (+) GTGA	S000378
EBOXBNNAPA	886 (-) CANNTG	S000144
MYCCONSENSUSAT	886 (-) CANNTG	S000407
EBOXBNNAPA	886 (+) CANNTG	S000144
MYCCONSENSUSAT	886 (+) CANNTG	S000407
BIHD1OS	897 (-) TGTCA	S000498
WRKY71OS	897 (+) TGAC	S000447
POLLEN1LELAT52	908 (-) AGAAA	S000245
DOFCOREZM	937 (-) AAAG	S000265
TAAAGSTKST1	937 (-) TAAAG	S000387
CACTFTPPCA1	945 (+) YACT	S000449
DOFCOREZM	952 (+) AAAG	S000265
WBOXHVISO1	954 (-) TGACT	S000442
WBOXNTERF3	954 (-) TGACY	S000457
WBOXATNPR1	955 (-) TTGAC	S000390
WRKY71OS	955 (-) TGAC	S000447
RAV1AAT	963 (-) CAACA	S000314

EECCRCAH1	967 (-) GANTTNC	S000494
ARR1AT	970 (-) NGATT	S000454
GTGANTG10	972 (-) GTGA	S000378
DOFCOREZM	976 (+) AAAG	S000265
NODCON1GM	976 (+) AAAGAT	S000461
OSE1ROOTNODULE	976 (+) AAAGAT	S000467
ARR1AT	978 (+) NGATT	S000454
EECCRCAH1	979 (+) GANTTNC	S000494
GT1CONSENSUS	980 (-) GRWAAW	S000198
POLLEN1LELAT52	982 (-) AGAAA	S000245
POLLEN1LELAT52	989 (+) AGAAA	S000245
DOFCOREZM	991 (+) AAAG	S000265
NODCON2GM	992 (-) CTCTT	S000462
OSE2ROOTNODULE	992 (-) CTCTT	S000468
DOFCOREZM	1000 (+) AAAG	S000265
GT1CONSENSUS	1006 (+) GRWAAW	S000198
DOFCOREZM	1009 (+) AAAG	S000265
GT1CONSENSUS	1018 (+) GRWAAW	S000198
PYRIMIDINEBOXOSRAMY1A	1021 (-) CCTTTT	S000259
DOFCOREZM	1022 (+) AAAG	S000265
-10PEHVPSBD	1030 (+) TATTCT	S000392
BOXIINTPATPB	1032 (-) ATAGAA	S000296
ARFAT	1039 (+) TGTCTC	S000270
SURECOREATSULTR11	1040 (-) GAGAC	S000499
POLLEN1LELAT52	1047 (-) AGAAA	S000245
EECCRCAH1	1062 (+) GANTTNC	S000494
DOFCOREZM	1064 (-) AAAG	S000265
EBOXBNNAPA	1070 (-) CANNTG	S000144
MYCATRD22	1070 (-) CACATG	S000174
MYCCONSENSUSAT	1070 (-) CANNTG	S000407
EBOXBNNAPA	1070 (+) CANNTG	S000144
MYCCONSENSUSAT	1070 (+) CANNTG	S000407
MYCATERD1	1070 (+) CATGTG	S000413
CACTFTPPCA1	1090 (-) YACT	S000449
CURECORECR	1091 (-) GTAC	S000493
CURECORECR	1091 (+) GTAC	S000493
SV40COREENHAN	1096 (+) GTGGWWHG	S000123
CGACGOSAMY3	1102 (+) CGACG	S000205
ACGTCBOX	1103 (-) GACGTC	S000131
ACGTCBOX	1103 (+) GACGTC	S000131
TGACGTVMAMY	1104 (-) TGACGT	S000377
ACGTATERD1	1104 (-) ACGT	S000415
HEXMOTIFTAH3H4	1104 (+) ACGTCA	S000053

ACGTATERD1	1104 (+) ACGT	S000415
ASF1MOTIFCAMV	1105 (-) TGACG	S000024
WRKY71OS	1106 (-) TGAC	S000447
SEF1MOTIF	1109 (+) ATATTTAWW	S000006
ROOTMOTIFTAPOX1	1109 (+) ATATT	S000098
TATABOXOSPAL	1110 (+) TATTTAA	S000400
POLASIG2	1112 (-) AATTAAA	S000081
CURECORECR	1135 (-) GTAC	S000493
CURECORECR	1135 (+) GTAC	S000493
CPBCSPOR	1140 (+) TATTAG	S000491
CACTFTPPCA1	1144 (-) YACT	S000449
MYBCORE	1146 (-) CNGTTR	S000176
CACTFTPPCA1	1150 (-) YACT	S000449
GATABOX	1154 (-) GATA	S000039
DOFCOREZM	1159 (+) AAAG	S000265
SEF4MOTIFGM7S	1163 (-) RTTTTTR	S000103
POLASIG3	1171 (-) AATAAT	S000088
TATABOX5	1172 (+) TTATTT	S000203
GT1CONSENSUS	1175 (-) GRWAAW	S000198
IBOXCORE	1176 (-) GATAA	S000199
GATABOX	1177 (-) GATA	S000039
DRE2COREZMRAB17	1188 (+) ACCGAC	S000402
DRECRTCOREAT	1188 (+) RCCGAC	S000418
CBFHV	1188 (+) RYCGAC	S000497
LTRECOREATCOR15	1189 (+) CCGAC	S000153
PYRIMIDINEBOXOSRAMY1A	1198 (-) CCTTTT	S000259
DOFCOREZM	1199 (+) AAAG	S000265
GT1CORE	1203 (+) GGTTAA	S000125
AMYBOX1	1213 (+) TAACARA	S000020
MYBGAHV	1213 (+) TAACAAA	S000181
GAREAT	1213 (+) TAACAAR	S000439
MYB1AT	1218 (+) WAACCA	S000408
REALPHALGLHCB21	1219 (+) AACCAA	S000362
CCAATBOX1	1221 (+) CCAAT	S000030
CAATBOX1	1222 (+) CAAT	S000028
CACTFTPPCA1	1229 (-) YACT	S000449
TAAAGSTKST1	1243 (+) TAAAG	S000387
DOFCOREZM	1244 (+) AAAG	S000265
ARR1AT	1258 (-) NGATT	S000454
NODCON1GM	1259 (-) AAAGAT	S000461
OSE1ROOTNODULE	1259 (-) AAAGAT	S000467
DOFCOREZM	1261 (-) AAAG	S000265
POLLEN1LELAT52	1262 (-) AGAAA	S000245

ARR1AT	1267 (-) NGATT	S000454
RYREPEATBNNAPA	1274 (-) CATGCA	S000264
RYREPEATBNNAPA	1276 (+) CATGCA	S000264
POLLEN1LELAT52	1281 (+) AGAAA	S000245
PYRIMIDINEBOXOSRAMY1A	1291 (+) CCTTTT	S000259
DOFCOREZM	1292 (-) AAAG	S000265
CACTFTPPCA1	1299 (-) YACT	S000449
GT1CONSENSUS	1304 (-) GRWAAW	S000198
ARR1AT	1310 (+) NGATT	S000454
POLLEN1LELAT52	1319 (+) AGAAA	S000245
DOFCOREZM	1322 (+) AAAG	S000265
NODCON1GM	1322 (+) AAAGAT	S000461
OSE1ROOTNODULE	1322 (+) AAAGAT	S000467
POLLEN1LELAT52	1331 (-) AGAAA	S000245
RAV1AAT	1336 (+) CAACA	S000314
ARR1AT	1350 (+) NGATT	S000454
MYBPZM	1356 (+) CCWACC	S000179
CACTFTPPCA1	1361 (+) YACT	S000449
CACTFTPPCA1	1368 (+) YACT	S000449
EBOXBNNAPA	1381 (-) CANNTG	S000144
MYCATRD22	1381 (-) CACATG	S000174
MYCCONSENSUSAT	1381 (-) CANNTG	S000407
EBOXBNNAPA	1381 (+) CANNTG	S000144
MYCCONSENSUSAT	1381 (+) CANNTG	S000407
MYCATERD1	1381 (+) CATGTG	S000413
GTGANTG10	1384 (+) GTGA	S000378
ROOTMOTIFTAPOX1	1394 (+) ATATT	S000098
ANAERO1CONSENSUS	1400 (-) AAACAAA	S000477
MARTBOX	1404 (+) TTWTWTTWTT	S000067
SEF4MOTIFGM7S	1416 (+) RTTTTTR	S000103
MARABOX1	1419 (-) AATAAAYAAA	S000063
POLASIG1	1419 (-) AATAAA	S000080
TATABOX5	1420 (+) TTATTT	S000203
POLASIG1	1423 (-) AATAAA	S000080
GT1CONSENSUS	1441 (+) GRWAAW	S000198
GT1CONSENSUS	1442 (+) GRWAAW	S000198
ROOTMOTIFTAPOX1	1445 (-) ATATT	S000098
GT1CONSENSUS	1452 (-) GRWAAW	S000198
IBOXCORE	1453 (-) GATAA	S000199
GATABOX	1454 (-) GATA	S000039
GT1CONSENSUS	1463 (-) GRWAAW	S000198
GT1GMSCAM4	1463 (-) GAAAAA	S000453
POLLEN1LELAT52	1465 (-) AGAAA	S000245

NODCON2GM	1468 (+) CTCTT	S000462
OSE2ROOTNODULE	1468 (+) CTCTT	S000468
GATABOX	1477 (+) GATA	S000039
IBOXCORE	1477 (+) GATAA	S000199
CAATBOX1	1482 (+) CAAT	S000028
ARR1AT	1496 (-) NGATT	S000454
POLLEN1LELAT52	1505 (+) AGAAA	S000245
DOFCOREZM	1507 (+) AAAG	S000265
-10PEHVPSBD	1509 (-) TATTCT	S000392
TOPOISOM	1519 (+) GTNWAYATTNAT	S000112
ROOTMOTIFTAPOX1	1522 (-) ATATT	S000098
SEF1MOTIF	1523 (+) ATATTTAWW	S000006
ROOTMOTIFTAPOX1	1523 (+) ATATT	S000098
POLASIG1	1526 (-) AATAAA	S000080
TATABOX5	1527 (+) TTATTT	S000203
GATABOX	1534 (-) GATA	S000039
NTBBF1ARROLB	1542 (+) ACTTTA	S000273
DOFCOREZM	1543 (-) AAAG	S000265
TAAAGSTKST1	1543 (-) TAAAG	S000387
POLASIG2	1544 (-) AATTAAA	S000081
CACTFTPPCA1	1550 (+) YACT	S000449
CARGCW8GAT	1552 (-) CWWWWWWWWG	S000431
CARGCW8GAT	1552 (+) CWWWWWWWWG	S000431
QELEMENTZMZM13	1560 (-) AGGTCA	S000254
WRKY71OS	1560 (+) TGAC	S000447
WBOXNTERF3	1560 (+) TGACY	S000457
TAAAGSTKST1	1565 (+) TAAAG	S000387
DOFCOREZM	1566 (+) AAAG	S000265
POLLEN1LELAT52	1568 (+) AGAAA	S000245
ANAERO1CONSENSUS	1571 (+) AAACAAA	S000477
GATABOX	1581 (-) GATA	S000039
MYBST1	1581 (-) GGATA	S000180
ARR1AT	1587 (-) NGATT	S000454
EBOXBNNAPA	1596 (-) CANNTG	S000144
MYCCONSENSUSAT	1596 (-) CANNTG	S000407
EBOXBNNAPA	1596 (+) CANNTG	S000144
MYCCONSENSUSAT	1596 (+) CANNTG	S000407
GATABOX	1601 (+) GATA	S000039
ROOTMOTIFTAPOX1	1602 (+) ATATT	S000098
POLASIG3	1604 (-) AATAAT	S000088
TATABOX5	1605 (+) TTATTT	S000203
GT1CONSENSUS	1607 (-) GRWAAW	S000198
CAATBOX1	1615 (-) CAAT	S000028

GATABOX	1618 (+) GATA	S000039
CACTFTPPCA1	1621 (-) YACT	S000449
ROOTMOTIFTAPOX1	1626 (+) ATATT	S000098
POLASIG3	1634 (+) AATAAT	S000088
-10PEHVPSBD	1644 (-) TATTCT	S000392
GT1CONSENSUS	1651 (+) GRWAAW	S000198
GT1GMSCAM4	1651 (+) GAAAAA	S000453
DPBFCOREDCDC3	1657 (+) ACACNNG	S000292
PRECONSCRHSP70A	1661 (+) SCGAYNRNNNNNNNNNNHD	S000506
GATABOX	1663 (+) GATA	S000039
GATABOX	1667 (+) GATA	S000039
ROOTMOTIFTAPOX1	1668 (+) ATATT	S000098
CAATBOX1	1670 (-) CAAT	S000028
AACACOREOSGLUB1	1674 (+) AACAAAC	S000353
ANAERO1CONSENSUS	1677 (+) AAACAAA	S000477
TATABOX5	1681 (-) TTATTT	S000203
NTBBF1ARROLB	1713 (-) ACTTTA	S000273
TAAAGSTKST1	1713 (+) TAAAG	S000387
DOFCOREZM	1714 (+) AAAG	S000265
CACTFTPPCA1	1716 (-) YACT	S000449
CURECORECR	1717 (-) GTAC	S000493
CURECORECR	1717 (+) GTAC	S000493
QELEMENTZMZM13	1722 (-) AGGTCA	S000254
WRKY71OS	1722 (+) TGAC	S000447
WBOXNTERF3	1722 (+) TGACY	S000457
CACTFTPPCA1	1753 (-) YACT	S000449
GTGANTG10	1754 (+) GTGA	S000378
SURECOREATSULTR11	1764 (+) GAGAC	S000499
ACGTATERD1	1767 (-) ACGT	S000415
ABRELATERD1	1767 (+) ACGTG	S000414
ACGTATERD1	1767 (+) ACGT	S000415
CURECORECR	1771 (-) GTAC	S000493
CURECORECR	1771 (+) GTAC	S000493
MYB1AT	1790 (+) WAACCA	S000408
REALPHALGLHCB21	1791 (+) AACCAA	S000362
DOFCOREZM	1795 (+) AAAG	S000265
TBOXATGAPB	1799 (-) ACTTTG	S000383
DOFCOREZM	1800 (+) AAAG	S000265
CACTFTPPCA1	1806 (-) YACT	S000449
NTBBF1ARROLB	1808 (-) ACTTTA	S000273
TAAAGSTKST1	1808 (+) TAAAG	S000387
DOFCOREZM	1809 (+) AAAG	S000265
POLLEN1LELAT52	1821 (+) AGAAA	S000245

GT1CONSENSUS	1822 (+) GRWAAW	S000198
GATABOX	1844 (-) GATA	S000039
MYBCORE	1847 (-) CNGTTR	S000176
DOFCOREZM	1865 (-) AAAG	S000265
POLLEN1LELAT52	1866 (-) AGAAA	S000245
DOFCOREZM	1869 (-) AAAG	S000265
TAAAGSTKST1	1869 (-) TAAAG	S000387
POLASIG2	1870 (-) AATTAAA	S000081
POLLEN1LELAT52	1875 (-) AGAAA	S000245
DOFCOREZM	1878 (-) AAAG	S000265
SEF4MOTIFGM7S	1891 (-) RTTTTTR	S000103
RAV1AAT	1901 (+) CAACA	S000314
CAREOSREP1	1904 (+) CAACTC	S000421
ACGTTBOX	1917 (-) AACGTT	S000132
ACGTTBOX	1917 (+) AACGTT	S000132
ACGTATERD1	1918 (-) ACGT	S000415
ACGTATERD1	1918 (+) ACGT	S000415
DOFCOREZM	1925 (-) AAAG	S000265
TAAAGSTKST1	1925 (-) TAAAG	S000387
ROOTMOTIFTAPOX1	1942 (-) ATATT	S000098
TATAPVTRNALEU	1956 (-) TTTATATA	S000340
TATABOX4	1956 (+) TATATAA	S000111
CACTFTPPCA1	1967 (+) YACT	S000449
NODCON2GM	1976 (+) CTCTT	S000462
OSE2ROOTNODULE	1976 (+) CTCTT	S000468
INRNTPSADB	1993 (+) YTCANTYY	S000395
NODCON2GM	1999 (+) CTCTT	S000462
OSE2ROOTNODULE	1999 (+) CTCTT	S000468
DOFCOREZM	2001 (-) AAAG	S000265
GT1CONSENSUS	2002 (-) GRWAAW	S000198
CACTFTPPCA1	2012 (+) YACT	S000449
GTGANTG10	2016 (-) GTGA	S000378
CACTFTPPCA1	2017 (+) YACT	S000449
MYB1AT	2022 (+) WAACCA	S000408
REALPHALGLHCB21	2023 (+) AACCAA	S000362
MARTBOX	2027 (-) TTWTWTTWTT	S000067
MARTBOX	2028 (-) TTWTWTTWTT	S000067
DOFCOREZM	2035 (+) AAAG	S000265
NODCON2GM	2036 (-) CTCTT	S000462
OSE2ROOTNODULE	2036 (-) CTCTT	S000468
POLLEN1LELAT52	2039 (+) AGAAA	S000245
CAATBOX1	2044 (+) CAAT	S000028
GT1CONSENSUS	2048 (-) GRWAAW	S000198

GT1GMSCAM4	2048 (-) GAAAAA	S000453

Appendix 7b: *In silico* Analysis of *FAωH1* P2 Promoter Sequence

List of promoter motifs identified by PLACE scan. Location (Loc.) given is 5' upstream of the translation start site on the coding strand (i.e. location of 1 would be 2056 bp upstream of the translation start site). Strand refers to the + or – orientation of the motif. Signal sequence is the consensus sequence attributed to the specific motif. Site # refers to the reference number for further information from the PLACE database. Grey represents promoter deletion series ABA-related elements; green represents other ABA-related elements; yellow represents wound-related elements; blue represents root-specific elements.

Factor or Site Name	Loc.	(Str.)	Signal Sequence	Site #
DOFCOREZM	4	(-)	AAAG	S00026
AMYBOX1	10	(+)	TAACARA	S00002
MYBGAHV	10	(+)	TAACAAA	S00018
GAREAT	10	(+)	TAACAAR	S00043
DOFCOREZM	14	(+)	AAAG	S00026
NODCON2GM	15	(-)	CTCTT	S00046
OSE2ROOTNODULE	15	(-)	CTCTT	S00046
POLLEN1LELAT52	18	(+)	AGAAA	S00024
GT1CONSENSUS	19	(+)	GRWAAW	S00019
GT1GMSCAM4	19	(+)	GAAAAA	S00045
MARTBOX	20	(-)	TTWTWTTWTT	S00006
MARTBOX	21	(-)	TTWTWTTWTT	S00006
ANAERO1CONSENSUS	28	(+)	AAACAAA	S00047
INRNTPSADB	35	(+)	YTCANTYY	S00039
GTGANTG10	36	(-)	GTGA	S00037
CACTFTPPCA1	37	(+)	YACT	S00044
CACTFTPPCA1	48	(+)	YACT	S00044
DOFCOREZM	50	(-)	AAAG	S00026
POLLEN1LELAT52	52	(-)	AGAAA	S00024
NODCON2GM	55	(+)	CTCTT	S00046
OSE2ROOTNODULE	55	(+)	CTCTT	S00046
CACTFTPPCA1	59	(+)	YACT	S00044
GATABOX	68	(+)	GATA	S00003
INRNTPSADB	85	(+)	YTCANTYY	S00039
ROOTMOTIFTAPOX1	94	(-)	ATATT	S00009
TATAPVTRNALEU	102	(-)	TTTATATA	S00034
TATABOX4	102	(+)	TATATAA	S00011
GT1CONSENSUS	121	(-)	GRWAAW	S00019
DOFCOREZM	126	(-)	AAAG	S00026
ARR1AT	133	(-)	NGATT	S00045
RAV1AAT	143	(+)	CAACA	S00031
CAREOSREP1	146	(+)	CAACTC	S00042
NODCON2GM	149	(+)	CTCTT	S00046
OSE2ROOTNODULE	149	(+)	CTCTT	S00046
SEF4MOTIFGM7S	153	(-)	RTTTTTR	S00010
ROOTMOTIFTAPOX1	157	(-)	ATATT	S00009

ROOTMOTIFTAPOX1	158	(+)	ATATT	S00009
CAATBOX1	160	(-)	CAAT	S00002
CACTFTPPCA1	166	(+)	YACT	S00044
DOFCOREZM	168	(-)	AAAG	S00026
POLLEN1LELAT52	169	(-)	AGAAA	S00024
DOFCOREZM	172	(-)	AAAG	S00026
TAAAGSTKST1	172	(-)	TAAAG	S00038
POLASIG2	173	(-)	AATTAAA	S00008
POLLEN1LELAT52	178	(-)	AGAAA	S00024
DOFCOREZM	181	(-)	AAAG	S00026
POLLEN1LELAT52	182	(-)	AGAAA	S00024
GATABOX	204	(-)	GATA	S00003
MYBST1	204	(-)	GGATA	S00018
CACTFTPPCA1	219	(+)	YACT	S00044
TATABOX5	225	(-)	TTATTT	S00020
POLASIG3	226	(+)	AATAAT	S00008
POLASIG2	229	(+)	AATTAAA	S00008
DOFCOREZM	234	(+)	AAAG	S00026
DOFCOREZM	242	(-)	AAAG	S00026
ERELEE4	244	(-)	AWTTCAAA	S00003
WBOXHVISO1	251	(+)	TGACT	S00044
WRKY71OS	251	(+)	TGAC	S00044
WBOXNTERF3	251	(+)	TGACY	S00045
ARR1AT	268	(-)	NGATT	S00045
CACTFTPPCA1	274	(-)	YACT	S00044
ROOTMOTIFTAPOX1	277	(+)	ATATT	S00009
EBOXBNNAPA	285	(-)	CANNTG	S00014
MYCATRD22	285	(-)	CACATG	S00017
MYCCONSENSUSAT	285	(-)	CANNTG	S00040
EBOXBNNAPA	285	(+)	CANNTG	S00014
MYCCONSENSUSAT	285	(+)	CANNTG	S00040
MYCATERD1	285	(+)	CATGTG	S00041
-300ELEMENT	289	(+)	TGHAAARK	S00012
PROLAMINBOXOSGLUB1	289	(+)	TGCAAAG	S00035
TBOXATGAPB	291	(-)	ACTTTG	S00038
DOFCOREZM	292	(+)	AAAG	S00026
CACTFTPPCA1	294	(-)	YACT	S00044
CURECORECR	295	(-)	GTAC	S00049
CURECORECR	295	(+)	GTAC	S00049
CACTFTPPCA1	296	(+)	YACT	S00044
DOFCOREZM	302	(+)	AAAG	S00026
CACGCAATGMGH3	308	(+)	CACGCAAT	S00036
CAATBOX1	312	(+)	CAAT	S00002
SEF4MOTIFGM7S	325	(+)	RTTTTTR	S00010
MYB1AT	331	(+)	WAACCA	S00040
CACTFTPPCA1	336	(-)	YACT	S00044
CURECORECR	337	(-)	GTAC	S00049
CURECORECR	337	(+)	GTAC	S00049

POLASIG1	365	(+)	AATAAA	S00008
MARABOX1	377	(+)	AATAAAYAAA	S00006
POLASIG1	377	(+)	AATAAA	S00008
ANAERO1CONSENSUS	380	(+)	AAACAAA	S00047
AACACOREOSGLUB1	381	(+)	AACAAAC	S00035
GATABOX	396	(+)	GATA	S00003
IBOXCORE	396	(+)	GATAA	S00019
MYBCORE	398	(-)	CNGTTR	S00017
LTREATLTI78	400	(+)	ACCGACA	S00015
DRE2COREZMRAB17	400	(+)	ACCGAC	S00040
DRECRTCOREAT	400	(+)	RCCGAC	S00041
CBFHV	400	(+)	RYCGAC	S00049
LTRECOREATCOR15	401	(+)	CCGAC	S00015
DOFCOREZM	409	(+)	AAAG	S00026
CACTFTPPCA1	429	(-)	YACT	S00044
TATABOX4	433	(-)	TATATAA	S00011
GATABOX	441	(+)	GATA	S00003
CACTFTPPCA1	443	(+)	YACT	S00044
DOFCOREZM	451	(-)	AAAG	S00026
POLASIG1	453	(-)	AATAAA	S00008
CAATBOX1	456	(-)	CAAT	S00002
CCAATBOX1	456	(-)	CCAAT	S00003
REALPHALGLHCB21	457	(-)	AACCAA	S00036
MYB1AT	458	(-)	WAACCA	S00040
SEF4MOTIFGM7S	460	(+)	RTTTTTR	S00010
CACTFTPPCA1	468	(-)	YACT	S00044
WBOXHVISO1	476	(-)	TGACT	S00044
WBOXNTERF3	476	(-)	TGACY	S00045
WRKY71OS	477	(-)	TGAC	S00044
ARR1AT	482	(-)	NGATT	S00045
ROOTMOTIFTAPOX1	488	(+)	ATATT	S00009
DOFCOREZM	498	(+)	AAAG	S00026
POLLEN1LELAT52	500	(+)	AGAAA	S00024
ARR1AT	503	(-)	NGATT	S00045
CACTFTPPCA1	508	(-)	YACT	S00044
TATABOX3	510	(+)	TATTAAT	S00011
TATABOX2	544	(+)	TATAAAT	S00010
L1BOXATPDF1	546	(+)	TAAATGYA	S00038
INRNTPSADB	553	(-)	YTCANTYY	S00039
POLLEN1LELAT52	559	(+)	AGAAA	S00024
GT1CONSENSUS	560	(+)	GRWAAW	S00019
GT1GMSCAM4	560	(+)	GAAAAA	S00045
DOFCOREZM	564	(+)	AAAG	S00026
ARR1AT	568	(-)	NGATT	S00045
CAATBOX1	574	(-)	CAAT	S00002
CCAATBOX1	574	(-)	CCAAT	S00003
CURECORECR	578	(-)	GTAC	S00049
CURECORECR	578	(+)	GTAC	S00049

L1BOXATPDF1	579	(-)	TAAATGYA	S00038
GT1CONSENSUS	583	(-)	GRWAAW	S00019
IBOXCORE	584	(-)	GATAA	S00019
GATABOX	585	(-)	GATA	S00003
CAATBOX1	588	(+)	CAAT	S00002
ARR1AT	592	(+)	NGATT	S00045
NODCON2GM	600	(+)	CTCTT	S00046
OSE2ROOTNODULE	600	(+)	CTCTT	S00046
DOFCOREZM	602	(-)	AAAG	S00026
GT1CONSENSUS	605	(-)	GRWAAW	S00019
ARR1AT	618	(+)	NGATT	S00045
TATABOX4	621	(-)	TATATAA	S00011
TATAPVTRNALEU	624	(-)	TTTATATA	S00034
TATABOX4	624	(+)	TATATAA	S00011
PYRIMIDINEBOXOSRAMY1A	629	(-)	CCTTTT	S00025
DOFCOREZM	630	(+)	AAAG	S00026
ROOTMOTIFTAPOX1	643	(-)	ATATT	S00009
ROOTMOTIFTAPOX1	644	(+)	ATATT	S00009
POLASIG3	646	(-)	AATAAT	S00008
TATABOX5	647	(+)	TTATTT	S00020
POLASIG1	650	(-)	AATAAA	S00008
TATABOX5	651	(+)	TTATTT	S00020
-300ELEMENT	653	(-)	TGHAAARK	S00012
GT1CONSENSUS	654	(-)	GRWAAW	S00019
GT1GMSCAM4	654	(-)	GAAAAA	S00045
INRNTPSADB	657	(+)	YTCANTYY	S00039
MARTBOX	661	(+)	TTWTWTTWTT	S00006
POLASIG1	662	(-)	AATAAA	S00008
TATABOX5	663	(+)	TTATTT	S00020
SEF4MOTIFGM7S	665	(+)	RTTTTTR	S00010
MARTBOX	667	(+)	TTWTWTTWTT	S00006
POLASIG1	668	(-)	AATAAA	S00008
TATABOX5	669	(+)	TTATTT	S00020
SEF4MOTIFGM7S	671	(+)	RTTTTTR	S00010
GT1CONSENSUS	674	(-)	GRWAAW	S00019
IBOXCORE	675	(-)	GATAA	S00019
GATABOX	676	(-)	GATA	S00003
NODCON1GM	677	(-)	AAAGAT	S00046
OSE1ROOTNODULE	677	(-)	AAAGAT	S00046
DOFCOREZM	679	(-)	AAAG	S00026
TBOXATGAPB	683	(-)	ACTTTG	S00038
DOFCOREZM	684	(+)	AAAG	S00026
CACTFTPPCA1	686	(-)	YACT	S00044
CURECORECR	689	(-)	GTAC	S00049
CURECORECR	689	(+)	GTAC	S00049
CACTFTPPCA1	690	(+)	YACT	S00044
GTGANTG10	702	(-)	GTGA	S00037
PALBOXLPC	707	(+)	YCYYACCWACC	S00013

GTGANTG10	709	(-)	GTGA	S00037
MYBPLANT	710	(+)	MACCWAMC	S00016
BOXLCOREDCPAL	711	(+)	ACCWWCC	S00049
MYBPZM	712	(+)	CCWACC	S00017
ARR1AT	726	(-)	NGATT	S00045
CBFHV	727	(+)	RYCGAC	S00049
CAREOSREP1	734	(+)	CAACTC	S00042
NODCON2GM	737	(+)	CTCTT	S00046
OSE2ROOTNODULE	737	(+)	CTCTT	S00046
DOFCOREZM	739	(-)	AAAG	S00026
TAAAGSTKST1	739	(-)	TAAAG	S00038
POLLEN1LELAT52	747	(+)	AGAAA	S00024
DOFCOREZM	750	(+)	AAAG	S00026
NODCON2GM	751	(-)	CTCTT	S00046
OSE2ROOTNODULE	751	(-)	CTCTT	S00046
PYRIMIDINEBOXOSRAMY1A	764	(+)	CCTTTT	S00025
DOFCOREZM	765	(-)	AAAG	S00026
GATABOX	770	(+)	GATA	S00003
IBOX	770	(+)	GATAAG	S00012
IBOXCORE	770	(+)	GATAA	S00019
IBOXCORENT	770	(+)	GATAAGR	S00042
ARR1AT	774	(+)	NGATT	S00045
EECCRCAH1	775	(+)	GANTTNC	S00049
GT1CONSENSUS	776	(-)	GRWAAW	S00019
GT1CONSENSUS	777	(-)	GRWAAW	S00019
ARR1AT	784	(-)	NGATT	S00045
DOFCOREZM	788	(+)	AAAG	S00026
ACGTATERD1	792	(-)	ACGT	S00041
ACGTATERD1	792	(+)	ACGT	S00041
CURECORECR	794	(-)	GTAC	S00049
CURECORECR	794	(+)	GTAC	S00049
TGACGTVMAMY	796	(-)	TGACGT	S00037
ACGTATERD1	796	(-)	ACGT	S00041
HEXMOTIFTAH3H4	796	(+)	ACGTCA	S00005
ACGTATERD1	796	(+)	ACGT	S00041
ASF1MOTIFCAMV	797	(-)	TGACG	S00002
WRKY71OS	798	(-)	TGAC	S00044
ARR1AT	805	(-)	NGATT	S00045
NODCON1GM	806	(-)	AAAGAT	S00046
OSE1ROOTNODULE	806	(-)	AAAGAT	S00046
DOFCOREZM	808	(-)	AAAG	S00026
POLLEN1LELAT52	809	(-)	AGAAA	S00024
ARR1AT	819	(-)	NGATT	S00045
RAV1AAT	835	(-)	CAACA	S00031
CAATBOX1	857	(+)	CAAT	S00002
CAATBOX1	866	(-)	CAAT	S00002
CCAATBOX1	866	(-)	CCAAT	S00003
GT1CONSENSUS	870	(+)	GRWAAW	S00019

EECCRCAH1	871	(-)	GANTTNC	S00049
GT1CONSENSUS	871	(+)	GRWAAW	S00019
ARR1AT	874	(-)	NGATT	S00045
POLASIG1	896	(-)	AATAAA	S00008
GT1CONSENSUS	899	(-)	GRWAAW	S00019
IBOXCORE	900	(-)	GATAA	S00019
GATABOX	901	(-)	GATA	S00003
SEF4MOTIFGM7S	904	(-)	RTTTTTR	S00010
DOFCOREZM	912	(+)	AAAG	S00026
BIHD1OS	921	(-)	TGTCA	S00049
WRKY71OS	921	(+)	TGAC	S00044
CAATBOX1	924	(+)	CAAT	S00002
MYB1AT	927	(-)	WAACCA	S00040
IBOXCORE	930	(-)	GATAA	S00019
SREATMSD	930	(+)	TTATCC	S00047
GATABOX	931	(-)	GATA	S00003
MYBST1	931	(-)	GGATA	S00018
AMYBOX2	931	(+)	TATCCAT	S00002
TATCCAYMOTIFOSRAMY3D	931	(+)	TATCCAY	S00025
TATCCAOSAMY	931	(+)	TATCCA	S00040
CAATBOX1	940	(-)	CAAT	S00002
ARR1AT	952	(+)	NGATT	S00045
TATABOX2	958	(-)	TATAAAT	S00010
CACTFTPPCA1	963	(+)	YACT	S00044
CAATBOX1	980	(-)	CAAT	S00002
ARR1AT	982	(+)	NGATT	S00045
CURECORECR	1001	(-)	GTAC	S00049
CURECORECR	1001	(+)	GTAC	S00049
DOFCOREZM	1024	(-)	AAAG	S00026
TAAAGSTKST1	1024	(-)	TAAAG	S00038
GT1CONSENSUS	1025	(-)	GRWAAW	S00019
IBOXCORE	1026	(-)	GATAA	S00019
GATABOX	1027	(-)	GATA	S00003
RAV1AAT	1044	(-)	CAACA	S00031
GT1CONSENSUS	1048	(+)	GRWAAW	S00019
GT1CONSENSUS	1049	(+)	GRWAAW	S00019
-300ELEMENT	1061	(+)	TGHAAARK	S00012
PYRIMIDINEBOXOSRAMY1A	1063	(-)	CCTTTT	S00025
DOFCOREZM	1064	(+)	AAAG	S00026
EECCRCAH1	1071	(-)	GANTTNC	S00049
GT1CONSENSUS	1071	(+)	GRWAAW	S00019
ARR1AT	1074	(-)	NGATT	S00045
POLLEN1LELAT52	1086	(-)	AGAAA	S00024
DOFCOREZM	1089	(-)	AAAG	S00026
GATABOX	1095	(+)	GATA	S00003
CACTFTPPCA1	1099	(+)	YACT	S00044
RAV1AAT	1106	(-)	CAACA	S00031
RAV1AAT	1109	(-)	CAACA	S00031

INRNTPSADB	1114	(-)	YTCANTYY	S00039
ROOTMOTIFTAPOX1	1130	(-)	ATATT	S00009
ROOTMOTIFTAPOX1	1131	(+)	ATATT	S00009
GT1CONSENSUS	1133	(-)	GRWAAW	S00019
ARR1AT	1141	(-)	NGATT	S00045
CBFHV	1142	(+)	RYCGAC	S00049
CGACGOSAMY3	1144	(+)	CGACG	S00020
ACGTATERD1	1146	(-)	ACGT	S00041
ACGTATERD1	1146	(+)	ACGT	S00041
RAV1AAT	1154	(-)	CAACA	S00031
ARR1AT	1160	(-)	NGATT	S00045
CACTFTPPCA1	1168	(-)	YACT	S00044
EECCRCAH1	1169	(-)	GANTTNC	S00049
CACTFTPPCA1	1180	(-)	YACT	S00044
CACTFTPPCA1	1183	(-)	YACT	S00044
CURECORECR	1199	(-)	GTAC	S00049
CURECORECR	1199	(+)	GTAC	S00049
CAATBOX1	1202	(+)	CAAT	S00002
ARR1AT	1203	(-)	NGATT	S00045
POLASIG1	1213	(+)	AATAAA	S00008
TAAAGSTKST1	1215	(+)	TAAAG	S00038
DOFCOREZM	1216	(+)	AAAG	S00026
CAATBOX1	1222	(-)	CAAT	S00002
ARR1AT	1224	(+)	NGATT	S00045
CAATBOX1	1233	(+)	CAAT	S00002
POLASIG3	1234	(+)	AATAAT	S00008
GT1CORE	1251	(-)	GGTTAA	S00012
ROOTMOTIFTAPOX1	1260	(+)	ATATT	S00009
-10PEHVPSBD	1261	(+)	TATTCT	S00039
DOFCOREZM	1265	(-)	AAAG	S00026
ARR1AT	1271	(+)	NGATT	S00045
HEXMOTIFTAH3H4	1281	(-)	ACGTCA	S00005
ASF1MOTIFCAMV	1281	(+)	TGACG	S00002
TGACGTVMAMY	1281	(+)	TGACGT	S00037
WRKY71OS	1281	(+)	TGAC	S00044
ACGTATERD1	1283	(-)	ACGT	S00041
ACGTATERD1	1283	(+)	ACGT	S00041
DOFCOREZM	1290	(-)	AAAG	S00026
TAAAGSTKST1	1290	(-)	TAAAG	S00038
BIHD1OS	1295	(+)	TGTCA	S00049
WBOXATNPR1	1296	(-)	TTGAC	S00039
WRKY71OS	1296	(-)	TGAC	S00044
CACTFTPPCA1	1300	(-)	YACT	S00044
CURECORECR	1301	(-)	GTAC	S00049
CURECORECR	1301	(+)	GTAC	S00049
AMYBOX1	1309	(+)	TAACARA	S00002
MYBGAHV	1309	(+)	TAACAAA	S00018
GAREAT	1309	(+)	TAACAAR	S00043

TBOXATGAPB	1312	(-)	ACTTTG	S00038
DOFCOREZM	1313	(+)	AAAG	S00026
CACTFTPPCA1	1315	(-)	YACT	S00044
GATABOX	1317	(-)	GATA	S00003
GTGANTG10	1319	(-)	GTGA	S00037
ROOTMOTIFTAPOX1	1323	(+)	ATATT	S00009
POLLEN1LELAT52	1332	(+)	AGAAA	S00024
MYBCORE	1337	(+)	CNGTTR	S00017
TATABOX4	1340	(-)	TATATAA	S00011
NAPINMOTIFBN	1345	(+)	TACACAT	S00007
DPBFCOREDCDC3	1346	(+)	ACACNNG	S00029
EBOXBNNAPA	1347	(-)	CANNTG	S00014
MYCCONSENSUSAT	1347	(-)	CANNTG	S00040
MYCATERD1	1347	(-)	CATGTG	S00041
EBOXBNNAPA	1347	(+)	CANNTG	S00014
MYCATRD22	1347	(+)	CACATG	S00017
MYCCONSENSUSAT	1347	(+)	CANNTG	S00040
EBOXBNNAPA	1349	(-)	CANNTG	S00014
MYCATRD22	1349	(-)	CACATG	S00017
MYCCONSENSUSAT	1349	(-)	CANNTG	S00040
EBOXBNNAPA	1349	(+)	CANNTG	S00014
MYCCONSENSUSAT	1349	(+)	CANNTG	S00040
MYCATERD1	1349	(+)	CATGTG	S00041
GTGANTG10	1352	(+)	GTGA	S00037
ARR1AT	1355	(+)	NGATT	S00045
CAATBOX1	1360	(+)	CAAT	S00002
POLLEN1LELAT52	1370	(+)	AGAAA	S00024
S1FBOXSORPS1L21	1383	(+)	ATGGTA	S00022
CURECORECR	1386	(-)	GTAC	S00049
CURECORECR	1386	(+)	GTAC	S00049
DPBFCOREDCDC3	1388	(+)	ACACNNG	S00029
ARR1AT	1405	(-)	NGATT	S00045
GATABOX	1416	(+)	GATA	S00003
ABRERATCAL	1428	(+)	MACGYGB	S00050
CGCGBOXAT	1429	(-)	VCGCGB	S00050
ABRERATCAL	1429	(-)	MACGYGB	S00050
CGCGBOXAT	1429	(+)	VCGCGB	S00050
GTGANTG10	1433	(+)	GTGA	S00037
ASF1MOTIFCAMV	1434	(+)	TGACG	S00002
WRKY71OS	1434	(+)	TGAC	S00044
GATABOX	1444	(+)	GATA	S00003
GT1CONSENSUS	1444	(+)	GRWAAW	S00019
IBOXCORE	1444	(+)	GATAA	S00019
TAAAGSTKST1	1446	(+)	TAAAG	S00038
DOFCOREZM	1447	(+)	AAAG	S00026
NODCON1GM	1447	(+)	AAAGAT	S00046
OSE1ROOTNODULE	1447	(+)	AAAGAT	S00046
MYB2CONSENSUSAT	1454	(-)	YAACKG	S00040

MYBCOREATCYCB1	1454	(-)	AACGG	S00050
MYBCORE	1454	(+)	CNGTTR	S00017
PYRIMIDINEBOXOSRAMY1A	1475	(-)	CCTTTT	S00025
DOFCOREZM	1476	(+)	AAAG	S00026
GT1CONSENSUS	1479	(+)	GRWAAW	S00019
TAAAGSTKST1	1481	(+)	TAAAG	S00038
DOFCOREZM	1482	(+)	AAAG	S00026
SEF4MOTIFGM7S	1486	(+)	RTTTTTR	S00010
CACTFTPPCA1	1499	(+)	YACT	S00044
BOXLCOREDCPAL	1510	(+)	ACCWWCC	S00049
GATABOX	1524	(+)	GATA	S00003
ARR1AT	1527	(+)	NGATT	S00045
CIACADIANLELHC	1528	(-)	CAANNNNATC	S00025
ARR1AT	1538	(+)	NGATT	S00045
SEF1MOTIF	1540	(-)	ATATTTAWW	S00000
TATABOXOSPAL	1541	(-)	TATTTAA	S00040
ROOTMOTIFTAPOX1	1544	(-)	ATATT	S00009
MYB1AT	1548	(+)	WAACCA	S00040
TBOXATGAPB	1555	(-)	ACTTTG	S00038
DOFCOREZM	1556	(+)	AAAG	S00026
WBOXNTCHN48	1580	(+)	CTGACY	S00050
QELEMENTZMZM13	1581	(-)	AGGTCA	S00025
WRKY71OS	1581	(+)	TGAC	S00044
WBOXNTERF3	1581	(+)	TGACY	S00045
DOFCOREZM	1585	(-)	AAAG	S00026
TAAAGSTKST1	1585	(-)	TAAAG	S00038
QELEMENTZMZM13	1595	(+)	AGGTCA	S00025
ELRECOREPCRP1	1596	(-)	TTGACC	S00014
WBOXNTERF3	1596	(-)	TGACY	S00045
WBOXATNPR1	1597	(-)	TTGAC	S00039
WRKY71OS	1597	(-)	TGAC	S00044
SORLIP1AT	1605	(-)	GCCAC	S00048
ASF1MOTIFCAMV	1609	(-)	TGACG	S00002
WBOXATNPR1	1610	(-)	TTGAC	S00039
WRKY71OS	1610	(-)	TGAC	S00044
CARGCW8GAT	1612	(-)	CWWWWWWWWG	S00043
CARGCW8GAT	1612	(+)	CWWWWWWWWG	S00043
TATABOX5	1613	(-)	TTATTT	S00020
POLASIG1	1614	(+)	AATAAA	S00008
LTRECOREATCOR15	1621	(-)	CCGAC	S00015
TATABOX5	1627	(+)	TTATTT	S00020
GT1CONSENSUS	1630	(-)	GRWAAW	S00019
GT1GMSCAM4	1630	(-)	GAAAAA	S00045
GT1CONSENSUS	1631	(-)	GRWAAW	S00019
GT1CORE	1638	(+)	GGTTAA	S00012
CAATBOX1	1649	(+)	CAAT	S00002
CACTFTPPCA1	1657	(+)	YACT	S00044
ROOTMOTIFTAPOX1	1663	(-)	ATATT	S00009

TATABOX2	1665	(+)	TATAAAT	S00010
ARR1AT	1669	(-)	NGATT	S00045
GATABOX	1675	(+)	GATA	S00003
SEF1MOTIF	1677	(-)	ATATTTAWW	S00000
TATABOX2	1677	(+)	TATAAAT	S00010
ROOTMOTIFTAPOX1	1681	(-)	ATATT	S00009
PREATPRODH	1688	(+)	ACTCAT	S00045
TAAAGSTKST1	1695	(+)	TAAAG	S00038
DOFCOREZM	1696	(+)	AAAG	S00026
ZDNAFORMINGATCAB1	1705	(+)	ATACGTGT	S00032
ACGTATERD1	1707	(-)	ACGT	S00041
ABRELATERD1	1707	(+)	ACGTG	S00041
ACGTATERD1	1707	(+)	ACGT	S00041
ARR1AT	1714	(-)	NGATT	S00045
TATABOX2	1723	(-)	TATAAAT	S00010
LECPLEACS2	1731	(-)	TAAAATAT	S00046
ROOTMOTIFTAPOX1	1731	(+)	ATATT	S00009
POLASIG2	1735	(-)	AATTAAA	S00008
MARABOX1	1740	(-)	AATAAAYAAA	S00006
ANAERO1CONSENSUS	1740	(-)	AAACAAA	S00047
POLASIG1	1744	(-)	AATAAA	S00008
TATABOX5	1745	(+)	TTATTT	S00020
EBOXBNNAPA	1752	(-)	CANNTG	S00014
MYCATRD22	1752	(-)	CACATG	S00017
MYCCONSENSUSAT	1752	(-)	CANNTG	S00040
EBOXBNNAPA	1752	(+)	CANNTG	S00014
MYCCONSENSUSAT	1752	(+)	CANNTG	S00040
MYCATERD1	1752	(+)	CATGTG	S00041
CACTFTPPCA1	1759	(-)	YACT	S00044
CAATBOX1	1765	(+)	CAAT	S00002
QELEMENTZMZM13	1780	(+)	AGGTCA	S00025
ELRECOREPCRP1	1781	(-)	TTGACC	S00014
WBBOXPCWRKY1	1781	(-)	TTTGACY	S00031
WBOXNTERF3	1781	(-)	TGACY	S00045
WBOXATNPR1	1782	(-)	TTGAC	S00039
WRKY71OS	1782	(-)	TGAC	S00044
EBOXBNNAPA	1788	(-)	CANNTG	S00014
MYCCONSENSUSAT	1788	(-)	CANNTG	S00040
MYB2CONSENSUSAT	1788	(-)	YAACKG	S00040
EBOXBNNAPA	1788	(+)	CANNTG	S00014
MYBCORE	1788	(+)	CNGTTR	S00017
MYCCONSENSUSAT	1788	(+)	CANNTG	S00040
CACTFTPPCA1	1797	(-)	YACT	S00044
GTGANTG10	1798	(+)	GTGA	S00037
ARR1AT	1799	(+)	NGATT	S00045
GATABOX	1809	(+)	GATA	S00003
GT1CONSENSUS	1809	(+)	GRWAAW	S00019
IBOXCORE	1809	(+)	GATAA	S00019

ARR1AT	1812	(-)	NGATT	S00045
ARR1AT	1831	(-)	NGATT	S00045
CAREOSREP1	1839	(+)	CAACTC	S00042
NODCON2GM	1842	(+)	CTCTT	S00046
OSE2ROOTNODULE	1842	(+)	CTCTT	S00046
DOFCOREZM	1844	(-)	AAAG	S00026
TAAAGSTKST1	1844	(-)	TAAAG	S00038
POLASIG1	1845	(-)	AATAAA	S00008
LTRE1HVBLT49	1851	(+)	CCGAAA	S00025
DOFCOREZM	1870	(-)	AAAG	S00026
GATABOX	1881	(+)	GATA	S00003
ROOTMOTIFTAPOX1	1882	(+)	ATATT	S00009
BOXLCOREDCPAL	1891	(+)	ACCWWCC	S00049
AMMORESIVDCRNIA1	1897	(+)	CGAACTT	S00037
TATABOXOSPAL	1902	(-)	TATTTAA	S00040
CACTFTPPCA1	1907	(+)	YACT	S00044
TATABOX5	1916	(+)	TTATTT	S00020
GT1CONSENSUS	1918	(-)	GRWAAW	S00019
POLLEN1LELAT52	1920	(-)	AGAAA	S00024
CAATBOX1	1925	(+)	CAAT	S00002
-300CORE	1944	(-)	TGTAAAG	S00000
DOFCOREZM	1944	(-)	AAAG	S00026
TAAAGSTKST1	1944	(-)	TAAAG	S00038
CACTFTPPCA1	1952	(-)	YACT	S00044
DOFCOREZM	1956	(+)	AAAG	S00026
POLLEN1LELAT52	1958	(+)	AGAAA	S00024
GT1CONSENSUS	1959	(+)	GRWAAW	S00019
POLLEN1LELAT52	1964	(-)	AGAAA	S00024
BOXIINTPATPB	1965	(-)	ATAGAA	S00029
ARR1AT	1972	(+)	NGATT	S00045
GT1CONSENSUS	1975	(-)	GRWAAW	S00019
GT1GMSCAM4	1975	(-)	GAAAAA	S00045
POLLEN1LELAT52	1977	(-)	AGAAA	S00024
DOFCOREZM	1980	(-)	AAAG	S00026
NODCON2GM	1994	(+)	CTCTT	S00046
OSE2ROOTNODULE	1994	(+)	CTCTT	S00046
MYBPZM	1999	(+)	CCWACC	S00017
HBOXCONSENSUSPVCHS	1999	(+)	CCTACCNNNNNNNCT	S00020
IBOXCORENT	2003	(-)	GATAAGR	S00042
IBOX	2004	(-)	GATAAG	S00012
IBOXCORE	2005	(-)	GATAA	S00019
GATABOX	2006	(-)	GATA	S00003
DOFCOREZM	2012	(-)	AAAG	S00026
POLLEN1LELAT52	2013	(-)	AGAAA	S00024
DOFCOREZM	2016	(-)	AAAG	S00026
GT1CONSENSUS	2017	(-)	GRWAAW	S00019
GT1GMSCAM4	2017	(-)	GAAAAA	S00045
POLLEN1LELAT52	2019	(-)	AGAAA	S00024

CACTFTPPCA1	2025	(-)	YACT	S00044
CAATBOX1	2028	(-)	CAAT	S00002
RAV1AAT	2033	(-)	CAACA	S00031
INRNTPSADB	2039	(-)	YTCANTYY	S00039
GT1CONSENSUS	2044	(+)	GRWAAW	S00019
GT1GMSCAM4	2044	(+)	GAAAAA	S00045
GT1CORE	2056	(+)	GGTTAA	S00012
CACTFTPPCA1	2065	(+)	YACT	S00044
GTGANTG10	2069	(+)	GTGA	S00037

Curriculum Vitae

MEG HAGGITT

EDUCATION

Ph.D in Department of Biology **2016**
University of Western Ontario, London, ON Canada
Dissertation: Role of *Fatty Acid omega-Hydroxylase 1* (*FAωH1*) and Abscisic Acid in Potato Tuber Suberin Formation

Western Teaching Certificate (to be completed December 2016) **2011-present**
University of Western Ontario, London, ON Canada

Honours Co-operative B.Sc. with Plant Specialization in Biology **2005**
University of Waterloo, Waterloo, ON Canada
Areas of Concentration: Molecular Biology and Genetics; Plant Anatomy, Development and Physiology

---

AWARDS

Alexander Graham Bell Canadian Graduate Scholarship (NSERC CGS) **2006-2011**
Held in Dr. Mark Bernards's Laboratory, University of Western Ontario, Canada

Julie Payette NSERC Research Scholarship **2005-2006**
Held in Dr. Vojislava Grbic's Laboratory, University of Western Ontario, Canada
Awarded to the top 24 Science and Engineering candidates across Canada entering graduate school.

Western Graduate Research Scholarship **2005-2012**
University of Western Ontario, Canada

NSERC Undergraduate Student Research Award (USRA) **2005**
Held in Dr. John Semple's Laboratory, University of Waterloo, Canada

Biology Upper Year Scholarship **2004-2005**
Based on academic excellence, University of Waterloo, Canada

NSERC Undergraduate Student Research Award (USRA) **2004**
Held in Dr. Vojislava Grbic's Laboratory, University of Western Ontario, Canada

J.R. Coutts International Experience Award **2003**
Held in Dr. Manfred Schenk's Laboratory, University of Hanover, Hanover, Germany

Honourable Mention for Best Poster Award **2002**
Canadian Society of Plant Physiologists National Conference; St. Catherines, Canada

Waterloo Undergraduate Research Award **2002**
University of Waterloo, Canada

NSERC Undergraduate Student Research Award (USRA) **2002**
Held in Dr. Carol Peterson's Laboratory, University of Waterloo, Canada

Queen Elizabeth II Aiming for the Top Scholarship **2000-2005**
Government of Ontario, Canada

Dr. Roger Downer Biology Entrance Award **2000**
University of Waterloo, Canada

POSITIONS HELD

Graduate Research Assistant: Ph.D Candidate **2006-present**
Dr. Mark Bernard's Laboratory, Department of Biology, Western University, London, ON Canada

Undergraduate Course Teaching Assistant **2004-2014**
Department of Biology, University of Western Ontario and University of Waterloo, Canada

Research Associate **2005**
Dr. John Semple's Laboratory, Department of Biology, University of Waterloo, Canada

Research Assistant **2004**
Dr. Vojislava Grbic's Laboratory, Department of Biology, University of Western Ontario, Canada

Histochemical Staining Techniques Consultant **2003**
Dr. Manfred Schenk's Laboratory, Institute of Plant Sciences, University of Hanover, Hanover, Germany

Research Assistant **2002-2003**
Dr. Carol Peterson's Laboratory, Department of Biology, University of Waterloo, Canada

RELATED EXPERIENCE

Young Members Committee: Phytochemical Society of North America **2012**

Organizer of Science Enrichment at Rural Communities **2006-2008**
Organized a scientific enrichment program at two rural secondary schools to increase awareness of novel scientific research and the implications in our society. This required the co-ordination of 15 volunteer graduate students from University of Western Ontario, acquiring the supplies necessary to run the experiments and coordinating with the local principals and science departments.

PUBLICATIONS

Hayter ML and Peterson CA. 2004. Can Ca^{2+} Fluxes to the Root Xylem be Sustained by Ca^{2+}-ATPases in Exo- and Endodermal Plasma Membranes. Plant Physiology 136: 4318-4325

Bjelica A, **Haggitt ML**, Woolfson KN, Lee DNP, Makhzoum AB, Bernards MA. 2016. Fatty Acid ω-Hydroxylases from *Solanum tuberosum*. Accepted to Plant Cell Reports.

Haggitt ML, Woolfson KN, Zhang Y, Kachura A, Bjelica A, Bernards MA. 2016. Differential Regulation of Polar and Non-Polar Metabolism During Wound-Induced Suberization in Potato (*Solanum tuberosum*) tubers. In preparation for submission to The Plant Cell.

SEMINAR AND CONFERENCE PRESENTATIONS

Bernards MA, **Haggitt ML**, Kurepin L, Zhang L, Bjelica A, Woolfson A. **2015**
Abscisic Acid Regulation of Wound-Induced Suberization
Oral Presentation, Plant Wax 2015, Ascona, Switzerland

Bernards MA, **Haggitt ML**, Kurepin L, Zhang Y, Bjelica A, Woolfson K. **2015**
Formation and Function of Suberin
Invited Talk, University of Bonn, Institute of Botany, Bonn, Germany

Bernards MA, **Haggitt ML**, Kurepin L, Zhang Y, Bjelica A, Woolfson K. **2015**
Formation and Function of Suberin
Invited Talk, University of Toronto, Department of Cell and Molecular Biology, Toronto, Canada

Haggitt ML, Kurepin L, Zhang Y, Bjelica A, Bernards MA. **2014**
Abscisic Acid Regulation of Wound-Induced Suberization
Poster Presentation, Annual Meeting of the Phytochemical Society of North America, North Carolina State University, Raleigh, NC

Haggitt ML, Kurepin L, Zhang Y, Bjelica A, Bernards MA. **2014**
Abscisic Acid Regulation of Wound-Induced Suberization
Oral Presentation, Banff Metabolism Conference, Banff, AB, Canada.

Haggitt ML, Kurepin LV, Bernards MA. **2012**
Effect of ABA on the *Fatty Acid ω-Hydroxylase 1* (*FAωH1; CYP86A33*) Wound-Induced Expression and Suberin Deposition in *Solanum tuberosum*.
Oral Presentation, Phytochemical Society of North America Annual Conference, London ON, Canada.

Haggitt ML, Kurepin LV, Bernards MA. **2012**
FAωH1 Wound-Induced Suberin Expression and Activity: The ABA Effect
Oral Presentation, 3rd Annual Biology Graduate Research Forum, University of Western Ontario, London, ON Canada.

Haggitt ML, Kurepin LV, Bernards MA. **2012**
Characterization of the *Fatty Acid ω-Hydroxylase 1* (*FAωH1; CYP86A33*) Wound-Inducible Promoter from *Solanum tuberosum.*
Poster Presentation, Banff Conference on Plant Metabolism, Banff AB, Canada.

Haggitt ML, and Bernards MA. **2009**
Identification and Functional Characterization of Suberin-associated ω-Hydroxylases in *Solanum tuberosum*.
Poster Presentation, Phytochemical Society of North America Annual Conference, Baltimore, USA.

Haggitt ML, and Bernards MA. **2007**
Biosynthesis of Potato (*Solanum tuberosum* L.*)* suberin: The ω-hydroxylation of Fatty Acids.
Poster Presentation, Canadian Society of Plant Physiologists National Conference, London, ON Canada

Hayter ML and Peterson CA. **2002**
Feasibility of Symplastic Ca^{2+} Movement through the Endodermis and Exodermis vis Ca^{2+}-ATPases in *Allium cepa* Roots.
Poster Presentation, Canadian Society of Plant Physiologists National Conference, St. Catherines, ON Canada.

MEMBERSHIPS

Phytochemical Society of North America **2009-2013**
Canadian Society of Plant Biologists **2002-2003**
